A Dynamic and Integrated Approach for Modeling and Managing Domino-effects (DIAMOND)

Chen, C.

DOI
10.4233/uuid:38a95ca3-6986-4723-8231-2c0bb11c12fc

Publication date
2021

Document Version
Final published version

Citation (APA)
Chen, C. (2021). *A Dynamic and Integrated Approach for Modeling and Managing Domino-effects (DIAMOND)*. [Dissertation (TU Delft), Delft University of Technology]. https://doi.org/10.4233/uuid:38a95ca3-6986-4723-8231-2c0bb11c12fc

A Dynamic and Integrated Approach for Modeling and Managing Domino-effects (DIAMOND)

Chao CHEN

Delft University of Technology

A Dynamic and Integrated Approach for Modeling and Managing Domino-effects (DIAMOND)

Dissertation

for the purpose of obtaining the degree of doctor

at Delft University of Technology,

by the authority of the Rector Magnificus Prof.dr.ir. T.H.J.J. van der Hagen,

chair of the Broad for Doctorates

to be defended publicly on

Thursday, 27 May 2021, at 15:00 o' clock

by

Chao CHEN

Master of Science in Oil and Gas Storage and Transportation Engineering,

Southwest Petroleum University, China

born in Guang'an, Sichuan, China

This dissertation has been approved by the promotors.

Composition of the doctoral committee:

Rector Magnificus	Chairman
Prof.dr.ir. G.L.L.M.E. Reniers	Delft University of Technology, promotor
Dr. M. Yang	Delft University of Technology, copromotor

Independent members:

Prof.dr.ir. P.H.A.J.M. van Gelder	Delft University of Technology
Prof.dr. V. Cozzani	University of Bologna, Italy
Prof.dr. F. Khan	Memorial University of Newfoundland, Canada
Prof.dr. W. Weng	Tsinghua University, China
Prof.dr.ir. H.J. Pasman	TUD/ Texas A&M University, USA

Reserve member:

Prof.ir. A.E.M. Huesman	Delft University of Technology

This research is funded by Delft University of Technology (TU Delft) and China Scholarship Council (CSC) under Grant 201708510111.

Cover illustration by: Chao Chen
Published and distributed by: Chao Chen
Printing: Ridderprint | www.ridderprint.nl

ISBN: 978-94-6384-221-1

Printed in the Netherland

To my fiancée Yu Yang

Preface

Looking back on my Ph.D. career, I clearly remember the skype meeting with Prof. Genserik Reniers on the Chinese New Year's Eve, 2017, which is the start of my research in the safety and security science domain. That fall, I left my hometown and started my journey in the Netherlands, as a Ph.D. candidate in TU Delft. During the journey, I have been growing under the help of many people. At the end of my Ph.D. program, I would like to thank everyone who helped, encouraged, and accompanied me.

I sincerely thank my promoter Prof. Genserik Reniers for his consistent support and supervision. When I contacted you for a possible Ph.D. position in TUD, you gave me a positive reply in a short time and tirelessly helped me improve the application materials. When I was lost in the first meeting on discussing my research proposal, you patiently emailed me about possible research ideas. When I wrote the first paper, you revised it four times and made it almost a new paper. You never urged my research progress, creating a relaxing and free research environment for me. You showed me how to be a good supervisor: knowledgeable, patient, super-effective, encouraging, friendly, etc. You are not only my supervisor but also my friend. I still remember our trip to China, in which we tasted varieties of Chinese food, took a boat tour on the Qinhuai River in the evening, and watched Sichuan Opera.

I would like to thank Dr. Nima Khakzad for being my co-promotor in the first two years. You always helped me revise papers and taught me many skills on how to organize a good paper. I obtained many ideas by learning from you and shaped my writing style inspired by your writings. I would also like to thank my current co-promotor, Dr. Ming Yang. Every talk we have together can generate sparks, and I enjoyed our conversation a lot. You lead me into the field of resilience research from our first conversation when you visited TU Delft in 2019. I often visited your home, and we chatted about everything.

I would also like to express my great appreciation to my master supervisor Prof. Changjun Li. Dear Prof. Li, thank you for being my life mentor in many aspects and let me step into the world of academia. It is you who encouraged me to pursue my academic dream and did everything to help me. From you, I have learned to constantly be ambitious and rigorous about academic research and work. Hard-working accompanies scholars throughout their lives. Besides, I would also like to thank Prof. Kexi Liao, Prof. Xiaoqing Song, Prof. Enbin Liu, Dr. Wenlong Jia, Dr. Xia Wu, Dr. Qian Huang, Dr. Yang Chen, Dr. Gang Liu, Dr. Ting Huang, Dr. Cheng Cao, Shikui Yan, Bo Wang, Yu Zou, Zenghui Cao, Longjun Chen, Lie Kong, Jie Zeng. You always helped me in academic research and daily life during these years.

I would also like to thank all the good colleagues met in the Safety and Security Science Group. You have given me many very unique and unforgettable experiences on countless things. I will never forget the exciting group dinners and activities where we share our knowledge about our own culture and history. The warm discussion we

have together also let me know much about different safety research topics, which I much appreciated. These beautiful colleagues are Prof. Pieter van Gelder, Prof. Jop Groeneweg, Prof. Fuqiang Yang, Prof. Yunxiao Fan, Prof. Yamin Huang, Dr. Paul Swuste, Dr. Wei Ge, Dr. Dan Jiang, Dr. Frank Guldenmund, Dr. Eleonora Papadimitriou, Dr. Peter Roelofsma, Dr. Laobing Zhang, Dr. Yulin Li, Dr. Pengfei Chen, Yunfeng Yang, Astrid Pinzger-van Staalduinen, Peter Blokland, Saba Chockalingam, Dick Hoeneveld, Karolien van Nunen, Xin Ren, Shuaiqi Yuan, Mengxia Li, Rongshui Qin, Jie Xue, Chaoning Lin, Gexin Shen, Weitao Xiong, and Xingyuan Zhou.

Moreover, I would like to share my gratitude towards my committee members for the doctoral defense. Your constructive comments and suggestions helped me obtained more profound insights into my work. Besides, I would like to thank these experts in our research domain who gave me help. They are Prof. Valerio Cozzani, Prof. Faisal Khan, Prof. Hans Pasman, Prof. Wenguo Weng, Prof. Fubao Zhou, Prof. Cheng Wang, Prof. Guohua Chen, Prof. Xuhai Pan, Prof. Jiansong Wu, Prof. Bing Zhang, Prof. Yi Liu, Dr. Jie Li, Dr. Mengqi Yuan, Dr. Dejian Wu, and Dr. Shengcai Li.

Besides, I will never forget the memories that I have together with my dear friends during these years in the Netherlands. I want to express my sincere appreciation to Dan Chen, Xiaomeng Liao, Xuandong Wang, Sjonnie Boonstra, Martina Casciano, Jari Rahul Capassi, Wenting Ma, Sihang Qiu, Min Jiang, Huanhuan Liu, Hongpeng Zhou, Jinyu Tang, Shuhong Li, Kailan Wu, and Fanxiang Xu.

I would also like to thank the China Scholarship Council (CSC) for the financial support for my PhD research.

另外，我想感谢我的父亲陈安平，母亲张文碧。一直以来, 你们给予我的无限支持和鼓励是我前进的动力。感谢姐姐陈开英和陈小燕对我们家庭和我一如继往的无私付出。感谢我所有的亲人对我从小到大的关心和帮助。

At last, I would like to thank my fiancée, Yu Yang. It is you who always support and encourage me to go through the tough times. Although we are 8000 kilometers apart, your love is always by my side. Now, we will create a warm family together.

Table of Contents

List of Figures

List of Tables

List of symbols

AIT	Autoignition temperature
$B_{i,\,k}$	Benefit of protection strategy *i* for a special attack scenario *k*
B_i	Expected benefit of protection strategy *i*
c_1	A constant in the equation of residual time to failure
c_2	A constant in the equation of residual time to failure
c_3	A constant in the equation of residual time to failure
c_4	A constant in the equation of residual time to failure
c_5	A constant in probit function of the damage due to overpressure
c_6	A constant in probit function of the damage due to overpressure
c_7	A constant in the probit function of acute intoxication
c_8	A constant in probit function of acute intoxication
c_9	A constant in probit function of acute intoxication
C_t	Concentration of toxic gas
$C_{ij,\,\mathrm{ini}}$	Initial costs of measure *j* in strategy *i*
$C_{ij,\,\mathrm{ins}}$	Installation costs of measure *j* in strategy *i*
$C_{ij,\,\mathrm{ope}}$	Annual operation costs of measure *j* in strategy *i*
$C_{ij,\,\mathrm{mai}}$	Annual maintenance costs of measure *j* in strategy *i*
$C_{ij,\,\mathrm{ins}}$	Annual inspection costs of measure *j* in strategy *i*
$C_{ij,\,\mathrm{log}}$	Annual logistics and transport costs of measure *j* in strategy *i*,
$C_{ij,\,\mathrm{con}}$	Annual contractor costs of measure *j* in strategy *i*
$C_{ij,\,\mathrm{oth}}$	Annual other costs of measure *j* in strategy *i*
C_r	Capability of resistant
d	Traffic density
E	Edges in a dynamic graph
E_c	Total combustion energy
EW	Edge weights
f_0	Performance of a chemical plant at the initial stage
f_1	Performance of a chemical plant at the end of disruption stage
f_2	Performance of a chemical plant at the end of escalation stage
f_3	Performance of a chemical plant in adaption stage
f_{ad}	Improved performance in the adaptation stage
f_{es}	Damaged performance in the escalation stage
f_{di}	Damaged performance in the disruption stage
$f(t)$	Performance function
g'	Relative density of a vapor
G	Dynamic graph
h	Height of a vapor cloud
I	Number of protection strategies

IT	Ignition time
J	Total number of (safety and security) measures
K	Total number of attack scenarios
L	Length of a road or railway section
L_k	Loss caused by attack k
$L_{k, n}$	Loss of installation n in attack k
$L_{k, n, sup}$	Loss of the supply chain f installation n in attack k
$L_{k, n, dam}$	Loss of damage of installation n in attack k
$L_{k, n, leg}$	loss of legal of installation n in attack k
$L_{k, n, ins}$	Loss of insurance of installation n in attack k
$L_{k, n, hum}$	Loss of human of installation n in attack k
$L_{k, n, env}$	Loss of environment of installation n in attack k
$L_{k, n, per}$	Loss of personnel of installation n in attack k
$L_{k, n, med}$	Loss of medical treatment of installation n in attack k
$L_{k, n, int}$	Loss of intervention of installation n in attack k
$L_{k, n, rep}$	Loss of reputation of installation n in attack k
$L_{k, n, inv}$	Loss of accident investigation and clean-up of installation n in attack k
$L_{k, n, sec}$	Loss of the security-related different from accidental losses of installation n in attack k
$P_{k, n}$	Damage probability of installation n in attack scenario k
$L_{0, k}$	Expected loss caused by attack scenario k under the protection of baseline strategy 0
$L_{i, k}$	Expected loss caused by attack scenario k under the protection of strategy i
m_i	Mass of flammable substances in installation i
m_t	Mass flow rate at time t
m_{TNT}	Equivalent mass of TNT
MIE	Minimum ignition energy
M_t	Total release mass at time t
$M_{f,\mathrm{t}}$	Mass of flammable substances in a vapor cloud
N	Number of hazardous installations
$NPVB_i$	Net present value of benefits of protection strategy i
N_v	Number of vehicles per hour
P^*	Probability of the minimal threat
P_o	Overpressure
P_a	Ambient pressure
P_{aut}	Probability of autoignition
PD	Probability of failure due to domino effects
P_f	Probability of failure due to direct disruptions

$P\left(FF \mid I_{t_2,IS1}\right)$	Conditional probability of FF given an ignition of source 1 at t_2
$P\left(VCE \mid I_{t_2,IS1}\right)$	Conditional probability of VCE given an ignition of source 1 at t_2
P_{IS}	Ignition probability of a ignition source
$P\left(I_{t_2,IS1} \mid \overline{I_{t_1}}\right)$	Conditional probability of the ignition of ignition 1 at t_2 given no ignition before time t_1
$P\left(I_{IS1} \mid \overline{I_{t_1}}\right)$	Conditional probability of no ignition before time t_1 given no immediate ignition
$P\left(\overline{I_{t_0}} \mid LOC\right)$	Conditional probability of no immediate ignition at time t_0 given a LOC event
P_C	Probability of guard communication
P_D	Probability of detection
P_E	Probability that the attack is successfully executed
P_{re}	Reliability of the available attack device
P_{pe}	Performance factor of adversaries when using the attack device
$P_{I,,k}$	Cumulative ignition probability caused by the ignition source k
PP	Probability of primary scenarios
P_r	Damage probability due to overpressure
P_S	Probability of a successful attack
P_{sc}	Scaled overpressure
$P_{IS1}(t_2)$	Ignition probability of source 1 before time t_2
$P_{IS1}(t_1)$	Ignition probability of source 1 before time t_1
$P_{IS2}(t_2)$	Ignition probability of source 2 before time t_2
$P_{IS2}(t_1)$	Ignition probability of source 2 before time t_1
$P_{t_2,IS1,VCE}$	Probability of VCE caused by ignition source 1 at t_2
$P_{t_2,IS1,VCE}$	Probability of FF caused by ignition source 1 at t_2
P_t	Death probability caused by acute toxicity
P_{Sta}	Probability of static discharge
PVC_i	Present value of cost with respect to protection strategy i
$PVC_{i,j}$	Present value of costs of the j-th safety or security measure in strategy i
$q_{i,j}$	Heat radiation from installation i to installation j
$q_{w,ij}$	Heat radiation from installation i to installation j under the protection of WDS
Q_j	Total heat radiation received by an installation j
Q_v	Volume flow rate of hazardous gas or vapor
r	Distance from the center of the explosion
r_d	Discount rate
r_s	Scaled distance
RP	Actual Release pressure
RT	Actual Release temperature
R_t	Radius of a vapor cloud at time t

RTF	Residual time to failure of installations
RTB	Residual time to burn out of installations
S	States
t	Release time
t_e	Exposed time that a human subject to toxic gas.
t_i	Time of step i
t_{IS}	Time of vapor cloud at an ignition source
t_g	Period time of graph g
t_{i+1}	Time of step i+1
t_{max}	Maximum time of resilience evolution scenarios
T_g	Time of graph g
T_l	Time lapse due to fireproof coatings
v	Average velocity of vehicle
V	Vertices
V_t	Volume of vapor cloud at time t
$V_{a,t}$	Volume of air in a vapor cloud at time t
$V_{f,t}$	Volume of flammable gas or vapor at time t
y	Number of years that the protection measure can operate in a chemical plant
Y_f	Probit value for fire
Y_P	Probit value for overpressure
Y_t	Probit value for toxic gas
Z	Scale distance of the TNT equivalency method
α	Vaporization rate
ΔH	Combustion heat of the flammable gas
ΔP	Peak overpressure
Δt	Time step
ρ_f	Density of flammable gas or vapor
ω	Ignition effectiveness
Φ	Normal distribution
$\triangle R$	Risk reduction

List of acronyms and abbreviations

BBC	British Broadcasting Corporation
BLEVE	Boing Liquid Expanding Vapor Explosion
CCPS	Center for Chemical Process Safety
CCTV	Closed-circuit television
CERs	Cost-effectiveness ratios
CFD	Computational Fluid Dynamics
CNN	Cable News Network
CSB	U.S. Chemical Safety and Hazard Investigation Board
DBN	Dynamic Bayesian network
DDET	Discrete dynamic event tree
DEG	Domino Evolution Graph
DET	Dynamic event tree
DGMC	Dynamic Graph Monte Carlo
DIT	Delayed ignition time
DVEA	Dynamic VCE evolution assessment
EDP	Emergency depressurization systems
ESD	Emergency shutdown systems
FEM	Finite Element Method
FF	Flash fire
FVC	Flammable vapor cloud
GDP	Gross Domestic Product
HAZOP	Hazard and operability study (HAZOP)
HSEG	Hazardous Scenario evolution graph
HSE	U.K. Health and Safety Executive
ICCA	Council of Chemical Associations
LNG	Liquefied natural gas
LOC	Loss of containment
LPG	Liquefied petroleum gas
ME	Multi Energy method
MET	Minimum evolution time
MINLP	Mixed integer nonlinear program
MPC	Multi-Plant Council
NPVB	Net present value of benefits
PFD	Probability of failure on demand
PPE	Personal protection equipment
PROTOPT	Protection optimization
PSV	Pressure Safety Valve

PVC	Present value of costs
QRA	Quantitative risk assessment
RQ	Research question
STED	Spatial-temporal evolution of domino effects
SRQ	Sub-research question
ttf	The time to failure
TNT	Trinitrotoluene
UPI	United Press International
VCE	Vapor cloud explosion
WDS	Water deluge systems

Chapter 1 Introduction

Process and chemical industrial areas consist of hundreds and even thousands of installations situated next to each other, where quantities of hazardous (e.g., flammable, explosive, toxic) substances are stored, transported, or processed. These installations are mutually linked in terms of the hazard level they pose to each other in the system. As a result, a primary undesired disruption (e.g., an accidental event, intentional attack, or natural disaster) may escalate to nearby installations, triggering a chain of accidents. This phenomenon is well known as the potential for “knock-on effects” or so-called “domino effects”. This dissertation is devoted to modeling the spatial-temporal evolution of domino effects, preventing the escalation, mitigating the consequences, thereby developing a safer, securer, and more resilient chemical industrial area. This chapter introduces the research background, motivations, questions, contributions, and the outline of the dissertation.

1.1 Background

The process and chemical industry is central to the global economy and has a prominent role in creating and maintaining modern-day life. In 2017, the chemical industry contributed $5.7 trillion (7%) to global GDP and provides 120 million jobs worldwide (ICCA, 2019). The chemical industry comprises chemical plants that produce, process, or store chemicals. Chemical plants are situated in an industrial area, which is called a chemical cluster or a chemical industrial park, such as the Antwerp industrial area, the Rotterdam chemical park, the Rhine-Ruhr industrial area, and the Shanghai chemical industrial park. These chemical industrial areas consisting of hundreds and sometimes thousands of hazardous installations situated next to each other are usually characterized by high complexity and interdependencies (Cozzani et al., 2005; Reniers and Cozzani, 2013; Zeng et al., 2019; Chen et al., 2020b). The chemical installations that store, transport, or process hazardous (e.g., flammable, explosive, toxic) substances usually operate under high-temperature high-pressure conditions. As a result, a primary undesired disruption may lead to major accidents[1] (Chen and Reniers, 2020). Moreover, Primary accidents may propagate to nearby installations, triggering a chain of accidents, resulting in overall consequences more severe than those of the primary event, a phenomenon which is well known as knock-on effects, or domino effects (Reniers and Cozzani, 2013; Chen et al., 2018). According to the definition, domino effects always concern the escalation due to the damage of secondary installations caused by the primary event rather than the escalation within the same installation caused by a low-severity initiating event (Cozzani et al., 2005). Once a major accident occurs in a chemical industrial area, it may result in huge property losses, casualties, severe environmental pollution as well as ecological and ethical problems (Yang et al., 2018; Yang et al., 2019; Chen et al., 2020c). This study focuses on domino effects in the process and chemical industry while domino effects (cascading effects) in other infrastructure systems such as power grids (Kinney et al., 2005) and traffic networks (Zheng et al., 2007) are not considered in this thesis.

Domino effects may be triggered by accidental events (unintentional domino effects) such as the Puerto Rico accident in 2009 (CSB, 2015) and the Buncefield domino accident in 2005 (Buncefield Major Incident Investigation Board, 2008). Compared with domino effects caused by accidental events, domino effects triggered by intentional attacks (intentional domino effects) may induce more severe consequences due to simultaneous damage of installations induced by multiple target attacks. For instance, three tanks in a French chemical plant were attacked via explosive devices in July 2015, causing two simultaneous tank fires (one damaged

[1] Major accident is defined by the Seveso Directive as “an undesired event such as a major emission, fire or explosion induced by uncontrolled developments in the course of an industrial activity, resulting in a serious danger to humans, immediate or delayed, inside or outside the establishment, and/or to the environment, and involving one or more dangerous substances”.

tank failed to be ignited) (BBC News, 2015). This possible attempt to induce a domino effect has luckily failed.

1.2 Motivations

In light of the severe consequences of domino effects, the second Seveso Directive (Directive 96/82/EC, also known as “Seveso-II” Directive) requires chemical companies to assess “domino” accident hazards inside and outside the industrial areas (Papadakis and Amendola, 1997). The third Seveso Directive (Seveso-III) highlights the role of exchanging information between chemical plants to prevent domino effects in chemical clusters (Council Directive 2012/18/EU, 2012). In the scientific and technical domain, growing attention on the assessment and management of domino effects can be observed since the 1990s (Bagster and Pitblado, 1991; Khan and Abbasi, 1998a; Salzano and Cozzani, 2003; Cozzani et al., 2005; Reniers et al., 2005a; Reniers et al., 2009; Khakzad et al., 2013; Chen et al., 2020c). A lot of research and advancements were made in recent decades, while, there are some open issues in modeling and managing domino effects in the chemical process industry.

(1) Modeling the evolution of domino effects is the basis for domino effect management, and it is also challenging due to the time dependencies and uncertainties related to the evolution. For instance, the probit models for fire-induced failure are developed to assess the first level escalation. Applying these models in the second or higher-level escalations may overestimate the likelihood of higher-level escalations. Besides, previous risk assessment methods such as the Bayesian network may not be suitable for chemical clusters with many installations. Moreover, more than one kind of scenario (hazards) exists in one domino accident, but previous modeling work mainly concentrates on one type of scenario (fire or explosion), ignoring possible hazard evolution, whereby one scenario develops into another type of scenario.

(2) Intentional attacks on chemical plants may damage multiple tanks, resulting in more severe domino effects. Besides safety barriers, security measures may also be used and needed to prevent domino effects. However, in literature, only scarce attempts have been made to assess the performance of security measures in the prevention of domino effects. To the best of the author’s knowledge, the integrated performance of a protection strategy (a combination of safety barriers and security measures) for intentional domino effects is overlooked. These disruptions (accidental events and intentional attacks) may be difficult to predict, and thus domino effects may be inevitable in some cases. In that case, enhancing the resilience of chemical plants may be a practical approach to mitigate the consequences of domino effects. Nevertheless, little attention has been paid to the role of adaptation and restoration capabilities in domino effect management.

This dissertation is expected to fill these research gaps to better protect chemical industrial areas.

1.3 Research questions

The research aims to model the spatial-temporal evolution of domino effects and manage domino effects based on the developed models, thus obtaining optimal protection strategies. To achieve the research objective, filling the gaps in modeling and managing domino effects, the main research question (RQ) is formulated, as follows:

RQ: *How can domino effects be modeled and managed, considering the time-dependencies and evolution uncertainties, to prevent and mitigate domino effects in the process industries?*

To answer the main question, a list of sub-questions should be addressed, as follows:

SRQ1: *What methods have been used to model and manage domino effects, and what research gaps need to be filled for better preventing and mitigating domino effects in the process industries?*

In recent decades, various methods have been developed to model and manage domino effects in the process industry. These years have seen several literature reviews such as one on past domino accidents (Abdolhamidzadeh et al., 2011), one on domino effect assessment methods (Necci et al., 2015), and a bibliometric analysis (Li et al., 2017). There is still a need to obtain deeper insight into what modeling and management methods have been used to deal with domino effects and how these models and methods have evolved, what have been the main areas of concern, and which issues need more attention in the future. A systematic literature review is conducted to answer these questions.

SRQ2: *How can the spatial-temporal evolution of domino effects induced by fire be modeled, considering superimposed effects and synergistic effects?*

The escalation of fire-induced domino effects depends on the time to failure (TTF) of installations exposed to fire. As a result, the fire-induced escalation may be regarded as a spatial-temporal evolution process. During the evolution, one installation may receive heat radiation from multiple fires (synergistic effects), and the received heat radiation may change over time. The effects of heat radiation in different stages should be superimposed when determining the TTF (superimposed effects). Besides, the time-lapse in the second or higher-level escalation should be considered in probit models. In light of these research gaps, a new model should be proposed for fire-induced domino effects.

SRQ3: *How can the vapor dispersion and delayed ignition time be considered in VCE-induced domino effects?*

Compared with fire, vapor cloud explosion (VCE) is more difficult to assess due to the uncertainty of ignition position, the uncertainty of delayed ignition time (DIT), and the complexity of overpressure intensity calculation. The VCE induced by the release of hazardous substances in chemical plants is a dynamic process along with the vapor cloud dispersion. However, previous risk analysis methods for VCE always assume that the explosion occurs immediately at the release place (Abdolhamidzadeh et al., 2010b; Zhou and Reniers, 2017b), which is inconsistent with the observations from large VCEs in recent years. As a result, a dynamic tool needs to be developed to address the vapor cloud dispersion and delayed ignition in the assessment of VCE-induced domino effects.

SRQ4: *How can the evolution of multi-hazardous scenarios be modeled in domino effects?*

Once a release occurs at an installation in a chemical industrial area, scenarios such as a toxic release, a VCE, and a fire may simultaneously or sequentially occur, and the generated scenarios can evolve spatially and result in a cascading disaster. Consequently, all the major accident scenarios (fire, explosion, and toxic release) can be simultaneously or sequentially present in a domino effect. Neglecting any known hazard may underestimate the risk of domino effects and result in more severe consequences. Therefore, modeling the spatial-temporal evolution of hazardous scenarios originating from the release of hazardous materials in industrial areas is essential for protecting staff, nearby residents, and emergency rescuers. As a result, a dynamic method should be developed to model multi-hazardous scenarios in domino effects.

SRQ5: *How can safety and security management be integrated and optimized for preventing and mitigating domino effects?*

Safety barriers are widely used to prevent and mitigate unintentional domino effects. Compared with unintentional domino effects, intentional domino effects may induce more severe consequences due to simultaneous damage of installations induced by sudden and uncertain multiple target attacks. The integration of safety and security measures is necessary to tackle intentional domino effects. Security measures can be taken to prevent intentional attacks, and mitigation barriers may be used to prevent possible escalations. Besides, the economic issues of safety and security play an indispensable role in the decision-making on the allocation of safety and security measures since companies usually face budget limitations. As a result, an integrated method is needed to economically allocate safety and security measures to prevent and mitigate domino effects.

SRQ6: *How can unpreventable domino effects be tackled?*

A disruption such as an intentional attack may be difficult to predict and prevent, thus safety and security measures may be insufficient for preventing domino effects. Once a domino effect occurs, an adaptation operation or a quick restoration can reduce the loss and thus mitigate the consequences of domino effects. Resilience refers to the capability of a chemical plant to resist, mitigate, adapt, and recover from undesired events, maintaining its desired performance. As a result, developing a resilient chemical plant may be a practical and effective way to deal with these disruptions. A resilience-based approach is needed to prepare a chemical plant to anticipate, absorb, adapt to, and restore from domino accidents.

1.4 Contributions

The contributions of this dissertation are summarized, as follows:

(1) A systematic review on domino effect research in the process and chemical industries is conducted, identifying the current research issues and approaches to modeling and managing domino effects, analyzing the research gaps, and discussing possible future research directions.

(2) A dynamic graph approach is developed to model the spatial-temporal evolution of fire-induced domino effects, considering the synergistic effects and superimposed effects and overcoming the limitations of probit models in higher-level escalation.

(3) A dynamic risk assessment method based on a discrete dynamic event tree (DDET) is established to integrate vapor cloud dispersion models and ignition sources into a stochastic simulation engine to model the timing dependencies and ignition uncertainty in the evolution of VCEs, assessing VCE-induced domino effects.

(4) A dynamic approach called "Dynamic Graph Monte Carlo" (DGMC) is developed to model the evolution of multi-hazardous scenarios and assess the vulnerability of humans and installations exposed to various hazards, considering the uncertainties and interdependencies among the agents (hazardous installations, humans and ignition sources) and their impacts on the evolution of hazards and possible domino effects.

(5) An integrated management method based on cost-benefit analysis is developed to allocate safety and security measures for preventing and mitigating domino effects, achieving the most profitable protection strategy.

(6) A resilience-based approach considering the resistant capability, the mitigation capability, the adaption capability, and the restoration capability, is established to prevent and mitigate domino effects and develop a resilient chemical plant.

1.5 Outline of the dissertation

Major hazardous scenarios such as fire and VCE are the most common hazardous scenarios that may be present in domino effects, this study focuses on modeling and managing domino effects that involve one or more of these scenarios. This dissertation consists of 8 chapters and the structure of this dissertation is shown in Figure 1.1.

Chapter 1 illustrates the background, motivations, research questions, contributions, and organization of this dissertation.

Chapter 2 provides a systematic literature review of domino effects in the process industry. This chapter reviews the risk assessment and modeling methods and safety and security management approaches of domino effects. The current approaches are also classified and discussed to identify the research gaps and explore future research directions. (Contribution 1)

Chapter 3 demonstrates the dynamic graph approach for modeling the spatial-temporal evolution of fire-induced domino effects. The core of this section is the developed Domino Evolution Graph (DEG) model and the Minimum Evolution Time (MET) algorithm for solving the model. A case study is provided to test the model while another case is used to show its application in chemical clusters with a large number of hazardous installations. (Contribution 2)

Chapter 4 develops a dynamic event tree (DET) approach to model the spatial-temporal evolution of VCEs, addressing the time dependencies in vapor dispersion and the ignition uncertainty. This chapter focuses on the developed model and its application in the vulnerability assessment of installations expose to VCEs. A case study is provided to illustrate the steps of the methodology and compare the results with a past accident. (Contribution 3)

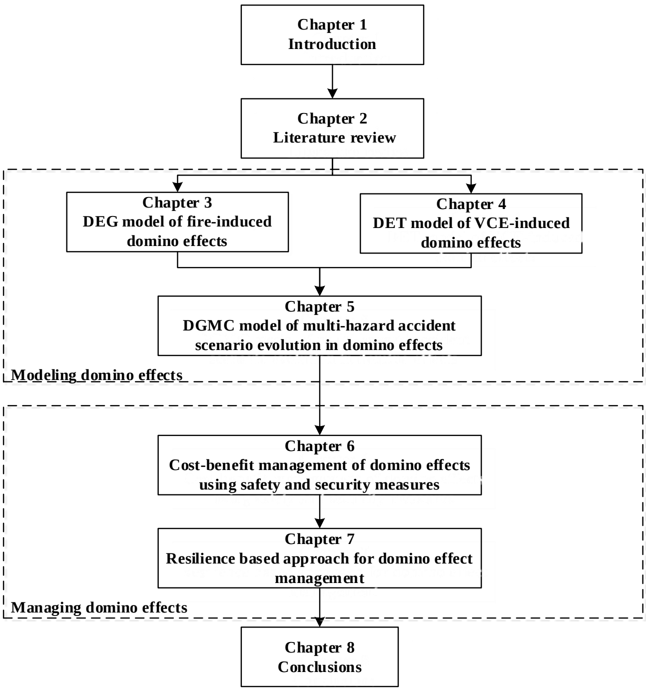

Figure 1.1 Outline of the dissertation

Chapter 5 develops a dynamic approach, “Dynamic Graph Monte Carlo” (DGMC), for modeling multi-hazard accident scenarios in domino effects. In this chapter, a chemical plant is modeled as a multi-agent system (installations, humans, and ignition sources), and the vulnerability of humans exposed to toxic gas, fire, and VCE are considered. (Contribution 4)

Chapter 6 provides a cost-benefit management approach for the investment and allocation of safety and security resources. An optimization algorithm called “PROTOPT” based on the “maximin” strategy is developed to achieve the most profitable protection strategy for preventing and mitigating domino effects. (Contribution 5)

Chapter 7 introduces the resilience concept in domino effect management. A stochastic dynamic method is developed to quantify the resistant capability, the mitigation capability, the adaption capability, and the restoration capability of chemical plants, supporting the allocation of safety barriers, security barriers, adaption measures, and restoration measures. Once a domino effect is inevitable, a resilient chemical plant may rapidly restore from the escalation disaster and reduce the losses. (Contribution 6)

Chapter 8 concludes the dissertation and discusses future research on modeling and managing domino effects in the process industry.

Chapter 2 Domino effects in the process industry: The state-of-the-art

Domino effects have received increasing attention in recent decades and various approaches have been developed to model and manage domino effects in the process industry. This chapter provides a thorough study on current & future research trends in the development of modeling methods and protection strategies for prevention and mitigation of large-scale escalating events or so-called domino effects in the process and chemical industries. First, we provide an overview of what constitutes domino effects based on the definition and features, characterizing domino effect studies according to different research issues and approaches. The modeling approaches are grouped into three types while the protection strategies are divided into five categories, followed by detailed descriptions of representative modeling approaches and management strategies in chemical plants and clusters. The current research trends in this field are obtained based on the analysis of research work on domino effects caused by accidental events, natural events, and intentional attacks over the past 30 years. A comparison analysis is conducted for the current modeling approaches and management strategies to pose their applications. Finally, this chapter offers future research directions and identifies critical challenges in the field, aiming at improving the safety and security of chemical industrial areas to prevent and mitigate domino effects.

The content of this chapter is based on the following published paper:
Chen, C., Reniers, G., Khakzad, N., 2020c. A thorough classification and discussion of approaches for modeling and managing domino effects in the process industries. Safety Science 125. 10.1016/j.ssci.2020.104618

2.1 Introduction

The chemical industry is central to the global economy and has a prominent role in creating and maintaining modern-day life. There is a long tradition of forming clusters in the chemical industry due to various reasons, such as benefits of scale, exchange of material streams, and optimization of energy streams. Reniers et al. (2014) defined a chemical industrial cluster as a geographically limited concentration of chemicals-using companies and service providers operating in the chemical industrial sector. Chemical industrial clusters can be found around the world, consisting of tens of different chemical plants and chemical logistic service providers situated in each other's vicinity.

Despite the many advantages of sharing benefits, the fact of increased overall risk cannot be neglected in chemical industrial clusters. Chemical industrial areas consist of hundreds and sometimes thousands of installations situated next to each other, where large quantities of hazardous (e.g., flammable, explosive, toxic) substances are stored, transported, or processed. These installations are mutually linked in terms of the hazard level they pose to each other in the system. As a result, a primary undesired scenario may propagate to nearby installations, triggering a chain of accidents, resulting in overall consequences more severe than those of the primary event, a phenomenon which is well known as knock-on effects or domino effects (Reniers and Cozzani, 2013).

Domino effects may be regarded as very low-frequency, very high-consequence events (Khakzad, 2015; Necci et al., 2015). Nonetheless, the risk of domino effects in the chemical and process industries should not be neglected, due to the severe consequences. Most recently, on March 21, 2019, a series of explosions and fires at Jiangsu Tianjiayi Chemical Company, China, almost fully destroyed the chemical plant, resulting in at least 78 deaths, 617 injuries, and huge property loss (UPI, 2019). On March 17, 2019, a fire-induced domino accident at Intercontinental Terminals Company in Deer Park, in Texas, the USA, led to the damage of 7 storage tanks, causing serious pollution of Tucker Bayou (CNN, 2019). The most well-known domino accident occurred in November 1984 in an LPG plant in Mexico City, resulting in 650 deaths and 6500 injuries (Pietersen, 1988; Chen et al., 2020a).

Since domino effects can induce catastrophic consequences, the second Seveso Directive (Directive 96/82/EC, also known as “Seveso-II” Directive) concerned with the prevention and mitigation of major accidents therefore required to assess “domino” accident hazards inside and outside the industrial areas (Council Directive96/82/EC, 1997; Papadakis and Amendola, 1997). The Seveso Directive concerning domino effects was further reinforced (Seveso III Directive) by forcing the owners of different chemical facilities to exchange information more intensively (Directive, 2012). Moreover, safety barriers and multiple safety layers are recommended by several technical standards aiming at reducing the risk of domino accidents (CCPS, 2011).

The first well-documented domino accident in the chemical and process industry can be traced back to 1947 in Texas City, but limited work related to domino effects were mostly dedicated to analyzing the failure behavior of pressured vessels exposed to fire engulfment, jet fire, and heat radiation before the 1990s (Anderson et al., 1974; Moodie, 1988). Since then, growing public attention has been drawn to the scientific and technical literature on the modeling and risk assessment of domino effects (Bagster and Pitblado, 1991; Khan et al., 1998; Khan and Abbasi, 1999). Early researches mainly focused on modeling and management of domino effects triggered by accidental events (Cozzani and Zanelli, 2001; Cozzani et al., 2005; Reniers et al., 2005a; Reniers and Dullaert, 2007). Scholars started to be concerned about domino effects caused by intentional attacks (security-related domino effects) since Reniers et al. (2008) proposed to prevent and deal with potential security-related domino effects in chemical clusters. Moreover, domino effects caused by natural hazards have received increasing attention in recent years (Fabbrocino et al., 2005; Cozzani et al., 2014; Necci et al., 2014; Khakzad et al., 2018b; Reniers et al., 2018a).

Several scholars reviewed domino effect related research including past accident investigations (Shaluf et al., 2003; Clini et al., 2010; Darbra et al., 2010; Abdolhamidzadeh et al., 2011; Hemmatian et al., 2014), review on assessment of domino effects, review on escalation thresholds (Alileche et al., 2015), bibliometric analysis (Li et al., 2017) as well as historical analysis (Swuste et al., 2019). However, there is still a need to obtain insight into which modeling approaches and protection strategies on domino effects have been used and how these models and methods have evolved, identifying what have been the main areas of concern and which issues need more attention in the future. This study therefore systematically reviews past progress in modeling and management of domino effects, highlights research approaches and evolution of research trends, and outlines possible future research needs from the perspective of previous domino accidents.

The outline of this chapter is as follows. Section 2.2 presents the method used in this study for the literature review; Section 2.3 elaborates the features and classifications of domino effects. In Section 2.4, various models and assessment methods on domino effects are illustrated and reviewed; Section 2.5 reviews past protection strategies and methods used in the management of domino effects. In Section 2.6 a discussion about these modeling approaches and protection strategies as well as possible future research paths are performed. Conclusions drawn from this work are presented in Section 2.7.

2.2 Method

To conduct the review of the current research issues and approaches on modeling and management of domino effects in the process and chemical industries, a four-step method based on systematic review and meta-synthesis techniques (Evans, 2002; Jones, 2004) was developed, as shown in Figure 2.1.

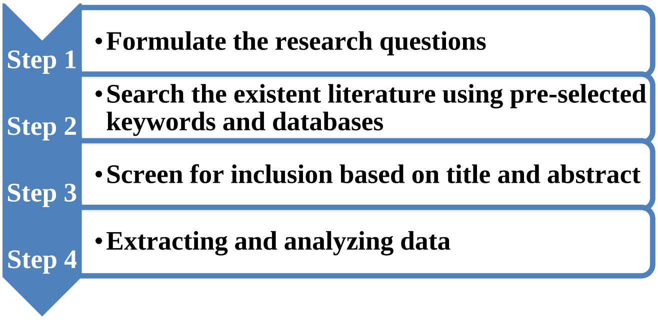

Figure 2.1 Procedures of literature investigation
(Chen et al., 2020c)

According to the procedures, we first propose the research questions given the research objective illustrated in Section 2.1, as follows: (1) What are the current criteria used to classify domino effects? (2) Which are the current approaches used for modeling and risk assessment of domino effects? (3) Which are the current protection strategies used for the management of domino effects? (4) What are the present research gaps between present research and past domino effect events?

Next, extensive literature is searched and collected using online resources from the library of Delft University of Technology. Two academic databases were selected: (i) Web of Science, (ii) ScienceDirect. Keywords used to collect relevant researches includes “domino effect”, “knock-on event”, “catastrophic effect”, “chain of accidents”, “escalating event”, “process industry” “chemical industry”, “chemical plant”, “chemical industrial cluster”, “chemical industrial park”, “oil”, “gas”, “petroleum”, “LNG” and “LPG”. The literature searching was finished on April 29th, 2019. Based on the 284 records extracted from the databases, all the titles and abstracts were examined thoroughly to further screen out references that are not closely related to the topic. As a result, 132 articles are obtained from 32 journals including Journal of Loss Prevention in the Process Industries, Journal of Hazardous Materials, Process Safety and Environmental Protection, Reliability Engineering & System Safety, and Safety Science. 57 of the papers published in the past five years (from 2015-2019) indicate that domino effects have gained increasing attention in the scientific literature. The authors include most frequently Valerio Cozzani, Genserik Reniers, Nima Khakzad, Gabriele Landucci, and Faisal Khan. Finally, we summarize, aggregate, organize, and compare the evidence extracted from the included studies. The analysis results are presented in Sections 2.3-2.5.

2.3 An overview of domino effects and the relevant researches

2.3.1 Classification of domino effects

There are several definitions of “domino effect” provided in the literature(Alileche et al., 2015; Necci et al., 2015). This study utilizes the widely accepted definition provided by Reniers and Cozzani (2013): a phenomenon in which a primary undesired event propagates within equipment (‘temporally’), or/and to nearby equipment (‘spatially’), sequentially or simultaneously, triggering one or more secondary unwanted events, in turn possibly triggering (higher-order) undesired events, resulting in overall consequences more severe than those of the primary event. According to the definition, a domino event can be characterized by the following elements: (i) a “primary event,” initiating the domino effect, (ii) escalation vectors responsible for possible accident propagation, (iii) one or more secondary accident events, (iv) the overall consequences far more severe than those of the primary event.

Primary events can be divided into three categories: fires, explosions, and the release of toxic materials. Toxic releases are always ignored since they do not directly lead to damage to secondary installations (Salzano and Cozzani, 2003). These primary events may be induced by accidental events (e.g., mechanical failure, human error, aging), natural disasters (e.g., earthquakes, floods, and hurricanes), and intentional events (e.g. terrorist attacks, sabotage, criminal actions). The primary events triggered by natural disasters in industrial plants are generally called “Natechs”. Accidental primary events and Natechs belong to the safety domain while intentional events involve security issues.

Abdolhamidzadeh et al. (2011) analyzed 224 accidents that occurred from 1910 to 2008 in the process industries, indicating that 43% of the recorded domino accidents were triggered by fires and 53% were triggered by explosions. Among the domino events initiated by fires, pool fire (80%) was the most frequent scenario found to trigger knock-on events. Among explosions, VCE (vapor cloud explosion) has been the most frequent cause. The historical analysis also shows that long-lasting stationary fires (i.e., pool fires and jet fires) are responsible for most of the escalation events in industrial accidents (Gomez-Mares et al., 2008). The analysis further showed that 44% of jet fire accidents had occurred in transportation, 36% in process plants, 11% during loading/unloading operations, and 9% in storage plants. The escalation vectors (physical effects) in terms of different primary events that are responsible of possible propagation are identified from historical domino accidents (Bagster and Pitblado, 1991; Khan and Abbasi, 1998a; Cozzani et al., 2006a), as shown in Table 2.1.

Table 2.1 Possible escalation vectors of different primary scenarios (Cozzani et al., 2006b)

Primary scenario	Escalation vector
Pool fire	Radiation, fire impingement
Jet fire	Radiation, fire impingement
Fireball	Radiation, fire impingement
Flash fire	fire impingement
BLEVE	Overpressure, fragment projection
Confined explosion	Overpressure, fragment projection
Mechanical explosion	Overpressure, fragment projection
VCE	Overpressure

BLEVE: Boing Liquid Expanding Vapor Explosion; VCE: Vapor Cloud Explosion

In case of propagation, domino events characterized by cardinality 0 are the initiating events or the “primary domino events”, whereas cardinality 1 refers to secondary domino events, cardinality 2 to tertiary domino events, etc. (Reniers and Cozzani, 2013). Propagation of a primary scenario to a secondary scenario may be called first-level propagation, while from a secondary scenario to a tertiary order of scenario may be called the second level propagation.

Darbra et al. (2010) studied 225 accidents involving domino effects that occurred in process/storage plants and during the transportation of hazardous materials from 1961-2007. Among these accidents, 5.8% were triggered by natural disasters (10 lightning, 1 earthquake, 1 extreme temperature, and 1 flooding), and 1 event was triggered by an intentional attack. Three domino accidents caused by Natechs were also listed in Abdolhamidzadeh et al. (2011). More recently, a survey (Hemmatian et al., 2014) shows that 6.4% of domino accidents are triggered by natural events while 0.6% of them are caused by sabotages.

In the process and chemical industry, natural disasters may induce major accidents, resulting in the damage of installations and the loss of containment (LOC) of hazardous substances, which are known as Natechs (Campedel et al., 2008; Antonioni et al., 2009a; Krausmann et al., 2011a; Krausmann et al., 2011b; Landucci et al., 2012b; Reniers et al., 2018a; Misuri et al., 2020). As a result, Natechs can be regarded as a special domino effect triggered by natural events: lightning (Necci et al., 2013; Necci et al., 2014; Necci et al., 2016), earthquakes (Fabbrocino et al., 2005; Antonioni et al., 2007; Campedel et al., 2008), floods (Cozzani et al., 2010; Landucci et al., 2012b; Landucci et al., 2014; Khakzad and Van Gelder, 2018; Yang et al., 2019), hurricanes (Misuri et al., 2019; Qin et al., 2020), wildfire (Scarponi et al., 2018). In this study, Natech domino effects are narrowly tailored as Natech events in which the damaged equipment furtherly causes escalation and results in major accident scenarios at other hazardous installations (Alessandri et al., 2018; Khakzad, 2018b; Khakzad et al., 2018b; Yang et al., 2018; Khakzad, 2019). Similarly, these escalation events originated from intentional attacks are called intentional domino effects.

Although the frequencies of domino effects caused by intentional attacks or natural disasters are less than those triggered by accidental events, the overall consequences may be more severe due to simultaneous damage of installations induced by multiple-target attacks or natural disasters (Antonioni et al., 2007; Chen et al., 2019b; Khakzad and Reniers, 2019). Moreover, safety barriers may be damaged and emergency response actions may be unavailable when a natural disaster occurs, leading to the evolution of the scenarios and the propagation of accidents rapidly. For example, the efficiency of emergency rescue might be largely reduced due to the damages of transportation systems, water supply infrastructures, power supply systems, communication, and medical facilities during a natural disaster. Compared with accidental domino effects and Natech domino effects, the tackling of intentional domino effects has to consider intelligent and strategic adversaries besides the uncertainty (or randomness) and complexity in the evolution of domino effects. Adversaries wanting to deliberately induce domino effects may adapt to changing circumstances caused by protection measures. Thus both safety and security are important for the prevention or mitigation of domino effects. More details on the differences among accidental domino effects, Natech domino effects, and intentional domino effects are described in Table 2.2.

Table 2.2 list of the characteristics of three categories of domino effects

Types	Accidental domino effects	Natech domino effects	Intentional domino effects
Natures of primary events	Unintentional	Unintentional	Intentional
Positions of primary events	Usually occurring at installations	Any positions within chemical plants or outside the area nearby	The most critical positions within chemical plants or outside the area nearby
Sources of hazards	Hazardous materials in chemical installations and hazardous materials form loading and unloading vehicles	Hazardous materials in chemical installations, and natural hazards, such as earthquakes, floods, and hurricanes	Hazardous materials in chemical installations, and external hazardous materials or weapons carried by attackers such as explosive devices
Main escalation vectors	Heat radiation, fire impingement, overpressure, and fragments	Heat radiation, fire impingement, overpressure, and fragments	Heat radiation, fire impingement, overpressure, and fragments
Simultaneous primary scenarios	Usually involving a single installation	Multiple installations are usually involved in large nature disasters	Multiple installations are usually attacked due to multiple target attacks
Protection measures	Safety barriers	safety barriers with a high probability of unavailability	Security measures and safety barriers

In light of these features, we classify domino effects into several categories according to different criteria, following the research by Reniers (2010), as shown in Table 2.3.

Table 2.3 Categories of domino events (excluding toxic domino effects)

Type	categories	Definition
1	Accidental	The domino effect caused by accidental events
	Natech	The domino effect caused by natural hazards

	Intentional	The domino effect caused by intentional attacks
2	Fire-induced	The primary event is a fire
	Explosion-induced	The primary event is an explosion
3	Internal	The start and end of the escalation vector characterizing the domino event are situated inside the boundaries of the same chemical plant
	External	The start and end of the escalation vector characterizing the domino event are not situated inside the boundaries of the same chemical plant
4	Direct	The domino event happens as a direct consequence of the previous domino event
	indirect	The domino event happens as an indirect consequence of a preceding domino event, not being the previous one
5	Temporal	The domino event happens within the same area as the preceding event, but with a delay
	Spatial	The domino event happens outside the area where the preceding event took place
6	Serial	The domino event happens as a consequent link of the only accident chain caused by the preceding event
	Parallel	The domino event happens as one of several simultaneous consequent links of accident chains caused by the preceding event
7	Heat radiation-induced	The escalation of the domino effect is caused by heat radiation
	Overpressure-induced	The escalation of the domino effect is caused by overpressure
	Fragment-induced	The escalation of the domino effect is caused by fragments
	Coupled	Multiple kinds of escalation vectors are present during the evolution of the domino effect

2.3.2 Characterization of current publications

To obtain a better insight into the current research on modeling and management of domino effects, a preliminary characterization for these papers is performed. Research topic, research issues, and research approaches are used to characterize a research paper. The research topics that we found, were ‘modeling domino effects’ and ‘management of domino effects’. Two research issues and six approaches related to the former research topic are identified while the latter topic involves five research issues and 13 approaches, as shown in Figure 2.2.

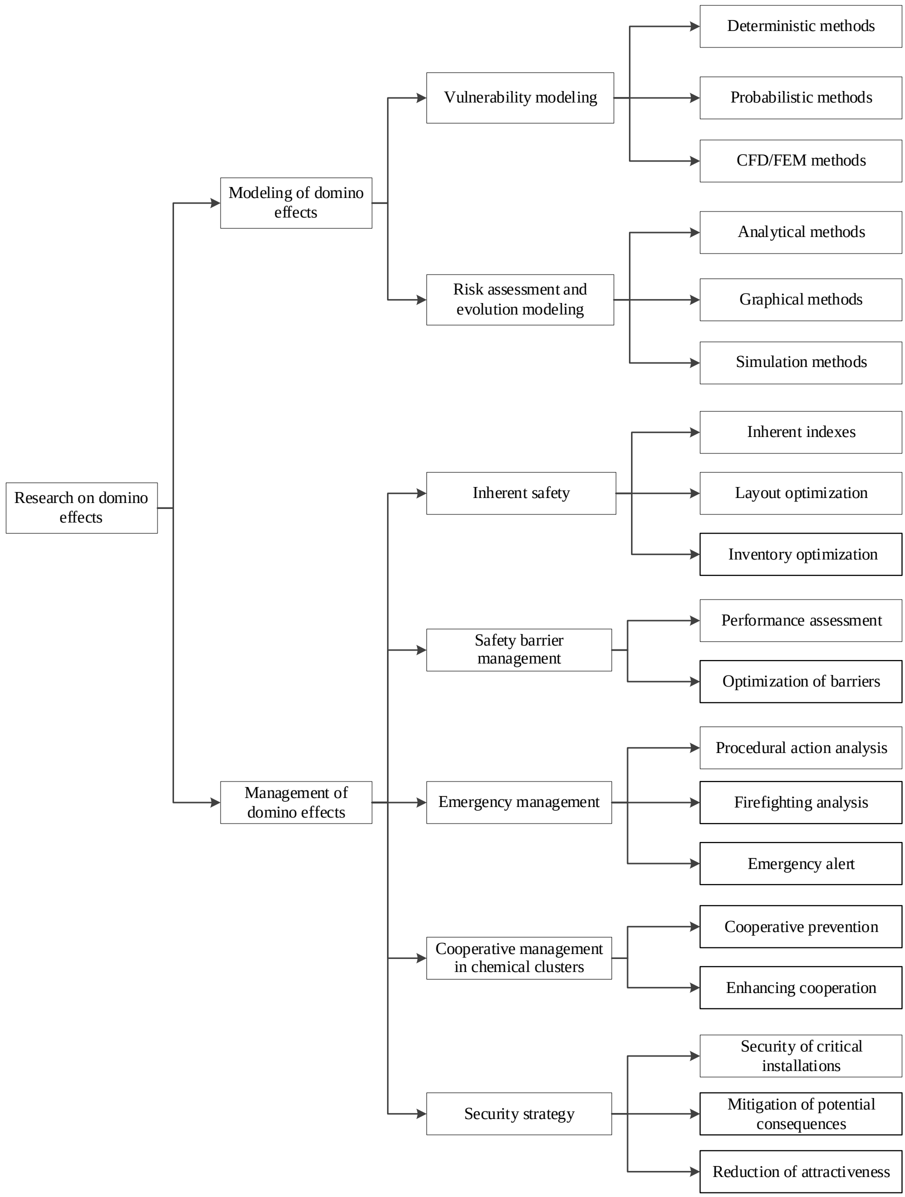

Figure 2.2 Characterization of current domino effect research (Chen et al., 2020c)

Each paper can be characterized according to the research topic, issue, approach, and other keywords, as shown in the Appendix (Table A.1). All the selected literature on modeling and management of domino effects will be discussed thereby.

2.4 Risk assessment and modeling of domino effects

2.4.1 Vulnerability of installations

A primary accident scenario usually propagates when the generated escalation vector results in the failure of other installations. The study of domino scenarios, therefore, requires analyzing the capability of a unit or process plant to foster either the onset or the escalation of potential cascading effects, which is defined as “vulnerability” (Khakzad and Reniers, 2015b).

(1) Deterministic methods

The earliest vulnerability analysis approach for the assessment of damage to installations uses escalation thresholds based on experiments or accident data (Anderson et al., 1974; Moodie, 1988). Threshold values provide the minimum intensity of physical effects able to cause an escalation, which may be effectively used to develop “rules of thumb” or as a screening tool for the preliminary assessment of possible escalation scenarios (Reniers and Cozzani, 2013). As a result, the minimum distance between two hazardous installations required to avoid an escalation event may be called “safety distance” or “effect distance” (Reniers and Dullaert, 2007; Necci et al., 2015). Table 2.4 lists escalation thresholds and safety distances of escalation vectors for different equipment recommended by Cozzani et al. (2006b).

Table 2.4 Escalation thresholds and safety distances
(Cozzani et al., 2006b; Alileche et al., 2015)

Scenario	**Escalation vector**	**Modality**	**Target category**	**Escalation threshold**	**Safety distance**
Flash fire	Heat radiation	Fire impingement	Floating roof tanks	Flame envelope	Max. flame distance
–			All other units	Escalation unlikely	-
Fireball	Heat radiation	Flame engulfment	Atmospheric	Q > 100 kW/m^2	Maximum flame distance
			Pressurized	Escalation unlikely	-
		Distant radiation	Atmospheric	Q > 100 kW/m^2	Maximum flame distance
			Pressurized	Escalation unlikely	-
Jet fire	Heat radiation	Fire impingement	All	Flame envelope	-
		Stationary radiation	Atmospheric	Q > 15 kW/m^2	50 m from flame envelope
			Pressurized	Q > 45kW/m^2	25 m from flame envelope
Pool fire	Heat radiation	Flame engulfment	All	Flame envelope	–
		Stationary radiation	Atmospheric	Q > 15 kW/m^2	50 m from flame envelope

			Pressurized	$Q > 45$ kW/m^2	25 m from flame envelope
VCE	Overpressure	Blast wave interaction	Atmospheric	$P_o > 22$ kPa	$r_s = 1.75$ (ME); 1.50(BS)
			Pressurized	$P_o > 20$ kPa	$r_s = 2.10$ (ME); 1.80 (BS)
			Elongated (toxic)	$P_o > 20$ kPa	$r_s = 2.10$ (ME); 1.80(BS)
			Elongated (flammable)	$P_o > 31$ kPa	$r_s = 1.35$ (ME); 0.85 (BS)
	Heat radiation	Fire impingement	Floating roof tanks	Flame envelope	Max. flame distance
			All other units	Escalation unlikely	-
Confined explosion	Overpressure	Blast wave interaction	Atmospheric	$P_o > 22$ kPa	20 m from vent
			Pressurized	$P_o > 20$ kPa	20 m from vent
			Elongated (toxic)	$P_o > 20$kPa	20 m from vent
			Elongated (flammable)	$P_o > 31$ kPa	20 m from vent
Mechanical explosion	Overpressure	Blast wave interaction	Atmospheric	$P_o > 22$ kPa	$r_s = 1.80$
			Pressurized	$P_o > 20$ kPa	$r_s = 2.00$
			Elongated (toxic)	$P_o > 20$ kPa	$r_s = 2.00$
			Elongated (flammable)	$P_o > 31$ kPa	$r_s = 1.20$
	Missile projection		All	Fragment impact	300 m (prob. < 0.05)
BLEVE	Overpressure	Blast wave interaction	Atmospheric	$P_o > 22$ kPa	$r_s = 1.80$
			Pressurized	$P_o > 20$ kPa	$r_s = 2.00$
			Elongated (toxic)	$P_o > 20$ kPa	$r_s = 2.00$
			Elongated (flammable)	$P_o > 31$ kPa	$r_s = 1.20$
	Missile projection		All	Fragment impact	300 m (prob.<0.05)
Point-source explosion		Blast wave interaction	Atmospheric	$P_o > 22$ kPa	-
			Pressurized	$P_o > 20$ kPa	-
			Elongated (toxic)	$P_o > 20$ kPa	-
			Elongated (flammable)	$P_o > 31$ kPa	-

Q: heat radiation intensity; P_o: static peak overpressure; r_s: energy scaled distance; ME: Multi Energy method; BS: Baker-Sthrelow method.

According to these threshold values, a safety distance may be obtained according to physical effect analysis (Van Den Bosh and Weterings, 1997; Uijt de Haag and Ale, 1999; Cozzani et al., 2006b). However, the vulnerability of installations not only depends on the complexity of escalation vectors but also on the features of target installations. In other words, a wide uncertainty exists in threshold values for domino escalation since a threshold value may be derived only from a special condition. As a result, different and apparently contradictory threshold values for equipment damage caused by overpressure or radiation are present in the literature and technical specifications (HSE, 1978; Bagster and Pitblado, 1991; Khan and Abbasi, 1998a; Uijt de Haag and Ale, 1999). As a result, the safety distance identified by comparing the result of consequence analysis of primary scenarios with the threshold values may not be conservative. Although the uncertainty of safety distances derived from thresholds and primary scenarios is inevitable, it is also adopted in inherent safety design (Tugnoli et al., 2008a; Cozzani et al., 2009) and technical specifications (Van Den Bosh and Weterings, 1997; Atkins, 1998) due to the simplicity and transparency of the approach. Consequently, the thresholds and safety distances recommended in different regulations and technical specifications are different from each other. For example, the recommended threshold values and safety distances span over an order of magnitude among different countries in the EU due to the lack of a harmonized approach to the assessment of major accident hazards in the European countries (Alileche et al., 2015).

(2) Probabilistic methods

To address the uncertainty of domino escalation and support for quantitative risk assessment (QRA) of domino effects, probability models are used to assess the vulnerability of installations.

1) Overpressure

Bagster and Pitblado (1991) proposed a probabilistic approach defining a damage probability function based on the distance from the center of the primary scenario and the safety distance. Khan and Abbasi (1998a) adopted a probit function approach to model the damage probability caused by overpressure, considering peak overpressure (static pressure) and dynamic pressure. The probit function was first developed by Eisenberg et al. (1975) and only peak overpressure was considered in the literature, as shown in Eq. (2.1).

$$Y = a + b\ln(P_o) \tag{2.1}$$

Where P_o is the static peak overpressure (kPa); Y is the probit value; a and b are constants. Then the damage probability P_d can be obtained using the cumulative standard normal distribution (Φ), as shown in Eq. (2.2).

$$P_d = \Phi(Y - 5) \tag{2.2}$$

Probit analysis is a well-known method to evaluate the dose-effect relationship for human responses to toxic substances, thermal radiation, and overpressure (Safety, 2000; Lees, 2012). In Eq. (2.1), the “dose” is the peak overpressure, and the “response” is the probit value representing the damage likelihood caused by overpressure on installations. Cozzani and Salzano (2004b) developed probit models for each category of equipment (atmospheric, pressurized, elongated, and small) rather than using a general model for all equipment. The equipment-specific models significantly reduced errors caused by the general probit model, presenting an important difference between the damage probabilities and the damage threshold of different categories of equipment. This work was improved by distinguishing the extent of damage and assigning a linear relationship between the probit value and the observed thresholds for each category of damage (Zhang and Jiang, 2008). Recently, Mukhim et al. (2017) furtherly improved the work of Zhang and Jiang (2008) by classifying the equipment into 11 categories and developing a probit model for each category of equipment. These vulnerability models for overpressure can also be applied to vulnerability assessment for installations subject to home-made explosives (Salzano et al., 2014; Landucci et al., 2015b). The probit models were coupled to simplified calculation models for peak overpressure to develop a straightforward approach for estimating safety distances caused by blast waves and damage probability as a function of the scaled distance. Besides, Salzano and Cozzani (2006) studied the intensity of the loss of containment following overpressure wave interaction with process equipment using a fuzzy set analysis based on accident data, supporting for assessment of second-level escalation.

2) Heat radiation

Compared to the damage caused by overpressure, the damage mechanism of heat radiation (or fire impingement) may be more complex since the damage caused by radiation is a gradual process, i.e., installations exposed to heat radiation do not fail immediately. As time goes by, the exposed installation’s vulnerability increases due to temperature/pressure build-up, and may be deemed as a failure when the loss of containment emerges. The time-lapse between the start of the fire and the failure of the target equipment is named “time to failure” (TTF) (Moodie, 1988). Therefore, emergency response has a huge impact on the vulnerability of installations besides heat radiation intensity (threshold). In this context, Landucci et al. (2009a) developed a probit model for estimating the damage probability of storage tanks exposed to fire based on the *TTF* obtained via empirical formulas and under the following assumptions (ii) 10% probability of failure for *TTF*= 5 min, which is equal to the minimum time required to start on-site emergency response operations; (iii) 90% probability of failure for *TTF* = 20 min, which is equal to the minimum time required to start the mitigation actions. The probit model is derived for assessing first-level domino effects, neglecting the time-lapse in higher-level escalations. The two assumptions may be adjusted according to the characteristics of the emergency response of a special industrial area to obtain more accurate results. Chen et al. (2018) extended this work to overcome the limitation of the “probit model” approach in higher-level propagations, addressing the uncertainty of emergency response using a probability distribution function.

3) Fragments

Several accidental primary scenarios can lead to fragments or missile hazards, such as boiling liquid expanding vapor explosions (BLEVE), physical explosions, confined explosions and runaway reactions, etc. Past accident data indicates that

BLEVE events account for most industrial accidents involving fragment projection and usually cause very severe consequences (Gubinelli and Cozzani, 2009b; Tugnoli et al., 2014a). Gubinelli et al. (2004) proposed a probabilistic model according to the event sequence to assess the damage probability induced by fragments, as follows:

$$f_{d,F} = f_p \times P_{gen,F} \times P_{imp,F} \times P_{dam,F} \tag{2.3}$$

Where $f_{d,F}$ denotes the damage probability induced by a fragment F; f_p represents the probability of primary event; $P_{gen,F}$ represents the probability of the fragment to be generated in the primary event; $P_{imp,F}$ denotes the probability of impact between the fragment and a target installation; $P_{dam,F}$ represents the probability of target damage given the impact with the fragment. As a result, the total damage probability was represented as the sum of the probability caused by each fragment (Gubinelli et al., 2004). This model characterized the impact of the likelihood of sequential events (were regarded as independent events) on the damage of an installation caused by fragments while ignoring low probability events that simultaneous damages are caused by multiple fragments on one installation. Projected fragments are capable of generating secondary accidents at relevant distances from the primary scenario due to possible large projection distances. The hazards associated with projected fragments are related to the number of fragments and mass and velocity. To assess the vulnerability of installations subject to fragments, the following steps are usually adopted: (i) calculate explosion energy, (ii) predict the number of fragments, (iii) calculate initial velocity, (iv) calculate the angle of departure, and (v) calculate trajectory (Hauptmanns, 2001a, b; Lisi et al., 2014; Lisi et al., 2015). It is rather difficult to accurately predict the initial velocity and the departure angle and thus thresholds for fragments are rare due to high uncertainties. Therefore, Monte Carlo simulation and probability density functions are always used to model the uncertainties in the assessment of fragment projection (Hauptmanns, 2001a; Lisi et al., 2014; Tugnoli et al., 2014a; Lisi et al., 2015). Zhang and Chen (2009) derived a formula for the initial projection velocity of fragments by taking the explosion moment as a polytropic process and solving the energy transformation equation.

(3) CFD/FEM methods

In recent years, advanced numerical methods such as Computational Fluid Dynamics (CFD) and the Finite Element Method (FEM) have obtained increasing attention due to their strengths in physical effect simulation. These advanced methods are considered to be a promising tool to support the assessment of complex accidental scenarios, such as three-dimensional pool fires and jet fires (Rum et al., 2018). Landucci et al. (2009a) modeled the failure of storage tanks exposed to fire using a commercial FEM code. The FEM model can simulate the thermal and mechanical parameters of vessel shells under heat radiation, such as heat radiation, wall temperature, and stress. A storage vessel is assumed to fail when the equivalent intensity of combined stress becomes greater than the maximum allowable stress. This work was extended to model the performance of different materials proposed for the passive fire protection of tanks (Landucci et al., 2009c). Jujuly et al. (2015) developed a three-dimensional computational fluid dynamics (CFD) simulation of a liquefied natural gas (LNG) pool fire using ANSYS CFX. In this study, shell temperature and heat radiation thresholds were used to determine the failure of storage vessels. The results show that wind speed has a significant contribution to the behavior of a pool fire and its possible accompanying domino effects. Besides, ANSYS FLUENT were also used to model the heat transfer and pressure build-up in LPG vessels exposed to fires (Landucci et al., 2016b; Rum et al., 2018). FLACS software developed by Gexcon AS was also be used to model flammable cloud dispersion and VCE explosion, supporting domino effect assessment (Dasgotra et al., 2018). These studies indicate that using advanced simulation tools can obtain a more precise assessment of failure conditions of vessels engulfed in fires, thus supporting the development of vulnerability models for process equipment exposed to fire. More recently, the Fire Dynamics Simulator (FDS) is adopted to simulate tank and dike pool fires in a tank farm (Ahmadi et al., 2019). CFD simulation may obtain more accurate results of physical effects and thus facilitate vulnerability assessment of installations exposed to escalation vectors, but it is very complex, time-consuming and very expensive (Assael and Kakosimos, 2010).

2.4.2 Risk assessment and evolution modeling

These available vulnerability assessment methods reviewed in the previous section can provide reliable models to estimate the possibility and probability of the escalation of primary events, which is a critical step in the risk assessment of domino effects. This section presents current methods on risk assessment and evolution modeling of domino effects, including likelihood assessment of domino effects, risk assessment of domino effects and evolution assessment of domino effects. The available methods are divided into three categories: analytical methods, graphical methods and simulation methods.

(1) Analytical methods

Although quantitative risk assessment (QRA) is most commonly used in the process industries to quantify the risks of ‘major accidents’, the QRA for domino effects is still very challenging due to the complexities and uncertainties associated with escalating accidents (Bagster and Pitblado, 1991; Uijt de Haag and Ale, 1999; Cozzani and Salzano, 2004b). To assess the likelihood of domino effects, Bagster and Pitblado (1991) developed a program based on a distance-based approach, addressing higher-order propagations, multiple escalation vectors and the damage directions of escalation vectors. The physical mechanisms of different escalation vectors were not fully considered since a squared decay function (convex function) was used for all escalation vectors.

Khan and Abbasi (1996) introduced a software package called MAXCRED based on maximum credible accident analysis to assess the potential consequences of a chemical plant or industrial complex to the surroundings and the environment. Probit models were used to assess the damage potential of different accident scenarios and the results indicate that a confined vapor cloud explosion followed by a pool fire would be the worst accident scenario and has the maximum potential of triggering non-intentional domino effects. Besides, an analytical approach is developed to model different domino effect scenarios in the chemical process industries, including fire, explosion, toxic release, simultaneous and interactive impacts of fire and explosion (Khan and Abbasi, 1998a). This work was coded to a user-friendly software (DOMIFFECT) for domino effect analysis (Khan and Abbasi, 1998b). The software was used for estimating possible hazards from loss of containment to explosions; handling of interaction among different domino accident scenarios; assessing the likelihood of different domino effect scenarios and estimating the potential consequences (Khan and Abbasi, 2000; Khan and Abbasi, 2001). Furtherly, the DOMIFFECT software was incorporated into a risk analysis methodology called Optimal Risk Analysis (ORA) as a consequence analysis module (Khan et al., 2001c).

Cozzani and Salzano (2004b) established a quantitative assessment methodology for overpressure based on equipment-specific probit models. Two case studies derived from an actual case of an oil refinery demonstrated that individual risk increases up to an order of magnitude when considering domino effects. Following this work, a systematic procedure for the quantitative assessment of the risk caused by domino effects was developed (Cozzani et al., 2005). This methodology can account for the main escalation vectors since probit models for fire and overpressure, and a probabilistic model for fragments are involved in this QRA framework. The overall consequences of domino effects to individual risk, societal risk, and the potential life loss index were obtained considering all the credible combinations of secondary events that may be triggered by each primary scenario. The QRA framework was implemented in a GIS-based software tool, Aripar-GIS (Cozzani et al., 2006a; Antonioni et al., 2009b). Application of the software in actual plant lay-outs can automatically identify possible escalation targets as well as directly calculate the individual and societal risk indexes caused by possible domino scenarios. Combining vulnerability assessment methods for installations subject to Natech events, the methodology may be extended to analyze domino effects caused by Natech events (Cozzani et al., 2014; Antonioni et al., 2015).

TNO developed a QRA tool for the external safety of industrial plants w.r.t. a dust explosion hazard, addressing first-order domino effects using safety distances (van der Voort et al., 2007). Zhang and Chen (2013) proposed a QRA methodology based on failure mechanism analysis to quantify domino effect risk and used a visualized risk cloud figure to show the risk of different zones. Kadri et al. (2013) introduced a concept of domino systems and presents a QRA methodology for domino effects caused by fire and explosion on storage areas. Zhou and Reniers (2018a) applied matrix operations in a quantitative risk assessment to take into consideration synergistic effects in fire-induced domino effects. Besides, a multi-plant QRA method was carried out to support decision-making on the acceptability of constructing a new chemical plant adjacent to an existing one (Baesi et al., 2013). Besides, several commercial QRA or consequence software can also facilitate domino effect assessment, such as FLACS developed by Gexcon AS, Shepherd and FRED developed by Shell as well as EFFECTS and RISKCURVES developed by TNO (Gexcon, 2018b).

In recent years, domino effects in parallel pipelines obtained increasing attention in the scientific literature (Ramirez-Camacho et al., 2015; Silva et al., 2016; Ramírez-Camacho et al., 2019). Different from domino effects in industrial areas, management of domino effects in oil and gas pipelines may be more difficult since they are frequently installed underground and over long distances. Ramirez-Camacho et al. (2015) established a mathematical model to estimate the likelihood of domino effects in parallel pipes. The likelihood was denoted as a function of the location of the hole, the jet direction and solid angle, the diameter of both pipelines, and the distance between them. In terms of underground parallel pipelines, Silva et al. (2016) developed an analytical model based on historical accident data and pipeline crater models. The study shows that a separation distance of 10 m would be sufficient to prevent accident escalation between parallel pipelines.

(2) Graphical methods

Chemical industrial areas consist of various hazardous installations with different domino effect potentials. Some installations exhibit a high probability of initiating domino accidents while other installations are more likely to propagate domino events. These installations can be regarded as nodes, and the quantitative possibility of accident propagation may be represented by the weight of the links between nodes in a network or graph (Reniers and Dullaert, 2007; Khakzad and Reniers, 2015b; Chen et al., 2018). Compared with analytical methods, graphical models may provide a framework for the evolution of domino effects, tackling complex domino scenarios and higher-order propagations.

1) Graph/network models

Reniers and Dullaert (2007) first modeled domino effects in chemical industrial areas using a directed graph G, as follows:

$$G = (N, A) \tag{2.4}$$

N represents the set of nodes (e.g., chemical installations), A denotes the set of arcs between each ordered pair of nodes, being represented as a matrix of $N \times N$. The weight of each arc represents the likelihood of propagation from a tail installation to a head installation. Since available threshold values or probit models are not always consistent, a distance-based matrix called Domino Danger Unites Matrix (DDU) was defined as the weight of arcs, characterizing possible accident scenarios from one installation to another (Reniers and Dullaert, 2007). Using this approach, hazardous installations in an industrial area can be modeled as a whole in terms of the danger they pose to each other. Therefore, this method can obtain critical installations with a high probability of initiating or propagating domino effects, supporting prevention decision-making (Reniers and Dullaert, 2007, 2008).

2) Graph metrics

Khakzad and Reniers (2015b) analyze the vulnerability of process plants in the context of domino effects using graph metrics such as betweenness, out-closeness, and in-closeness in directed graphs, and closeness in undirected graphs. The betweenness of a vertex is defined as the fraction of geodesic distances (or the weights of edges) between all pairs of nodes that traverse the node of interest. The out-closeness of a node can be defined as the number of steps needed to reach every other node of the graph while the in-closeness of a node can be defined as the number of steps needed to reach the node from every other node of the graph. The out-closeness metric reflects installations' potential contribution to the escalation of domino effects while the in-closeness metric represents the vulnerability of installations to get damaged during domino effects. This method is therefore able to identify the critical installations or most vulnerable installations in process industrial areas (Khakzad and Reniers, 2015b; Khakzad et al., 2016).

3) Dynamic graphs

Chen et al. (2018) developed a dynamic graph approach to model the spatial-temporal evolution of domino accidents, overcoming the limitation of the "probit model" w.r.t only able to estimate the damage probability of the first level propagation. Synergistic effects and parallel effects of the spatial evolution, as well as superimposed effects of the temporal evolution possibly occurring in complex domino evolution processes, are considered in this study. Different from static graph models, the structure of a dynamic graph with the evolution of a domino accident, is shown in Figure 2.3.

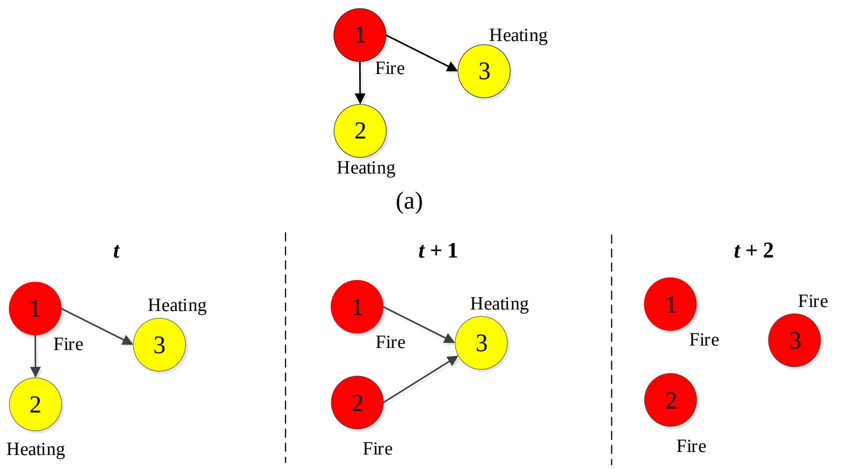

(b)
Figure 2.3 The structure of graph models of domino effects
(Note: (a) a static graph model and (b) dynamic graph model, adapted from (Chen et al., 2020c))

The dynamic graph approach seems to be able to model the dynamic evolution of domino effects (escalation sequence) compared to the static graph which provides merely a snapshot of the whole process at once.

4) Bayesian network

Bayesian network (BN) is a powerful probabilistic graphical tool widely used in the area of safety and risk assessment and of artificial intelligence to model uncertain knowledge and dependency in probabilistic systems (Khakzad et al., 2011; Khan et al., 2015; Chen et al., 2019c; Li et al., 2019). Khakzad et al. (2013) introduced a Bayesian network (BN) methodology to model the domino effect evolution and to estimate the domino effect probability at different escalation levels, considering possible synergistic effects occurring when several scenarios of a lower level trigger a higher level scenario. Considering the complex interaction and conditional dependencies among the units involved in the domino effect, several limiting assumptions such as independent events or random or binomial selection of target units can be relaxed using the Bayesian network approach (Khakzad et al., 2013). Figure 2.4 shows a possible propagation pattern of a domino effect represented by a BN.

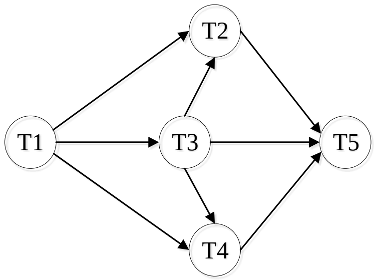

Figure 2.4 A possible propagation pattern represented by BN
(Note: the corresponding sequence of failures: T1→T3→T2, T4→T5), adapted from Khakzad et al. (2013))

Besides, BN was also used to analyze domino effects caused by dust explosions (Yuan et al., 2016) and lightning (Yang et al., 2018).

5) Dynamic Bayesian network

Different from the ordinary Bayesian network, Khakzad (2015) developed a dynamic Bayesian network (DBN) model to take into account both the spatial and temporal escalation of domino effects. The improved methodology explicitly takes time dependencies into account and identifies the most probable sequence of accidents, reflecting the characteristics of a domino effect much better than the most probable combination of accidents offered by ordinary BN (Zeng et al., 2019). Since determining the structure of BN is the first step of BN analysis, only the most probable sequence of accidents is obtained. To model the uncertainty of the sequence of events during a domino scenario, a new DBN model with a more complex structure is proposed by Khakzad et al. (2018a). Besides, an approach combining DBN with a fuzzy inference system was also developed to deal with the uncertainty of domino effects (Ji et al., 2018). Most recently, DBN was employed to analyze wildfire spread in wildland-industrial interfaces and domino effects caused by wildfire (Khakzad et al., 2018b; Khakzad, 2019).

6) Petri-net models

Petri-nets can be regarded as a directed graph, consisting of two sets of nodes: the set of places representing system objects and the set of events or transitions determining the dynamics of the system. Petri-nets are always used to analyze and simulate concurrent systems (Murata, 1989; David and Alla, 2005). Zhou and Reniers (2017b) proposed a Petri-net model to analyze domino effects caused by vapor cloud explosions. The probabilistic dependency relationship between events was modeled by the token of a place with a probability value. Similar to the BN method, the structure of the Petri-net is developed based on threshold values, and consecutively the probability calculation is performed according to the developed network (Zhou and Reniers, 2017b; Zhou and Reniers, 2018b). Kamil et al. (2019) modeled the complex interaction and time dependencies among units during the evolution of fire-induced domino effects using a Petri-net.

(3) Simulation methods

Abdolhamidzadeh et al. (2011) proposed a simulation approach based on the Monte Carlo method for assessing the probability of domino effects and the failure frequency of installations, avoiding the complexity of analytical techniques used by QRA approaches. Later, this simulation method was improved to extend its capabilities in multi-scenario and higher-level escalations (Rad et al., 2014). The simulation approach successfully models the spatial evolution of domino accidents but the shortcoming is obvious, i.e. it is time-consuming. Besides, similar to the QRA approach (Cozzani et al., 2005), it is a purely probabilistic tool based on randomly generated numbers, ignoring the actual accident propagation mechanisms. An agent-based simulation tool considering installations' states was proposed to analyze the higher-level propagations and temporal dependencies (Zhang et al., 2018). The Monte Carlo simulation method is also used to solve the model, also taking huge computation time, especially for realistic chemical clusters with a large number of installations.

2.5 Safety and security management of domino effects

Risk management in the process industries aims to reduce the hazard of a process, the probability of an accident, or both using a wide variety of strategies, techniques, procedures, policies, and systems (Bollinger and Crowl, 1997). Reniers et al. (2008) indicated that both safety and security are important for the management of domino effects. Domino effect management, therefore, requires taking a wide variety of safety and security measures to prevent or mitigate possible intentional domino effects and unintentional domino effects. Bollinger and Crowl (1997) divided risk reduction strategies into four categories: inherent, passive, active, and procedural. Current measures for preventing and controlling domino effects including LOC prevention, safety distance, safety inventory, layout optimization, safety barriers and security measures and emergency response, etc.

2.5.1 Inherent safety

The main difference between inherent safety and the other three categories is that inherent safety aims to remove the hazard at the source, as opposed to accepting the hazard and attempting to mitigate the effects. Application of inherent safety strategies may be the most effective and straightforward approach and has received the majority of attention in prior development of assessment tools (Khan and Amyotte, 2003). In terms of domino effects, inherent safety strategies can prevent the initiation of the accident as well as reduce the potential for propagating an accident or terminate the accident sequence. Kletz (2003) proposed five well-known principles for inherently safer design: intensification or minimization, substitution, moderation by attenuation, simplification, and moderation by limitation of effects. These principles may be applied to identify and define inherent safety actions aimed at escalation prevention, although these principles are sometimes difficult to implement in practice, and not all these principles may be applied at the design stage in which the domino effect assessment should be afforded (Cozzani et al., 2007). The five principles are described in Table 2.5.

Table 2.5 Inherently safer principles
(Khan and Amyotte, 2003; Kletz, 2003; Cozzani et al., 2007)

Inherently safer principles	Description
Intensification or minimization	Using so little of the hazardous material that there are no significant risks if it all leaks out
Substitution	using a less hazardous material or a process that is less likely to develop into a runaway reaction
Moderation by attenuation	Using the hazardous material in the least hazardous form
Simplification	Using simpler plants that provide fewer opportunities for error and less equipment that can fail
Moderation by limitation of effects	Using the design and operation that are less likely to induce severe effects

(1) Inherent safety indexes

Cozzani et al. (2007) analyzed possible escalation scenarios to identify inherent safety actions w.r.t. prevention and mitigation of domino effects. They indicated that the principle of “limitation of effects” is more effective and the integration of inherent safety criteria with passive or active protections may be a promising route for the prevention of severe domino accidents in chemical and process plants. Cozzani et al. (2009) defined a set of indexes based on the assessment of inherent safety distances calculated using specific escalation thresholds for the calculation of process and layout hazards related to escalation events. The hazard indexes may be used to identify actions aimed at escalation prevention both in layout design and in the design of single units. Tugnoli et al. (2008a) examined the five inherent safety principles and found that “attenuation”, “simplification” and “limitation of effects” are practical for layout design. According to these three principles, they developed an index-based approach for plant layout design, taking into consideration the actual consequences of possible escalation scenarios and scores the subsequent accident propagation potential (Tugnoli et al., 2008b). For comparative analysis of reference technologies proposed for hydrogen storage, Landucci et al. (2008) developed a set of inherent safety key performance indicators (KPIs) based on consequence assessment and credit factors of possible LOC events. These studies highlight the need for the application of inherent safety principles early in layout design to avoid domino effects.

(2) Layout optimization

Besides comparative analysis, the optimization based on inherent safety principles and indexes is also widely used in plant layout design. Lee et al. (2005) proposed nonlinear programming to optimize the allocation of explosive facilities, considering possible domino effects caused by fire, overpressure, and fragments. The optimization objective is to minimize the total escalation probabilities caused by different escalation vectors, neglecting the likelihood difference among different primary events. The developed computer-aided module based on this approach may be used for the sequential allocation of hazardous facilities in a limited land (Lee et al., 2006). This optimization algorithm was further extended to obtain the optimized plant layout for minimizing the total weighted consequences of different escalation scenarios (So et al., 2011), and minimizing the total costs (the sum of pipeline connection cost, protection cost, and land-use cost) (Dan et al., 2015).

Jung et al. (2011) developed an optimization approach for facility siting and layout by using a mixed-integer nonlinear program (MINLP). MINLP is widely used in optimization problems with continuous and discrete variables and nonlinear functions in the objective function and/or the constraints. This optimization aimed at determining safe locations of new facilities to minimize the overall cost including land costs, interconnection cost between facilities, and risk cost derived from possible structural damage caused by overpressures. The optimization results can be used to facilitate decision-making for creating low-risk layout structures and determining whether a proposed plant could be safely and economically configured in a particular area. The MINLP approach was also applied to obtain the optimal plant layout for reducing domino effects based on probit models and domino effect indexes (López-Molina et al., 2013; de Lira-Flores et al., 2014; de Lira-Flores et al., 2018). Besides, an MINLP formulation is proposed for process plant layout optimization, considering possible domino effects of them (Latifi et al., 2017).

A multi-objective optimization was employed to optimize the design of storage facilities by combining inherent safety design and quantitative risk assessment (Bernechea and Arnaldos, 2014). Multi-objective optimization is a decision-making tool based on multiple criteria, simultaneously optimizing two or more objectives subjected to different restrictions. As a result, it can be used to balance the conflict between minimization of domino effects and reduction of investment costs (Bernechea and Arnaldos, 2014). Plant layout design according to QRA results can also be found in Nomen et al. (2014) in which a simple criterion based on the surface enclosed in isorisk curves is used for the comparison of different QRA results. Khakzad and Reniers (2015a) developed a multi-criteria decision analysis tool based on an analytic hierarchical process for chemical plant design. The developed BN combined with multi-criteria decision analysis techniques in their study can be applied to a wide range of chemical plants with a variety of hazardous units and multiple accident scenarios.

(3) Inventory optimization

Besides plant layout, the quantity of hazardous substances is also a key factor for creating an inherently safe plant. Thus optimization of the allocation of chemical inventories may be a good option when reducing the mass of hazardous substances is impossible. Khakzad et al. (2014) proposed a risk-based approach based on DBN to optimize the chemical plant inventory to reduce the risk of domino accidents. The study indicated that optimization of the allocation of hazardous inventories can be of great importance for existing process plants in which it is not possible to prevent domino effects via the extension of safety distances.

2.5.2 Management of safety barriers

Passive barriers in process safety management can be defined as any measures that reduce either the frequency or consequence of the hazard without the active functioning of any device, such as dikes, firewalls, fireproofing coatings, and pressure safety valves. Active barriers are any measures that are aimed at detecting and responding to process deviation from normal operation using controls, alarms, safety instrumented systems or functions, and mitigation systems (e.g. water deluge systems (WDS), emergency shutdown systems (ESD), emergency depressurization systems (EDP) (Bollinger and Crowl, 1997; Cozzani et al., 2007; Landucci et al., 2015a; Khakzad et al., 2017a; Chen et al., 2019b). In recent years, increasing researches on passive and active barriers have been focused on protecting process industrial areas from fire-induced domino effects.

(1) Performance assessment of safety barriers

The performance of a safety barrier for escalation prevention depends on the "availability" and "effectiveness" of the barrier. The availability is defined as the complement of the probability of failure on demand (PFD) of the safety barrier while the effectiveness is characterized by the conditional probability of the escalation being successfully prevented given the barrier is activated. Landucci et al. (2015a) proposed a quantitative assessment method for the performance of safety barriers including passive barriers, active barriers, and emergency response. A fault tree was developed to quantitatively assess the PFD of safety barriers, and the frequency of domino effects was obtained using a developed event tree considering the performance of relevant safety barriers (Landucci et al., 2015a; Landucci et al., 2017b). The performance of different barrier types accounting for specific site factors can be determined by combining the quantitative study with key performance indicator analysis (Landucci et al., 2016a). Then, the event tree approach was extended to account for the influence of harsh environmental conditions on the emergency response and on the performance of hardware safety barriers (Landucci et al., 2017a; Bucelli et al., 2018). Table 2.6 shows the PFD values of different safety barriers.

Table 2.6 The PFD values of safety barriers
(CCPS, 2001; Landucci et al., 2015a)

Safety barrier	Actuation type	Proportioning method	PFD
Foam-water sprinkler system	Pneumatic	In-line educator	5.43×10^{-3}
		Metering proportioning	5.01×10^{-3}
		Bladder tank	3.76×10^{-3}
	Electric	In-line educator	5.39×10^{-3}
		Metering proportioning	4.96×10^{-3}
		Bladder tank	3.72×10^{-3}
WDS for LPG vessels protection	Pneumatic	-	1.89×10^{-2}
	Electric	-	4.33×10^{-2}
WDS for horizontal separator protection	Pneumatic	-	2.24×10^{-2}
	Electric	-	2.24×10^{-2}
ESD system	-	-	3.72×10^{-4}
Pressure Safety Valve (PSV)	-	-	1.00×10^{-2}
Fireproofing coating	-	-	1.00×10^{-3}
Emergency intervention	-	-	1.00×10^{-1}

To address the degradation of safety barriers during domino events, Khakzad et al. (2017a) developed a dynamic Bayesian network methodology considering the temporal evolution of domino effects and the time dependency of fire protection systems' performance. In this study, exponential probability distribution was used to model the availability of safety barriers while time-dependent fragility models were adopted to assess the failure probability of tanks exposed to fire. These studies on performance assessment of safety barriers show the role of safety barriers in reducing the probability of fire escalation by several orders of magnitude.

(2) Optimization of the allocation of safety barriers

Fireproof coatings are a crucial safety barrier for the prevention and mitigation of fire-induced domino accidents. However, it is impossible to apply fireproof coatings in all equipment of a chemical industrial area due to economic issues. Tugnoli et al. (2012) thus developed a risk-based methodology to identify fireproofing zones in the initial phases of layout definition, considering the escalation caused by both pool fire and jet fire. In their study, a risk matrix was adopted to rank the severity of different LOC scenarios to identify the reference scenarios. Then the fireproof zones were obtained using the plotted envelops corresponding to the reference LOCs (Tugnoli et al., 2012; Tugnoli et al., 2013). Besides, an approach for determining the water application rate was established for the protection of storage tanks against heat radiation from an external non-contacting fire (Ghasemi and Nourai, 2017). This study indicates that there will be at least 25% saving in a tank farm area by calculating the water application rate to reduce the separation distance between adjacent tanks.

Janssens et al. (2015) proposed an optimization method to allocate safety barriers for mitigating the consequences of possible domino effects triggered by fire. The optimization objective is to maximize the total failure time associated with a domino effect within a chemical plant using safety barriers given a limited budget. The decision-making on the allocation of safety barriers was thus considered as a knapsack problem and a metaheuristic algorithm was developed to obtain the optimal allocation strategy. This approach can guide the decision-maker to allocate a limited budget to increase the time needed for emergency response actions and thus prevent possible fire escalation.

Besides, a cost-effective analysis was used to support decision-making on the allocation of safety barriers for the mitigation of domino effects (Khakzad and Reniers, 2017; Khakzad et al., 2018c). Compared with cost-benefit analysis, cost-effectiveness analysis does not strictly require the monetization of benefits, but always needs to compute cost-effectiveness ratios (CERs) and use these ratios to select the most effective strategies (Reniers and Van Erp, 2016). The effectiveness of safety barriers may be represented by graph metrics (Khakzad et al., 2017b), quantified risk (Khakzad and Reniers, 2017), or avoided loss (Khakzad et al., 2018c). Therefore, the cost-effective analysis based on the results obtained from graph metrics, Bayesian network, or limited memory influence diagram can identify a cost-effective allocation of safety barriers to mitigate possible fire-induced domino accidents.

2.5.3 Emergency response

Emergency response plans in the chemical industry are essential to protect installations, the public, and workers' health and safety, to reduce the environmental impacts, and the recovery time of normal operations. The emergency response also influences the development of the accident and has important impacts on the occurring of domino effects. However, the evaluation of emergency response is rather complex due to the uncertainties related to human factors involved in the performance of emergency response tasks (Chen et al., 2019b). For example, the effectiveness of firefighting strongly depends on the skills and preparedness of emergency responders, the number of firefighting trucks as well as the distance of water resources from the plant (Zhou et al., 2016; Khakzad, 2018d). Besides, the effectiveness of emergency response actions highly depends on the time required to start the emergency operations. For instance, considering the cooling strategy of installations exposed to heat, time is needed for the shell temperature to drop under the failure threshold (Cincotta et al., 2019). In the case of terrorist attacks on chemical facilities, more than one fire may occur simultaneously, and these fires may lead to domino effects at different locations in a chemical industrial area due to multiple-target attacks. In that case, emergency management might be more significant and challenging since it is not so easy to allocate limited emergency resources to different locations.

(1) Procedural action analysis

Zhou and Reniers (2016b) analyzed the emergency response to multiple simultaneous large-scale fires using a Petri-net based simulation method. The simulation method addresses the executing actions and the system status (e.g. fire thermal radiations) during an emergency response process, considering the strategies of the allocation of firefighters. The simulation results show that in most cases the allocation of firefighters should be based on fire severity rather than average distribution; the effects of backups for firefighters depend on special fire scenarios thus it is not always necessary to enhance the backups (Zhou and Reniers, 2016b). A further analysis based on timed colored hybrid Petri-net shows that cooling adjacent tanks is much more important for preventing domino effects triggered by fire (Zhou and Reniers, 2018c). This work was extended to deduce the consequence-antecedent relationship between an accident and the emergency response actions by using a fuzzy Petri-net (Zhou and Reniers, 2017a). Besides, an approach combining event sequence diagram and Monte Carlo simulation was developed to assess emergency response actions for the prevention of fire escalation, considering multiple influence factors, such as sequence, duration, correctness, and mutual interaction (Zhou et al., 2016). Therefore, these methods may be used to identify the defects during an emergency response due to multiple fires, facilitating the decision-making on emergency strategies.

(2) Firefighting analysis

Recently, a risk-informed approach based on DBN for emergency response analysis in oil terminals was developed to identify optimal firefighting strategies, especially when the number of fire trucks is not sufficient to handle all the vessels in danger (Khakzad, 2018d). The study shows that cooling an exposed vessel would immediately reduce the likelihood of fire escalation whereas suppressing a burning vessel would not quickly reduce the emitting heat radiation, leaving some chance for fire escalation. The results from a graph-based approach demonstrated that suppression and cooling of tanks with the highest out-closeness index will result in an optimum firefighting strategy (Khakzad, 2018a). In addition to this firefighting optimization based on risk reduction, Cincotta et al. (2019) proposed a new optimization concept based on resilience analysis for the optimization of firefighting strategies, maximizing the resiliency of process plants. A resilience metric based on the failure probability of installations was developed to measure the performance of firefighting strategies. However, the developed resilience metric mainly focused on the vulnerability phase, ignoring the recoverability phase. Thus the results obtained from this study are not much different from those of previous studies.

(3) Emergency Alertness in chemical industrial clusters

Hosseinnia et al. (2018b) established an emergency response decision matrix to tackle domino effects in chemical clusters. The methodology consists of a decision tree of emergency levels and an alert notification system based on a decision matrix. The decision tree was developed to determine the emergency level of each company within the cluster based on the attack outcomes. The alert notification system was set to determine the security level of other critical assets due to either the possibility of an imminent threat or the occurrence of an actual attack against a particular asset. Compared with safety-related domino effects, the emergency management for security-related domino effects needs to consider the security forces. Besides hazard analysis, the attractiveness of installations to adversaries should be addressed in target identification. Also, the consequence analysis should take into consideration both the vulnerability of installations against intentional attacks and the vulnerability of installations subject to possible domino effects (Hosseinnia et al., 2018a, b).

2.5.4 Cooperative prevention

Multiple chemical plants belonging to different companies may be in a chemical industrial park or so-called chemical cluster. As a result, safety and security resources allocated in one chemical plant have a benefit for nearby plants due to the mitigation of possible external domino effects while it may also relatively increase the security risk of nearby plants because of the change of attractiveness for possible common adversaries. Cooperative prevention is thus proposed to prevent domino effects in chemical industrial clusters.

(1) External domino effects and cooperative prevention

According to the possible affected area of domino accidents in a chemical industrial cluster, domino effects can be divided into two categories: internal domino effects and external domino effects, as already indicated before. The former is defined as the domino effect occurring within the boundaries of the plant where the domino accident originates while the latter is defined as the knock-on effect that escalates outside the boundaries of the plant where the domino accident originates (Reniers et al., 2004; Reniers et al., 2005a). Due to possible external domino effects, a terrorist attack on chemical installations or storage tanks belonging to company A may affect company B, or indeed a simultaneous attack on both companies may take place, causing a major catastrophic disaster. Besides, these scenarios may unfold if the terrorist has access to sufficient and accurate information. Since several companies may be involved in such catastrophes, it is in the best interest of all plants composing a chemical industrial cluster to collaborate in optimizing cross-plant loss prevention and making it as effective and as efficient as feasibly possible (Reniers and Soudan, 2010). Even if a company has fully invested in the prevention of domino effects while its neighbor has not, the company may experience a major accident caused by an initial event that occurs in an adjacent chemical enterprise in the chemical industrial cluster. However, the neighboring company itself becomes more of a target for a terrorist attack since its attractiveness increases if no security investments are made (Reniers, 2009; Reniers and Soudan, 2010).

To prevent and mitigate external domino effects, Reniers et al. (2005b) examined risk analysis tools used by 24 chemical plants in Belgium, to identify the current practice in the chemical industry subject to European Seveso legislation and to examine how the present methods can be integrated to improve the safety policy. The survey shows that the exchange of expertise and cooperation will lead to a safer working environment. It was also demonstrated that HAZOP, what-if analysis, and the method of risk matrix are promising for designing a standardized safety analysis scheme that may stimulate inter-company cooperation. As a result, an external domino accident prevention framework based on the three risk analysis methods was developed, which was called “Hazwim”. External industry evaluation indicated that the Hazwim framework consisting of a process scheme and an organized schedule is a very useful instrument for decision-making for the prevention of external domino accidents (Reniers et al., 2005a).

To support prevention investments, the decision-making of different plants within a chemical cluster was modeled by using a cooperative game. A win-win strategy or so-called Nash equilibrium where both companies win by investing in security prevention measures can be obtained by using game theory (Reniers et al., 2009). Further study demonstrated that security may truly be optimized within a chemical industrial area if academic research would further lead within chemical clusters to set up a supra-plant institution at cluster level with the ability to persuade neighboring plants to change their strategic behaviors (e.g., increasing trust, making unambiguous agreements) (Reniers, 2010).

(2) Enhancing safety and security cooperation

Security investments are completely different from safety investments in which a company can become safer from a neighboring company’s investment in safety barriers. In that case, chemical plants are not inclined to invest in cross-plant preventive measures besides those legally required due to the extremely low probabilities of external domino effects, trust, and confidentiality concerns (Reniers, 2010). Pavlova and Reniers (2011) thus developed a sequential-move game to enhance safety and security cooperation within chemical clusters dealing with domino effects. The sequential game with two stages is illustrated in Figure 2.5.

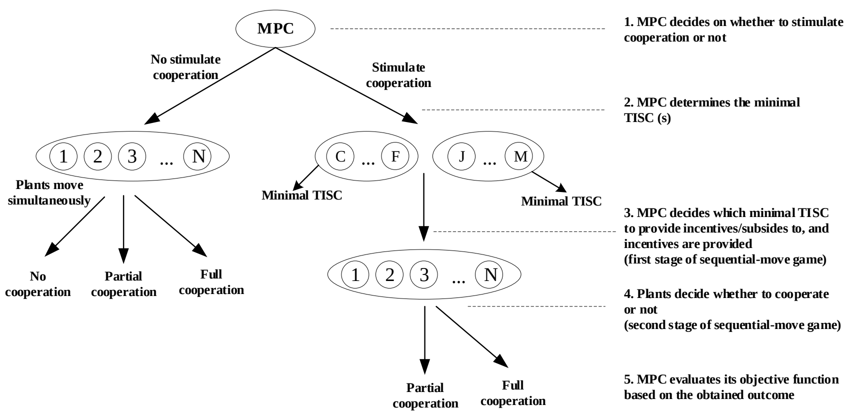

Figure 2.5 The decision procedures of two-stage sequential move game
(Note: adapted from Pavlova and Reniers (2011))

As shown in Figure 2.5, Pavlova and Reniers (2011) recommended to set up an institution, the so-called Multi-Plant Council (MPC), to stimulate the prevention cooperation in a chemical industrial cluster. The MPC would be responsible for a continuous follow-up of external safety (and security) improvements at the individual companies belonging to the industrial cluster. In the two-stage game, the MPC is a leader who has the opportunity to decide to stimulate cooperation or not among the cluster companies. The MPC's objective is to achieve full cooperation among players through establishing a system of incentives at minimum expense. The individual chemical companies are followers. After the leader makes a decision, the followers may decide to invest in the cooperative prevention of domino accidents and play a Nash equilibrium. The solution of the game is obtained as a subgame perfect equilibrium. The minimum expense provided by MPC is used to induce cooperation among the rest of the players. Therefore, one of the main objectives of the sequential-move game is to find out the minimal cooperative expense.

2.5.5 Security strategies for intentional domino effects

The U.S. Department of Homeland Security identified chemical industrial facilities as one of 16 critical infrastructure sectors that their incapacitation or destruction would have a debilitating effect on security, national economic security, national public health or safety, or any combination thereof (U.S. Department of Homeland Security, 2013). Securing chemical infrastructures has gained increasing concern in scientific and technical literature since the 9/11 attack in New York City, 2001 (Baybutt, 2002; American Petroleum Institute (API), 2004; Whiteley and Mannan, 2004; Apostolakis and Lemon, 2005; Bier et al., 2005; Moore et al., 2007; API, 2013; Zhang and Reniers, 2016). However, little attention had been paid to preventing domino effects caused by intentional events before Reniers et al. (2008) proposed to deal with intentional domino effects in chemical clusters. Different from other critical infrastructures, an intentional attack on one or more hazardous installations may trigger a chain of hazardous events, resulting in more severe consequences than that of the primary attack. Intentional domino effects may be triggered due to the following motivations (i) adversaries execute an attack with the purpose of triggering domino effects, inducing catastrophic accidents; (ii) adversaries attack target installations resulting in unplanned domino effects; (3) adversaries indirectly attack a target installation via domino effects (Reniers and Audenaert, 2014; Landucci et al., 2015b; Khakzad and Reniers, 2019).

In terms of the protection strategies used in literature, the present review divided current research on the management of intentional domino effects into three categories: security of critical installations, mitigation of potential consequences, and reduction of attractiveness.

(1) Security of critical installations

A chemical industrial area is always characterized by many hazardous installations. The domino potential of hazardous installations depends on the danger they pose to each other, relevant to the amount of substances present, the physical and toxic properties of the substances, and the specific process conditions, etc. These installations that exhibit a high probability of initiating or propagating domino accidents may be regarded as critical installations, in terms of domino effects. In that case, these critical installations are more attractive and so have a higher probability to be exploited by adversaries to trigger catastrophic disasters. The concept of securing critical installations is a reasonable and feasible strategy to protect chemical industrial areas from possible intentional domino effects.

The strategy of securing critical installations was first proposed to address security-related issues in domino effect management (Reniers et al., 2008). The installations with a high potential to propagate domino effects are defined as domino hubs (critical installations) within the industrial network. Thus, enhancing the security of domino hubs can improve the overall security of the chemical industrial area. In that case, an entire chemical industrial area is divided into smaller chemical sub-clusters in which no domino effects can enter or leave the physical boundaries. A case study indicated that protecting as few as 7 of 225 installations in a chemical industrial area might already have an important security impact (Reniers et al., 2008; Reniers and Dullaert, 2008). Besides, the Borda algorithm approach can be used to obtain an ordinal ranking of decision preferences based on vulnerability assessment, facilitating the allocation of security resources. Readers interested in the algorithm’s application in this issue can refer to Reniers and Audenaert (2014).

From the perspective of resilience, Reniers et al. (2014) proved that the layout of a chemical industrial area might follow a power-law distribution. In other words, only a few installations exhibit very high escalation danger connectivity while others (the vast majority of installations) may have only relatively unimportant domino dangerousness links. Securing those high-danger installations leads to decreasing the possible consequences of an attack since the large chemical industrial area disintegrates into smaller areas of possible escalation. As a result, the chemical industrial area would be more resilient against intentional attacks. Bubbico and Mazzarotta (2014) explored the role of layout on security risk in chemical industrial areas, highlighting the significance of planning plant layout from a security perspective. In that case, the most critical zones should be preliminarily identified when planning a plant layout, including process areas, control room(s), storage installations of hazardous materials, loading and unloading facilities, and fired heated equipment. According to the concept of the layers of protection, the most critical assets should be set in the middle, providing concentric levels of security and increasing the number and the complexity of the barriers moving toward the center (Bubbico and Mazzarotta, 2014). Therefore, securing critical installations is a feasible strategy, avoiding the difficult issue in chemical security that is determining the probability or the likelihood of an attack on a chemical industrial area.

(2) Mitigation of potential consequences

When eliminating terrorist groups and intentional attacks seem impossible, mitigating the potential consequences of intentional attacks can be considered as an effective approach for protecting chemical industrial plants against terrorist attacks. Besides, using safety measures to mitigate the potential consequences of intentional attacks can contribute to the prevention of accidental domino effects and Natech domino effects. As a result, the application of this protection strategy may result in not only a safer chemical industrial area but also a more secure surrounding.

Srivastava and Gupta (2010) developed a Stepped Matrix Procedure method to deal with domino effects, considering safety barriers needed so that the intentional event would not cascade into domino effects. Reniers and Audenaert (2014) proposed to minimize potential consequences of domino effects based on vulnerability assessment of installations subject to possible domino effects, reducing the security risk of chemical industrial areas, avoiding security vulnerability assessments and threat assessments. The approach proposed in their study can also be used to identify the most vulnerable installations of a chemical industrial area in the early design phase or to solve layout or site location problems to reduce the potential consequences. Khakzad and Reniers (2019) proposed the cost-robust low-capacity utilization of process plants as a way to tackle intentional domino effects in process plants based on vulnerability analysis. This study proposed a cost-robust mitigation strategy to keep some of the storage tanks empty in the case of imminent terrorist attacks. The robustness of the plant against intentional attacks can be increased temporarily by applying this protection strategy. Consequently, any safety measures for escalation prevention may be used to mitigate the potential consequence of intentional attacks, avoiding intentional domino effects.

(3) Reduction of attractiveness

Coster and Hankin (2003) summarized nine factors relevant to the attractiveness of hazardous facilities: access, security, visibility, opacity, secondary hazard, robustness, law enforcement response, victim profile, and political value. Attractiveness analysis should consider the perceived value of a target to the threat as well as the threat's choice of targets to avoid discovery and to maximize the probability of success (API, 2013). Since terrorists usually launch attacks with the aim of causing as much damage as possible, inducing mass casualties and panic and drawing media attention (Reniers and Audenaert, 2014; Khakzad, 2018c), both the strategies of security of critical installations and mitigation of potential consequences can lead to a reduction of the attractiveness to adversaries. Combining safety and security resources to the protection of chemical industrial areas from possible intentional domino effects may be regarded as a strategy for the reduction of attractiveness.

Khakzad (2018c) emphasizes the importance of reducing the attractiveness of chemical plants to terrorist attacks, recommending using safety concepts such as inherently safer design and land use planning to improve the security of chemical plants. These safety concepts can reduce both the attractiveness of the chemical plant and the severity of the consequences of likely attack scenarios. Chen et al. (2019b) proposed an integrated approach to protecting chemical industrial areas from intentional domino effects, considering the vulnerability of installations w.r.t. intentional attacks as well as the vulnerability of installations subject to possible domino effects caused by the attacks. The developed resource allocation method in this study can largely reduce a chemical cluster's attractiveness as well as the potential consequences.

2.6 Discussion

2.6.1 Current research trends

(1) Modeling first and higher level propagations

According to the domino effect definition (Reniers and Cozzani, 2013), a primary accident scenario must trigger one or more secondary accident scenarios (first-level propagation), and the secondary accident scenarios may trigger one or more tertiary accident scenarios, and so on (higher-level propagation). Early quantitative research on modeling domino effects mainly forced on the first-level escalations, assessing the likelihood of domino effects in a chemical industrial area (Cozzani et al., 2005; Salzano and Cozzani, 2005; Abdolhamidzadeh et al., 2010b). Only considering the first-level escalation may underestimate the consequences of domino effects. Modeling second and higher level escalation is a challenging work due to the uncertainty associated with higher-order scenarios (e.g., failure types, failure sequences, or intensity of escalation vector) and the complexity of higher level propagation (e.g., synergistic effects and parallel effects). Increasing attempts have been made in recent years to model higher-level propagations since 2013 (Khakzad et al., 2013; Cozzani et al., 2014; Rad et al., 2014; Chen et al., 2018; Zhou and Reniers, 2018b). Graphic methods provide a visible framework for the evolution of domino effects and thus have some advantages in modeling higher-level propagation. Previous research establishes graph structures mainly based on threshold values, which may present the most probable sequence of a domino effect. Since a graph/network only represents one possible evolution sequence of domino effects, and multiple graphs or a more complex structure should be established if the uncertainty of the evolution sequence is considered. Monte Carlo based simulation is a widely used method to deal with propagation uncertainty, but it may take huge computation time.

(2) Modeling spatial and temporal evolution

Bagster and Pitblado (1991) considered a domino accident as a spatial escalation initiated by a loss of containment and resulting in a major incident on a nearby installation. Since then, modeling the spatial evolution of domino effects and then obtaining the likelihood of domino effects and the failure frequency of installations have been the main tasks for the risk assessment of domino effects (Bagster and Pitblado, 1991; Khan and Abbasi, 1998a; Khakzad et al., 2013; Yuan et al., 2016). Domino effects can also be regarded as a chain of accidents and these hazardous events may occur simultaneously or sequentially, so the evolution of domino effects may be a time-dependent or dynamic process (Delvosalle, 1998; Reniers and Cozzani, 2013). For example, the propagation caused by heat radiation is delayed since the build-up of temperature and pressure depends on time (time to failure). Dynamic tools are thus needed in modeling the evolution of domino effects and to accurately assess the vulnerability of installations subject to domino effects, supporting the decision-making on emergency response actions. The available dynamic approaches for modeling domino effects include dynamic Bayesian network (DBN) (Khakzad, 2015), agent-based modeling (Zhang et al., 2018), Dynamic graphs (Chen et al., 2018), and Petri-nets (Kamil et al., 2019). By applying these dynamic tools, the heat radiation received by an installation in different stages can be superimposed to determine the residual time to failure at the next stage since the heat radiation intensity may be different in different stages (superimposed effects). As a result, dynamic tools are widely used to model fire-induced domino effects. In terms of domino effects triggered by overpressure or fragments, temporal evolution is ignored since the failure caused by these physical effects is almost instantaneous.

(3) Management of domino effects in chemical industrial clusters
In a chemical industrial cluster, chemical plants may be operated by different companies. Therefore, the hazards possibly leading to domino effects at a chemical company not only depend on the company's own decisions but also the decisions of other chemical plants situated within the chemical cluster due to possible external domino effects. As a result, corporation management of domino effects is undoubtedly the best protection strategy in a chemical cluster (Reniers et al., 2005a; Reniers et al., 2009). However, achieving full cooperation among different plants is challenging since it is related to technical and organizational problems, such as a standardized risk analysis method accepted by all involved companies. To achieve prevention corporation in a chemical cluster, a prevention framework based on widely used risk analysis methods was developed (Reniers et al., 2005a), and a Multi-Plant Council (MPC) was recommended to prompt the corporation. Besides, decision-making on alert levels in a chemical industrial cluster was also proposed to prevent external domino effects (Hosseinnia et al., 2018b). To promote cooperation in a real chemical industrial cluster, more strategic and proactive cooperation should be explored, addressing organizational issues in the overall management process.

(4) Safety and security of domino effects
Past research on domino effects management is mainly concerned with accidental domino effects including inherent safety (Cozzani et al., 2007, 2009; Khakzad and Reniers, 2015a), safety barriers (Landucci et al., 2015a; Khakzad et al., 2017b), and emergency response (Zhou et al., 2016; Khakzad, 2018d; Zhou and Reniers, 2018c), yet with much less focus on Natech domino effects and intentional domino effects. Although these protection strategies can also be used to prevent or mitigate domino effects triggered by Natech or intentional attacks, special characteristics related to the prevention of these domino effects are not fully highlighted. For Natech domino effects, active measures have a high probability of being unavailable since protection systems may be damaged. Besides, emergency response actions may be also impossible due to the inaccessibility of other critical infrastructures nearby, such as water supply systems. In terms of the prevention of domino effects caused by intentional events, there are three main strategies: security of critical installations using security measures (Reniers et al., 2008; Reniers and Audenaert, 2008), mitigation of potential consequences using safety measures (Srivastava and Gupta, 2010; Khakzad and Reniers, 2019) and reduction of attractiveness using both safety and security resources (Reniers and Audenaert, 2014; Khakzad, 2018c). However, little attention has been paid to adversaries' strategies which may result in large losses. For example, multiple fires may be induced by multiple-target attacks, resulting in uncontrolled escalation due to possible synergistic effects.

(5) Decision-making on prevention measures

Multiple protection strategies may be present based on one or more protection principles. Decision-making tools (e.g., comparative analysis, optimization, and cost-effective analysis) are thus needed to identify the best strategy according to a decision criterion. Decision-making based on inherent safety has drawn much attention, including comparative analysis (Landucci et al., 2008; Tugnoli et al., 2008b), layout optimization (Lee et al., 2005; So et al., 2011; Dan et al., 2015), and inventory optimization (Khakzad et al., 2014). Optimization tools are also used for the allocation of safety barriers (Tugnoli et al., 2012; Ghasemi and Nourai, 2017). Besides, cost-effective analysis (Khakzad and Reniers, 2017; Khakzad et al., 2018c) is also applied to address the influence of costs on decision-making for safety barriers. Moreover, game theory is used to deal with the decision-making among different plants in a chemical industrial cluster (Reniers et al., 2010; Pavlova and Reniers, 2011). Current research mainly focuses on one kind of protection measure or is only based on one protection principle, lacking decision-making on multiple measures since multiple protection measures are always used in a chemical industrial area. In addition to the costs of protection measures, the protection benefits may also be interesting for safety and/or security managers because both the costs and benefits related to protection measures are important for any company's profitability in the long term.

2.6.2 Comparison of modeling approaches and protection strategies

(1) Comparison among different modeling approaches

Many approaches have been proposed for modeling domino effects in the process and chemical industries. For different stakeholders in the process and chemical industries, due to their various and different interests of concern, different approaches may be chosen. Consequently, a comparison among different approaches is performed based on several criteria, as follows.

(1) Source: the reference of the approach;
(2) Category: the category of the approach;
(3) Vulnerability basis: the vulnerability models used in the approach;
(4) Escalation vector: the escalation vector considered in the approach;
(5) Evolution: the evolution level and possible temporal evolution considered in the approach;
(6) Computation cost: the computation cost is based on the complexity and time needed for performing the approach.

According to the analysis in Section 2.4, 11 main approaches for modeling domino effects are selected and analyzed based on the six foregoing criteria. The comparison results are shown in Table 2.7.

Table 2.7 Comparison of different modeling approaches

Source	Category	Vulnerability basis	Escalation vector	Evolution	Computation cost
Bagster and Pitblado (1991)	Analytical method	Safety distances	Multiple	Higher-level	High in large scale case
Khan and Abbasi (1998a)	Analytical method	Probabilistic models	Multiple	First-level	Low
Cozzani et al. (2005); (Cozzani et al., 2014)	Analytical method	Probit models	Multiple	First-level Extend to higher levels	Low High in large scale case
Reniers and Dullaert (2007)	Network method	Safety distances	Multiple	Higher-level	low
Abdolhamidzadeh et al. (2010b); (Rad et al., 2014)	Model-Carlo simulation	Probit models	Multiple	First-level Extend to higher levels	high
Khakzad et al. (2013)	Bayesian network	Probit models and thresholds	Multiple	Higher-level	High in large scale case
Khakzad (2015)	Dynamic Bayesian network	Probit models and thresholds	Heat radiation	Higher-level Temporal evolution	High in large scale case
Khakzad and Reniers (2015b)	Graph metrics	thresholds	Multiple	Higher-level	Low
Zhou and Reniers (2017b); (Kamil et al., 2019)	Petri-net	Probit models	Multiple	Higher-level	Low High
Zhang et al. (2018)	Agent-based simulation	Probit models	Heat radiation	Higher-level Temporal evolution	High
Chen et al. (2018)	Dynamic graph model	Time to failure	Heat radiation	Higher-level Temporal evolution	Low

(2) Comparison of different management strategies

The fundamental objective of domino effect research is the prevention and mitigation of domino effects in chemical industrial areas. Different protection approaches are proposed according to different protection strategies including inherent safety, safety barriers, emergency response, cooperative prevention in chemical industrial clusters, and security of domino effects. To protect a chemical industrial area from domino effects, the possible causes of domino effects should be first analyzed since different areas may face different hazards. For accidental domino effects, hazards are mainly located within the chemical industrial area while in the case of intentional- and

Natech-related domino effects external threats can be involved. Safety measures for escalation prevention (i.e., inherent safety, safety barriers, and emergency response) can reduce the risk of domino effects caused by intentional attacks, accidental events, and Netechs. Security measures are mainly for preventing intentional attacks to reduce the probability of intentional domino effects. A cooperative prevention strategy is proposed to prevent possible external domino effects, enhancing the safety and security of all chemical plants in a chemical industrial cluster from a systemic viewpoint. Therefore, stakeholders should choose one or more protection strategies according to their safety and security threats, concerns, and the performance of different protection strategies, as shown in Figure 2.6.

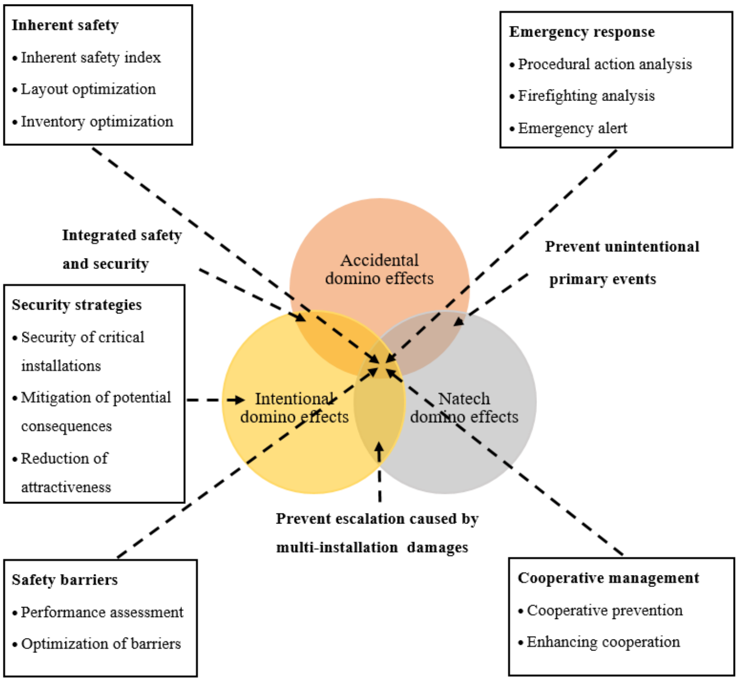

Figure 2.6 Protection strategies for managing domino effects (Chen et al., 2020c)

2.6.3 Future directions and challenges

According to the review of modeling and management issues and approaches of domino effects in the process and chemical industries approach in previous sections, this subsection identifies the following research directions and challenges:

(1) Vulnerability assessment with advanced consequence simulation tools

The vulnerability of hazardous installations subject to escalation vectors is the basis for judging whether a hazard scenario propagates or not. Although many attempts have been done on vulnerability assessment, many of these researches are based on simple assumptions, lacking detailed analysis for physical mechanisms. The failure of installations is a complex phenomenon with a lot of uncertainty. The failure of installations depends on the installations' parameters such as installation types, wall thickness, wall materials, and internal pressure, as well as the plant layout and meteorological factors which may have a great impact on the received intensity of escalation vectors. To accurately model the vulnerability of installations, experiments, or simulation tools may be used. Experiments may not be used frequently due to the huge costs (especially for full-scale experiments). Consequently, a numerical simulation may be more feasible by using advanced consequence simulation software, such as ANSYS, FLUENT, FLACS, FDS, etc. More detailed results can be obtained using these advanced CFD/FEM tools to improve vulnerability assessment models.

(2) Modeling the evolution of coupled domino effects

Modeling the evolution of domino effects, especially higher-level evolution and temporal evolution, has obtained worldwide concern. Most previous models for domino effect evolution only consider one escalation vector (i.e., heat radiation, overpressure, or fragments). However, past accident surveys indicate that multiple escalation vectors are always present in the evolution of a domino accident. In other words, a primary fire may trigger an explosion at neighboring equipment while an explosion can also induce a fire at installations nearby. Therefore, modeling the evolution of domino effects coupled with multiple escalation vectors may be one of the future research issues.

(3) Modeling the uncertainty of domino effects

Graphical models provide a framework for modeling the knock-on evolution and make it possible to predict the most probable sequence of events and the escalation probability, addressing the complexity of domino effects, such as synergistic effects, parallel effects, and superimposed effects. However, accurately modeling domino effects is still a challenging work due to the uncertainty involved in the evolution of domino effects. The uncertainty can be divided into two parts, the uncertainty of accident scenarios and the uncertainty of propagation. The former involves heat radiation intensity, overpressure value, and the number, weight, and velocity of fragments. The latter is related to the failure likelihood of installations subject to hazardous scenarios, failure types, and the subsequent scenarios caused by loss of containments. To improve the inaccuracy due to the simple assumptions used in previous models, modeling the uncertainty of domino effects is needed work.

(4) Management of domino effects in extreme condition

The availability of safety barriers in a normal environment is relatively high, but their reliability or avoidability may decrease sharply due to extreme conditions caused by, for instance, extreme weather or natural accidents. In that case, safety barriers may be damaged and unavailable, and the needed time for starting emergency response actions may be delayed, resulting in uncontrollable domino effects. For example, an earthquake can not only trigger a domino accident but also may damage safety barriers and other infrastructures nearby, making the prevention or mitigation of the domino effect impossible. Therefore, assessing the vulnerability of safety barriers exposed to extreme conditions and selecting alternative or spare safety strategies should be investigated in the future.

(5) Optimizing decision-making on the management of domino effects
As illustrated before, there are many protection strategies for preventing domino effects. A safety manager may select inherent safety design, apply safety barriers or enhance the capability of emergency response teams, or a combination of several measures. These measures, which may be used in different stages of the entire operation life, have different performances and costs. Thus both the protection costs and potential avoided losses should be considered since protection strategies are important for the company’s profitability in the long term. As a result, economic models and optimization methods may be used to support the decision-making on prevention and mitigation related to domino effects.

(6) Integrating safety and security resources to protect domino effects
Domino effects can be induced by accidental events, Natechs, and intentional attacks. Safety barriers can reduce the likelihood and consequences of accidental domino effects, Natech domino effects, and intentional domino effects. Security resources are essential to reduce the threat of domino effects caused by intentional attacks and also decrease the attractiveness of the attacked target, hence its likelihood. Previous studies on domino effect management mainly focused on accidental domino effects, largely neglecting Natech domino effects and intentional domino effects which may result in even more severe consequences. Thus we may consider the integrated performance of protection strategies for different kinds of domino effects from a systemic perspective. In terms of domino effect management in chemical industrial clusters, the influence of safety barriers and security measures are different for other plants nearby. As a result, balancing the investments in safety barriers and security measures as well as the investments in different plants in a chemical cluster may be another research issue in the future.

(7) Optimization of the cooperative management in chemical industrial clusters
Although the advantages of cooperative prevention of domino effects in chemical industrial clusters are obvious, enforcing full cooperation in a real chemical cluster is still challenging due to organizational factors related to the overall management. More strategic and proactive cooperation in real industrial practice should be explored where organizational structure is optimized and management from the different plants belonging to one cluster is inter-connected.

2.7 Conclusions

Over the past 30 years, the significance of domino effect modeling and management has been well recognized among researchers and practitioners in the process and chemical industries. An increasing effort has been devoted to assess the likelihood of domino effects, model the evolution of domino effects, and prevent or mitigate domino effects, but challenges still exist. This chapter reviews the research issues and approaches in modeling and management of domino effects, as well as their evolution in the literature. Existing approaches to modeling domino effects are broadly grouped into three categories: Analytical approaches, graphical approaches, and simulation approaches. Current management strategies are divided into five types: inherent safety, management of safety barriers, emergency response, cooperative prevention, and security strategies. For each type of approach or strategy, this chapter organizes pertinent studies in terms of research issues, modeling rationale, and contributions, etc. It provides a very clear picture of the evolution of the research issues and approaches for modeling and management of domino effects. Besides, different types of modeling approaches and management strategies are further compared according to several criteria, to position their applications and drive the research directions in the future.

Despite current studies have contributed a lot to modeling and managing domino effects, there are still many challenges left, such as modeling the evolution of coupled domino effects, management of domino effects in extreme conditions, integrating safety and security resources to prevent domino effects, studying the optimal way to manage domino effects in chemical clusters, etc., summarized in Section 6.3. In sum, this chapter not only presents an introduction to the modeling approaches and management strategies of domino effects to new scholars and different stakeholders in the field but also identifies the future research directions and challenges to better protect chemical industrial areas from domino effects caused by accidental events, Natechs, and intentional attacks.

Chapter 3 Modeling the spatial-temporal evolution of fire-induced domino effects

Past accident analyses indicate that fire escalation is responsible for most of the domino effects in the process industry. The evolution of domino accidents triggered by fire is different from domino accidents triggered by other primary scenarios since the escalation caused by heat radiation is delayed with respect to the start of the fire. In this study, a dynamic approach involving a Domino Evolution Graph (DEG) model and a Minimum Evolution Time (MET) algorithm is proposed to model the spatial-temporal evolution of domino accidents. Synergistic effects and parallel effects of spatial evolution, as well as superimposed effects of temporal evolution possibly occurring in complex domino evolution processes, are considered in this study. A case study demonstrates that the approach can not only capture the spatial-temporal dimension but also overcome the limitation of the “probit model” w.r.t only able to estimate the damage probability of the first-level propagation. Besides, different from simulation or Bayesian approaches, this methodology with the MET algorithm can rapidly obtain the evolution graphs (paths), the evolution time, and the corresponding probability, given a primary scenario. Therefore, this approach can also be applied to domino risk assessment at an industrial park level and provide support for the allocation decision of safety and security resources.

The content of this chapter is based on the following published papers:
Chen, C., Reniers, G., Zhang, L., 2018. An innovative methodology for quickly modeling the spatial-temporal evolution of domino accidents triggered by fire. Journal of Loss Prevention in the Process Industries 54, 312-324.
Chen, C., Reniers, G., Khakzad, N., 2019. Integrating safety and security resources to protect chemical industrial parks from man-made domino effects: a dynamic graph approach. Reliability Engineering & System Safety 191.

3.1 Introduction

Safety and security are different in the nature of incidents: safety is unintentional whereas security is intentional (Hessami, 2004; Reniers and Pavlova, 2013b). Regardless of the nature of incidents, they may become a primary accident in a chain of accidents, a phenomenon which is well known as a domino effect (Reniers and Cozzani, 2013). Therefore the modeling or assessment of the evolution of domino events is essential for protecting chemical and process installations against knock-on accidents. A growing public concern since the 1990s raised the attention in the scientific and technical literature on domino effects (Necci et al., 2015).

Traditional risk identification and evaluation approaches such as HAZOP analysis, What-If analysis, and the risk matrix are recommended for domino risk analysis in chemical industrial clusters (Reniers et al., 2005a). Chemical industrial parks consist of various hazardous installations with different domino effect potentials. Some installations exhibit a high probability of initialing domino accidents while other installations are more likely to propagate domino events. These installations can be regarded as nodes, and the quantitative possibility of accident propagation may be represented by the weight of the links between nodes in a network graph (Reniers and Dullaert, 2007). Based on this concept, critical installations contributing to possible domino effects can be identified and this information may support the allocation of domino prevention resources (Reniers et al., 2008; Zhang and Chen, 2011). The methodology was extended for vulnerability analysis and protection decision making by using graph theory metrics (e.g. betweenness and closeness) (Khakzad and Reniers, 2015b; Khakzad et al., 2016; Khakzad et al., 2017d). These quick and reliable graph-based approaches can assess domino risks within an entire industrial area and identify the most critical units. They are however unable to capture temporal evolution characteristics.

A Quantitative Risk Assessment (QRA) framework was proposed for domino effects mainly including three steps: the identification of domino scenarios, a frequency analysis, and a consequence assessment (Cozzani et al., 2005). Only the first level propagation is considered in the framework due to the complexity of higher level propagations. The damage probability models used in the QRA methodology were extended and improved by considering different escalation vectors such as radiation, overpressure, and fragments (Gubinelli and Cozzani, 2009b, a; Landucci et al., 2009b; Landucci et al., 2012a; Jia et al., 2017). For example, a damage probability model for fire escalation assessment is established based on the results of finite element models (FEM) and experimental data (Landucci et al., 2009b), as shown in Eq. (3.1). The damage probability model is called the "probit model" and the probit value is related to the time to failure (TTF) of installations, the estimated time required to start the emergency operations, and the estimated time required to start the mitigation actions. The model is determined by considering the uncertainty of emergency response and the TTF in the first level propagation. Hence the "probit model" may be unreasonable for accurately estimating the damage probability of installations in second-level or higher-level propagations due to the delay of the "time to failure" compared with the first level propagation. In other words, using the model may result in over-estimation of the probability propagation in second or higher levels. Taking an extreme case as an example, if a primary fire was controlled by emergency actions (such as cooling with water, external firefighters arriving) before the second level propagation, the propagation probability of the second level would be zero.

Besides, a simulation approach was proposed based on the Monte Carlo method to model higher-level propagations. The approach successfully models the spatial evolution of domino accidents but the shortcoming is obvious, i.e. it is time-consuming (Abdolhamidzadeh et al., 2010a). An agent-based modeling approach considering installations' states was proposed to analyze the higher-level propagations and temporal dependencies (Zhang et al., 2017). The Monte Carlo simulation method is also used to solve the model, also taking huge computation time, especially for realistic chemical clusters with a large number of installations. Other simulation work concentrates on emergency response assessment and optimization (Zhou and Reniers, 2016b; Zhou et al., 2016). Besides, a Bayesian network methodology was proposed to model domino effect propagation (Khakzad et al., 2013; Khakzad, 2015). The methodology can model higher-level propagations while it is difficult to apply it to chemical clusters with a large number of installations (Khakzad and Reniers, 2015b).

In the light of these findings and of the evolution of domino effect research, the present work aims to establish a dynamic graph approach for modeling the spatial-temporal evolution of domino effects and overcoming the above shortcomings. The spatial propagation and the temporal propagation are integrated using dynamic graphs. First, we briefly introduce the theory of dynamic graphs in section 3.2. Next, the Domino Evolution Graph (DEG) model is illustrated in Section 3.3, and the corresponding algorithm of Minimum Evolution Time (MET) is elaborated and explained in section 3.4, following by a case study in section 3.5. Finally, conclusions are drawn in section 3.6.

3.2 Dynamic graph

Graph theory provides a mathematical approach for studying interconnections among elements in natural and manmade systems. Initially, interactions of elements were limited to binary relations denoted by vertices of the graph. Subsequently, functions were associated with graphs that assign a real number to each edge of a graph for quantifying the relationship between any pair of elements in a given system. So a classic graph consists of a set of vertices (nodes) and a set of edges (arcs) with the assumption that the structure of the graph is static.

However, graphs may change over time in many applications, such as in computer programming languages and artificial intelligence. Dynamic graph models were systematically proposed in the 1990s to solve these practical dynamic applications. And the corresponding algorithms have been improved to study the dynamic graphs, such as Shortest Path algorithms. A dynamic graph, similar to the structure of static graphs, can be an undirected graph, a directed graph, or a weighted graph (network).

The three different structures of dynamic graphs are briefly described as follows. (Bondy and Murty, 1976; Harary and Gupta, 1997; Casteigts et al., 2012)

- An undirected graph is a pair G = (V, E), where V is a set of vertices, and E is a set of edges. Each edge is an unordered pair where v_i and $v_j \in V$.
- A directed graph is a pair $G = (V, A)$, where V is again a set of vertices, and A is a set of arcs. Each arc is an ordered pair (v_i, v_j), $i \neq j$.

There are three kinds of weighted graphs (networks): a node-weighted graph, an edge-weighted graph, and a full weighted graph. A full weighted graph $G= (V, E, f, g)$, f: $V \rightarrow N_V$, g: $E \rightarrow N_E$, where N_V (N_E) is some numbered system, assigning a value or a weight of a node. The weights may be real numbers, complex numbers, integers, elements of some group, etc.

A dynamic graph G is updated when one or more than one of the following four entities change: V (a set of nodes), E (a set of edges), f (map vertices to numbers), and g (map edges to numbers). The dynamic graph can be divided into four basic categories according to the variation of different entities.

- A node-dynamic graph: the set V changes over time and the nodes may be added or removed. When a node is removed, the related edges are also eliminated.
- An edge-dynamic graph: the set E changes over time and the edges may be added or removed.
- A node-weighted dynamic graph: the function f changes over time and the weights on the nodes update.
- An edge-weighted dynamic graph: the function g changes over time and the weights on the edge also update.

Any combination of the above basic types can occur in real applications. An update on a graph is an operation that adds or removes nodes or edges, or changes in weights of nodes and edges. Between two updates, the graph can be regarded as a static graph. So a dynamic graph can be viewed as a discrete sequence of static graphs and each graph can be studied by using the developed knowledge of static graph theory. Dynamic graph models may vary with different applications and the related algorithms can be developed according to the update rules of the dynamic graph (Harary and Gupta, 1997).

3.3 Domino Evolution Graph model

3.3.1 Definition

A Domino Evolution Graph (DEG) is defined as a dynamic graph indicating installations' vulnerability features in the evolution process of domino effects caused by unintentional or intentional events. The dynamic graph starts when there is a primary fire scenario and ends when the evolution is over. For illustration purposes, only the fire scenario is considered in the model, but it can be extended to other scenarios such as explosions and even the scenario evolution between fire and explosion. The dynamic graph can be represented, as follows:

$$G = (N, E, NW, EW) \tag{3.1}$$

(1) *N* is a set of nodes denoting installations in a chemical industrial park. The number of nodes (*N*) will not change in the entire evolution process.
(2) *E* is a set of directed edges from installations causing heat radiations to installations receiving the heat radiations. If there is an edge from node *i* to node *j*, node *i* is often called tail while node *j* is called head ($i \neq j$).
(3) *NW* is a group of node weights (indicators) indicating the vulnerability or harmfulness of installations, as follows:

$$NW = (S, Q, RTF, RTB, PP, PD) \tag{3.2}$$

- *S* is a set of states denoting the role of installations in a domino evolution. According to installations' vulnerable or harmful attributes in the evolution of domino effects, three states are defined: "vulnerable", "harmful" and "dead". The description of these states is shown in Table 3.1. For the sake of clear representation, an installation in the "vulnerable" state is marked as yellow, in the "harmful" state it is marked as red, and in the "dead" state it is marked as gray in the dynamic graph.

Table 3.1 State description

State	Description	Marked color
Vulnerable	The installation is not physically damaged but it may receive heat radiation from other installations. The installation's temperature or internal pressure may increase in this state.	Yellow
Harmful	The installation is on fire due to unintentional or intentional events or due to escalation from other installations. Installations in this state have a harmful impact on other installations receiving their heat radiation.	Red
Dead	The fire on the installation is extinguished due to the burning out of flammable substances or emergency response actions. All edges connected to the node will be removed if the installation's state transfers from "harmful" to "dead".	Gray

- *Q* is a weight of nodes denoting the total heat radiation received by installations, in kW/m^2. Installations in the "vulnerable" state receive heat radiations from installations in a "harmful" state ($Q \geq 0$). The *Q* is equal to zero if an installation is in the "harmful" state or the "dead" state.

- *RTF* is a weight of nodes representing the residual time to failure (*RTF*) of installations, in min. The installation is assumed to be damaged when *RTF* is equal to zero.

- *RTB* is a weight of nodes denoting the residual time to burn out (*RTB*) of installations, in min. The fire on an installation is regarded to be extinguished when *RTB* is equal to zero.

- *PP* is a set of primary probabilities of installations being damaged. It denotes the vulnerability of installations directly against undesired events. The *PP* may be decreased by taking safety and security measures.

(4) *EW* is the weight of directed edges. It only represents heat radiations from tail installations to head installations, kW/m^2. The *EW* can be expressed by an adjacent matrix (a square matrix of dimension $N \times N$), as follows:

$$EW = \begin{bmatrix} 0 & q_{12} & \cdots & q_{1n} \\ q_{21} & 0 & \cdots & q_{2n} \\ \cdots & \cdots & 0 & \cdots \\ q_{n1} & q_{n2} & \cdots & 0 \end{bmatrix} \tag{3.3}$$

where q_{ij} is the heat radiation from installation i to installation j. q_{ij} is equal to zero if there is no directed edge from installation i to installation j or i is equal to j. In the matrix, row i indicates the harmfulness of installation i for other installations, and column j characters the vulnerability of installation j.

3.3.2 Graph update

- Time update

A Domino Evolution Graph (DEG) can be regarded as a chain of static graphs. The initial graph (graph 1) arises when a primary scenario caused by unintentional or intentional events occurs. A new static graph will occur if an update operation is executed. The graph index (g) is also updated, as follows:

$$g = \begin{cases} 1 & \text{initial graph} \\ g+1 & \text{after a new update} \end{cases} \tag{3.4}$$

The period between two update operations is called “graph time” (t) in min. The total evolution time at the beginning of graph g (T_g, in min) can be obtained, as follows:

$$T_g = \begin{cases} 0 & g = 1 \\ T_{g-1} + t_{g-1} & g > 1 \end{cases} \tag{3.5}$$

- State update

There are two update types among the three states, as shown in Figure 3.1. In the initial graph, the damaged installation is in the “harmful” state and other installations are in the “vulnerable” state. An installation’s state will be updated from “vulnerable” to “harmful” if it is damaged by escalation from external installations. Besides, an installation in a “harmful” state will be updated to a “dead” state if the fire on the installation is extinguished. Finally, the update will end when there is no escalation under the following conditions: (i) no installation in the “vulnerable” state; (ii) no installation in the “harmful” state.

Figure 3.1 State transition of installations
(Chen et al., 2019b)

- Directed edge update

Directed edges connect installations in “harmful” states with installations in “vulnerable” states. Thus the directed edges should be added when any installation’s state is updated. All directed edges from other installations to an installation in a “vulnerable” state will be deleted and the directed edges from the installation to other installations will be added when the installation’s state transfers to “harmful”. The directed edges from an installation to other installations will be deleted when the installation’s state transfers to “dead”.

- Heat radiation update

Installations with a “vulnerable” state in a domino evolution process may receive heat radiation from multiple installations with “harmful” states; this is known as “synergistic effects”. Conversely, an installation in the “harmful” state may pose heat radiation on multiple installations being in “vulnerable” states; this is known as “parallel effects”. Figure 3.2a shows the graph model of a parallel effect while Figure 3.2b shows a synergistic effect as a graph.

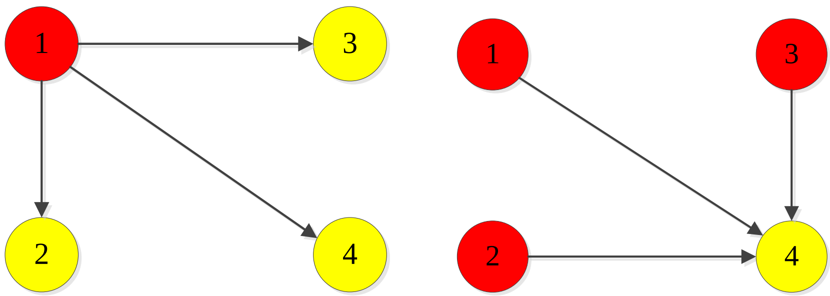

(a) Parallel effects (b) Synergistic effects
Figure 3.2 Graph models of the spatial evolution of domino effects
(Chen et al., 2019b)

According to the synergistic effect, the total heat radiation received by an installation *j* in a “vulnerable state” (Q_j) should be the sum of heat radiations received from other installations in “harmful” states, as follows:

$$Q_j = \sum_{i=1}^{N} q_{ij} \tag{3.6}$$

The heat radiation received by each installation may vary over time due to new occurrences of harmful installations or dead installations. For update operations, the potential heat radiation values between each pair of installations can be calculated by software such as ALOHA (ALOHA, 2016).

- Residual time to failure update

The *RTF* of installations may vary with time in the spatial-temporal evolution because of superimposed effects. Besides, passive protection systems also have great impacts on the *RTF*, such as fireproof coatings. Considering an installation *j* begins receiving effective heat radiation (Q_j > 15 kW/m^2 (Cozzani et al., 2009)) at evolution time T_g, the *RTF* can be calculated (Landucci et al., 2009a), as follows:

$$RTF_{j,\,g} = \frac{\exp\left(c_1 \times V^{c_2} + c_3 \ln(Q_j) + c_4\right)}{60} \tag{3.7}$$

Where $RTF_{j,g}$ is the residual time to failure of installation *j* at T_g, in min; c_1-c_4 are parameters related to vessel types, as presented in Table 3.2. Eq. (3.7) can also be rewritten, as follows:

$$60 \times RTF_{j,\,g} = \exp\left(c_1 \times V^{c_2} + c_4\right) \times Q_j^{c_3} \tag{3.8}$$

According to Eq. (3.7), $RTF_{j,g}$ is directly proportional to $Q_j^{c_3}$. If $RTF_{j,\,g} > t_g$, the installation *j* will not be physically damaged at T_{g+1} and the residual time to failure of installation *j* in the “vulnerable” state at the time T_{g+1}will be updated according to superimposed effects: the heat radiation in different stages received by an installation should be superimposed to determine the residual time to failure at the time of T_{g+1}, (Chen et al., 2018), as follows:

$$RTF_{j,\,g+1} = \left(\frac{Q_{j,\,g+1}}{Q_{j,\,g}}\right)^{c_3} \cdot \left(RTF_{j,\,\mathrm{g}} - t_g\right) \tag{3.9}$$

The $RTF_{j,\,g}$ is regarded as infinite when the installation *j* is in the “harmful” state or the “dead” state.

Table 3.2 The parameter value of c_1, c_2, c_3, and c_4 based on simulations (adapted from Landucci et al. (2009a))

Installation	c_1	c_2	c_3	c_4
Atmospheric tank	-2.67×10^{-5}	1	-1.13	9.9
Pressurized tank	8.845	0.032	-0.95	0

- Residual time to burn out update

Assuming an installation *i* is on fire at the evolution time of T_g, the residual time to burn out of installation *i* at the time of T_g can be represented by the ratio of flammable substance mass to the burning rate, as follows:

$$RTB_{i,\,g} = \frac{m_i}{v_i} \tag{3.10}$$

Where m_i is the mass of flammable substances in installation *i*, kg; v_i is the burning rate of flammable substances in installation *i*, kg/min; $RTB_{i,\,g}$ is the time to burn out of installation *i* at the evolution time of T_g.

If $RTB_{j,\,g} > t_g$, the installation *i* will continue to be on fire at T_{g+1} and the residual time to burning out of installation *i* at T_{g+1} will be updated, as follows:

$$RTB_{i,\,g+1} = RTB_{i,\,g} - t_g \tag{3.11}$$

- Damage probability update

Emergency response is essential for eliminating possible escalation or mitigating the consequence of domino effects in the chemical industry (Zhou and Reniers, 2016a). So emergency response should be considered in the vulnerability assessment of plant installations. However, the evaluation of emergency response is rather complex due to the uncertainties related to human factors in the performance of emergency response tasks. For simplification reasons, we assume that the domino effect evolution will be controlled when the emergency mitigation actions are started (Landucci et al., 2009a). Taking into account the uncertainty of emergency response, a cumulative log-normal distribution (LND) function is used to model the time required to control domino effects (*TTC*), as follows:

$$\log TTC \sim N\left(u, \sigma^2\right) \tag{3.12}$$

Where *u* is the mean of log *TTC* or expectation of the distribution; *σ* is the standard deviation of log *TTC* and σ^2 is the variance. These parameters can be obtained using Maximum Likelihood Estimation (MLE) based on the results of expert judgment, emergency exercises, or simulations. Therefore, if an installation *j* is supposedly damaged at T_g with a certain probability during the evolution, the conditional probability of installation *j* being damaged by domino effects ($P_{d,j}$) given a primary scenario can be obtained, as follows:

$$P_{d,j} = \left(1 - \mathrm{LND}\left(T_g\right)\right) \tag{3.13}$$

3.4 Algorithm

This section describes the algorithm based on the DEG model to obtain the evolution path, the evolution time of each graph, and the damage probability of installations due to domino effects, as shown in Figure 3.3. The Minimum Evolution Time (MET) algorithm is described and explained as follows. First, basic data needed for performing the method is inputted, including chemical industrial area information, potential heat radiations, and primary scenarios, etc. Then, the parameters (E, S, q) of the DEG model are initialized after selecting a primary scenario. Next, the *RTF* and *RTB* are calculated according to Eq. (3.7), Eq. (3.9), and Eq. (3.10). The initial DEG is updated at T_{g+1} when T_{g+1} is equal to the minimum value of RTF_i and RTB_i. The parameters of E, S, q are calculated again after updating. If q is equal to zero, the graph update will stop and the damage probability of each installation is calculated. Otherwise, the update will proceed.

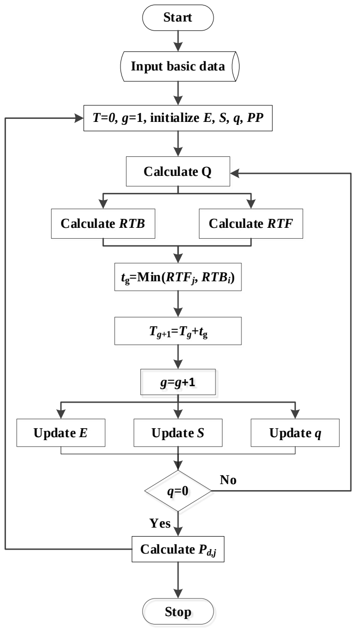

Figure 3.3 Flow diagram of the MET algorithm for the DEG model (Chen et al., 2019b)

3.5 Case study

In this section, illustrative examples aiming at interpreting the procedures and validation of the proposed method are given. Besides, the method is applied to a chemical cluster to show the method's advantages for such an implementation situation.

3.5.1 Example 1: A single plant

According to the dynamic graph approach, we first collect the plant information and installation data of the chemical plant, as follows. Figure 3.4 shows the schematic of an illustrative single chemical plant with four storage tanks. The features of these tanks are summarized in Table 3.3. The weather condition is assumed as follows: ambient temperature of 20℃, the wind blowing from the West with a speed of 1.5m/s, relative humidity of 50%, and a stability class D. The heat radiation caused by pool fire and the burning rate of each tank are calculated through the ALOHA software. The heat radiation caused by tank *i* on tank *j* (i.e., q_{ij}) and the time to burn out (*TTB*) of each tank is shown in Table 3.4. Assuming a log-normal distribution of the time to control effectively (*TTC*), the mean of *TTC* is equal to 10 min and the corresponding variance is equal to 2 min (Chen et al., 2018).

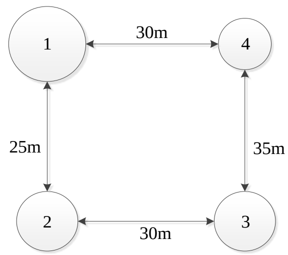

Figure 3.4 Layout of an illustrative chemical storage plant (example 1) (Chen et al., 2019b)

Table 3.3 Features of chemical storage tanks

Tank	Type	Dimension	Chemical substance	Volume (m^3)	Chemical content (t)	Consequence (1,000 EUR)
1	Atmospheric	30×10	Benzene	6000	4000	2900
2	Atmospheric	20×10	Acetone	2500	2000	2400
3	Atmospheric	20×10	Toluene	2500	1500	900
4	Atmospheric	10×6.5	Toluene	500	200	100

Table 3.4 The Heat Radiation q_{ij} and the time to burn out (*TTB*) of tanks

Tank *i, j*	q_{ij} (kW/m^2)				*TTB* (min)
	1	2	3	4	
1	-	32.5	25.1	12.9	1666.7
2	17.7	-	13.2	4.1	1369.9
3	8.7	17.6	-	13.8	980.4
4	10.1	3.5	8.3	-	233.9

The second step is to analyze possible threats and identify the corresponding primary scenarios. Table 3.5 illustrates the primary scenarios caused by possible intentional events and the conditional probability of primary scenarios (CPP) given an intentional attack.

Table 3.5 Possible primary scenarios caused by attacks

Attacks	Primary scenario	*CPP*
A1	Pool fire at Tank 1	0.5
A2	Pool fire at Tank 2	0.5
A3	Pool fire at Tank 3	0.5
A4	Pool fire at Tank 4	0.5

The DEG model proposed in this chapter is used to assess the vulnerability of the tanks in the chemical plant. In this step, the failure time and failure probability of each tank following escalation caused by attacks are obtained, as shown in Table 3.6 and Table 3.7.

Table 3.6 The damage time of tanks (min)

Tank	A1	A2	A3	A4
1	0	11.01	19.17	-
2	6.08	0	12.16	-
3	7.36	16.06	0	-
4	13.52	20.30	22.19	0

Table 3.7 The conditional probability of installations being damaged

Tank	A1	A2	A3	A4	AFP
1	0.50	0.11	6.71×10^{-7}	0	0.15
2	0.50	0.50	0.04	0	0.26
3	0.49	1.48×10^{-4}	0.50	0	0.25
4	6.70×10^{-3}	8.52×10^{-8}	2.45×10^{-9}	0.5000	0.13
ADP	0.50	0.31	0.27	0.13	0.20

Table 3.7 presents the damage probability of each Tank in different primary scenarios. It indicates that the domino effect caused by the attack on Tank 1 may be inevitable due to the fastest evolution. The average damage probability (ADP) represents the escalation capability of the attacked installations while the average failure probability (AFP) characterizes the vulnerability of installations. Thus installations are more likely to initiate or propagate domino effects if their rankings of *ADP* are higher than that of *ACP*. Alternatively, installations with higher rankings of *AFP* than that of *ADP* exhibit a high probability of being damaged by domino effects occurring in the area. Tank 2 with the highest *AFP* is more susceptible to domino effects caused by other tanks while scenario 1 with the highest *ADP* is more likely to cause domino effects.

Taking primary scenario 1 as an example to show the evolution process, Tank 1 is on fire caused by a direct intentional attack at $T = 0$ min (Figure 3.5a). The heat radiation emitted from Tank 1 can cause credible damage to Tank 2, resulting in a fire at Tank 2 at $T = 6.08$ min. After catching fire, the state of Tank 2 transfers from "vulnerable" to "harmful", inducing a synergistic effect on Tank 3 and Tank 4, as shown in Figure 3.5b. Consequently, Tank 3 is on fire at $T = 7.36$ min (Figure 3.5c) due to a superimposed effect of stage 1 and stage 2. Tank 4 is the last one to catch fire. The damaged time of each tank in different primary scenarios is shown in Table 3.6. The evolution speed of primary scenario 1 is the fastest while that of primary scenario 4 is the slowest.

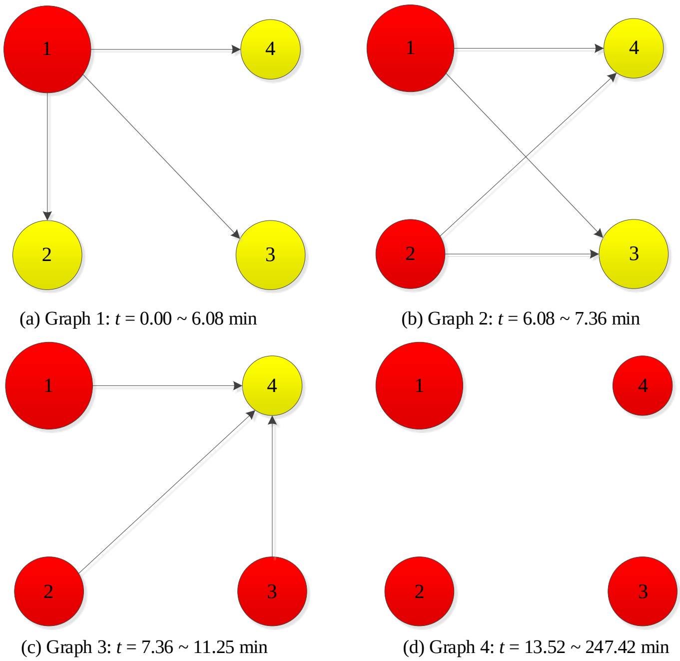

Figure 3.5 The DEG of the attack on Tank 1
(Chen et al., 2019b)

If the superimposed effect is neglected, the failure time of Tank 3 is much delayed (from 7.36 to 11.13 min) and the failure probability is largely underestimated (from 0.49 to 0.10). If the synergistic effect is ignored, Tank 3 catches fire at $T = 8.14$ and the failure probability is 0.46. Consequently, both the synergistic effect and the superimposed effect cannot be ignored in the evolution of domino effects. Besides, the attacks may result in the damages of multiple installations. Considering Tank 1 and Tank 2 are simultaneously on fire due to the attack at T=0, the failure time of Tank 3 decreases from 7.36 to 5.05, and the escalation may be inevitable since the conditional probability of escalation is equal to 1.0.

To validate the method, the results are compared with the results of a static graph approach (Khakzad and Reniers, 2015b). Employing the static graph methodology, the out-closeness metric reflects installations' potential contribution to the escalation of domino effects while the in-closeness metric represents the vulnerability of installations to get damaged during domino effects. The static graph model of the chemical storage plant is shown in Figure 3.6 (threshold value is also equal to $15kW/m^2$).

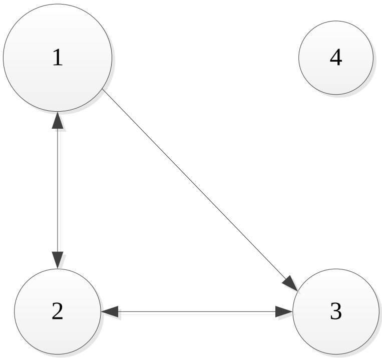

Figure 3.6 Static graph model of the chemical storage plant in example 1 (Chen et al., 2019b)

The results of two graph metrics (out-closeness and in-closeness) of the four tanks are illustrated in Table 3.8. It indicates that the method proposed in this study is valid since the ranking of units based on their out-closeness is the same as their ranking based on their *ADP* (Table 3.7); likewise, the ranking of units based on their in-closeness is also identical to their ranking based on their respective *AFP* (Table 3.7). The dynamic graph approach seems to be able to grasp the dynamic evolution of domino effects compared to the static graph which seems to provide merely a snapshot of the whole process at once.

Table 3.8 The results of graph metrics for the graph shown in Figure 3.6

Tank	Out-closeness	In-closeness
1	0.42	0.17
2	0.19	0.34
3	0.17	0.22
4	0	0

3.5.2 Example 2: A chemical cluster

A complex example is used to illustrate the application of the method to a chemical industrial park with a large number of installations. Figure 3.7 shows the layout of an area including three chemical storage plants. The plant information and tank data are shown in Table 3.9. All the tanks (150 in total) may be potentially attacked with the same conditional probability of successful attack (*CPS*) of 0.5. Assuming the mean of *TTC* (μ) is equal to 20 min and the corresponding variance (σ) is equal to 5 min. The wind speed is 5m/s and other parameters are the same as in example 1.

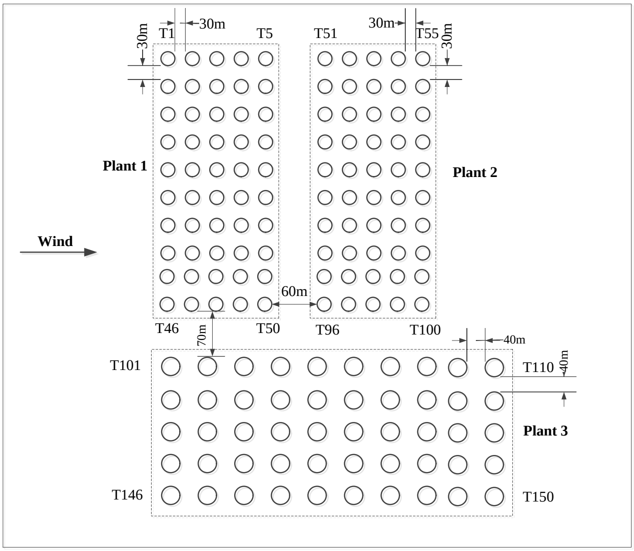

Figure 3.7 Layout of a chemical industrial park
(Chen et al., 2019b)

Table 3.9 Tank features in each plant

Plant	Tank number	Tank Type	Chemical substance	Volume of each tank (m^3)	Chemical content of each tank (t)	*TTB* of each tank (min)
1	50	Atmospheric	Toluene	2500	2500	1634
2	50	Atmospheric	Acetone	2500	1000	685
3	50	Atmospheric	Benzene	6000	2000	833

The average damage probability (*ADP*) of the 150 attack scenarios and the average failure probability (*AFP*) of the 150 installations are obtained via the algorithm presented in section 3.4, as shown in Figure 3.8. The total computational time is 4.1 s using a personal computer (Intel (R) Core (TM) i5 CPU, 4GB RAM). The maximum *ADP* in Plant 1 is 0.11 (an attack on Tank 26), in Plant 2 it is 0.03 (an attack on Tank 76), and in Plant 3 it is 0.09 (an attack on Tank 123). The *ADP* of attacks in Plant 2 are obviously smaller than those in Plant 1 and Plant 3 since the wind blows from west to east (i.e., the tank is more likely to be damaged by the heat radiation caused by the tank in the west), and the heat radiation caused by tanks in Plant 3 is greater than in Plant 2. The red curve in Figure 3.8 shows the *AFP* of each tank. The tanks located in the east have a higher *AFP* than those located in the west due to the effect of the wind. The maximum *AFP* in Plant 1 is 0.10 (Tank 30), in Plant 2 it is 0.03 (Tank 74), and in Plant 3 it is 0.09 (Tank 127).

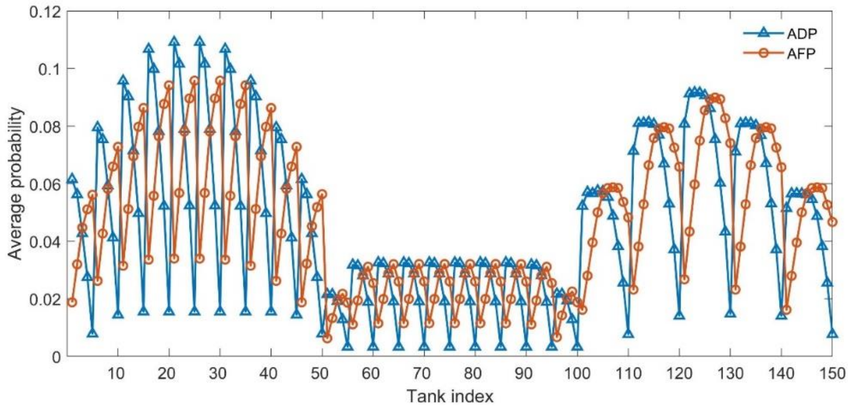

Figure 3.8 The ADP of each scenario and AFP of each installation
(Chen et al., 2019b)

Figure 3.9 shows the required time of external domino effects if a tank in Plant 1 is attacked. The minimum time required for initiating external domino effects in Plant 2 is 21.3 min with a maximum probability of 0.13, and that in Plant 3 is 26.5 min with a maximum conditional probability of 0.0024. The attacks in Plant 3 can also induce external domino effects in Plant 1 and Plant 2, and the maximum conditional probabilities are 0.21 and 0.23 separately. However, the external domino effects caused by attacks in Plant 2 may be impossible and Plant 3 is thus more likely to suffer from external domino effects since it is located downwind. The external domino effects can be eliminated by improving emergency response capabilities. For example, the maximum probability of external domino effects in Plant 3 triggered by Plant 1 will decrease to 2.19×10^{-4} if the emergency response time is shortened to 10 min.

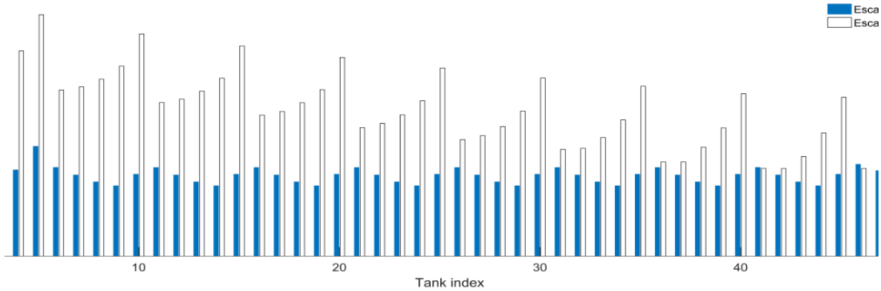

Figure 3.9 Required time of external domino effects
(Chen et al., 2019b)

3.6 Conclusions

In this chapter, an approach including a Domino Evolution Graph (DEG) model and a Minimum Evolution Time (MET) algorithm is proposed to model the spatial-temporal evolution of domino effects. The evolution process is divided into stages according to chronological order. All the graphs of a domino evolution process are sequentially connected by superimposed effects, making up a dynamic graph (Domino Evolution Graph). The Minimum Evolution Time (MET) algorithm based on the principle of minimum evolution time is proposed to solve the DEG model. The model results, including evolution graphs, evolution time, and the evolution probability, can be quickly obtained by using this algorithm. The results demonstrate that the dynamic graph approach can grasp the dynamic evolution of domino effects while the static graph seems to provide merely a snapshot of the whole process at once. The proposed methodology cannot only capture the spatial-temporal dimension but also overcome the limitation of the "probit model" in higher-level propagations. Besides, the results indicate that the synergistic effects and the superimposed effects have important repercussions on domino evolution and cannot be ignored. The primary scenario related to the damage of multiple installations cannot be ignored in which domino effects may be inevitable due to synergistic effects. This study is the first work to employ a dynamic approach modeling the spatial-temporal evolution of domino effects. The outcome of this research can be used to support the decision-making of safety and security barriers and emergency resources. Furthermore, this approach can also be extended to domino effect assessment related to multi-hazardous accident scenarios (fire, explosion, and toxic release).

Chapter 4 Modeling the dynamic evolution of VCE-induced domino effects

Vapor cloud explosion (VCE) accidents in recent years, such as the Buncefield accident in 2005, indicate that VCEs in process plants may lead to unpredicted overpressures, resulting in catastrophic disasters. Although many attempts have been made to assess VCEs in process plants, little attention has been paid to the spatial-temporal evolution of VCEs. This study, therefore, aims to develop a dynamic methodology based on the discrete dynamic Event Tree to assess the likelihood of VCEs and the vulnerability of installations. The developed methodology consists of six steps: (i) identification of hazardous installations and potential loss of containment (LOC), (ii) analysis of vapor cloud dispersion, (iii) identification and characterization of ignition sources, (iv) explosion frequency and delayed time assessment using the dynamic event tree, (v) overpressure calculation by the Multi-Energy method and (vi) damage assessment based on probit models. This methodology considers the time dependencies in vapor cloud dispersion and in the uncertainty of delayed ignitions. The application of the methodology to a case study shows that the methodology can reflect the characteristics of large VCEs and avoid underestimating the consequences. Besides, this study indicates that ignition control may be regarded as a delay measure. Effective emergency actions are needed for preventing VCEs.

The content of this chapter is based on the following published paper:

Chen, C., Khakzad, N., Reniers, G., 2020a. Dynamic vulnerability assessment of process plants with respect to vapor cloud explosions. Reliability Engineering & System Safety 200. 10.1016/j.ress.2020.106934

4.1 Introduction

In petroleum and chemical industrial plants, fire, explosion and toxic release arising from loss of containment (LOC) are concerned as major hazards (Pietersen, 1990; Lees, 2012; Chen et al., 2020c). Fire is the most common major scenario while explosion may impact a wider area and cause severe consequences, leading to multiple fatalities and extensive damage to property (Khan and Abbasi, 1999). Concerning the amount and rate of vaporization, large releases often result in vapor cloud explosion (VCE) rather than fires (Bellamy et al., 1989). Abdolhamidzadeh et al. (2011) investigated 224 domino accidents that occurred in the process industries and indicated that explosion is the most frequent cause of domino effects (57%). VCE has been responsible for 84% of the domino effects induced by explosions. Several catastrophic accidents occurred in recent years due to VCEs, such as the Puerto Rico explosion (2009, USA), the Sitapura explosion (2009, India), and the Amuay explosion (Venezuela, 2012). The Amuay disaster caused by a large VCE at the Amuay refinery, situated in northwestern Venezuela, led to over 50 fatalities and more than 100 injures, damaging 1600 houses and resulted in financial losses up to $1 billion (Mishra et al., 2014; Schmidt et al., 2016).

Although VCEs have frequently occurred in the petroleum and chemical industries, the mechanism of the blast is not well understood (Taylor, 2003). For example, the VCE in the Buncefield depot, in the UK, brought about an unexpected overpressure with the maximum value of more than 2000 kPa (Taveau, 2012). A release of hazardous substances can induce a fire if the released substance is immediately ignited while it is more likely to result in a VCE when the ignition is delayed. The subsequent fast expansion of flames produces the overpressure or so-called shock wave, resulting in damaging effects (Uijt de Haag and Ale, 1999). Many factors influence the evolution and the intensity of a VCE, including the type and quantity of the released flammable substance, the delayed time to ignition (DTI), the space figuration of the release position, the position and the number of ignition sources in the affected area, etc. (Assael and Kakosimos, 2010).

Many attempts have been conducted to model the vapor cloud dispersion or estimate the overpressure created by VCEs. The TNT equivalent method (Van den Berg and Lannoy, 1993) is the most widely used method in risk analysis (Lea and Ledin, 2002; Cozzani and Salzano, 2004b). This method provides a simple method for estimating a far-field blast effect, neglecting the space configuration where the explosion takes place, ignition sources and the dispersion of the vapor cloud, thus usually underestimating the overpressure (Baker et al., 1996; Van Den Bosh and Weterings, 1997). The Multi-Energy method based on the gas explosion mechanism, which considers the VCE as a number of sub-explosions inside special obstructed areas, is recommended as an alternative method for the TNT equivalent method (Uijt de Haag and Ale, 1999). This method is more suitable for estimating the significant overpressure produced by a large VCE in fuel storage plants (Taveau, 2012; Mishra et al., 2013, 2014). Other widely used overpressure evaluation methods for VCEs include the Baker-Strehlow method (Baker et al., 1998) and CFD simulation (Qiao and Zhang, 2010; Tauseef et al., 2011).

Compared with fire scenarios, the VCE phenomenon is more difficult to assess due to the uncertainty of ignition position, the uncertainty of delayed ignition time (DIT) and the complexity of overpressure intensity calculation. In fact, the VCE induced by the LOC of hazardous substances in chemical plants is a dynamic process along with the vapor cloud dispersion. However, previous risk analysis methods (Ramírez-Marengo et al., 2015; Sierra et al., 2018) for VCE always assume that the explosion takes place immediately at the release place, which is inconsistent with the observations from large VCEs in the recent years. The position of a vapor cloud explosion depends on the vapor cloud dispersion and ignition sources that can be inside or outside chemical plants. On November 28, 2018, a vapor cloud explosion outside a chemical plant at Zhangjiakou (China) was for instance caused by a Vinyl chloride release inside the plant, leading to 23 fatalities and 22 injuries (Chen and Reniers, 2020).

The present study aims to establish a dynamic risk assessment methodology based on a discrete dynamic event tree (DDET) to integrate plant physical models and ignition sources into a stochastic simulation engine to model the timing dependencies and ignition uncertainty in the evolution of VCEs. The overpressure induced by VCE is calculated by the Multi-Energy method while the damage probability of installations is calculated using probit models. VCE, its characteristics, and previous studies are represented in Section 4.2. Section 4.3 illustrates the dynamic accident evolution methodology. A case study is presented in Section 4.4 and a discussion based on the results is present in Section 4.5. Finally, conclusions are drawn in Section 4.6.

4.2 Vapor cloud explosion

4.2.1 Explosion mechanism

A flammable vapor cloud (FVC) is formed by mixing released flammable gases or evaporated flammable liquids and air during the leakage of flammable substances. Flash fire (FF) and VCE are the possible consequences of vapor cloud ignition. The ignition may take place if the concentration of flammable gases lies within the flammability limits (between the lower flammability limit and the upper flammability limit) and an ignition source is present for supplying the required energy (usually of the order of 10 J). FFs can result from the sudden ignition of a FVC, where the flame is not accelerated due to insufficient obstacles or the influence of turbulent dispersion. Alternatively, the flame speed may accelerate to sufficiently high velocities and produce significant blast overpressure (Assael and Kakosimos, 2010).

The expansion mechanism of a VCE can be analyzed according to the flame speed which is proportional to the developed overpressure. Following an ignition, the flame starts to propagate away from the point of ignition, with a speed of 5-30 m/s, producing very low overpressure. Next, a wrinkled-flame front appears due to the unstable nature of the flame and large turbulent eddies, resulting in an increase of the flame surface and thus an acceleration of flame speed (30-500 m/s.) and forming an overpressure of up to 2-3 mbar. The presence of obstacles in the flow induces a further increase in the flame speed (500-1,000 m/s), leading to an overpressure of up to 1 bar. This physical process of flame speed acceleration is a deflagration. If the flame speed continues to increase, and the reactive mixture in the front zone of turbulent combustion is compressed and heated due to mixing with combustion products, a shock wave can be created when the reactive mixture's temperature is higher than the self-ignition. This physical effect is called detonation, resulting in a flame speed up to 2,200 m/s and overpressures up to 20 bar. Johnson and Tam (2017) explained the large VCEs in industrial plants by using the deflagration to detonation transition (DDT) while Atkinson et al. (2017b) demonstrated that episodic deflagrations might be responsible for very large VCEs due to natural flame instability. Consequently, the VCE mechanisms need to be further studied in the future since there is no consistent statement to explain the VCEs in open areas.

4.2.2 Impact assessment of vapor cloud explosions

The available models to simulate or predict the effects of vapor cloud explosions can be categorized as empirical analytic models and numerical models. The empirical analytic models include Congestion Assessment method, TNT Equivalent method, Multi-Energy method, Baker-Strehlow method, etc. (Lea and Ledin, 2002) while numerical models are mainly based on CFD codes, such as Flacs and Fluent (Tauseef et al., 2011; Dasgotra et al., 2018).

(1) Multi-Energy method

The Multi-Energy method is based on gas explosion mechanism that regards the VCE as a number of sub-explosions inside special obstructed areas (Uijt de Haag and Ale, 1999). The layout of the space where the cloud is spreading is characterized as a strength coefficient in this method. The value of the coefficient is proportional to the blast overpressure which increases with augmenting the obstacle density in the area. In general, the TNT equivalent method can be used to quickly calculate the overpressure as a function of the distance while the results of Multi-Energy method is usually more accurate and closer to actual conditions (Assael and Kakosimos, 2010).

(2) Baker-Strehlow method

The Baker-Strehlow method (Baker et al., 1998), based on the Multi-Energy method, takes into account the flame propagation speed. The flame propagation speed depends on the way the flame front propagates, the reactivity of the fuel, and the density of the obstacles (Lea and Ledin, 2002).

(3) Numerical models

Numerical methods based on CFD codes have received much attention in recent years (Maremonti et al., 1999; Qiao and Zhang, 2010; Tauseef et al., 2011). These methods are able to model the effects of terrain shape and the presence of obstacles on the dispersion of a vapor cloud (Gant and Atkinson, 2011). The CFD simulation of the whole industrial facility can lead to more accurate results, but it is very complex, time-consuming and expensive, thus may be unsuitable for risk analysis of large and complex process plants (Assael and Kakosimos, 2010). The accuracy of CFD codes especially in the case of VCE simulation in congested environments depends upon the adopted combustion models, turbulence closure models and the constants for the computation of turbulence and the description of the complex interaction between fame front and turbulent flow field (Maremonti et al., 1999).

4.2.3 Frequency assessment of vapor cloud explosions

Event tree has been widely employed to analyze scenarios and frequencies of accidents induced by a LOC event in the process and chemical industries (Moosemiller, 2011; Badri et al., 2013; Ramírez-Marengo et al., 2015; Khakzad et al., 2016; Alileche et al., 2017). Figure 4.1 shows a general event tree analysis for the release of hazardous liquid substances from an atmospheric storage tank.

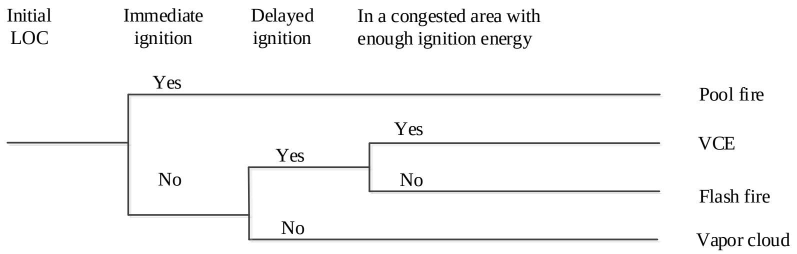

Figure 4.1 General event tree analysis for LOC-induced accident scenarios (Chen et al., 2020a)

Following a LOC event, a pool fire scenario can occur if the released substance is ignited immediately. Otherwise, the released substance would vaporize and form a vapor cloud. In case of a delayed ignition, A FVC can induce a VCE or FF during the dispersion process. If there is no immediate ignition and delayed ignition, the release event may form a large hazardous vapor cloud that may be harmful to surrounding people or damage the environment.

Assessment of fire accidents triggered by immediate ignition based on the general event tree analysis is reasonable since there is no delay, and the fire can be regarded to occur at the release position. However, it ignores the uncertainty of delayed ignition time (DIT) and the uncertainty of ignition and the uncertainty of delayed ignition position that is essential for the assessment of VCEs. First, the size of the vapor cloud increases over time, which has a great impact on the ignition likelihood and the explosion intensity. Conversely, the ignition position also influences the explosion intensity and the damage effects on other installations. Table 4.1 lists the DIT values of several large VCE accidents that occurred in the process and chemical industry (U.S. National Transport Safety Board, 1993; Dweck et al., 2004; Chang and Lin, 2006; Johnson, 2013; Mishra et al., 2014; CSB, 2015; Atkinson et al., 2017a).

As shown in Table 4.1, the DIT values range from 20s to 4500s and ignition source areas can be inside (e.g., pump house, wastewater treatment areas) or outside (e.g., vehicles) chemical plants. Therefore, neglecting the uncertainties caused by vapor cloud dispersion may result in significant errors. Besides, most of these accidents occurred in no-wind or low-wind conditions, which indicates that stable and large vapor clouds are more likely to form in these weather conditions (Atkinson et al., 2017a; Atkinson et al., 2017b).

Table 4.1 A summary of DIT values and ignition sources in VCE incidents

Incident	Plant type	Ignition source	DIT (s)
Flixborough, UK 1974	Chemical plant	Reactor	20-30
Newark, NJ 1983	Gasoline storage	Incinerator	> 900
Brenham, TX 1992	LNG storage	Driving car	3600
Skikda, Algeria 2004	LNG facility	Boiler explosion	< 300
Buncefield, UK 2005	Gasoline storage	Pumphouse	1380
San Juan, Puerto Rico 2009	Gasoline storage	Wastewater treatment area	1560
Jaipur, India 2009	Gasoline storage	Control room	4500
Amuay, Venezuela 2012	LPG storage	Vehicle	4080
Zhangjiakou, China 2018	Chemical plant	Furnace	418

4.3 Dynamic vulnerability assessment methodology

Although a lot of work has been done on the vulnerability of installations subject to vapor cloud explosion caused by LOC, the spatial-temporal evolution of such accidents has been overlooked. However, the vulnerability of installations depends on the intensity of overpressure caused by the VCE which is relevant to the spatial-temporal evolution of vapor clouds before ignition. This section thus aims to establish a dynamic VCE evolution assessment (DVEA) methodology, integrating the dispersion process of vapor cloud and ignition uncertainty into a stochastic simulation engine to assess the vapor cloud explosion risk in process industrial areas. The flow chart of the DVEA methodology is shown in Figure 4.2. The subsequent steps of the methodology are more thoroughly explained in the following subsections.

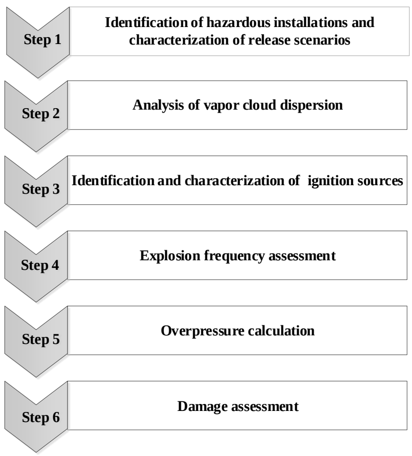

Figure 4.2 Flow chart of DVEA methodology procedures
(Chen et al., 2020a)

4.3.1 Step 1: Identification of hazardous installations and characterization of LOC scenarios

In process industrial areas, large quantities of hazardous (flammable/ explosive/ toxic) substances are handled, transported, and stored via all kinds of installations, such as process vessels, pipelines, valves, flanges, heat exchangers, pumps, storage tanks, etc. The inherent hazard of an installation depends on the quantity of substance present, the hazardous properties of the substance as well as the specific operation conditions (e.g., temperature, pressure) (Cozzani et al., 2009). Since this study mainly focuses on fire and explosion accidents, the toxic effects of hazardous substances are ignored. Therefore, only the hazardous installations that may become a release source of flammable or explosive substances are identified in the first step of the developed methodology.

Following the identification of hazardous installations, the loss of containment (LOC) events should be characterized to obtain the LOC scenarios and the corresponding frequency of each scenario. Both LOCs caused by unintentional events and intentional events should be identified in this step. The former should include generic LOCs, external-impact LOCs, loading and unloading LOCs, and others (Uijt de Haag and Ale, 1999). Generic LOCs cover all failure causes not considered explicitly, such as corrosion, construction errors, welding failures, and blocking of tank vents. External-impact LOCs are tailored for transport units. Loading and unloading LOCs are those that occur during loading and unloading operations (Chen et al., 2019a), such as overfilling. To estimate the frequency of LOCs, some specific information may be employed. In terms of intentional LOCs (e.g., deliberately opening valves (Villa et al., 2017b)), security risk analysis according to available information should be conducted, including threat analysis, attractiveness analysis, vulnerability analysis, and consequence analysis, etc. (Baybutt, 2017; Khakzad et al., 2018d; Reniers et al., 2018b). Based on the analysis of LOC scenarios, the parameters used for vapor cloud analysis such as initial pressure and temperature of hazardous substances in facilities, the mass of hazardous substances, and the possible leak sizes should be characterized.

4.3.2 Step 2: Analysis of vapor cloud dispersion

The results of hazardous installation identification and LOC scenario characterization such as release position, maximum release time, and mass flow rate, are the prerequisite for the formation and dispersion analysis of a vapor cloud. This step serves, therefore, to model the vapor cloud dispersion process over time, achieving the vapor cloud volume and position over time. The total release mass (M_t) at time t (the initial release time is zero) for a time-varying release scenario can be expressed as the integral of the mass flow rate (m_t) with respect to time:

$$M_t = \int_0^t m_t \, \mathrm{d}t \tag{4.1}$$

where m_t is the mass flow rate which can be represented as a function of time t. In order to simplify the calculation, the time period t can be divided into n discrete segments, then m_t can approximately be expressed as the sum of the masses in each segment, as shown in Eq (4.2). If the mass flow rate can be regarded as a constant (m) independent of release time, Eq. (4.2) can also be simplified as Eq. (4.3)

$$M_t = M_{t_1} + M_{t_2} + M_{t_3} + \ldots + M_{t_n} \tag{4.2}$$

$$M_t = m \times t \tag{4.3}$$

The mass flow rate m of a leakage from a hole can be obtained by using Eq. (4.4) as follows [11]:

$$m = \begin{cases} C_d A_h P_o K \sqrt{\dfrac{W_g}{\gamma RT}} & \text{leakage of gases} \\ C_d A_h \sqrt{2\left(P - P_a\right)} & \text{leakage of liquids} \end{cases} \tag{4.4}$$

where C_d represents the discharge coefficient; A_h (m^2) denotes the cross-sectional area of the leakage hole; P_o (Pa) denotes the initial gas pressure in the vessel (for each time step); W_g (kg/mol) represents the molecular weight of the gas; γ denotes the Poisson ratio; R represents the universal gas constant (8.314 $Jmol^{-1}K^{-1}$); T (K) denotes the temperature of the gas; Pa (Pa) represents the ambient pressure; ρ (kg/m^3) represents the density of the liquid. Other methods for the calculation of leak rates were also developed (Van Den Bosh and Weterings, 1997; Assael and Kakosimos, 2010).

The mass of the flammable substance in the vapor cloud $M_{f,t}$ is represented as the released mass multiplied by the ratio of the evaporation rate to flow rate α which is equal to 1 if the released substance is a gas. In that case, the volume of the flammable gas ($V_{f,t}$) is represented as:

$$V_{f,t} = \frac{\alpha \times M_{f,t}}{\rho_f} \tag{4.5}$$

where ρ_f is the density of the flammable gas. A vapor cloud is deemed as a mixture of air and flammable gas. As a result, the total volume of the vapor cloud (V_t) can be obtained as:

$$V_t = V_{f,t} + V_{a,t} \tag{4.6}$$

where $V_{a,t}$ is the volume of air mixed in the vapor cloud. $V_{a,t}$ can be determined by considering that the flammable gas is fully mixed with oxygen (Assael and Kakosimos, 2010).

In the Multi-Energy method, the vapor cloud shape is modeled as a hemisphere (Van den Berg and Lannoy, 1993). Figure 4.3 shows a sketch of the vapor cloud hemisphere model and the possible hazardous installations, ignition sources, and obstacles covered by the vapor cloud. In that case, the boundary of the vapor cloud can be characterized by the radius of the hemisphere (R_t), as shown in Eq. (4.6).

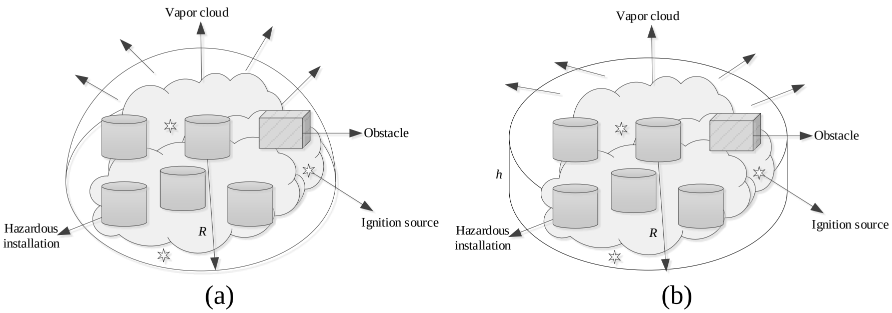

Figure 4.3 A sketch of vapor cloud dispersion in a process industrial plant ((a) hemispherical model and (b) cylindrical model, adapted from Chen et al. (2020a))

$$R_t = \left(\frac{3V_t}{2\pi}\right)^{\frac{1}{3}} \tag{4.7}$$

In terms of dense gas, a cylindrical shape (CCPS, 1996; Uijt de Haag and Ale, 1999; Atkinson and Coldrick, 2012) can be used to model the dispersion process, as shown in Figure 4.3b. The dispersion is characterized by a consistent height *h* and a radius of *R*, as follows:

$$R_t = \left(\frac{V_t}{h\pi}\right)^{\frac{1}{2}} \tag{4.8}$$

However, the height of the vapor cloud varies with the cloud location and evolves. Besides, it can not address dilution effects and meteorological conditions such as wind. In this study, a simplified gravity-driven model developed by Atkinson (2017) is adopted to model the dispersion of dense gas, as follows:

$$R_t = \left(\frac{4}{3}\right)^{0.75} C_E^{\,0.5} \left(\frac{g'}{2\pi}\right)^{0.25} Q_v^{\,0.25} t^{0.75} \tag{4.9}$$

C_E is an empirical constant and varies from 0.91 to 1.15. Q_v is the vapor cloud flow rate, g' is the relative density of the vapor. This method is developed based on experiments and simulation results in low-wind conditions in which most large VCE accidents occurred; it is, therefore, more conservative to model the vapor cloud dispersion when wind velocity is very low. (From a risk assessment perspective, it is more conservative as it would result in more devastating shock waves). Besides the analytical methods based on the hemisphere or cylinder assumption, the available software for dispersion modeling includes ALOHA (Tseng et al., 2012), PHAST (Zarei et al., 2013), EFFECTS (Gexcon, 2018a), etc. CFD software such as FLUENT (Tauseef et al., 2011), CFX (Qi et al., 2010), and FLACS (Dasgotra et al., 2018) may obtain more accurate results by addressing meteorological parameters, salient relief, and plant layout. In this study, analytical methods are adopted to model vapor cloud dispersion since a large number of release scenarios may involve risk assessment, overcoming the time-consuming aspect of CFD software.

4.3.3 Step 3: Identification and characterization of ignition sources

Identification and characterization of ignition sources is a critical step for the dynamic accident evolution assessment given a LOC event. The first task of this step is to identify ignition sources that may contribute to immediate ignition or delayed ignition, such as flare, boiler, and vehicles. In the chemical and process industries, measures for eliminating possible ignition sources are regarded as a significant and practical way to reduce the risk of fire and explosion; such measures may include decreasing the flow rate during loading and unloading operations for preventing static electricity and ground rods for preventing lightning. However, it is impossible to eliminate all ignition sources in an industrial environment. Besides, the ignition sources outside the industrial area have been responsible for some large vapor cloud explosion accidents that occurred in the chemical and petrochemical industries (Dweck et al., 2004; Mishra et al., 2014). Therefore, this step should identify as many as possible ignition sources within the chemical plant as well as outside the chemical plant. In other words, the possible ignition sources within the maximum area of the vapor cloud should be identified, no matter whether they are (in the chemical plant or not). The maximum vapor cloud can be determined by the dispersion model recommended in Step 2, under the premise that the hazardous substance inside the installation is completely released.

As shown in the event tree in Figure 4.1, ignition can be divided into immediate ignition and delayed ignition. Immediate ignition is defined as ignition at or near the release source and occurring quickly enough to preclude the formation of an appreciable vapor cloud (Moosemiller, 2011). Thus, the immediate ignition depends upon both the likelihood of autoignition and the likelihood of static discharge, which can be deemed as irrelevant to release time and vapor cloud dispersion. The probability of autoignition (P_{Aut}) and the probability of static discharge (P_{Sta}) can be determined as follows (Moosemiller, 2011):

$$P_{\mathrm{Aut}} = 1 - 5000\mathrm{e}^{-9.5(RT/AIT)} \tag{4.10}$$

$$P_{Sta} = 0.0024\left(RP / MIE^{2}\right)^{1/3} \tag{4.11}$$

AIT (F) is the autoignition temperature, *MIE* (mJ) is the minimum ignition energy, *RT* (F) is the actual release temperature, and *RP* (psig) is the pressure of the release source. The values of *AIT* and *MIE* for some common chemicals are presented in

Appendix (Table A.2). If $\frac{RT}{AIT} < 0.9$, $P_{Aut} = 0$ while $P_{Aut} = 1$ when $\frac{RT}{AIT} > 1.2$. This method assumes that there is always a likelihood of non-immediate ignition if T is no more than 200°C and higher than the AIT. These correlations were developed based on a combination of ignition data and expert judgments. Therefore users should use these correlations with discretion, select conservative values of input parameters, and should not read more accuracy into their predictions than is warranted (Moosemiller, 2011). Certainly, other correlations and data can be easily included in the developed methodology according to different users and applications.

A delayed ignition can be defined as any ignition other than immediate ignition, where there is a delayed time that allows the formation and dispersion of a vapor cloud. More ignition sources may involve in the accident evolution due to the vapor cloud dispersion. The cumulative probability of ignition caused by an identified ignition source (IS) can be modeled as a function of time when the ignition source is present in the vapor cloud (t_{IS}) and the ignition effectiveness (ω), as shown in Eq. (4.12) (Uijt de Haag and Ale, 1999).

$$P_{IS} = 1 - e^{-\omega t_{IS}} \tag{4.12}$$

The ignition effectiveness ω (s^{-1}) depends on a lot of factors, such as ignition source types, ignition energy, ignition control measures, etc. (Rew and Daycock, 2004; Šrekl and Golob, 2011). The estimation of ω is a key step in the assessment of the delayed ignition probability of a flammable vapor cloud. In this study, we adopt the ignition probability estimation method developed by HSE (Rew and Daycock, 2004), considering the type of hazardous area, properties of on-site ignition sources (strength, frequency and duration of activity, and density), and ignition control measures in place. Since the ignition probability is expressed by an exponential time-independent function, the probability of ignition is equal to the probability of ignition in one minute which in turn can be used to calculate the ignition effectiveness. It should be marked that this equation can only be used when the ignition source is active and covered by the vapor cloud. Therefore, the cumulative probability should be equal to zero before the ignition source is active or before the vapor cloud arrives. In terms of the ignition caused by vehicles on a road or railway near the plant, the ignition probability can be determined by the average traffic density d. The average traffic density d is defined as:

$$d = N_v L / v \tag{4.13}$$

N_v is the number of vehicles per hour, L is the length of a road or railway section, v is the average velocity of the vehicle. Therefore, the ignition probability caused by vehicles on a road or a railway can be calculated using Eq. (4.14) (Uijt de Haag and Ale, 1999).

$$P_{IS} = \begin{cases} d\left(1-e^{-\omega t_{IS}}\right) & d \le 1 \\ 1-e^{-d\omega t_{IS}} & d > 1 \end{cases} \tag{4.14}$$

4.3.4 Step 4: Explosion frequency and delayed time assessment

This step aims to assess the explosion frequency and the temporal dependencies caused by a LOC event in process plants using a dynamic probabilistic tool. The widely used dynamic probability tools include dynamic event tree (Acosta and Siu, 1993), dynamic fault tree (Dugan et al., 1992), dynamic bow-tie (Khakzad et al., 2012), dynamic Bayesian network (Khakzad, 2015) and Monte Carlo simulation (Durga Rao et al., 2009). Siu (1994) classified dynamic risk assessment methods into three categories: digraph-based methods (e.g., dynamic event tree), explicit state-transition methods (e.g., explicit Markov chain models) and implicit state-transition approaches (e.g. discrete event simulation). Dynamic event tree is recommended as a typical digraph-based tool for modeling system evolution while considering its stochastic behavior and possible dependencies among failure events (Siu, 1994; Aldemir, 2018). In order to directly present the accident evolution process and the possible accident scenarios, a discrete dynamic event tree (DDET) is employed in the present study. The DDET is used as a framework to simulate and analyze the dynamic interactions among the vapor cloud dispersion and ignition sources, as shown in Figure 4.4.

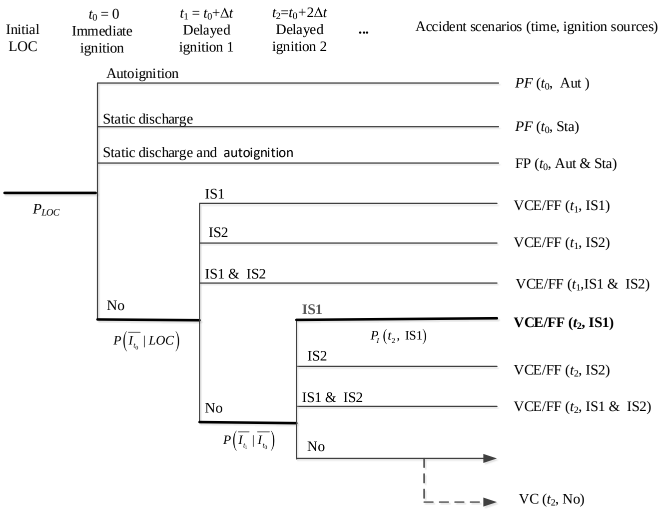

Figure 4.4 A discrete dynamic event tree for accident evolution assessment (Chen et al., 2020a)

Figure 4.4 shows a VCE evolution process with four ignition sources: autoignition, static discharge, ignition source 1, and ignition source 2. Taking the scenarios marked in bold as an example, the probability of VCE/FF caused by the ignition of source 1 at t_2, can be obtained:

$$P_{t_2,IS1,VCE} = P_{LOC} P\left(\overline{I_{t_0}} \mid LOC\right) P\left(\overline{I_{t_1}} \mid \overline{I_{t_0}}\right) P\left(I_{t_2,IS1} \mid \overline{I_{t_1}}\right) P\left(VCE \mid I_{t_2,IS1}\right) \quad (4.15)$$

$$P_{t_2,IS1,FF} = P_{LOC} P\left(\overline{I_{t_0}} \mid LOC\right) P\left(\overline{I_{t_1}} \mid \overline{I_{t_0}}\right) P\left(I_{t_2,IS1} \mid \overline{I_{t_1}}\right) P\left(FF \mid I_{t_2,IS1}\right) \quad (4.16)$$

where $P_{t_2,IS1,VCE}$ is the probability of VCE caused by ignition source 1 at t_2, $P_{t_2,IS1,FF}$ is the probability of FF caused by ignition source 1 at t_2, $P\left(VCE \mid I_{t_2,IS1}\right)$ is the conditional probability of VCE given delayed ignition caused by ignition source 1 at t_2, $P\left(FF \mid I_{t_2,IS1}\right)$ is the conditional probability of FF given delayed ignition caused by ignition source 1 at t_2, $P\left(I_{t_2,IS1} \mid \overline{I_{t_1}}\right)$ is the conditional probability of the delayed ignition caused by ignition source 1 at t_2 given no ignition before time t_1, $P\left(\overline{I_{t1}} \mid \overline{I_{t0}}\right)$ is the conditional probability of no ignition before time t_1 given no immediate ignition at time t_0, $P\left(\overline{I_{t_0}} \mid LOC\right)$ is the probability of no immediate ignition at time t_0 given a LOC event, and P_{LOC} is the probability of the LOC event. According to Eq. (4.17), $P\left(I_{t_2,IS1} \mid \overline{I_{t_1}}\right)$ can be calculated as:

$$P\left(I_{t_2,IS1} \mid \overline{I_{t_1}}\right) = \left\{P_{IS1}(t_2) - P_{IS1}(t_1)\right\} - \left\{P_{IS1}(t_2) - P_{IS1}(t_1)\right\}\left\{P_{IS2}(t_2) - P_{IS2}(t_1)\right\} \quad (4.17)$$

where $P_{IS1}(t_2)$ is the ignition probability of source 1 before time t_2, $P_{IS1}(t_1)$ is the ignition probability of source 1 before time t_1, $P_{IS2}(t_2)$ is the ignition probability of source 1 before time t_2, $P_{IS2}(t_1)$ is the ignition probability of source 2 before time t_1.

To simplify the calculation, a constant time step ($\Delta t = t_{i+1} - t_i$) is recommended in dynamic event tree analysis. The value of Δt should be determined based on the required calculation accuracy and the needed calculation time. The event tree will end when the probability of the vapor cloud is less than a threshold, which means that the accident scenarios with a probability lower than the threshold can be ignored.

4.3.5 Step 5: Overpressure calculation

In this section, the Multi-Energy method is introduced to calculate the overpressure of VCE scenarios identified in Step 4. To apply the method, two parameters should be determined: (i) strength coefficient and (ii) scaled distance. The coefficient of the strength which characterizes the strength of the explosion blast depends on the obstacle density of the explosion area. The coefficient ranges from 1 to 10 and increases with the increase of obstacle density. The obstacle density is used to characterize the congestion level of the area covered by a vapor cloud. Low obstacle density is defined for areas in which there are few obstacles in the flame path, or the obstacles are widely spaced and there are only one or two layers of obstacles. High obstacle density areas have three or more closely spaced obstacle layers with a blockage ratio of 40% or more (Van Den Bosh and Weterings, 1997). Since obstacle density is the most difficult to quantify in the Multi-Energy method, uncertainty exists in the determination of the strength coefficient. As a result, the coefficient value may be determined by using guidance. Appendix A.2 describes the guidance adopted in this study for estimating the strength coefficient (*SC*). Since it may be difficult for users to determine the value of the strength coefficient, a conservative value is recommended by TNO (The Netherlands Organization for Applied Scientific Research) to avoid underestimating the blast strength (Van Den Bosh and Weterings, 1997). The scaled distance (r_{sc}) is calculated by Eqs. (4.18) and (4.19).

$$r_{sc} = \frac{r}{\left(E / P_a\right)^{1/3}} \tag{4.18}$$

$$E = M_f \times \Delta H \tag{4.19}$$

where E (J) is the total combustion energy; P_a (Pa) is the ambient pressure; r (m) is the distance from the center of the explosion; ΔH (J/kg) is the combustion heat of the flammable gas. The scaled overpressure (P_{sc}), as a function of the scaled distance and the strength coefficient of the explosion blast, can be read from a blast chart (Van den Berg, 1985), as shown in Appendix A.2. As a result, the overpressure can be obtained as:

$$P_o = P_{sc} \times P_a \tag{4.20}$$

It should be marked that the uncertainty exists in each commonly used calculation method for the VCE. For example, the main uncertainty parameter in the Equivalent TNT Mass method is the fraction of energy released as shock wave (coefficient f_E), while in the Multi-Energy method the unknown parameter is the coefficient of the strength of the explosion blast.

4.3.6 Step 6: Damage assessment

To address the uncertainty of domino escalation and support for vulnerability assessment of installations subject to domino effects induced by a VCE, probability models were used to assess the vulnerability of installations. Bagster and Pitblado (1991) proposed a probability approach defining a damage probability function based on the distance from the center of primary scenarios and the safety distance. Khan and Abbasi (1998a) adopted a probit function to model the damage probability caused by overpressure, considering peak overpressure (static pressure) and dynamic pressure. The probit function was first developed by Eisenberg et al. (1975) and only peak overpressure was considered in the literature, as shown in Eq. (4.21).

$$Y = c_5 + c_6 \ln(\Delta P) \tag{4.21}$$

where $\triangle P$ (Pa) is the peak overpressure; Y is the probit value; c_5 and c_6 are constants. Then the damage probability P_r can be calculated using the cumulative standard normal distribution (Φ), as shown in Eq. (4.22).

$$P_r = \Phi(Y - 5) \tag{4.22}$$

Cozzani and Salzano (2004b) developed probit models for each category of equipment (atmospheric, pressurized, elongated, and small) rather than using a general model for all equipment. The equipment-specific models significantly reduced the error caused by the general probit model, presenting the important difference between the damage probabilities and the damage threshold of different categories of equipment. Therefore, this study adopts these special probit models to estimate the damage probability of installations.

4.4 Case study

The large VCE accident in the Buncefield oil storage and transfer depot, 4.8 km from the town center of Hemel Hempstead, Hertfordshire, on 11 December 2005 (Buncefield Major Incident Investigation Board, 2008), is used as a case study to illustrate the developed methodology.

4.4.1 Description of the plant and the VCE accident

The layout of the Buncefield oil depot is shown in Figure 4.5. It typically stores 150,000 tons of fuel (gasoline, fuel oil, kerosene) with a total capacity of 273,000 m^3. The main 35 storage tanks are numbered and shown in Figure 4.5.

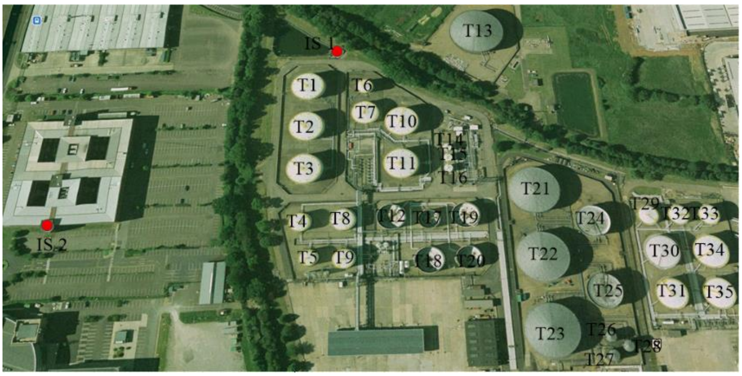

Figure 4.5 Layout of the Buncefield oil depot before 2005, the UK (Chen et al., 2020a)

Before the explosion, overfilling occurred during a delivery operation of unleaded petrol via a pipeline to Tank 2, forming a large vapor cloud that covered part of the plant. The overfilling lasted about 23 minutes before the vapor cloud was ignited, resulting in a powerful VCE and the following fires. The accident damaged 23 storage tanks and injured 43 people (Buncefield Major Incident Investigation Board, 2008; Gant and Atkinson, 2011; HSE, 2011). Since the primary VCE event escalated and resulted in overall consequences more severe than the primary event, a domino effect was involved in the Buncefield accident. This study mainly focuses on the assessment of the VCE accident and thus ignores any second-level or higher-order escalation of domino effects (Chen et al., 2020b).

4.4.2 Methodology application

To apply the methodology illustrated in Section 4.3 to the Buncefield plant, we first should identify hazardous installations and characterize the possible LOC scenarios. The main hazardous installations include 35 ground storage tanks, pipelines linking with these installations, loading and unloading facilities, and other components such as valves and pumps. The possible LOC scenarios may be releases from storage tanks, tank overfilling during loading and unloading operations, and leakages from pipelines. To illustrate and validate the proposed methodology, only the overfilling scenario is considered, i.e., the excessive liquid flowed down from the vents in the fixed tank roof. The mass flow rate is estimated as a constant of 115 kg/s (Atkinson and Coldrick, 2012). The probability of valve failure (i.e., the leakage) is considered to be 5×10^{-2} per year referred to the failure frequency estimation during loading and unloading operations in the process industry (Hauptmanns, 2004).

According to the characteristics of the LOC scenario, a vapor cloud analysis in step 2 can be conducted to obtain the vapor cloud dispersion over time. The ratio of the evaporation rate to flow rate, α, is approximately equal to 0.17 given an evaporation rate of 19.5 kg/s. Consequently, the vapor addition rate to the cloud is estimated as 199 m^3/s based on empirical formulas developed by Atkinson and Coldrick (2012). Since the gasoline vapor is denser than air, the gravity-driven model is used to analyze vapor cloud evolution, considering $C_E = 1$ and $g' = 0.5$ (Atkinson, 2017). As a result, the vapor cloud radius r_t can be calculated according to Eq. (4.7) given a delayed time t. Figure 4.6 shows the vapor cloud contour at each time slice. The vapor cloud contour is idealized neglecting the effects of site topology and obstacles, etc. It should be noted that by considering these parameters via more advanced CFD methods one may obtain more accurate contours which may be irregular in shape, offset in one direction, or of different thickness (Gant and Atkinson, 2011).

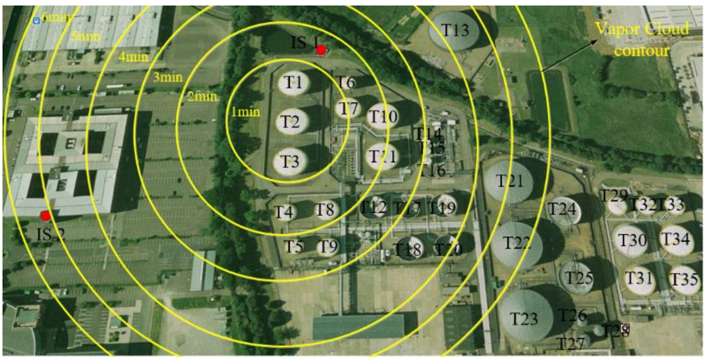

Figure 4.6 Vapor cloud contour evolution
(Chen et al., 2020a)

Since the ambient temperature was very low during the accident, the autoignition probability P_{ia} is considered to be zero. The ignition probability of static discharge P_{is} is 0.0156 given the minimum ignition energy of 0.23 mJ. According to the accident investigation (Health and Safety Executive, 2009; Bakke et al., 2010), there are two possible ignition sources in the oil storage depot, i.e., the pump house (IS1) and the Northgate emergency generator (IS2). Figure 4.7 shows the dynamic event tree up until 25 min with 66 possible VCE scenarios.

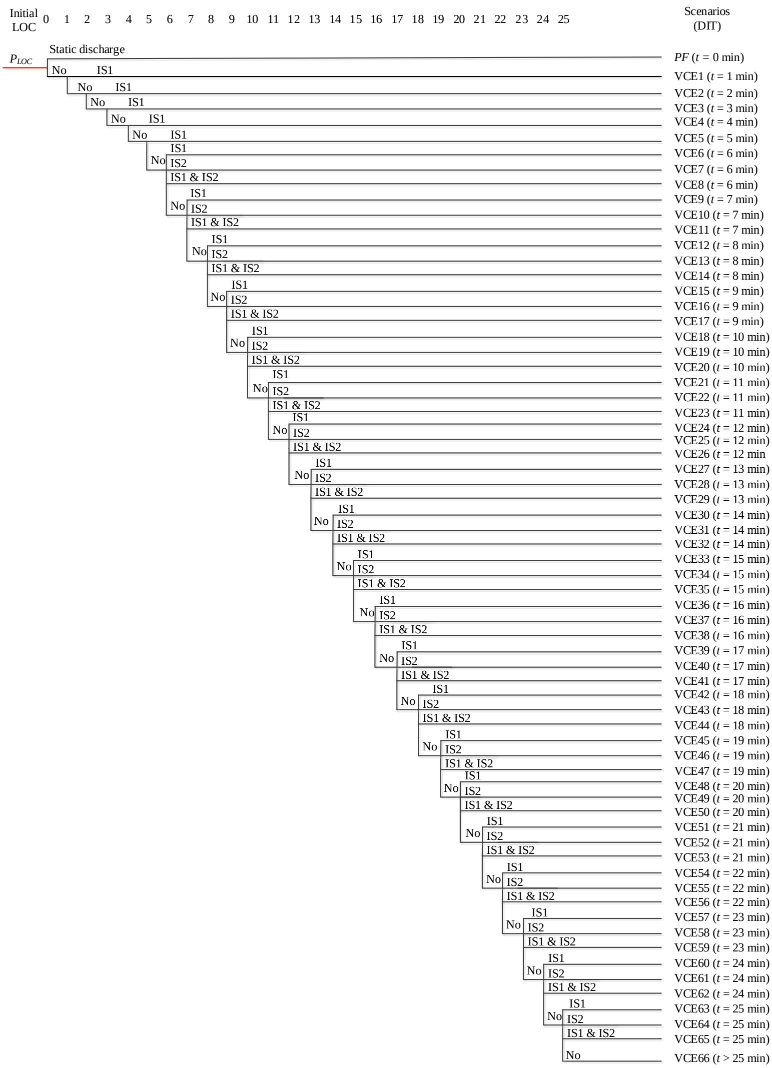

Figure 4.7 A discrete DET for Buncefield explosion assessment (Chen et al., 2020a)

For illustration, other possible ignition sources such as the vehicles parked nearby are not considered in this case study. Both the primary ignition probabilities of the two sources are considered to be 0.1/min (with 'good' ignition controls (Rew and Daycock, 2004)) since the two equipment items were not in operating condition during the accident. As a result, the parameters of ω in Eq. (4.10) of the two ignition sources is equal to 0.0018. IS1 is active after t = 1.5 min while IS2 is active at t = 5 min. The next step is to estimate the explosion probability and possible delayed time using a dynamic event tree for a time step Δt = 1 min.

Based on the event tree, the cumulative probability of ignition over time can be obtained, as shown in Figure 4.8. The cumulative probability increases over time while the increased rate decreases after the vapor cloud reaches the second ignition source. At t = 1 min, the delayed ignition probability is zero since the vapor cloud hasn't covered any ignition source. The cumulative probability reaches 0.98 at 23 min and still increases over time, finally approaching 1.

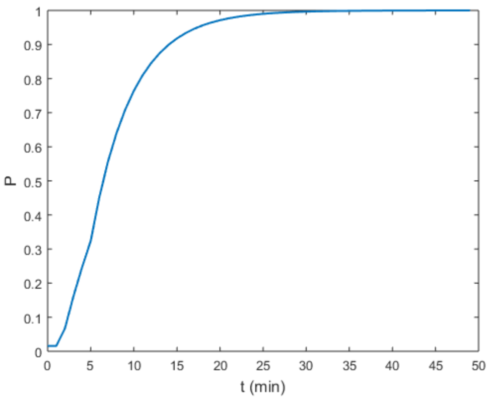

Figure 4.8 The cumulative probability of ignition over time
(Chen et al., 2020a)

There are four possible ignition causes: immediate ignition caused by static discharge, delayed ignition at the pump house (SI1), delayed ignition at the Northgate emergency generator (SI2), or simultaneous ignitions at the pump house (SI1) and the Northgate emergency generator (SI2). Figure 4.9 shows the ignition probabilities of different ignition causes over time. The maximum ignition probability is in the 6th min when the vapor cloud reaches the Northgate emergency generator and the two ignition sources are active. The ignition probability in the 2^{nd} min is lower than that in the 3rd min because the vapor cloud reaches the pump house at t = 1.5 min (i.e., the ignition source active from 1.5 min). The ignition probability decreases rapidly over time as the cumulative ignition probability increases, so a VCE with a long DIT may be regarded as a low-probability event.

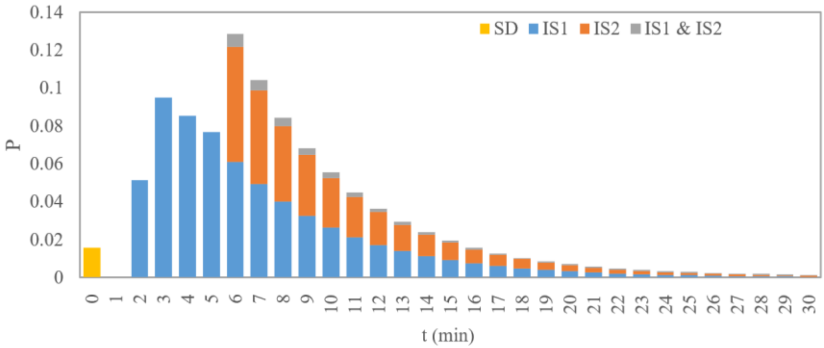

Figure 4.9 The conditional probabilities of different ignition scenarios (Chen et al., 2020a)

Based on the spatial-temporal dispersion results, Step 5 can obtain the overpressure caused by VCE at each discrete time using the Multi-Energy method. Since the industrial area was blocked by various buildings, tanks, and plants, a conservative strength coefficient of 10 (the maximum value) is considered for all the VCE scenarios. Figure 10 shows the overpressure caused by VCE scenarios at different distances.

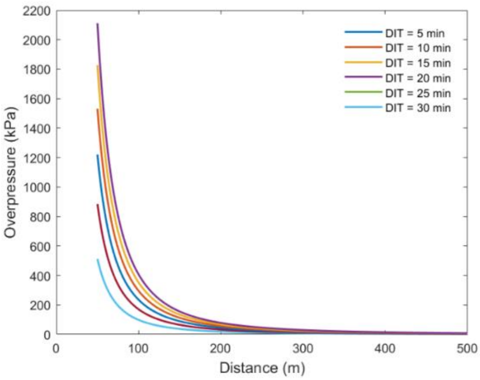

Figure 4.10 Calculation results of overpressure (Chen et al., 2020a)

The overpressure increases over the delayed ignition time (DIT) due to the increase of total explosion energy. The maximum overpressure can reach 2000 kPa which is consistent with the previous study on Buncefield accident investigations (Taveau, 2012; Mishra et al., 2013). But the overpressure rapidly decreases with increasing the distance from the center of the explosion. So, equipment with a large distance from the center of the explosion may survive from the VCEs, such as T34 and T35.

The final step assesses the vulnerability of hazardous installations, obtaining the damage probability of installations and the likelihood of domino effects caused by possible VCE scenarios. The parameter values of a and b are considered as −9.36 and 1.43, respectively, for atmospheric tanks (Zhang and Jiang, 2008). Consequently, the damage probability of installations subject to these VCEs can be calculated using Eq. (4.21) and Eq. (4.22). Figure 4.11 shows the conditional probability of damage to T20 and T35. The damage probability of T35 is lower than that of T20 for a VCE since the distance from the explosion to T35 is larger than that to T20. The conditional probability of damage for each tank increases with the increase of delayed ignition time (DIT). The explosion caused by simultaneous ignitions at SI1 and SI2 leads to more severe consequences than the explosion caused by single ignition at SI1 or SI2.

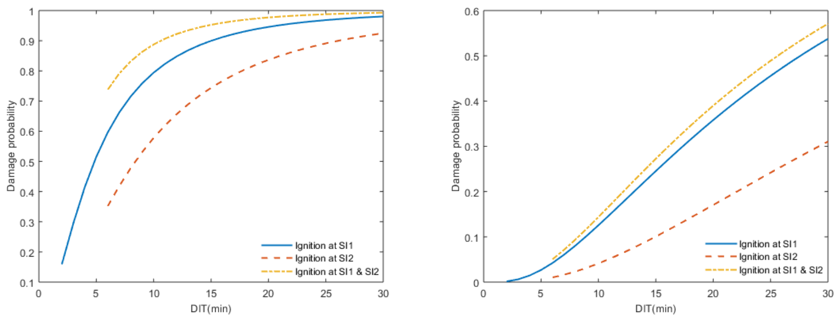

(a) (b)

Figure 4.11 Damage Probability of tanks subject to VCEs at different times ((a) tank 20 and (b) tank 35, adapted from Chen et al. (2020a))

Figure 4.12 shows the damage probability of tanks caused by the VCE scenario at *t* = 23 min (the Buncefield explosion accident in 2005). The results indicate that Tanks 1-21 are very likely to be destroyed by the explosion due to the high damage probabilities (> 0.9).

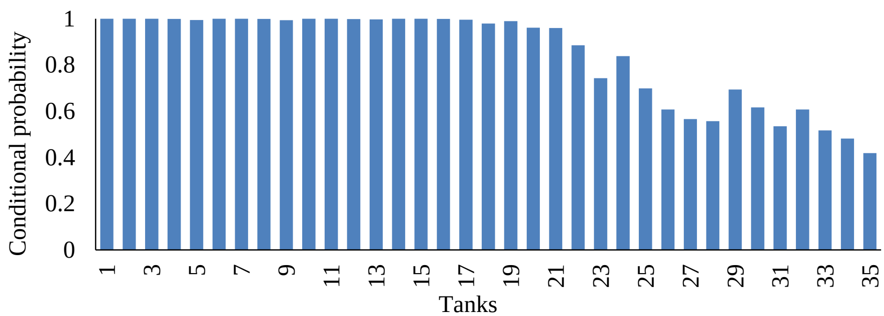

Figure 4.12 Damage probability of tanks caused by the VCE at *t* = 23 min (Chen et al., 2020a)

Figure 4.13 shows the layout of the Buncefield plant after the accident in 2005. The real damaged tanks can easily be identified and these 21 tanks (marked by yellow circles) are very likely to have been destroyed by the explosion due to the high damage probabilities (> 0.9). Among the 21 tanks, only T5 and T9 were not really damaged in the accident, which indicates that the results obtained by the developed methodology are almost in agreement with the real Buncefield accident.

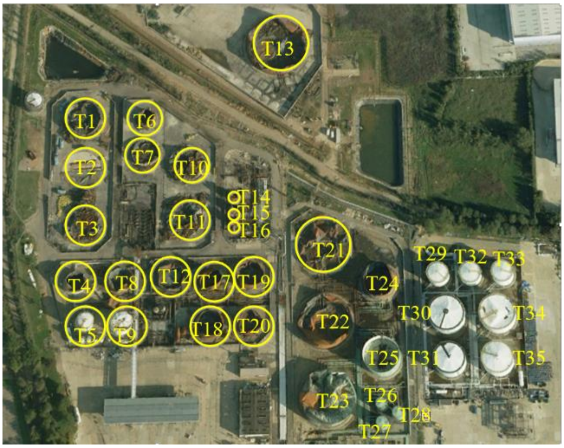

Figure 4.13 A comparison of the results and real damaged tanks (Chen et al., 2020a)

Finally, we can obtain the conditional probability of damage of installations subject to possible VCEs given an overfilling scenario at Tank 2, as shown in Figure 4.14.

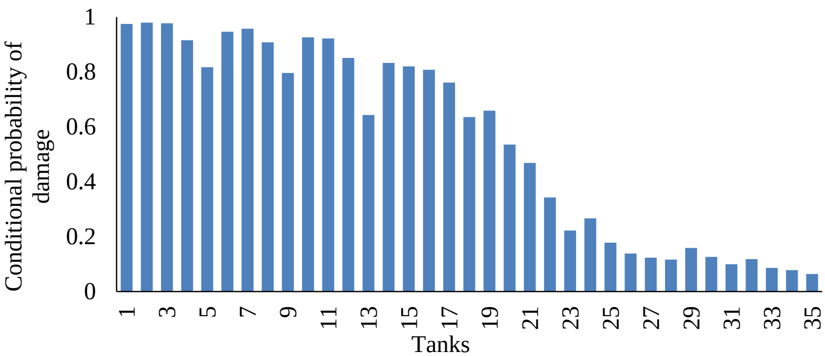

Figure 4.14 Conditional damage probability of tanks given an overfilling (Chen et al., 2020a)

Tanks 25-35 have a lower damage probability than other tanks since they are situated at a substantial distance from the release tanks. The number of expected damaged tanks (the sum of damage probability of each tank) is 16. In that case, domino effects may be inevitable. The results indeed indicate that a large vapor cloud explosion can lead to the damage of multiple tanks or knock-on effects, resulting in severe consequences. This was the case for instance with the Buncefield VCE accident in 2005, the San Juan VCE accident in 2009, and the Jaipur VCE accident in 2009.

4.5 Discussion

The case study indicates that the developed dynamic assessment methodology can model the influence of the spatial-temporal evolution of a vapor cloud and the uncertainty of delayed ignition on the vulnerability of installations subject to the major accident scenario “vapor cloud explosion” (VCE). The obtained results are consistent with the accident investigations for the past large VCEs. This section analyzes the critical parameters in the methodology and the possible future research issues to further improve this study.

In a real chemical plant, multiple ignition sources may be present within or outside the plant. As a result, collecting and characterizing the main ignition sources is a critical step in the developed methodology. The ignition probability of a single source depends on a lot of factors, such as the type of the source, the ignition energy of the source, and also the control measures for the source. Figure 4.15 shows the cumulative probability of ignition over time with different values of ignition effectiveness (ω).

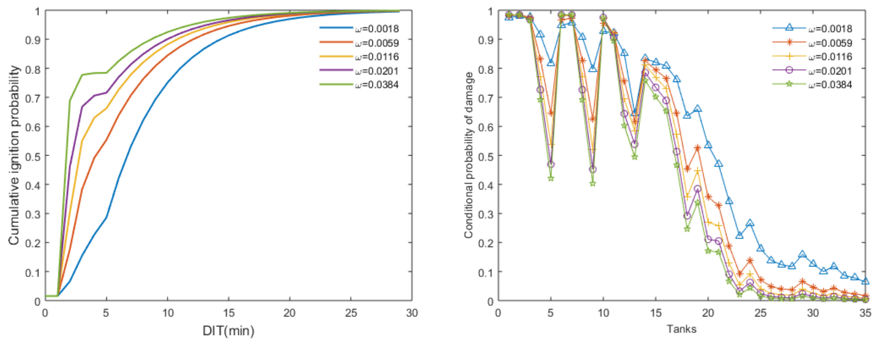

Figure 4.15 The effects of ignition effectiveness (ω)
(Note: (a) the cumulative probability of ignition and (b) the conditional probability of damage of tanks given the overfilling scenario, adapted from Chen et al. (2020a))

As shown in Figure 4.15a, the ignition probability increases with augmenting the ignition effectiveness of single sources. Therefore, ignition control is widely used to decrease ignition effectiveness to prevent major accidents in the process and chemical industries. However, ignition cannot be completely eliminated by ignition control measures. Besides, due to ignition control measures, a VCE may be delayed, resulting in a larger vapor cloud and thus a larger VCE of more severe consequences. As shown in Figure 4.15b, the conditional damage probability of the tanks decreases with increasing the distance between the tanks and the VCE center (the dips in the figure are due to situations where the higher numbered tanks are actually further away from the ignition source). Moreover, the conditional damage probability of the tanks increases with decreasing the ignition effectiveness. Therefore, ignition control can be considered as a delay measure, which may not be adequate to prevent VCEs. To prevent VCEs, ignition control measures may be integrated with emergency response actions such as diluting oil vapor using water vapor. In other words, ignition control may be used to provide enough time for emergency response actions to prevent VCEs.

The Multi-Energy method was adopted to calculate the overpressure caused by VCEs in this study. The key issue in the application of this method is to determine the strength coefficient based on the congestion (obstacle density) of process plants. Obstacle density is the most difficult parameter to quantify in the application of the Multi-Energy method. Although TNO has already published the yellow book to guide the application of the Multi-Energy method, it is still difficult for users to determine the value of the strength coefficient due to the uncertainty of obstacle density. Since the actual overpressure can easily be underestimated according to experimental results, it is recommended to be conservative in the determination of the strength coefficient (Van Den Bosh and Weterings, 1997). Taking the case in Section 4.4 as an example, the maximum conditional damage probability subject to VCEs caused by overfilling at T2 decreases to 0.35 if the strength coefficient of 10 is substituted by 3. Thus, the strength coefficient should be determined by meticulously analyzing the layout of a process plant in the application of the developed methodology. Otherwise, the worst strength coefficient should be adopted to obtain conservative results in vulnerability assessment.

To make the developed methodology user-friendly, we adopted an analytic method to predict the dispersion of vapor clouds, neglecting the VCE dilution with distance. As a result, the application of this methodology would lead to more conservative results in risk assessment. To account for VCE dilution with distance as well as upper and lower explosion limits, CFD methods may be integrated into this methodology to obtain more accurate results in future studies. With the rapid improvement of computational resources, applying CFD methods in risk assessment may become easier and acceptable for engineers in the future. Monte Carlo simulation can also be integrated into this methodology to evaluate the frequency of each scenario when the number of possible accident scenarios becomes too large due to the increase in the number of ignition sources. The developed methodology in this study was illustrated and verified by the VCE at the Buncefield oil storage facility as a case study. The results agree with the observations that more than 20 tanks were damaged by the VCE. Besides the real accident scenario, other possible scenarios were also obtained by the application of the developed methodology which shows the effectiveness of the methodology in considering the uncertainties (more than one accident scenario could have occurred). In this study, second or higher-level escalation was neglected, which could be considered for future work. Besides the application in risk assessment, the developed method combined with Bayesian theory may be used in accident investigations to identify the most likely ignition source based on evidence-based reasoning.

4.6 Conclusions

This study introduced a new methodology based on a dynamic event tree (DET) to model the vulnerability of process plants to VCEs, considering both the spatial-temporal dispersion of a vapor cloud and the uncertainty of delayed ignition time

(DIT). This work demonstrated how DET can effectively be used to assess the damage probability of critical installations exposed to VCEs caused by loss of containment. The dynamic methodology can address severe consequences caused by a large VCE due to a long DIT, such as the Buncefield accident in 2005.

Different from previous work on vulnerability assessment for vapor cloud explosions, the key outcomes of the present study can be summarized. Firstly, the time dependencies in vapor cloud dispersion and the uncertainty of delayed ignition should be considered to assess the VCE; this is crucial for reflecting the characteristics of possible large VCEs and for avoiding the underestimation of their consequences. Secondly, the vulnerability of installations to VCEs depends on the congestion of the plant layout and DIT. A long-delayed explosion may result in multiple-failure of installations, resulting in catastrophic disasters. Thirdly, the DIT is related to the distance between the release position and the ignition sources, the type of ignition sources, and the ignition control measures in place. The ignition control measures can decrease the ignition probability of single sources and may delay (if not fully eliminate) the VCE. However, a delayed ignition (which might be considered a good thing) could actually lead to a larger VCE and more severe consequences. Lastly, combining ignition control measures with emergency response actions (e.g., diluting oil vapor by water vapor) may be a way to prevent VCEs in process plants since ignition control might provide enough time for emergency response actions to prevent VCEs.

Chapter 5 Modeling multi-hazardous scenario evolution of domino effects

In the chemical industry, multi-hazard (toxic, flammable, and explosive) materials such as acrylonitrile are stored, transported, and processed in large quantities. A release of multi-hazard materials can simultaneously or sequentially lead to acute toxicity, fire, and explosion. The spatial-temporal evolution of hazards may also result in cascading effects. In this study, a dynamic methodology called "Dynamic Graph Monte Carlo" (DGMC) is developed to model the evolution of multi-hazard accident scenarios and assess the vulnerability of humans and installations exposed to such hazards. In the DGMC model, chemical plants are modeled as a multi-agent system with three agents: hazardous installations, ignition sources, and humans while considering the uncertainties and interdependencies among the agents and their impacts on the evolution of hazards and possible domino effects. A case study is analyzed using the DGMC methodology, demonstrating that the risk can be underestimated if the spatial-temporal evolution of multi-hazard scenarios is neglected. Vapor cloud explosion (VCEs) may lead to more severe damage than fire. The safety distances implemented only based on fire hazards are not sufficient to prevent chemical plants from the damage of VCEs.

The content of this chapter is based on the following published paper:

Chen, C., Reniers, G., Khakzad, N., 2021b. A dynamic multi-agent approach for modeling the evolution of multi-hazard accident scenarios in chemical plants. Reliability Engineering & System Safety 207. 10.1016/j.ress.2020.107349

5.1 Introduction

The past decades have witnessed an increase in the number, size, and diversity of chemical plants due to the increasing population and the increasing requirement for products (energy, chemicals, commodities, and food, etc.) (Reniers and Cozzani, 2013; Khan et al., 2015). The rapid expansion of the process plants and infrastructures brings huge economic benefits while unavoidably increasing the exposure to major hazards caused by hazardous materials in chemical industrial areas, resulting in human losses, environmental damage, and economic losses (Reniers and Audenaert, 2014; Necci et al., 2015; Ge et al., 2020; Wang and Wu, 2020; Yang et al., 2020). Major hazards such as fire, explosion, and toxic release arising from loss of containments may occur due to intentional or unintentional causes (Wang et al., 2018; Chen et al., 2019b; Yang et al., 2019; Wang et al., 2020). Intentional hazards are security-related threats, including terrorist attacks, sabotage, thief, etc. Unintentional hazards consist of accidental hazards (e.g., corrosion, fatigue, mechanical damage) and natural hazards (e.g., earthquake, flood, and lightning). In hazardous chemical areas, fire is the most frequent hazard (44%), followed by explosion (36%). Toxic release without fire and explosion accounts for 20% of all major accidents and toxic substances are involved in almost 30% of these accidents (Vilchez et al., 1995). Besides, chemical industrial areas are usually congested with hazardous storage tanks, complex piping, high-pressure compressors, and separators in which a loss of containment (LOC) event may lead to cascading effects and multiple hazardous scenarios.

All the major hazards of fire, explosion, and toxic release can be simultaneously or sequentially present in one disaster due to the evolution of hazardous scenarios. Many catastrophic disasters in the past two decades originated from the hazardous release of process vessels and evolved to VCEs and finally fires. On October 23, 2009, a large VCE happened at the Caribbean Petroleum Corporation terminal in Bayamón, Puerto Rico, during the offloading of gasoline from a tanker (CBS, 2015). The subsequent fires triggered by the explosion lasted about 60 h and resulted in significant damage to 17 of the 48 petroleum storage tanks and other equipment (CBS, 2015). On November 28, 2018, a Vinyl chloride release in a chemical plant at Zhangjiakou (China) caused a VCE outside the chemical plant, triggering fires on tank trucks and leading to 23 fatalities and 22 injuries (The accident investigation team for “11.28” accident, 2019).

In light of these past disasters and due to the severe consequences of unpredicted hazardous scenarios, modeling the spatial-temporal evolution of hazardous scenarios originating from the release of hazardous materials in industrial areas is essential for protecting staff, nearby residents, and emergency rescuers (Georgiadou et al., 2007; Zhou and Reniers, 2018c, 2020). For example, in the Tianjin port disaster in 2015, which was caused by a spontaneous ignition of nitrocellulose, many of the emergency rescuers were killed in the disaster due to an unpredicted evolution of the fire to an explosion. Besides, the disasters caused by natural hazards (Na-tech) can make emergency response more difficult due to the damage to safety barriers and other infrastructures, resulting in more severe consequences (Li et al., 2018; Misuri et al., 2019; Chen et al., 2020c; Olivar et al., 2020). To avoid such catastrophic disasters, many post-accident analyses have been conducted to predict the overpressure induced by explosions (Maremonti et al., 1999; Taveau, 2012; Mishra et al., 2013; Sharma et al., 2013; Mishra et al., 2014) and vapor cloud dispersion (Gant and Atkinson, 2011; Dasgotra et al., 2018; Mishra, 2018). Besides, a lot of work has been done on vulnerability assessment of installations to VCEs, risk assessment of domino effects caused by VCE (Salzano and Cozzani, 2003; Cozzani and Salzano, 2004b, a; Zhang and Jiang, 2008; Mukhim et al., 2017; Zhou and Reniers, 2017b) and domino effects triggered by fire (Khakzad et al., 2016; Khakzad et al., 2017b; Yang et al., 2018). Regarding the evolution of fire, the time to failure of equipment exposed to fire is critical for assessing the vulnerability of installations. As a result, dynamic methods were used to assess the vulnerability of installations exposed to fire and fire-induced domino effects (Khakzad, 2015; Chen et al., 2018; Kamil et al., 2019; Zeng et al., 2019; Ding et al., 2020). Among these dynamic tools, the dynamic graph approach and the dynamic Bayesian network approaches can model the spatial-temporal evolution of domino effects caused by fire and visualize the escalation paths of fire (Khakzad, 2015; Wang et al., 2018; Chen et al., 2019b). Monte Carlo simulation has also been applied to address the evolution uncertainty of domino effects (Abdolhamidzadeh et al., 2010b).

Compared to the research devoted to VCE or fire evolution, little attention has been paid to the evolution of possible toxic release, VCE and fire in a catastrophic disaster, and the assessment of human exposure to multiple hazardous scenarios. Jiang et al. (2019) analyzed the vulnerability of tanks exposed to fire and explosion in different accidents but overlooked the possible evolution between different hazardous scenarios. He and Weng (2019) studied the synergic effects of multi-hazard on vulnerability assessment but ignored the dynamic evolution process. The evolution of toxic release to VCE and vice versa is a dynamic process along with a vapor cloud dispersion (Chen et al., 2021b). The present study, therefore, aims to establish a dynamic methodology for human and facility vulnerability assessment considering the spatial-temporal evolution of multiple hazards: toxic release, VCE, and fire. In our study, chemical plants are modeled as a multi-agent (component) system (Zhang et al., 2018; Alrabghi, 2020; Galbusera et al., 2020; Zhang and Si, 2020) through the application of dynamic graphs. Graph-based methods have been used for domino effect analysis (Zhang and Si, 2020), vulnerability and reliability analysis (Su et al., 2018), and resilience assessment (Goldbeck et al., 2019). Besides, Monte Carlo simulation (Chakraborty et al., 2020; Jensen et al., 2020; Liu et al., 2021) is used in this study to solve the dynamic multi-agent model. Consequently, both the uncertainty of ignition and the uncertainty of the evolution of different hazardous scenarios are taken into consideration in the present study. The model is developed in Section 5.2 and the corresponding update rules and algorithm are developed in Section 5.3. A case study is provided in Section 5.4 to show the application of the developed methodology. A discussion based on the results of the case study is presented in Section 5.5. The conclusions of this study are summarized in Section 5.6.

5.2 Modeling

Graph-based methods are commonly used and are effective tools to analyze multiple interacting agents in a system (Harary, 1969; Jafari et al., 2011). In a graph, the agents are modeled by nodes and their dependencies are represented by edges (Khakzad et al., 2017b; Ding et al., 2020; Jiang et al., 2020). As a result, graph-based methods provide a visible structure (graph or network) to represent the complex agent interactions while agent-based modeling focuses on agent behaviors (e.g., attributes and interactions), making it very flexible to model socio-technical systems (Stroeve et al., 2013; Rai and Hu, 2018; Zhang et al., 2018). Graph metrics such as betweenness and closeness have been used to assess domino effects and the vulnerability of installations subject to fire and explosion scenarios (Khakzad and Reniers, 2015b; Khakzad et al., 2017b). The time-dependent escalation of fire can also be modeled by dynamic graphs (Chen et al., 2018). The dynamic graph approach can model the dynamic evolution of fire scenarios while static graph methods provide merely a snapshot of the whole process at once. When it comes to modeling the evolution between different hazardous scenarios, it is difficult to address the uncertainty in hazardous scenario evolution by merely using the dynamic graph approach. Compared with analytical methods, Monte Carlo simulation is widely used to model uncertainties that cannot be easily accounted for due to the intervention of random variables, avoiding complex mathematical calculations (Joy, 1995; Kuczera and Parent, 1998; Rubinstein and Kroese, 2016). In this study, a new methodology is developed based on dynamic graphs and Monte Carlo simulation to model the complexity and uncertainty of hazardous scenario evolution. The methodology is called Dynamic Graph Monte Carlo (DGMC). The DGMC is defined as a dynamic graph with time-dependent parameters and random parameters in which Monte Carlo simulation is used to solve the model.

To model the hazardous scenario evolution process and thereby dynamically assess human vulnerability exposed to the possible toxic cloud, heat radiation, and overpressure, we define a Hazardous Scenario Evolution Graph (HSEG) based on the developed DGMC method. The HSEG can be defined as a dynamic graph with a nine-tuple, as shown in Eq. (5.1).

$$HSEG = \left(T, M, N, K, S, E, C, O, H\right) \tag{5.1}$$

5.2.1 Evolution time

$T = [T_1, T_2, T_3, \ldots, T_G]$ represents the evolution time of hazardous scenarios starting from a hazardous release (T_1=0). The dynamic graph *HSEG* is sliced into *G* static graphs by these time nodes. The *HSEG* parameters are updated at each time node T_g due to the change of hazardous scenarios, human states, and installation states. If an ignition occurs, t_2 is equal to the ignition time (*IT*). *IT* is a random variable that depends on the number of ignition sources, ignition effectiveness, and vapor cloud dispersion, etc. The *IT* is equal to zero if the released materials are immediately ignited. In the chemical industry, the likelihood of immediate ignition is always determined by the autoignition of flammable substances and the static discharge caused by the release (Chen et al., 2020a). If the ignition is delayed, the possible ignitions caused by different ignition sources are considered as independent events, and the ignition probability of a single ignition source depends on the ignition effectiveness and the period that the ignition source is covered by the flammable vapor (t_{IS}), as shown in Eq. (4.12) (Uijt de Haag and Ale, 1999). To determine t_{IS}, the vapor cloud dispersion model developed by (Atkinson and Coldrick, 2012) is adopted, as shown in Eq. (4.9).

5.2.2 Numbering hazardous installations

$N = [1, 2, 3, \ldots, n]$ is a set of nodes representing the hazardous installations that may be involved in the evolution of hazardous scenarios.

5.2.3 Numbering human positions

$M = [n + 1, n + 2, n + 3, \ldots, n+m]$ is a set of nodes denoting the human position that may be affected by toxic release, fire, or overpressure hazards.

5.2.4 Numbering ignition sources

$K = [m + n + 1, m + n + 2, m + n + 3, \ldots, m + n + k]$ is a set of nodes denoting the ignition sources that may cause the ignition of a flammable vapor cloud.

5.2.5 Node states

S is a node parameter indicating the state of installations, humans, and ignition sources at the evolution time T. According to possible major hazards in industrial areas and the vulnerability characteristics of hazardous installations and humans, five states of hazardous installations, three human states, and three states of ignition sources are defined, as shown in Tables 5.1-5.3.

Table 5.1 States of hazardous installations

State	Description
Operational	The hazardous installation is not physically damaged and is operational.
Release	The hazardous installation is physically damaged, resulting in the loss of containment of hazardous materials and/or poisoning humans nearby.
Fire	The installation is on fire due to immediate ignition, causing heat radiation on humans and/or other installations.
VCE	The installation’s loss of containment induces a vapor cloud explosion due to delayed ignition.
Extinguished	The installation is physically damaged but does not generate any hazardous effects.

As shown in Table 5.1, the state of “operational” is an initial state while the state of “extinguished” is a terminal state. The states of “release”, “fire” and “VCE” are harmful to other installations and humans. If a release occurs at an installation, the state of the installation changes from “operational” to “release”. The state of “fire” is caused by an immediate ignition while the state of "VCE" results from delayed ignition.

Table 5.2 shows human states including one initial state "safe" and two terminal states "injured" and "dead". Table 5.3 lists the states of ignition sources, including one initial state (inactive), one terminal state (ignited), and one intermediate state (active). It should be noted that all the foregoing states are time-dependent and may be updated with the spatial-temporal evolution of the scenarios.

Table 5.2 States of humans

State	Description
Safe	The human does not receive any hazardous effects.
Injured	The human is injured due to exposure to toxic gas, heat radiation, or overpressure.
Dead	The human is decreased due to exposure to toxic gas, heat radiation, or overpressure.

Table 5.3 States of ignition sources

State	Description
Inactive	Flammable vapor is not present at the ignition source, or the concentration of the vapor is out of the flammability limit.
Active	Flammable materials are present at the ignition source, and the concentration of the vapor is between the lower and upper flammability limits.
Ignited	The ignition source has ignited the flammable vapor.

5.2.6 Physical effects

E is a set of directed edges denoting the physical effects that may cause damage to hazardous installations or be harmful to humans. In this study, the heat radiation induced by fire, the overpressure caused by VCEs, and the toxicity induced by toxic vapor are considered. There are six kinds of directed edges: the heat radiation from installation nodes to installation nodes or human nodes, the overpressure from installation nodes to installation nodes or human nodes, and the toxic effects from installation nodes to human nodes or ignition nodes.

5.2.7 Acute intoxication

C is a set of edge parameters from release source to human denoting the concentration of toxic vapor at human positions. The acute intoxication of exposed humans caused by a toxic cloud depends on the toxic concentration (C_t) and exposure time (t_e). The probit function for acute intoxication is used to quantify the death probability due to human exposure to toxic vapor, as follows:

$$Y_t = c_7 + c_8 \ln\left(C_t^{c_9} \times t_e\right) \tag{5.2}$$

where c_7, c_8, and c_9 are constants that vary with different toxic substances. These constants for different toxic substances can be adopted from the Green Book (Van Den Bosh et al., 1989). Y_t is the probit value of human vulnerability exposure to toxic gas. It should be remarked that besides the toxic concentration and exposure time, other factors such as demographics (e.g. ages) and Personal Protection Equipment (PPE) are not considered in this formula.

5.2.8 Damage induced by VCEs

O is an edge parameter denoting the overpressure generated by VCEs when the flammable vapor is ignited by an ignition source. The commonly-used overpressure estimation methods include the TNT equivalent method, the Baker-Strehlow method, and CFD simulation, etc. The TNT equivalent method is a simple approach based on the TNT explosion mechanism to calculate overpressure, which neglects the effects of space configuration, ignition sources, and flammable gas distribution and thus may underestimate the overpressure. The Multi-Energy method is developed for gas explosions, dividing the explosion as a number of sub-explosions and addressing the effects of congestion levels, ignition and gas distribution in obstructed areas. Netherlands Organization for Applied Scientific Research (TNO) recommended the Multi-Energy method for overpressure calculation in quantitative risk analysis (Uijt de Haag and Ale, 1999). Consequently, the Multi-Energy method (Atkinson and Coldrick, 2012) is adopted to calculate the overpressure obtained by different installations and humans. More details of this method are described in Chapter 4.

The damage probability of hazardous installations and death probability caused by overpressure can also be calculated by the application of probit functions, as follows:

$$Y_p = c_5 + c_6 \ln\left(P_o\right) \tag{5.3}$$

where c_5 and c_6 are constants, as shown in Table 5.4.

Table 5.4 Probit function parameters for overpressure

Installations	Atmospheric	Pressurized	Elongated	Auxiliary	Human
c_5	-9.36	-14.44	-12.22	-12.42	-77.1
c_6	1.43	1.82	1.65	1.64	6.91

2.2.9 Damage induced by fires

H is a $m\times\left(m+n\right)$ matrix representing the heat radiations generated by nodes in "fire" states. $q_{i,j}$ is an element of the matrix denoting the heat radiation induced by an installation i in a "fire" state to installation or human j, as follows:

$$Q = \begin{bmatrix} 0 & q_{1,2} & \cdots & q_{1,m+n} \\ q_{1,2} & 0 & \cdots & q_{2,m+n} \\ \cdots & q_{i,j} & 0 & \cdots \\ q_{m,1} & \cdots & q_{m,m+n-1} & q_{m,m+n} \end{bmatrix} \tag{5.4}$$

Q is not a square matrix in this chapter because people can only receive but not generate heat radiation. Considering possible synergistic effects (Chen et al., 2019b) induced by multiple installations in the "fire" states, the heat radiation received by a node j (Q_j) can be calculated as:

$$Q_j = \sum_{i=1}^{m} q_{i,j} \tag{5.5}$$

Based on the heat radiation matrix, the Domino Evolution Graph (DEG) model developed in Chapter 3 can be used to calculate the heat radiation received by humans and installations at different evolution times. Then the vulnerability of humans exposed to heat radiation is estimated by using the exposure time and the received heat radiation (Q). Consequently, the probit value of human vulnerability exposure to multiple fires can be estimated as:

$$Y_f = -14.9 + 2.56 \ln\left(6 \times 10^{-3} \times Q^{1.33} \times t_e\right) \tag{5.6}$$

The heat radiation received by people (Q) varies with the number of hazardous installations in the "fire" state during the spatial-temporal evolution of hazardous scenarios. Therefore, the hazardous effects caused by heat radiation on humans at different periods should be superimposed (e.g., the superimposed effects of heat radiation on human vulnerability). At evolution time T_g, the probit value (Y_{f,T_g}) can be estimated as:

$$Y_{f,\,t_G} = -14.9 + 2.56 \ln\left(6 \times 10^{-3} \times \sum_{g=1}^{g=G}\left(Q_g^{\ 1.33} \times t_g\right)\right) \tag{5.7}$$

5.3 Graph update rules and simulation algorithm

5.3.1 Graph update rules

Figure 5.1 shows the state transitions and physical effects due to different states in HSEGs. As shown in Figure 5.1, dotted lines represent the state transition of nodes and solid lines denote physical effects caused by a node to other nodes. Humans may be injured due to acute toxicity caused by installations in the "release" state, heat radiation induced by installations in the "fire" state, as well as overpressure caused by installations in the "VCE" state. Since human vulnerability to heat radiation and toxic vapor depends on the intensity of the physical effects and the exposure time, humans may die after a period time of exposure. But the overpressure induced by

VCEs may induce an immediate death since the death likelihood caused by explosions is determined by the explosion intensity regardless of the exposure time. In a hazardous scenario evolution caused by overfilling, a human may suffer from different hazardous scenarios at different subsequent times.

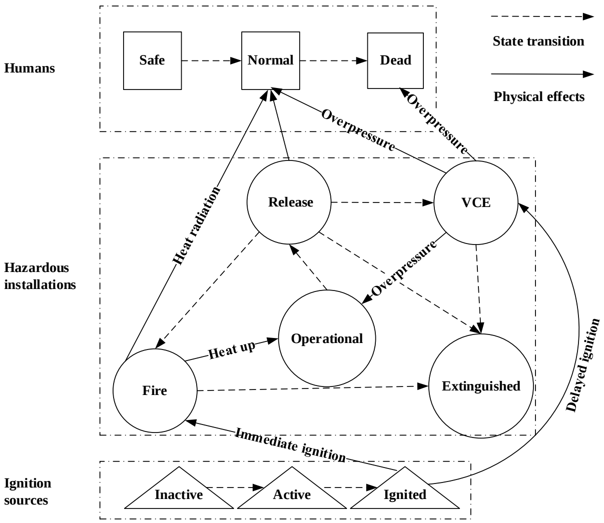

Figure 5.1 State transition and physical effects among different states (Chen et al., 2021b)

To further illustrate the graph update rules, Figure 5.2 shows an example of a HSEG with 9 static graphs. As shown in Figure 5.2, a hazardous installation's state changes from "operational" to "toxic release" when a toxic release occurs at the installation (e.g., T1 in Figure 5.2a) due to accidental events, natural events, or intentional attacks. If the released material is ignited immediately, the installation's state will change to "fire" and induce heat radiation on humans and other hazardous installations. Otherwise, a vapor cloud may form and disperse along with the vaporization of the release material, resulting in acute toxicity, as shown in Figure 5.2b. As the vapor cloud continues to spread, the ignition source may change from an "inactive" state to an "active" state (Figure 5.2c). As a result, a VCE may occur when the vapor cloud is ignited, resulting in the damage of hazardous installations and casualties. As shown in Figure 5.2d, T2 and T4 are damaged by the VCE while T3 is not. At time t_4, both H1 and H2 become exposed to the overpressure caused by the VCE but the injury of H1 may be more severe than that of H2 since the former suffers from acute toxicity as well. Simultaneously, T2 and T4 may be on fire because the explosion can release a lot of heat and energy which increases the likelihood of immediate ignition at the two damaged tanks. As shown in Figure 5.2e, the two tanks in "fire" states induce synergistic effects of heat radiations on H1, H2, and T3. H1 may die at time t_5 (Figure 5.2f) while H2 may die at time t_6 (Figure 5.2g). The state of T4 changes from "fire" to "extinguished" at t_7 due to the burn-out of flammable substances. Finally, the fire at T2 is extinguished and T3 survives since the escalation is blocked by firefighting actions. The evolution ends since there is no escalation.

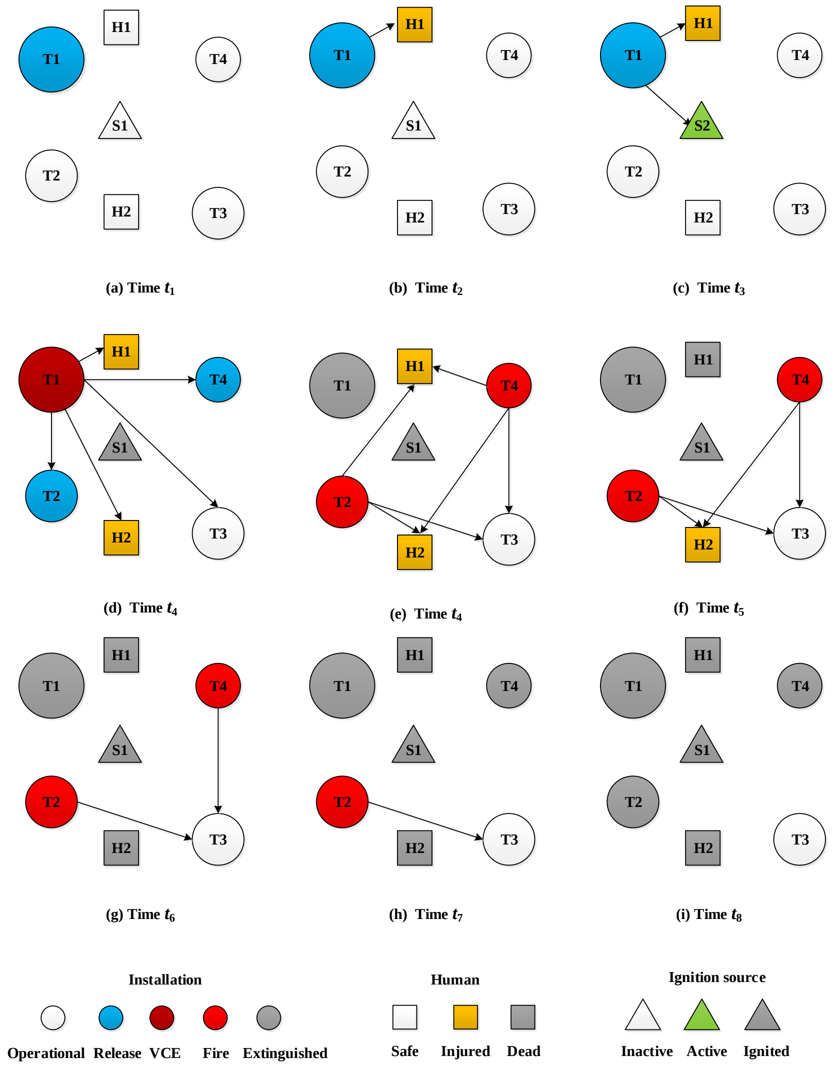

Figure 5.2 A HSEG with 9 static graphs
(Chen et al., 2021b)

5.3.2 Simulation algorithm

Figure 5.2 uses a dynamic graph to represent an evolution process of hazardous scenarios originating from a toxic release. Evolution uncertainties such as the ignition time and the death probability of humans cannot be fully considered by listing all the possible hazardous scenario evolution paths. Besides, the evolution may be more complex when it comes to real chemical storage areas with multiple ignition sources and many hazardous installations. As a result, Monte Carlo simulation is employed to generate HSEGs, addressing the time-dependencies and uncertainties in the hazardous scenario evolution process. Figure 5.3 shows the developed algorithm based on the HSEG model and the Monte Carlo simulation.

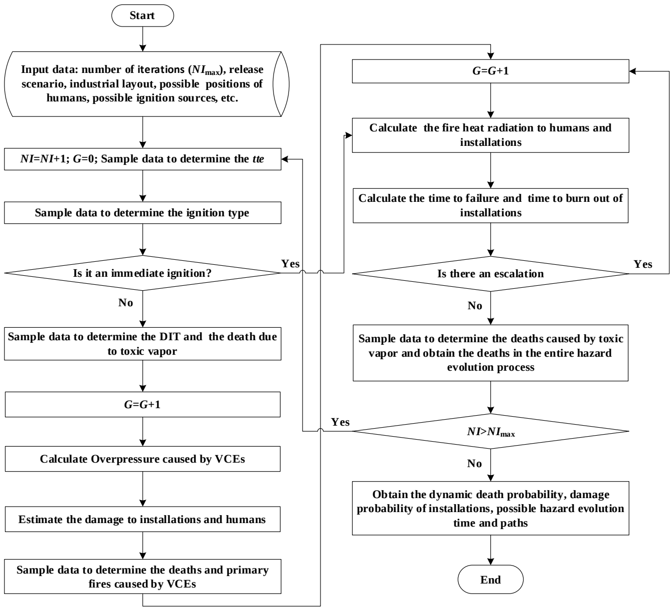

Figure 5.3 Simulation algorithm for the HSEG model (Chen et al., 2021b)

According to the simulation algorithm, at first, basic data is inputted, including the number of iterations (NI_{max}), the industrial layout, release scenarios, possible ignition sources, etc. Next, the ignition type is determined by random sampling. If it is a delayed ignition, the ignition time (*IT*) and the ignition source are determined by random sampling based on Eq. (5.2). Death caused by toxic vapors can also be determined using Eq. (5.4). At the *IT*, the HSEG updates and the curves in the graph represent overpressure. The overpressures suffered by humans and hazardous installations can be calculated based on Eq. (5.6). As a result, the fatalities and the subsequent fires caused by the overpressure can be obtained by random sampling based on Eq. (5.7). The graph will be updated again at the *IT*, and the curves in the graph will then represent heat radiation. The heat radiation can be calculated by the application of ALOHA, and then the time to failure of hazardous installations can be determined using Eqs. (5.10) and (5.11). If there is an immediate ignition, the calculation procedures for explosion and toxic vapor are neglected, and the heat radiation is immediately calculated. During the fire escalation period, the graph is updated when a new fire occurs, or an existing fire is extinguished when the evolution is over.

The above calculations are repeated $NI_{\max}$ times. Finally, the death probability and failure probability of installations during the dynamic hazardous evolution are obtained. Besides, the possible evolution paths, evolution time nodes, expected DIT can also be determined using the simulation.

5.4 Application of the methodology

The DGMC methodology consisting of the HSEG model and the simulation algorithm was developed in Section 5.2. To demonstrate its application to a dynamic hazardous scenario evolution, an illustrative case study is used in this section.

5.4.1 Case study

A chemical storage facility including 37 chemical storage tanks (T1-T37) in three tank areas (I, II, III), 5 possible human positions (H1-H5), and two possible ignition sources (S1-S2) is considered in this study. The layout of the chemical storage facility is shown in Figure 5.4. Table 5.5 summarizes the main characteristics of the storage tanks considered in the dynamic vulnerability analysis.

Figure 5.4 Chemical storage facility considered in the case study (Chen et al., 2021b)

Table 5.5 Characteristics of chemical storage tanks

Tank	Type	Dimension × Height (m)	Chemical substance	Nominal volume (m^3)	Chemical content (m^3)
T1-T6	Atmospheric	21.0 × 16.6	Acrylonitrile	5000	4000
T7-T9, T12-T15	Atmospheric	17.0 × 15.4	Gasoline	3000	2400
T10, T11	Atmospheric	7.0 × 13.6	Gasoline	500	400
T16-T27	Atmospheric	14.5 × 12.7	Gasoline	2000	1600

An overfilling of acrylonitrile at T1 with a filling rate of 100kg/s was considered as the primary scenario. The release of acrylonitrile can result in acute intoxication and the subsequent explosions and fires may lead to human exposure to overpressure and heat radiation. The released acrylonitrile vaporizes and disperses around. The ambient temperature is 0 °C and the wind speed is equal to zero. According to the vapor cloud dispersion model in Eq. (5.8), the ignition source S1 is active after 5.1 min while S2 is active after 2.8 min. The autoignition probability P_{ia} is zero and the ignition probability due to static discharge P_{is} is estimated as 0.02 given the minimum ignition energy of 0.16 mJ (Haase, 1977) and the autoignition temperature of 481 °C (Brazdil, 2000). The possible heat radiations induced by tanks and the burning rates of fires are calculated through the ALOHA software. The number of iterations (NI_{max}) is set as 10^5 in which the computation time is 3.9 min, and the average deviation of two computations is lower than 0.001. In terms of large chemical plants with many installations, the computation time will increase though being still acceptable. Taking the case with 150 tanks (Chen et al., 2019b) as an example, the computation time would be 21 min. This computation is conducted by an ordinary personal computer (Intel (R) Core (TM) i7 CPU, 8GB RAM). The computation time can be deviously reduced by using a computer with better computation performance.

5.4.2 Results

Due to the spatial-temporal evolution of hazardous scenarios, humans may get exposed to different hazardous scenarios. The death probabilities caused by different hazardous scenarios at H1-H5 are shown in Figure 5.5.

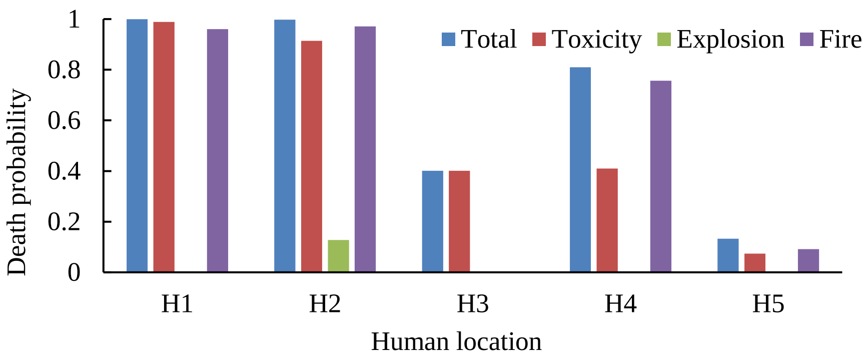

Figure 5.5 Death probabilities caused by hazardous scenarios at H1-H5 (Chen et al., 2021b)

As shown in Figure 5.5, both the total death probabilities at H1 and H2 are around 0.99, indicating that people at H1 and H2 will die due to the toxicity and fire. The total death probabilities at H1 and H2 are approximately equal to their death probabilities caused by toxicity or fire. It demonstrates that people at H1 and H2 may simultaneously or sequentially receive multiple hazardous scenarios. Humans at H1, H4, and H5 are mainly threatened by toxicity and fire while the main hazardous scenarios at H2 include toxicity, VCE, and fire. The hazardous scenarios at H3 are dominated by toxicity since it is far from T1, and it is not in the storage tank area. Although there is a long distance between T1 and H5, fire can escalate from tanks nearby T1 to the tanks close to H5. The results can be explained by analyzing the spatial-temporal evolution between the hazardous scenarios. In this case, explosion is not the main cause of fatalities, but it can cause injures such as eardrum rupture. The probability of eardrum rupture at H1 and H2 is 0.34 and 0.68, respectively. According to these results, different kinds of PPEs can be assigned to humans in different positions. For example, humans at H3 only need to take a gas mask while protective clothing to protect against potential heat is also needed for humans at H1, H2, H4 and H5 due to possible multi-hazardous scenarios. More details of PPE are presented in the Discussion.

Figure 5.6 shows the failure probabilities caused by fires and explosions of the 27 hazardous tanks due to the overfilling of acrylonitrile at T1. The failure probabilities of T1-T6 in tank area I is around 0.98 since they are close to the release source. The failure probabilities of tanks in storage area II obviously decrease with increasing the distance between the release sources and the tanks (e.g., T7-T11, T12-T15). The failure probabilities of tanks in tank area III are much lower than those of the tanks in storage areas I and II since they are located farther from the release source T1. Besides, the fires cannot escalate from area II to area III due to the safety distance between these areas. However, the explosion at tank areas I and II can damage the tanks in area III, possibly resulting in fires. It indicates that the safety distances provided for preventing fire escalation are not sufficient to prevent the damage caused by VCEs.

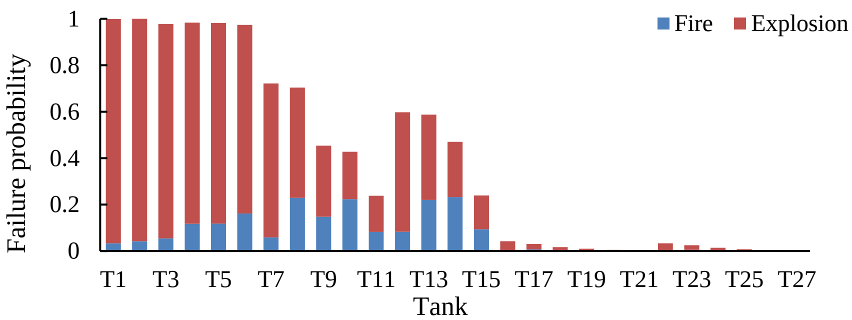

Figure 5.6 Failure probabilities of tanks caused by fire and explosion (Chen et al., 2021b)

The tanks around T1 (i.e., T1-T8 and T12) are more likely to be directly damaged by explosions (VCEs). These damaged tanks may result in multiple fires, and the fires may escalate spatially as well as temporally, resulting in the damage of other tanks such as T10 and T11. Figure 5.7 exemplifies one of the possible hazardous scenario evolutions: acrylonitrile starts releasing from T1 at t = 0; the released acrylonitrile forms a flammable vapor cloud, and the vapor cloud disperses around. People at H1 and H2 get exposed to the toxic gas at t = 1.3 min and t = 3.0 min, respectively. The ignition source S2 is active at t = 2.8 min while S2 is active at T = 5.1 min. Then the vapor cloud is ignited by S2 at t = 7.6 min, resulting in a VCE. During the vapor dispersion process, people at H1 and H2 die due to acute toxicity. At t = 7.6 min, 11 tanks (T1-T9, T11, T12, and T15) are damaged and catch fire due to the overpressure caused by the VCE. The fires rapidly escalate to T10, T13 and T14. Finally, people at H4 die due to heat radiation.

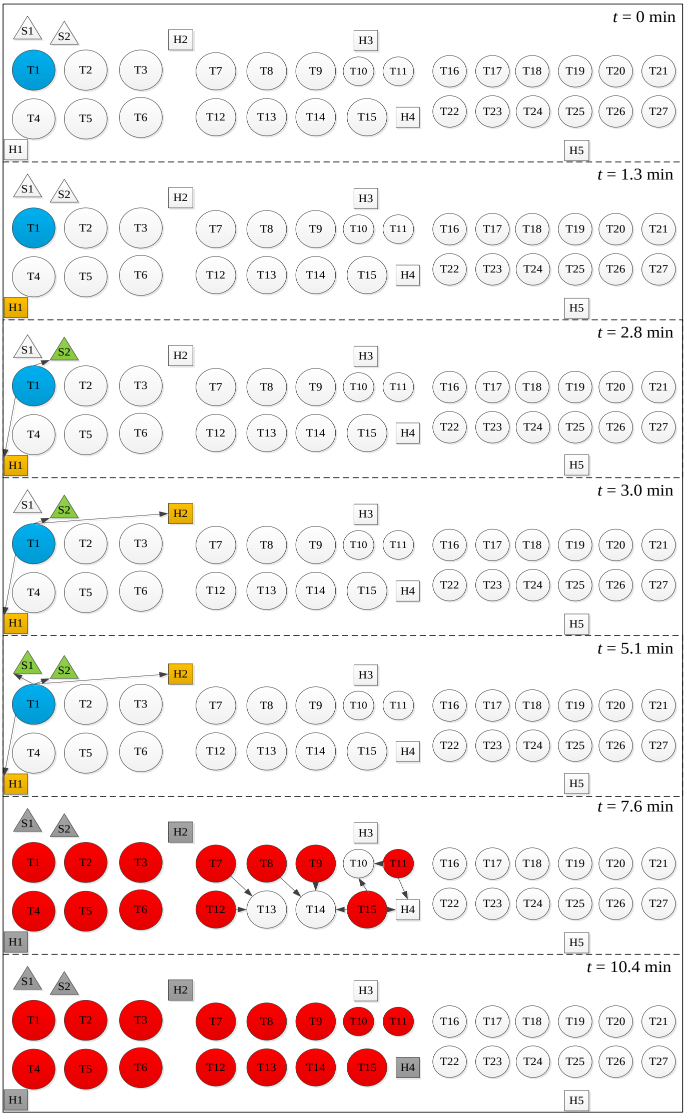

Figure 5.7 One scenario evolution including toxic release, VCE, and fire (Chen et al., 2021b)

As shown in Figure 5.7, T10, T13, and T14 are damaged by multiple fires at t = 10.4 min due to synergistic effects. The result demonstrates that fire escalation after a delayed VCE is usually inevitable. Despite the fact that the fire cannot escalate from tank storage area II to tank storage area III due to the physical distance between them, there is a low probability for the tanks in storage area III to get damaged (0.0 ~ 0.1) and for people at H5 to die (0.09) in a fire: This case may happen if a VCE causes damage to the tanks in the storage area III and subsequently triggers fire in the area. It indicates that the tanks are more vulnerable to VCEs and the safety distances solely based on fire risk assessment would be ineffective for VCEs. Due to the hazardous scenario evolution, the death probabilities of humans at H1, H2, and H4 change over time. Figure 5.8 shows the cumulative probabilities of death at H1, H2, and H4. People at H1 start inhaling toxic vapor at t =1.3 min when the toxic vapor spreads to H1 and the death probabilities increase over time due to the amount of inhaled toxic vapor. The cumulative probability of death at H2 increases from t = 3.0 min when the people at H2 when people at H2 begin to be exposed to toxic gas. At t = 7.6 min, multiple tank fires are induced by the VCE, resulting in hazardous effects at H1, H2, and H4. As a result, the cumulative probability of death at H4 starts to increase due to the induced heat radiation, and that at H1 and H4 further increases due to toxicity and heat radiation.

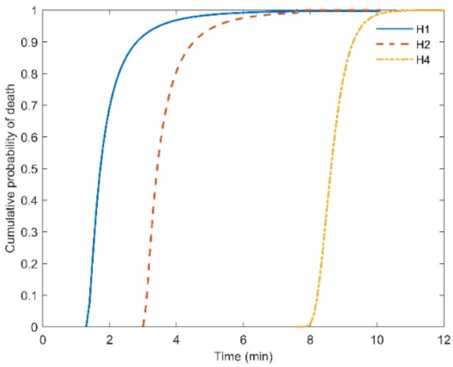

Figure 5.8 The cumulative probabilities of death at different positions (Chen et al., 2021b)

5.5 Discussion

The case study in Section 5.4 demonstrates that multi-hazard chemicals (e.g., acrylonitrile) in the process industry can simultaneously or sequentially lead to multiple hazardous scenarios to humans and installations due to the cascading effects. The results are consistent with the characteristics of the disaster in Zhangjiakou, China (2019). Based on the case study, this section discusses parameters that may have considerable effects on human vulnerability and the multi-hazard evolution.

5.5.1 Atmosphere parameters

Atmosphere parameters such as ambient temperature and wind have an impact on the evaporation of liquid hazardous materials and the dispersion of vapor clouds. Both wind speed and direction have been shown to affect the vulnerability of humans and facilities during cascading effects [41, 57]. Since large disasters caused by overfilling usually occur at low wind conditions (Atkinson, 2017), only the effects of temperature on the death probability of humans and the failure of hazardous tanks are discussed in this study. As shown in Figure 5.9, both the death probability of humans and the failure probability of tanks increase with the rise of ambient temperature. As shown in Figure 5.9a, the death probability of humans at H3 only slightly increases with rising temperature, indicating that acute toxicity is not sensitive to temperature. The reason is that the rise of ambient temperature increases the toxic gas concentration while decreases the delayed ignition time (DIT). The failure probabilities of tanks in tank area III (T16-T27) are much lower than those in area II since the physical distance between tank area II and III becomes a barrier for fire escalation between the two areas. When the ambient temperature rises, the likelihood of tank failure in tank area III increases rapidly since the overpressure caused by VCEs increases so does the damage likelihood of tanks in area III. In general, humans with lower death probabilities and tanks with lower failure probabilities are more sensitive to ambient temperature. It can be demonstrated that the damage effects increase with increasing ambient temperature.

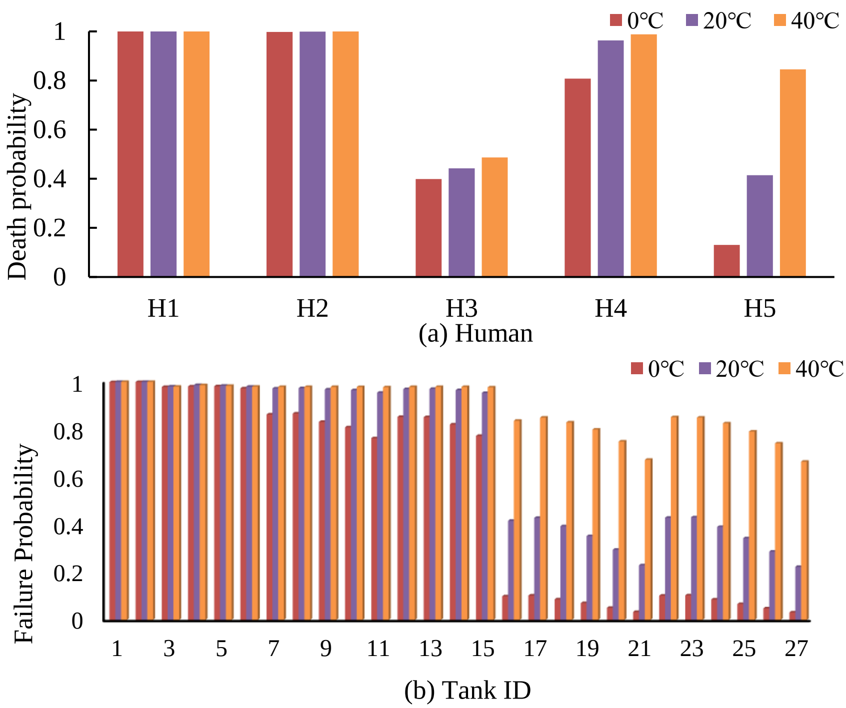

Figure 5.9 The effects of ambient temperature on humans and installations (Note: (a) the total death probability of humans, and (b) the total failure probability of installations, adapted from Chen et al. (2021b))

5.5.2 Flow rate

The flow rate is a key parameter for characterizing a loss of containment. Since the amount of hazardous material released is proportional to the flow rate, the death probability increases with increasing flow rate, as shown in Figure 5.10a. The death probability at the five positions slightly rises with the increase of the flow rate. Figure 5.10b shows the effects of flow rate on the failure probabilities of hazardous tanks. All the failure probabilities of the 27 tanks display an increasing trend when increasing the flow rate. Therefore, it can be demonstrated that a larger release is more likely to result in more severe consequences, no matter what hazardous scenarios the release causes. By comparing Figure 5.10 with Figure 5.9, it can be demonstrated that the effect of flow rate is much smaller than that of ambient temperature since the evaporation rate of toxic vapor is more sensitive to ambient temperature than the flow rate. For example, the concentration of toxic vapor increase by 34% if the flow rate increases from 80kg/s to 160kg/s while that increases by 170% when the ambient temperature increases from 20℃ to 40℃.

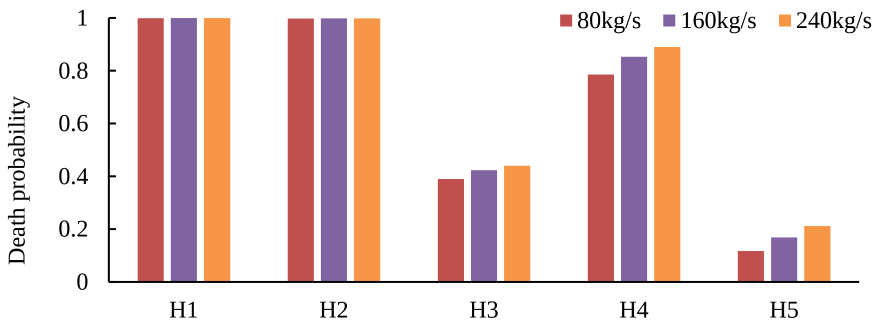

(a) Human

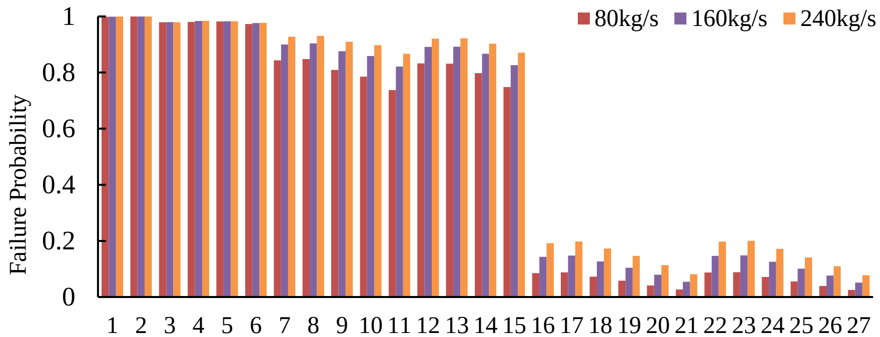

(b) Tank

Figure 5.10 The effects of flow rate
(Note: (a) the total death probability of humans and (b) the total failure probability of tanks, adapted from Chen et al. (2021b))

5.5.3 Probability of immediate ignition

An immediate ignition can lead to fire but the increase of the probability of immediate ignition (PII) decreases the likelihood of VCEs and toxicity. Figure 5.11 illustrates the effects of FII on the total death probability of humans and the total failure probability of the tanks. Both the death probability and failure probability decrease with an increase of the PII. It indicates that the damage caused by the fire is lower than the damage caused by VCEs and toxicity. The total risk caused by hazardous materials towards individuals and facilities may be underestimated if only fire hazard is considered in the hazardous scenario evolution. The tanks close to the release source are more sensitive to the PII because an increase of PII sharply decreases the damage probability caused by VCEs, as shown in Figure 5.11b.

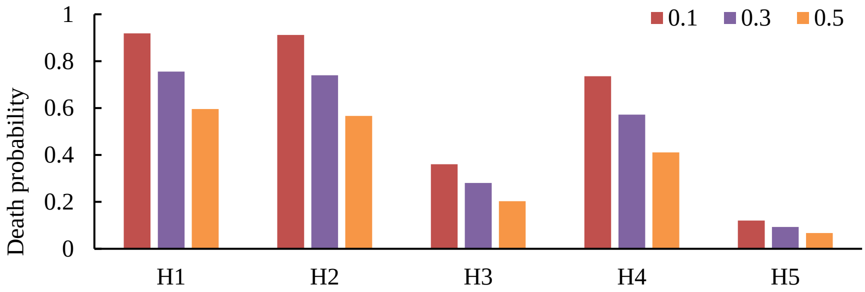

(a) Human

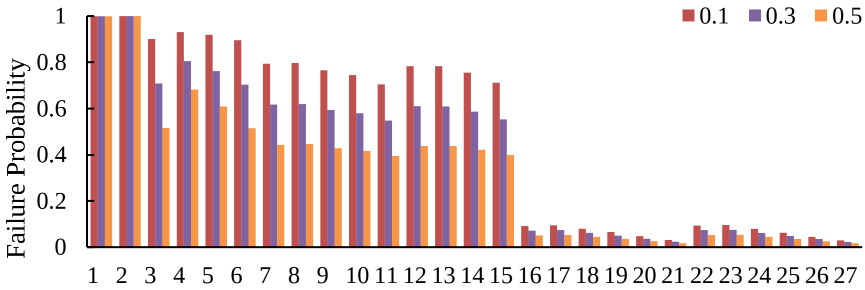

(b) Tank

Figure 5.11 The effects of the probability of immediate ignition (PII)
(Note: (a) the total death probability and (b) the total failure probability, adapted from Chen et al. (2021b))

5.5.4 Emergency response

The time needed for effective emergency response (t_e) is essential for mitigating the consequences of a disaster by cutting or delaying the spatial-temporal escalation of hazardous scenarios. In this study, a log-normal distribution is used to model the uncertainty of t_e. The effects of the average values of t_e (μ) on the total death probability and failure probability are shown in Figure 5.12. As shown in Figure 5.12a, The death probability of humans far from the release source increases with increasing the time needed for the emergency response while the death probability at H1 and H2 close to the release source is not sensitive to the t_e. It is more difficult to rescue people near the release source via emergency response. The failure probability of tanks also increases with the increase of tee. Besides, tanks that are more vulnerable to fire are more likely to survive since the emergency response can largely decrease the possibility of fire escalation.

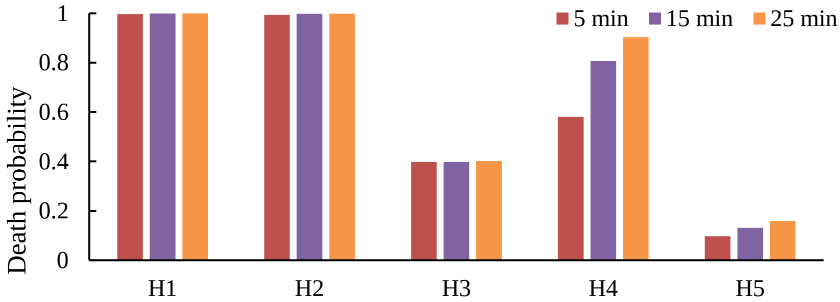

(a) Human

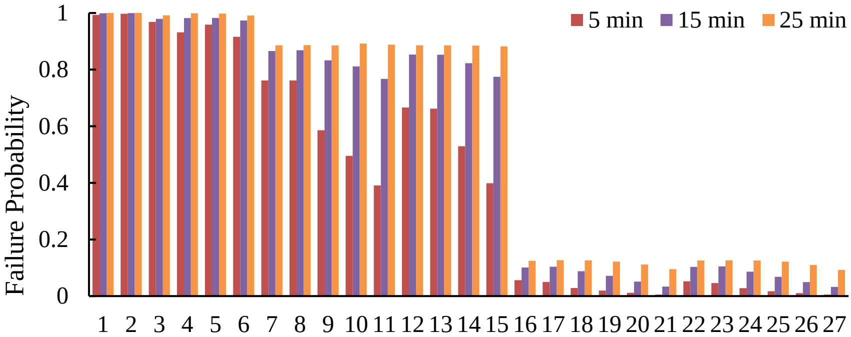

(b) Tank

Figure 5.12 The effects of emergency response parameter μ
(Note: (a) the total death probability of humans and (b) the total failure probability of tanks, adapted from Chen et al. (2021b))

5.5.5 Personal protection equipment

PPE is used to minimize human exposure to hazardous scenarios, such as respirators, protective clothing, helmets, goggles, glasses and other garments that are designed to prevent the wearer from hazardous scenarios (OSHA, 2019). In the case study, the main hazards for humans are toxic gas and heat radiation. Respirators are commonly used for protecting humans from toxicity by filtering out toxic gases in the air (Greenawald et al., 2020). In case PPE is available in chemical plants, a human response time of 5 s for humans to respond to hazardous scenarios is considered (Van Den Bosh et al., 1989). Figure 5.13 shows the death probabilities of humans with respirators in different positions. Compared to Figure 5.5 (without respirators), the death probability caused by acute intoxication is largely reduced. For example, the death probability at H1 decreases from 0.99 to 0.05, decreasing by 95%. However, the total death probabilities at H1, H2 and H4 don't decrease since people at these positions are also threatened by heat radiation. As a result, thermal protective clothing is needed to provide enough time for humans to escape from fire scenarios (Van Den

Bosh et al., 1989; Guowen et al., 2010). Figure 5.14 shows the death probabilities under the protection of respirators and thermal protective clothing.

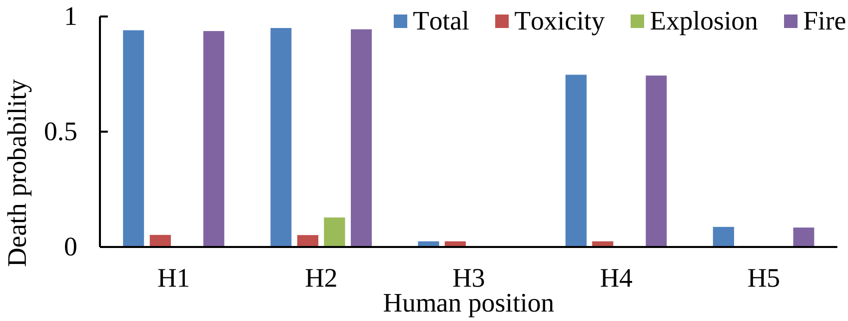

Figure 5.13 The effects of respirators on the death probabilities (Chen et al., 2021b)

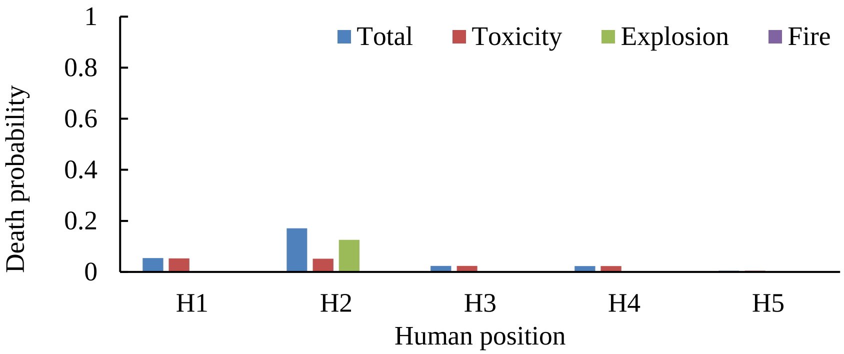

Figure 5.14 The effects of respirators and thermal protective clothing (Chen et al., 2021b)

As shown in Figure 5.14, the total death probabilities at H1-H5 are decreased due to the application of respirators and thermal protective clothing. In the case scenario, both respirators and thermal protective clothing are needed for people at H1, H2, H4 and H5 while only respirators are needed in H3 since people may only be exposed to toxic hazardous scenarios. Consequently, this study can facilitate the allocation of PPE for people at different positions and avoid underestimating hazardous scenarios and unreasonable allocation of protection resources.

Besides the discussed issues, in the future, CFD may be used to model the dispersion of toxic gas, considering the influences of wind velocity and obstacles on dispersion, thus improving the accuracy of the proposed method. In terms of Monte Carlo simulation, the application of more advanced computers may be needed for the case with hundreds of installations and multiple ignition sources.

5.6 Conclusions

There are many installations for storage, transport, or process of hazardous materials in chemical process plants. Once a release occurs at an installation, hazardous scenarios such as toxic release, VCE and fire can simultaneously or sequentially occur, and the generated hazardous scenarios can evolve spatially and result in a cascading disaster.

In this study, a dynamic methodology based on dynamic graphs and Monte Carlo simulation is developed to assess the vulnerability of humans and facilities if they are exposed to multiple hazardous scenarios while considering the spatial-temporal evolution of the hazardous scenarios. A case study was used to illustrate the application of the methodology and its capabilities in modeling the occurrence and evolution of time-dependent multi-hazard under uncertainty.

The main achievements of the present study can be summarized as follows: (i) The methodology can effectively model simultaneous and sequential multiple hazards caused by the release of hazardous materials; (ii) only considering one type of hazard in vulnerability assessment may largely underestimate the risk, possibly resulting in ineffective allocation of personal protection equipment (PPE); (iii) humans in different locations may be threatened by different hazards, thus different protection strategies may be formulated for people within and around the chemical plants; (iv) VCE and toxic release may result in more severe consequences than fire as long-delayed ignition can result in the damage of multiple installations and acute toxicity of people around the release source; (v) the concurrent fires resulting from a VCE may be inevitable due to a rapid escalation rate and limited emergency resources; (vi) hazardous installations are more vulnerable to VCEs, and the safety distances based on fire hazards are not sufficient for VCEs; (vii) people close to the release source are prone to multi-hazardous scenarios while the deaths outside the hazardous storage areas are mainly caused by acute toxicity and VCEs.

Chapter 6 Cost-benefit management of domino effects

Domino effects may be triggered by unintentional events or intentional attacks in chemical industrial areas comprising many hazardous installations. Compared with accidental domino effects, intentional domino effects may be more difficult to prevent since intelligent and strategic adversaries can adapt their tactics according to protection measures. Thus, this chapter integrates safety and security resources to prevent and mitigate domino effects. Safety and security measures are divided into three categories: detection measures, delay barriers, and emergency response. However, it is impossible to take all of the possible safety and security measures in a chemical industrial area since protection resources and safety budgets are always limited. As a result, this chapter further proposes a cost-benefit management methodology to support decision-making on protection measures, obtaining the optimal protection strategy. The net present value of benefits (NPVB) is employed and quantified in the cost-benefit analysis to determine whether a protection strategy is profitable or not. Besides, an optimization algorithm called “PROTOPT” is developed to achieve the most profitable protection strategy. An illustrated case study shows that this approach can obtain the optimal protection strategy, making the protection more effective.

The content of this chapter is based on the following published papers:

Chen, C., Reniers, G., Khakzad, N., 2020b. Cost-Benefit Management of Intentional Domino Effects in Chemical Industrial Areas. Process Safety and Environmental Protection 134, 392-405.

Chen, C., Reniers, G., Khakzad, N., Yang, M., 2021. Operational safety economics: Foundations, current approaches and paths for future research. Safety Science. 105326

6.1 Introduction

The prevention and mitigation of domino effects in the chemical process industries have received increasing attention in scientific and technical literature since the 1990s (Bagster and Pitblado, 1991). Domino effects can be triggered by either unintentional (safety-related) events (e.g., mechanical failure, human error, and natural disasters) or intentional (security-related) events (e.g., terrorist attacks). Public concern pays attention to domino effects caused by intentional attacks (security-related domino effects) since Reniers et al. (2008) proposed to deal with intentional domino effects in chemical clusters. Adversaries may execute an attack to trigger domino effects, inducing catastrophic events, or indirectly damaging installations. Besides, intentional attacks might result in unplanned domino effects due to the interaction between the target installation and the nearby installations. Compared with domino effects caused by unintentional events, intentional domino effects may induce more severe consequences due to simultaneous damage of installations induced by multiple target attacks. For example, three tanks in a French chemical plant were attacked via explosive devices in July 2015, inducing two simultaneous tank fires (one damaged tank failed to be ignited) (BBC News, 2015).

To prevent or mitigate accidental and intentional domino effects, Reniers and Soudan (2010) recommended setting up an institution, the so-called Multi-Plant Council (MPC) for stimulating the prevention cooperation in a chemical industrial cluster. Reniers and Audenaert (2014) proposed to reduce the potential consequences of intentional domino effects based on vulnerability analysis, providing a systematic method to intelligently protect chemical industrial areas against intentional attacks. Landucci et al. (2015b) assessed the vulnerability of industrial installations subject to attacks by homemade explosives. The results indicated that domino effects can be triggered by explosion attacks only in the case that homemade explosives are positioned inside the facility or near hazardous installations outside the industrial area. Zhou and Reniers (2016b) studied emergency strategies for multiple simultaneous fires caused by intentional attacks. Hosseinnia et al. (2018a) established an emergency response decision matrix to determine the emergency level of each company tackling terrorist attacks with improvised devices in chemical clusters. Khakzad and Reniers (2019) applied graph theory and dynamic Bayesian network to identify critical units and proposed a strategy whereby some of the storage tanks are made empty to mitigate intentional domino effects.

The previous work for domino effect management neglects the integrated performance of safety and security resources, possibly result in resource overlaps and unsuitable allocation of protection resources. Besides, economic issues of risk play an indispensable role in the decision-making process concerning safety and security management since companies usually face budget limitations. Economics reminds us that protection resources are always limited and the resources allocated to one target are not available for others (Poole, 2008; Paltrinieri et al., 2012; Birk, 2014). Although economic issues of risk may only be one part of risk management, it has a great impact on the effectiveness of a company's prevention policy as well as the company's profitability in the long term (Reniers and Van Erp, 2016). Economic models, therefore, are usually used to optimize the allocation of protection resources and thus maximize the protection effectiveness, such as the prevention investment decision model based on cost-benefit analysis (Reniers and Sorensen, 2013; Villa et al., 2017a) and the domino mitigation model using cost-effective analysis (Janssens et al., 2015; Khakzad et al., 2018c). Besides the application in resource allocation, economic models of terrorism provided new insights into the motivation and strategy behind terrorist events from economic perspectives by analyzing the costs and benefits of terrorism (Blomberg et al., 2004; Brück, 2007).

However, there is a research gap between economic models and domino effect management due to the complexity and uncertainty of domino effect evolution as well as the fact that there are intelligent and strategic adversaries. This study aims to develop a methodology to employ economic models for preventing and mitigating domino effects in chemical industrial areas. First, the methodology with five steps is elaborated in Section 6.2. Second, we expound on threat analysis to obtain the likelihood and possible undesired scenarios in Section 6.3. After introducing the vulnerability assessment of installations against direct attacks, the dynamic graph approach for assessing the vulnerability of installations subject to domino effects is provided in Section 6.4. Next, a cost-benefit analysis based on threat and vulnerability analysis is elaborated in Section 6.5. Moreover, an optimization algorithm is developed in Section 6.5 to achieve the optimal cost-benefit protection strategy within budget constraints. A case study is provided in Section 6.6 while conclusions drawn from this work are presented in Section 6.7.

6.2 Methodology

6.2.1 The dependencies between safety and security of domino effects

Safety barriers for preventing domino effects in process industries are generally divided into three categories: (i) active protection systems; (ii) passive protection systems and (iii) emergency measures (De Dianous and Fievez, 2006; CCPS, 2011). Previous researches on the management of domino effects mainly focus on accidental domino effects. Landucci et al. (2015a) developed a fault tree methodology to quantify the performance of safety barriers in fire-induced domino effects. Janssens et al. (2015) developed an optimization model to allocate safety barriers for the sake of maximum the *ttf* of chemical installations. Khakzad et al. (2017a) proposed a DBN approach for the performance assessment of fire protection systems during domino effects, taking into account the dynamic failure process of fireproofing coatings. (Khakzad et al., 2018c) also developed an approach based on a limited memory influence diagram (LIMID) to multi-attribute decision analysis of safety measures. Also, advanced tools such as Petri-net and event sequence diagrams were applied to assess emergency response actions during fire-induced domino effects (Zhou et al., 2016; Zhou and Reniers, 2018c).

A few attempts to manage intentional domino effects are based on securing critical installations or reducing potential consequences using safety barriers, ignoring the integration of safety barriers and security measures. Figure 6.1 shows the dependencies in the decision-making on safety and security resources, assuming possible domino effects occurring after the allocation.

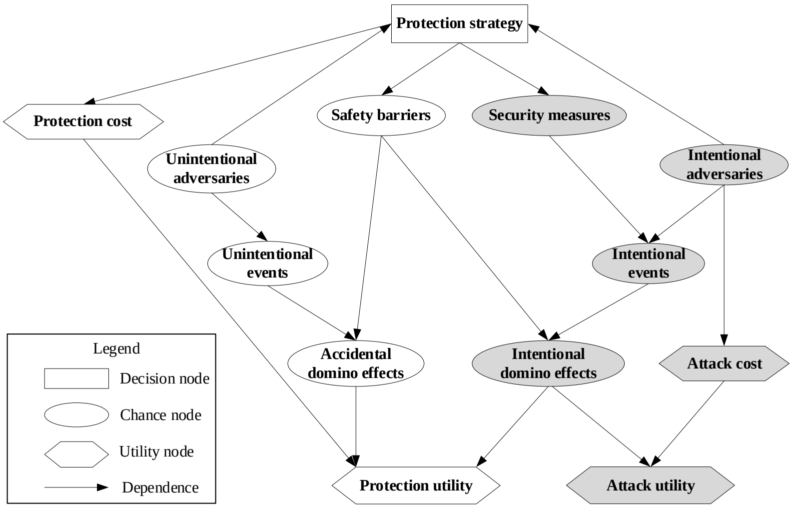

Figure 6.1 The diagram for the allocation of safety and security resources

Safety barriers can not only prevent or mitigate accidental domino effects but also have great impacts on intentional domino effects. For instance, safety barriers may reduce the potential consequences of intentional events and thus decrease the attractiveness of chemical industrial areas. In terms of cross-plant areas, safety and security resources allocated in one chemical plant have a benefit for plants nearby due to the mitigation of possible external domino effects while it may also relatively increase the security risk of nearby plants because of the change of attractiveness. Therefore, safety and security resources should be integrated to prevent or mitigate all possible domino effects caused by safety or security events.

6.2.2 Classification of protection measures

In light of possible intentional and accidental domino effects, both safety and security measures may be used in domino effect management. A new classification of protection measures (safety or security measures) for preventing and mitigating domino effects in chemical industrial areas is proposed, as shown in Figure 6.2.

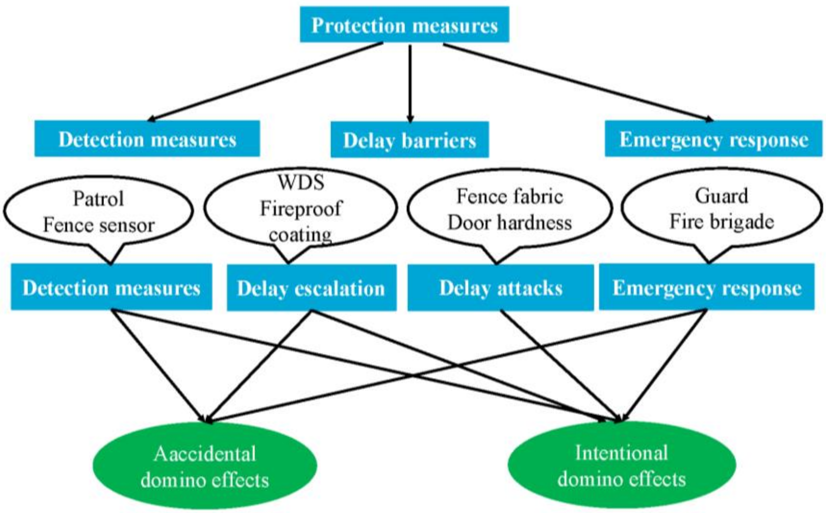

Figure 6.2 Classification of protection measures related to domino effects

According to the function of protection measures, protection measures are divided into three categories: detection measures, delay barriers, and emergency response actions.

(1) Detection measures

Detection measures are used to detect intentional and unintentional abnormal events such as accidental release and adversary actions. The detection function consists of a series of sub-functions: discovery, alarm, and assessment, etc. A detection for an abnormal event is successful only when the functions are correctly executed. As a result, the detection performance depends on the probability that detection sensors or persons successfully discover abnormal events, the probability that the alarm related to the events are successfully communicated, the probability that the alarm is successfully assessed, and the time needed from the entire detection process (detection time). An additional detection performance indicator is the nuisance alarm rate. A nuisance alarm is any alarm that is not caused by abnormal events. In an ideal detection system, the detection probability would be 1 and the nuisance alarm rate would be zero. However, in a chemical plant, all sensors interact with their environment and they may be disturbed by other disturbances in their detection zones, such as vegetation, wildlife, and weather conditions. In a chemical plant, a typical detection system may consist of exterior and interior intrusion sensors, video alarm assessment, entry control, and alarm communication systems. Video alarm assessment is always conducted by closed-circuit television (CCTV) camera coverage of each sensor sector. An entry control system allows authorized personnel and material to get into and out of facilities while detecting and possibly prevent the access of unauthorized movements. Alarm communication aims to transport an alarm and information to a center, and possibly present and assess the information (Garcia, 2007; Reniers et al., 2015).

(2) Delay barriers

Delay barriers may be divided into two categories: delay attack measures and delay escalation measures. Delay attack measures are barriers that can increase the time that an adversary needs to carry out an action and such measures can thus delay the implementation of an attack. An effective protection system first requires that the detection system successfully discovers the abnormal event. In that case, response force (e.g., guards, police) can work to prevent the attack when the alarm is correctly assessed and delivered to the response force. However, the start of an effective response force needs time and if the time is larger than the time needed for completing the adversary attack, the response force would be ineffective and the attack could not be prevented. As a result, after an adversary action is detected, delay measures are employed to delay the implementation of the attack until an effective response force is available. Therefore, response force can successfully interrupt the adversary attack before the attack goal is achieved only when the adversary is detected and the response force is available (active) before the attack is implemented (Garcia, 2007; Chen et al., 2020b). Delay escalation barriers are barriers used to delay the escalation of domino effects, such as fireproof coatings and water delivery systems. For example, fireproof coatings can block the transfer of heat radiation from the installation on fire to nearby installations exposed to the fire, increasing the time to failure (TTT) of the exposed installations (Chen et al., 2019b, 2020c).

(3) Emergency response

Response force refers to any response personnel and measures that may be involved in the response to intentional attacks or hazardous scenarios in a chemical plant. As a result, emergency response in a chemical plant is essential to protect installations, the public, workers, and the environment. The response force may be on-site and offsite, including security guards, police, medical emergency team, and fire brigade, etc. Guards and police may be regarded as a preventive response which may prevent the completion of an attack if the attack is successfully detected and the delay measures provide enough time for the start of the response force. Medical emergency teams and fire brigades are used to mitigate the consequences of attacks. Protection of different targets may require different response plans and the performance of response force depends on the threat types. For example, it is almost impossible to use security guards to prevent drone attacks. This is one of the reasons that the drone attack on the Abqaiq oil plant in 2019 led to a 50% reduction in Abqaiq’s oil production and a nearly 15% increase in the crude oil price (Chen et al., 2021a). Therefore, different chemical plants may need different protection strategies and an effective protection strategy requires a reasonable arrangement of detection, delay, and response measures (Garcia, 2007; Reniers et al., 2015; Chen et al., 2020b).

6.2.3 Cost-benefit management

Based on the integrated protection measures, a methodology based on cost-benefit analysis is developed to obtain the most profitable protection strategy for domino effects in the process and chemical industries. Figure 6.3 shows the steps of the methodology. The methodology for preventing and mitigating domino effects consists of five parts: threat and hazard analysis, vulnerability assessment of installations directly against undesired events, vulnerability assessment of installations subject to possible domino effects induced by the undesired event, cost-benefit analysis, and optimization. The first step aims to determine the threat probability (the likelihood of the threat) and possible accidental hazards. Due to domino effects, installations may be damaged by direct undesired events or the consequent domino effects. Therefore, steps 2 & 3 deal with the vulnerability of installations directly to undesired events and consequent domino effects respectively. The performance of protection measures is also considered in the vulnerability assessment. According to the results of threat analysis and vulnerability assessment, a cost-benefit analysis is conducted in step 4 to determine whether a protection strategy (a combination of protection measures) is profitable, or not. Finally, the cost-benefit protection strategy is obtained through an optimization algorithm in step 5. The five steps will be elaborated hereafter.

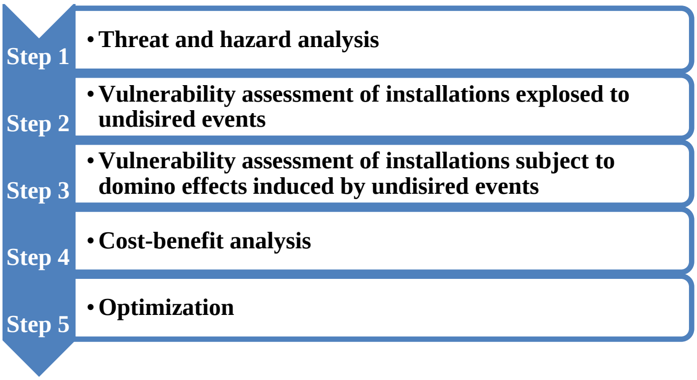

Figure 6.3 Procedures of the developed methodology
(Chen et al., 2020b)

6.3 Threat and hazard analysis

Threat and hazard analysis which provides the basic data (e.g., threat likelihood, possible undesired scenarios) for vulnerability analysis, is needed for economic analysis for managing domino effects. Unintentional threats (hazards) can be easily analyzed by hazard identification methods such as the Hazard and Operability Study (HAZOP) method and the checklist method. An intentional threat may be regarded as an indication, a circumstance, or an event that possibly leads to losses of, or damage to, facilities (API, 2013). The first step of intentional threat analysis is to collect information on possible threats, such as motivations, attack types, attack capability, and attack objectives. According to adversaries’ motivations, domino effects caused by intentional attacks may be categorized into three types: (i) adversaries may execute an attack to trigger domino effects, inducing catastrophic consequences; (ii) adversaries attack target installations resulting in unplanned domino effects; (iii) adversaries indirectly attack an object installation via domino effects. The objective of threat analysis for tackling intentional domino effects is, therefore, to identify possible scenarios caused by intentional attacks and to determine the threat probability.

Intentional attacks may result from internal adversaries, external adversaries, or internal adversaries working in collusion with external adversaries. The adversaries encompass individuals, groups, organizations, or governments possibly executing these intentional events. So a threat analysis should consider as many adversaries as possible, such as intelligence services of host nations, or third-party nations, political and terrorist groups, criminals, rogue employees, cybercriminals, and private interests (API, 2013). Besides, the capability and the resources of the attackers in terms of available information, instruments, and tools should be considered in the analysis. However, quantifying adversaries is a considerable challenge since it requires a multitude of data and knowledge, and modeling the motivations, intents, characteristics, capabilities, and tactics of adversaries (Paté-Cornell and Guikema, 2002; Baybutt, 2017). Expert judgment methods may be applied to determine the threat probability, P_T (the likelihood of the threat) based on available data and information. In this study, a five-level threat assessment method recommended by the American Petroleum Institution (API) is adopted, as shown in Table 6.1.

Table 6.1 SRA methodology for threat assessment
(Note: adapted from API (2013))

Threat level	Description
Very low	Indicates little or no credible evidence of capability or intent and no history of actual or planned threats against the asset or similar assets (e.g. "no expected attack in the life of the facility's operation").
Low	Indicates that there is a low threat against the asset or similar assets and that few known adversaries would pose a threat to the asset (e.g. "1 event or more is possible in the life of the facility's operation").
Medium	Indicates that there is a possible threat to the asset or similar assets based on the threat's desire to compromise similar assets, but no specific threat exists for the facility or asset (e.g. "1 event or more in 10 years of the facility's operation").
High	Indicates that a credible threat exists against the asset or similar assets based on knowledge of the threat's capability and intent to attack the asset or similar assets, and some indication exists of the threat specific to the company, facility, or asset (e.g. "1 event or more in 5 years of the facility's operation").
Very high	Indicates that a credible threat exists against the asset or similar assets; that the threat demonstrates the capability and intent to launch an attack; that the subject asset or similar assets are targeted or attacked on a frequently recurring basis; and that the frequency of an attack over the life of the asset is very high (e.g. "1 event/event per year").

In case of unacceptable high consequences caused by intentional domino effects or insufficient information and data available to implement the five-level threat assessment method, a conditional threat approach may be applied: assuming $P_T = 1$ (Mueller and Stewart, 2011; Villa et al., 2017a). This conservative approach indicates that the potential consequences of possible intentional attacks are so severe that the threat likelihood assessment is not necessary. In that case, security management may focus on assessing the vulnerability of chemical installations, the potential consequences of intentional domino effects, and the cost-benefit of protection measures.

6.4 Vulnerability assessment

A vulnerability assessment for installations against intentional domino effects should consider (i) the vulnerability of installations directly against threats and hazards as well as (ii) the vulnerability of installations subject to possible domino effects caused by the attacks. Since the vulnerability of installations exposed to hazards can be obtained by using several traditional methods such as fault tree analysis and Bayesian network (Khakzad et al., 2011), this section mainly focuses on the vulnerability of installations against direct intentional attacks and domino effects.

6.4.1 Vulnerability assessment of installations against direct intentional attacks

The vulnerability of installations against direct intentional attacks can be regarded as any weakness that may be exploited by an attacker to gain access to direct targets and to successfully execute an attack (API, 2013). An intentional attack can be interrupted when the attack is detected and the guard communication to the response force is of success (Garcia, 2007). Therefore, the probability of a successful attack (P_S), indicating the likelihood that a target installation is directly damaged by the attack, can be expressed as follows:

$$P_S = P_T \cdot (1 - P_D \cdot P_C) \cdot P_E \tag{6.1}$$

where P_C is guard communication probability usually with a value of at least 0.95; P_D is detection probability; P_E is the probability that the attack is successfully executed. According to the EASI model (Garcia, 2007), P_D depends on the attack path, detection measures along the path, and guard response time. If the needed time for an attacker to pass the segment between a detection position and the attack target is less than the guard response time, the detection measures should not be accounted for. To successfully interrupt intentional attacks, detection measures and delay measures should be arranged reasonably. Detection measures consist of fence sensors, door sensors, personnel, etc., and delay measures include fence fabric, door hardness, wall hardness, etc. To assess the damage probability of installations caused by direct attacks, it is required to quantify the detection probability of each detection measure and to calculate the delayed time of each delayed measure.

The factors that affect P_C include the training in the use of communication equipment, maintenance, dead sport in radio communication, and the stress experienced during actual attacks (Garcia, 2007). The P_E depends on the capability and the resources of the attackers, which is relevant to available information, instruments, and tools. It was simplified as the product of the reliability of the available device (P_{re}) and the performance factor (P_{pe}) of adversaries when using the device (Stewart and Mueller, 2012), as follows:

$$P_E = P_{re} \cdot P_{pe} \tag{6.2}$$

In terms of explosion attacks launched by terrorist organizations, 4 types of explosive device complexity are defined. The corresponding values of P_{re} and P_{pe} are reported in Table 6.2.

Table 6.2 Values of P_{re} and P_{pe} w.r.t. explosion attacks (Stewart and Mueller, 2012; Villa et al., 2017a)

Device complexity	Representative device	P_{re}	P_{pe}
Simple	Pipe bomb	0.931	0.981
Medium	Mobile phone initiated VBIED*	0.920	0.980
Complex	Improvised mortar	0.910	0.905
No information available	Conservative assumption	1	1

*VBIED: Vehicle Borne Improvised Explosive Device

According to the above analysis, the possible primary hazardous scenarios initiating domino effects can be identified via cause-consequence analysis methods, such as what-if analysis and fault tree analysis (Reniers et al., 2005a; Chen and Reniers, 2018). The primary hazardous scenario (H) can be expressed as a conditional probability of successful attacks, $P(H \mid S)$. Thus the probability of primary scenarios caused by intentional attacks is represented, as follows:

$$P_H = P_S \cdot P(H \mid S) \tag{6.3}$$

The probability of primary hazardous scenarios (P_H) is deemed to be a prior probability to obtain the vulnerability of installations exposed to possible intentional domino effects in the considered chemical industrial area.

6.4.2 Vulnerability assessment of installations subject to domino effects

The main objective of vulnerability assessment for domino effects is to determine the damage probability of installations subject to possible domino effects caused by undesired events. A chemical industrial area consists of various hazardous installations situated next to each. An undesired event to one or more than one hazardous installation may trigger a chain of hazardous events, resulting in more severe consequences than that of the primary event. These hazardous events may occur simultaneously or sequentially, so the evolution of domino effects may be a time-dependent or dynamic process. Therefore, a dynamic tool is more suitable for modeling the evolution of domino effects and to assess the vulnerability of installations subject to domino effects. The dynamic graph approach developed in Chapter 3 is introduced to assess the vulnerability of installations exposed to possible domino effects, considering the performance of escalation barriers and emergency response.

(1) The performance of active escalation barriers

Active escalation barriers are safety measures that their protection functions need to be triggered by a device or a system. These measures are widely used to detect and respond to process deviation from normal operation, such as water deluge systems (WDS), emergency shutdown systems (ESD), and emergency depressurization systems (EDP). A common-used active barrier is WDS. The heat radiation received by installations can be reduced by WDS. The WDS mitigates fire exposure by keeping a water film on exposed surfaces to absorb radiant heat and to cool the steelwork, thus reducing the heat radiation received by installations. In this study, WDS is used as an example of an active barrier in the evolution of domino effects. The heat radiation with WDS ($q_{w,ij}$) can be obtained using a radiation reduction factor (φ) and an effectiveness parameter (η) when the installation i is on fire, as follows:

$$q_{w,ij} = (1-\eta\times\varphi)\times q_{ij} \tag{6.4}$$

q_{ij} is the heat radiation caused by installation i on installation j without WDS, in kW/m^2; η is an effectiveness parameter of active protection systems; φ is the radiation reduction factor. If the active protection system is available, parameter values are assumed as follows: φ = 60%, η = 75%; otherwise, both parameters are equal to zero (Landucci et al., 2015a).

(2) The performance of passive escalation barriers

Different from active barriers, passive safety barriers such as firewalls and fireproofing coatings don't need any trigger devices and systems. Fireproofing coatings are always used on the surface of hazardous vessels to decrease the incoming heat radiation and mitigate the heat-up of the vessel, avoiding failure caused by external fire. In case of the presence of fireproof coatings, a time-lapse (T_l) should be considered since the failure time of installations is delayed due to the existence of fireproof coatings. Considering a hazardous installation starts receiving heat radiation at time T_g, the residual time to failure with fireproof coatings ($RTF_{c,j,g}$) can be obtained, as follows:

$$RTF_{c,j,g} = RTF_{j,g} + T_l \tag{6.5}$$

In this study, a conservative T_l of 70 min (Landucci et al., 2015a) for a 10mm fireproof coating is used in the present study if the fireproof coating is available; otherwise, the T_l should be zero.

(3) The performance of emergency response

Emergency response in the chemical industry is essential to protect installations, employees, the public, and the environment (Hosseinnia et al., 2018) when an undesired event occurs. In terms of domino effects, emergency response actions such as firefighting can effectively suppress fire escalations and thus prevent and mitigate domino effects (Zhou and Reniers, 2017). In chapter 3, a cumulative log-normal distribution (LND) function is used to model the time required to control domino effects (*TTC*). As a result, any measures that can induce the mean value of *TTC* can be used to enhance the capability of emergency response. The performance of emergency measures can be characterized by the reduced mean-time of *TTC* (u_r). As a result, the new distribution function with an emergency measure can be obtained, as follows:

$$\log ttc \sim N\left(u-u_r, \sigma^2\right) \tag{6.6}$$

Considering the performance of safety barriers, the evolution of domino effects and the failure probability of installations can also be obtained using the Minimum Evolution Time (MET) algorithm developed in Chapter 3.

6.5 Cost-benefit analysis

6.5.1 Cost analysis

To be able to implement a protection strategy or to update existing protection systems, cost analysis of a protection strategy is indispensable since companies are always confronted with budget limitations. In this section, the various costs related to a protection strategy that a company may decide to implement are considered. The protection costs consist of investments that occur at present time such as initial costs and installation costs, and also the costs that occur throughout the remaining lifetime of the facility (Reniers and Brijs, 2014). In other words, cost analysis for a protection measure should include direct economic costs of applying the safety or security measures and indirect costs associated with their use. Eight cost categories of protection measures are listed in Table 6.3 (Reniers and Van Erp, 2016) and security measures.

Table 6.3 Categories of protection costs
(Reniers and Van Erp, 2016; Villa et al., 2017a)

Cost category	Subcategories
Initiation	Investigation, selection and design material, training, changing guidelines and informing
Installation	Production loss, start-up, equipment, installation team
Operation	Utilities consumption and labor Utilities
Maintenance	Material, maintenance team, production loss, start-up
Inspection	Inspection team
Logistics and transport	Transport and loading/unloading of hazardous materials, storage of hazardous materials, drafting control lists, relative documents
Contractor	Contractor selection, training
Other	Office furniture, insurance, and stationery items

The present value of costs ($PVC_{i,j}$) caused by the implementation of the *j*-th protection measure in a protection strategy *i* is the sum of the initiation costs, installation cost, and the discounted present value of other six cost types, as follows:

$$PVC_{i,j} = C_{i,j,\text{ini}} + C_{i,j,\text{ins}} + \frac{(1+r)^y - 1}{r_d(1+r_d)^y}\left(C_{i,j,\text{ope}} + C_{i,j,\text{mai}} + C_{i,j,\text{ins}} + C_{i,j,\log} + C_{i,j,\text{con}} + C_{i,j,\text{oth}}\right) \tag{6.7}$$

where $C_{i,j,\text{ini}}$ represents the initial costs of measure *j* in strategy *i*, $C_{i,j,\text{ins}}$ concerns the installation costs of measure *j* in strategy *i*, $C_{i,j,ope}$ equals the annual operation costs of measure *j* in strategy *i*, $C_{i,j,\text{mai}}$ concerns the annual maintenance costs of measure *j* in strategy *i*, $C_{i,j,\text{ins}}$ represents the annual inspection costs of measure *j* in strategy *i*, $C_{i,j,log}$ represents the annual logistics and transport costs of measure *j* in strategy *i*, $C_{i,j,\text{con}}$ represents the annual contractor costs of measure *j* in strategy *i*, $C_{i,j,\text{oth}}$ represents the annual other costs of measure *j* in strategy *i*, r_d is the discount rate, *y* is the minimum value of the number of years that the protection measure will operate and the remaining lifespan of the facility. For more information for the cost calculation of subcategories listed in Table 6.3, readers are kindly referred to Reniers and Van Erp (2016).

In terms of a protection strategy *i*, there may be multiple safety or security measures, so the total annual present value of costs due to the use of a protection strategy can be expressed, as follows:

$$PVC_i = \sum_{j=1}^{J} PVC_{ij} \tag{6.8}$$

where PVC_i is the present value of cost for protection strategy *i*, *J* is the total number of protection measures taken to prevent or mitigate domino effects.

6.5.2 The overall expected loss of domino effects

To analyze the overall expected loss, both the direct damage caused by the undesired event and the damage resulting from subsequent domino effects should be considered. There may be multiple attack scenarios since the intelligent and strategic adversary may adapt to changing circumstances in terms of protection measures. Considering *K* attack scenarios and *U* accidental scenarios may be present in a chemical industrial area, the overall expected losses caused by the *k*-th (k = 1, 2, 3… *K*) attack scenario and the *u-th* accidental scenario can be simplified as the sum product of the installations' damage probabilities and their loss:

$$L_k = \sum_{n=1}^{N} P_{k,n} \cdot L_n \tag{6.9}$$

$$L_u = \sum_{n=1}^{N} P_{u,n} \cdot L_n \tag{6.10}$$

where L_k, is the total loss caused by attack *k*. $P_{k,n}$ is the damage probability of installation *n* in attack scenario *k*, L_n is the loss due to the damage to installation *n*; L_u

is the total loss caused by accidental scenario u. $P_{u,\,n}$ is the damage probability of installation n in attack scenario u.

The assessment of losses caused by domino effects should take into account economic loss, casualties, as well as any other influences such as psychological and political effects (Stewart and Mueller, 2011). Both the direct losses that are immediately visible and tangible and the indirect losses that are intangible and invisible are important to analyze avoided losses (Jallon et al., 2011; Reniers and Van Erp, 2016). The direct avoided losses consist of these avoided losses caused by damage to installations, products, and equipment, medical expenses, paying fines, and insurance premium rise while the indirect avoided losses include capacity losses, production schemes, recruitment, and wage costs (Gavious et al., 2009). The quantification of indirect losses is more difficult since they consist of hidden or invisible components, usually resulting in underestimation of the avoided losses (Jallon et al., 2011). One simple method to estimate the indirect losses is using an indirect to direct loss ratio based on the assessment results of direct losses. The ratio varies in academic literature and this makes it induce difficult for users to choose a suitable ratio. For example, a widely used loss ratio of 4 is proposed based on an analysis of 7500 accidents while a range of 1 to 20 has been proposed on different industrial sectors and methods used (Dorman, 2000). In the present study, we adopt the loss assessment method proposed by Reniers and Brijs (2014) to account for the losses of major accidents in chemical industrial areas and to address the losses related to intentional attacks, including reputation, symbolic, psychological, and political effects (Reniers and Van Erp, 2016). Therefore, the total loss caused by the damage of an installation can be estimated as a sum of eleven contributions, as follows:

$$\begin{aligned} L_n = {} & L_{n,\,sup} + L_{n,\,dam} + L_{n,\,leg} + L_{n,\,ins} + L_{n,\,hum} + \\ & L_{n,\,env} + L_{n,\,per} + L_{n,\,med} + L_{n,\,int} + L_{n,\,inv} + L_{n,\,oth} \end{aligned} \tag{6.11}$$

where $L_{n,\,sup}$ is the supply chain loss, $L_{n,\,dam}$ is the damage loss, $L_{n,\,leg}$ is the legal loss, $L_{n,\,ins}$ is the insurance loss, $L_{n,\,hum}$ is the human loss, $L_{n,\,env}$ is the environmental loss, $L_{n,\,per}$ is the personnel loss, $L_{n,\,med}$ is the medical loss, $L_{n,\,int}$ is the intervention loss, $L_{n,\,rep}$ is the reputation loss, $L_{n,\,inv}$ is the accident investigation and the cleanup loss, $L_{n,\,sec}$ is the security-related loss which is different from accidental losses. The avoided loss of each category can be calculated as the sum of the subcategories presented in Table 6.4.

Table 6.4 Categories of protection costs
(Reniers and Van Erp, 2016)

Cost category	Subcategories
Supply chain	Production, start-up, schedule
Damage	Damage to own material/property, other companies' material/property, surrounding living areas, public material/property

Legal	Fines, interim lawyers, specialized lawyers, internal research team, experts at hearings, legislation, permit, and license
Insurance	Insurance premium
Human	Compensation victims, injured employees, recruitment,
Environmental	Environmental damage and clean-up
Personnel	Productivity of personnel, training of new or temporary employees, wages
Medical	Medical treatment at location, medical treatment in hospitals and revalidation, using medical equipment and devices, medical transport
Intervention	The service from fire department, police department or ambulance
Investigation	Accident investigation
Other	Reputational, symbolic, psychological, and political effects

6.5.3 Net benefits analysis

The benefits of an integrated protection strategy can be estimated by expressing the difference between expected losses of domino accidents without and with the implementation of protection measures. To calculate the benefits of a protection strategy, a baseline ($k = 0$) should be defined. The baseline can be the strategy without any safety or security measures, or the initial strategy before protection upgrade. In that case, the benefits of a protection strategy i for a special scenario can be defined as follows:

$$B_{i,k} = L_{0,k} - L_{i,k} \tag{6.12}$$

$$B_{i,u} = L_{0,u} - L_{i,u} \tag{6.13}$$

where $B_{i,k}$ is the benefit of protection strategy i for a special attack scenario k, $L_{0,k}$ is the expected loss caused by attack scenario k under the protection of baseline strategy 0, $L_{i,k}$ is the expected loss caused by attack scenario k under the protection of strategy i; $B_{i,u}$ is the benefit of protection strategy i for a special accidental scenario u, $L_{0,u}$ is the expected loss caused by accidental scenario u under the protection of baseline strategy 0, $L_{i,u}$ is the expected loss caused by accidental scenario u under the protection of strategy i.

Different from accidental threats, adversaries with bad intentions may adapt to the changing circumstances caused by a protection strategy to maximize their malevolent inspired benefits. According to the Stackelberg leadership model (Pita et al., 2009; Kroshl et al., 2015), the defender can be considered as the ‘leader’ (on the first step moves, taking the prior decision on protection) while the attacker is viewed as the ‘follower’ who knows the protection strategy before launching an attack. A reasonable assumption is that the attacker is a benefit maximizer aiming to maximize the damage. In terms of a protection strategy i, the attacker would adapt to the protection by selecting an attack scenario k maximizing $L_{i,k}$. In other words, the benefit of a protection strategy *i* for intentional attacks should be represented by the attack scenario which causes the minimal expected benefit. Therefore, the total benefit of protection *i* for intentional attacks and accidental events can be obtained:

$$B_i = \min_k B_{i,k} + \sum_{u=1}^{U} B_{i,u} \tag{6.14}$$

where B_i is the expected benefit of protection strategy *i*. In that case, the net present value of benefits (*NPVB*) of protection strategy *i* ($NPVB_i$) can be defined as the difference between the protection benefit and the protection cost of strategy *i*, as follows:

$$NPVB_i = \frac{(1+r_d)^y - 1}{r_d(1+r_d)^y} B_i - PVC_i \tag{6.15}$$

A protection strategy *i* is usually recommended if the annual net benefit exceeds a threshold (e.g., $NPVB > 0$), otherwise, it is considered to be not cost-effective or inefficient. (Stewart and Mueller, 2013; Reniers and Van Erp, 2016). Given $NPVB = 0$, the minimal threat probability (P^*) or risk reduction ($\triangle R$) needed for a special protection strategy *i* to be cost-benefit can be obtained by 'break-even' analysis. (Stewart and Mueller, 2014) Therefore, the *NPVB* can be regarded as a robust index for decision-making on protection strategies, addressing the intelligent and strategic actions of adversaries and the uncertainties in accidental events and possible domino effect evolution.

6.5.4 Optimization

According to the cost-benefit analysis a protection strategy is recommended if the so-called net present value of benefits (*NPVB*) is greater than a threshold. However, companies usually face budget limitations and are expected to maximize the *NPVB* when it comes to decision-making on protection investments. This section thus aims to find out the most profitable protection strategy under budget limitations.

The allocation of protection resources in chemical industrial areas can be tackled according to the so-called "Knapsack problem", well-known in the field of Operations Research (Reniers and Sorensen, 2013; Villa et al., 2017a). In terms of intentional domino effects, a chemical industrial area with large quantities of hazardous installations may be regarded as an interdependent system. A non-linear optimization model can be obtained as follows:

$$\begin{cases} \max\limits_{n} NPVB_i \\ C_i \le C_{\text{Budget}} \\ i = 1, 2, \ldots, I \end{cases} \tag{6.16}$$

Eq. (6.16) indicates that *NPVB* of possible protection strategies should be maximized within the constraint of available protection budget C_{Budget}. The monetary cost of a protection strategy *i* should then obviously not exceed C_{Budget}. To simplify the problem, a robust optimization strategy called "PROTOPT" for PROTection OPTimization, is proposed to sequentially allocate safety and security measures, maximizing a chemical plant's *NPVB*, as shown in Figure 6.4.

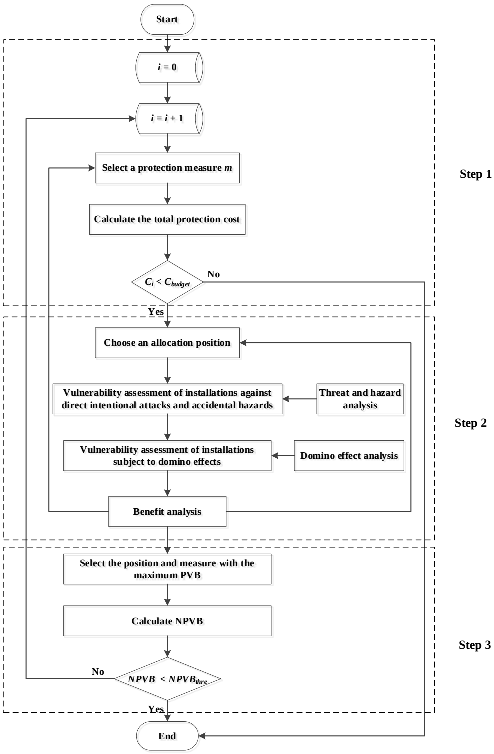

Figure 6.4 The "PROTOPT" algorithm
(Chen et al., 2020b)

As shown in Figure 6.4, the PROTOPT algorithm consists of three steps: cost analysis, benefit analysis, and optimization. The algorithm will end when the *NPVB* is lower than the threshold of *NPVB* ($NPVB_{thre}$). The *NPVB* can be considered to be zero, which means that only profitable protection strategies should be recommended. Besides, $NPVB_{thre}$ can be calculated using a Disproportionate Factor (DF) which is a threshold value to determine whether the protection measure is grossly disproportional or not. (Talarico and Reniers, 2016) Applying this optimization algorithm, we can not only obtain the optimal protection strategy under an available protection budget but also obtain a recommended protection cost and relevant protection strategy to maximize the protection *NPVB* when there is no budget restriction.

6.6 Case study

6.6.1 Case study description

To demonstrate the application of the proposed integrated methodology in tackling domino effects using safety barriers and security measures, consider a petrochemical plant in Berre L'Etang, France, as shown in Figure 6.5. The chemical industrial area was attacked in 2015, resulting in two tank fires, environmental pollution, yet no casualties (BBC News, 2015).

Figure 6.5 The layout of a chemical storage plant
(Chen et al., 2020b)

The petrochemical plant considered in this case covers an area of around 720,000 m², consisting of 32 gasoline storage tanks (T1-T34) and 6 dismissed tanks (T35-T40). The characteristics of the three types of gasoline storage tanks (small, middle, and large tanks) are summarized in Table 6.5.

Table 6.5 Characteristics of petrochemical storage tanks

Tank	Type	$D \times H$ (m)	Chemical substance	Volume (m^3)	Content (m^3)	Symbol
T1-T15	Atmospheric	42×7.2	Gasoline	9975	8000	Small
T16-T30	Atmospheric	48×7.2	Gasoline	11966	10000	Middle
T31-T34	Atmospheric	60×5.4	Gasoline	15268	13000	Large

These tanks are surrounded by tank dikes and each dike contains one or two tanks. To detect any abnormal events of tanks, cameras are installed in the dikes (E1~E19 as shown in Figure 6.5), considering a detection probability of 0.9 for each camera. The west side of the plant concern other chemical facilities and loading and unloading zones are located in the North part of the plant. The curve marked in white in Figure

6.5 is the simple wired perimeter fence on the eastern and northern boundaries of the plant.

6.6.2 The threat and hazard to the chemical plant

According to the procedures of the methodology, we should first analyze possible threats and hazards. Since the chemical plant was maliciously attacked in 2015, consider an external adversary to sabotage tanks (setting fires), trying to maximize the company's loss. Besides, the threat level is regarded as high and the threat likelihood P_T is equal to 0.2 according to Table 6.1. The possible adversary may cut the simple wired fence at a special site (I1~I9), run into one tank dike (E1-E20), and attack one tank or two tanks sequentially in the dike. As a result, the possible 48 attack scenarios considered in this case study are shown in Figure 6.6, there are 34 attack scenarios with a single target and 14 attack scenarios with two targets. Since intentional attacks are the main threats to the chemical plant, possible accidental hazards are ignored in this case study.

6.6.3 The vulnerability of tanks against intentional attacks

The second step is to carry out a vulnerability assessment of installations against direct attacks. According to the procedures and paths of the possible attack scenarios presented in Figure 6.6, the needed time to get through each path section for different attack scenarios can be calculated. A standard running speed of 3 m/s is assumed during the attack process of adversaries without any load (Villa et al., 2017a). Since the adversaries may take some weapons or equipment, speed reduction factors of 0.5 and 0.75 are given to attacks with weapons to two targets and a single target respectively. In that case, the mean delay time during running in each path section of different attacks can be obtained. A mean delayed time of 10 s is assumed to cut the fence and the mean delayed time to get to the dike (due to the height of the wall) is considered as 30 s.

The detection probability of cameras after entering a tank dike is equal to 0.9. The probability of response communication is 0.95 and the mean response time equals 5 min. To deal with the uncertainty of delay-related time and response-related time, a standard deviation of 30% of the mean value is assumed according to the conservative assumption based on the normal distribution (Garcia, 2007). Both ($P(H|S)$) and (P_E) are equal to 1. In that case, a single target attack scenario may result in one tank fire or no tank fire while a multiple-target attack can result in one tank fire, two tank fires, or no tank fire. The likelihoods of possible primary hazardous scenarios caused by these attacks are listed in Table 6.6.

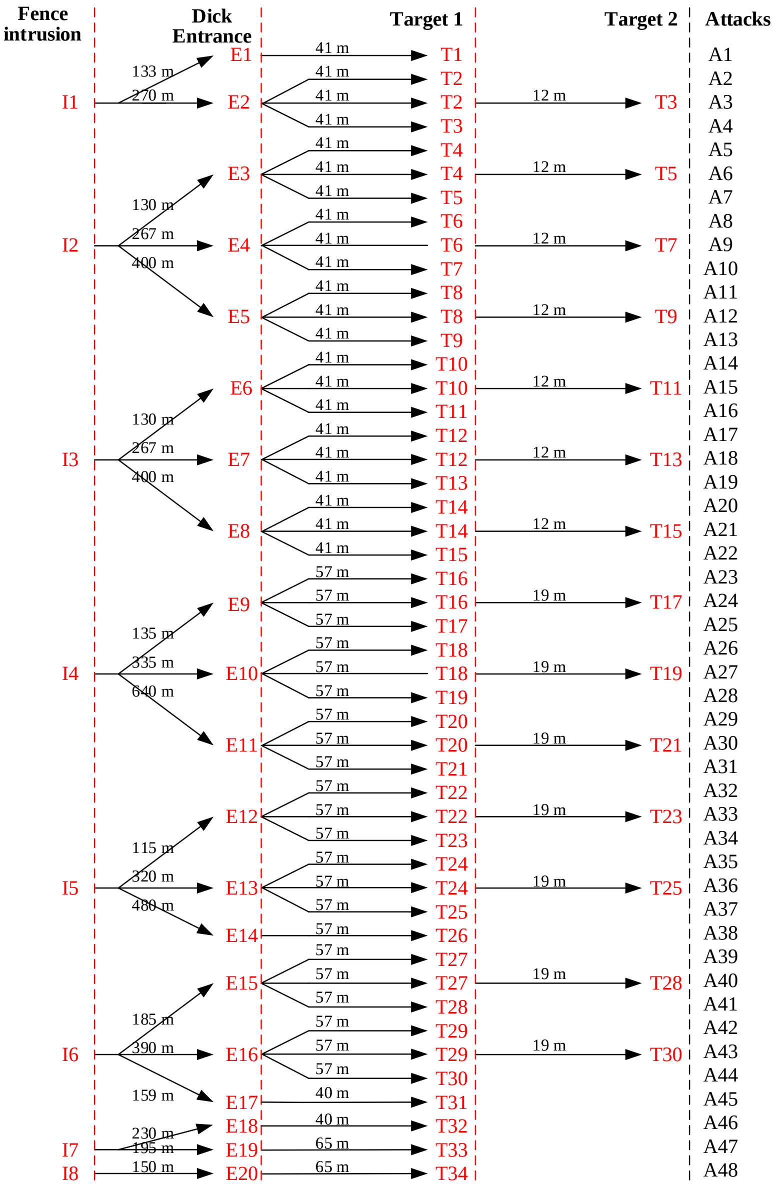

Figure 6.6 The possible attack scenarios considered in this case study (Chen et al., 2020b)

Table 6.6 Primary scenarios caused by different attack scenarios

Attack	Hazardous scenario	Conditional probability	Attack	Hazardous scenario	Conditional probability
A1	T1 on fire	0.959	A24	T16 & T17 on fire	0.624
A2	T2 on fire	0.959	A25	T17 on fire	0.953
A3	T2 on fire	0.295	A26	T18 on fire	0.953
	T2 & T3 on fire	0.669	A27	T18 on fire	0.333
A4	T3 on fire	0.959		T18 & T19 on fire	0.624
A5	T4 on fire	0.959	A28	T19 on fire	0.953
A6	T4 on fire	0.295	A29	T20 on fire	0.953
	T4 & T5 on fire	0.669	A30	T20 on fire	0.333
A7	T5 on fire	0.959		T20 & T21 on fire	0.624
A8	T6 on fire	0.959	A31	T21 on fire	0.953
A9	T6 on fire	0.295	A32	T22 on fire	0.953
	T6 & T7 on fire	0.669	A33	T22 on fire	0.333
A10	T7 on fire	0.959		T22 & T23 on fire	0.624
A11	T8 on fire	0.959	A34	T23 on fire	0.953
A12	T8 on fire	0.295	A35	T24 on fire	0.953
	T8 & T9 on fire	0.669	A36	T24 on fire	0.333
A13	T9 on fire	0.959		T24 & T25 on fire	0.624
A14	T10 on fire	0.959	A37	T25 on fire	0.953
A15	T10 on fire	0.295	A38	T26 on fire	0.953
	T10 & T11 on fire	0.669	A39	T27 on fire	0.953
A16	T11 on fire	0.959	A40	T27 on fire	0.333
A17	T12 on fire	0.959		T27 & T28 on fire	0.624
A18	T12 on fire	0.295	A41	T28 on fire	0.953
	T12 & T13 on fire	0.669	A42	T29 on fire	0.953
A19	T13 on fire	0.959	A43	T29 on fire	0.333
A20	T14 on fire	0.959		T29 & T30 on fire	0.624
A21	T14 on fire	0.295	A44	T30 on fire	0.953
	T14 & T15 on fire	0.669	A45	T31 on fire	0.959
A22	T15 on fire	0.959	A46	T32 on fire	0.959
A23	T16 on fire	0.953	A47	T33 on fire	0.949
A24	T16 on fire	0.333	A48	T44 on fire	0.949

As shown in Table 6.6, single-target attacks would result in one primary hazardous scenario while two-target attacks may result in two scenarios: the fire at the first target and the fires at both targets. Although the path distances between different single attacks are different, the tank fire probabilities caused by these attacks are the same or have small differences since the distance difference before reaching the detection measures (i.e., cameras) is meaningless according to Garcia (2007) For example, the tank fire probabilities of attack 1 and attack 2 are identical although the path of attack 2 is longer than the path of attack 1 (as shown in Figure 6.6). Besides, the probabilities of primary hazardous scenarios are quite high which indicates that the effectiveness of the baseline security system is poor. The cameras should be installed near the start point of attacks to provide enough time for response communication and response force actions.

6.6.4 The results of domino effect analysis

The identical probabilities do not mean that the expected consequences of different attacks are not different because each tank may have a different potential to initiate domino effects. This is why the vulnerability of installations to possible domino effects caused by these primary hazardous scenarios should be assessed. According to the vulnerability assessment method presented in Section 4.2, we first obtain the potential heat radiation q_{ij} between each pair of tanks if tank i is on fire, as shown in the Appendix (Table A.4). The potential evolution path, evolution time, and installation damage probability due to domino effects caused by different primary hazardous scenarios can be obtained using the dynamic graph model. The analysis shows that T26, T33, and T34 can not initiate domino effects if they are attacked. Besides, the chemical industrial area can be divided into five domino islands where any primary hazardous event within the area can not escalate outside the area, as shown in Figure 6.7.

Figure 6.7 Five domino islands within the chemical plant
(Chen et al., 2020b)

A domino island can be analyzed independently since no escalation vector links with installations outside the area. The domino effect risk decreases with increasing the number of domino islands. The installation damage sequences caused by 48 possible primary hazardous scenarios are listed in Appendix (Table A.5). The results of the domino effect analysis demonstrate that the attack on tanks in domino island 1 can lead to a more severe disaster (the damage of 24 tanks).

6.6.5 Protection strategies

The results of threat analysis and vulnerability assessment show that the plant is susceptible to intentional attacks, and the attack may lead to catastrophic consequences due to possible domino effects. As a result, additional safety and security measures might be proposed to protect the plant against intentional attacks. Assuming the protection budget is €2.5M, six protection upgrades are proposed, including three security strategies (PS1-PS3), one safety strategy (PS4), and two integrated protection strategies (PS5, PS6), as follows:

PS1) install fence sensors on the perimeter;

PS2) updating the perimeter delay measure by building a concrete reinforced external wall;

PS3) reducing response force time by building an additional guard dispatch;

PS4) applying fireproof coating on all storage tanks;

PS5) adding fence sensors on the perimeter and building an additional guard dispatch;

PS6) adding fence sensors on the perimeter and applying fireproof coating on critical tanks.

6.6.6 Cost analysis (Step 1 of the PROTOPT algorithm)

The cost calculation for each of the six protection strategies proposed in the previous section is carried out according to the cost categories and cost calculation method described in Section 6.5.1. The remaining lifespan of all the protection measures *y* is considered as 10 years and the discount factor for cost calculation is 0.035 (HSE, 2016). The conversion rate from USD to EUR is 0.888 based on the real exchange rate (wisselkoers, 2019). Fence sensor units used in PS1 are installed every 10m along the 5750 m perimeter (Villa et al., 2017a). The concrete reinforced wall proposed in PS2 is 2.65 m high, 0.098m thick, and 5750 m long. The initial costs of a concrete-reinforced wall consist of concrete cost, forms cost, and reinforced steel costs, the costs of labor and equipment used in construction are considered in installation costs while the operation costs are ignored (Craftsman, 2018). The costs of PS3 are mainly from a new building and additional guards. To calculate the operation costs caused by additional guards, the average salary of €23/h and 8760 working hours/year are adopted (Explorer, 2019). A 10 mm fireproof coating is recommended in PS4 for all the tanks to make sure a delayed failure time of 70 min is present (Paltrinieri et al., 2012; Khakzad et al., 2018c). The sum of initial costs and installation costs of the fireproof coating is €24/mm/m^2. The final proposal only applies fireproof coating on the top six critical tanks (T6, T7, T11, T12, T23, T24) based on the vulnerability of the tanks subject to domino effects. More cost details are shown in the Appendix (Table A.6). The final cost calculation results are represented as the present value of costs (PVC) in Table 6.7.

Table 6.7 Cost calculation results

Protection strategies	Description	Performance	*PVC* (€)
PS1	575 fence sensors along 5750 m perimeter	Detection probability at the perimeter is 0.9	4.7×10^5
PS2	A concrete reinforced external wall (2.65m × 0.098m ×5750 m)	Delayed time at the perimeter is 180s	2.9×10^6
PS3	A new building with several guards near the chemical plant	Response time is reduced to 150s	1.8×10^6
PS4	10 mm fireproof coating for each storage tank	The delayed time of tank damage is 70min.	1.1×10^7
PS5	PS1+PS3	PS1+PS3	2.3×10^6
PS6	PS1+PS4	PS1+PS4	$\leq 2.5\times10^6$

As shown in Table 6.7, PS2 and PS4 should be excluded since the PVCs of building a concrete reinforced external wall and fireproof coating of all the tanks exceed the protection budget. The rest of the protection strategies should further be assessed via a benefit analysis.

6.6.7 Benefit analysis of protection strategies (Step 2 of the PROTOPT algorithm)

The overall expected losses should be evaluated according to adversaries' attack strategies, protection strategies, and the vulnerability of installations. Different from the consequence assessment of general security events, the loss assessment of intentional domino effects is a rather complex task since many scenarios with multiple contemporary events may take place. To simplify the calculation, a catastrophic case scenario where all the tanks are damaged with 30 fatalities and 3000 injuries is defined. (Reniers and Van Erp, 2016) Besides, assuming that the different categories of costs are proportional to the damage of the tanks, the losses of different domino scenarios can be obtained according to the catastrophic case scenario.

The supply chain losses are estimated by considering the storage profit, i.e., €0.58/(barrel · month) (Reuters, 2015). The supply chain losses caused by tank damage are considered to be the storage profit of the tank per year. In the calculation of damage losses, both the tank damage and the loss of gasoline in the tank are taken into consideration. Considering the loss of €711 k, €800 k and €933 k for the small-, middle- and large-sized tanks respectively, (Matches, 2014) the loss of gasoline can be represented by the product of the volume and the price of gasoline €1.45/L (GlobalPetrolPrices, 2019). The fines-related costs in legal losses are considered as €251.3 K if all tanks are damaged, referring to a previous accident in France (Reniers and Van Erp, 2016).

To calculate the costs of human life, the value of a statistic life (VSL) of €5.8 M (Birk, 2014) and the value of a statistical injury of €31 K (Kuhn and Ruf, 2013) are adopted for a case study. The insurance costs of €5 M, reputation costs of €384 M, and intervention costs of €30 K for the worst-case scenario are retrieved from a previous study (AFP, 2012). The environment costs, personnel costs, medical costs, investigation, and clean-up costs are also estimated based on the above figures. As a result, the losses of the catastrophic case scenario and the expected losses related to the attacks are obtained, as displayed in Table 6.8.

Table 6.8 The losses of the worst scenario and the losses of attacks

Cost category	Losses related to the worst-case scenario (€/year)	The expected losses from other possible attacks (€/year)
Supply chain	1.2×10^6	7.6×10^5
Damage	5.9×10^8	3.3×10^6
Legal	2.5×10^5	1.4×10^4
Insurance	5.0×10^6	2.8×10^5
Human	2.7×10^8	1.5×10^7
Environmental	1.2×10^8	6.6×10^6
Personnel	2.3×10^5	1.3×10^4
Medical	5.3×10^7	3.0×10^6
Intervention	3.0×10^4	1.7×10^3
Investigation	5.4×10^6	3.0×10^5
Other	3.8×10^8	2.1×10^7
In total	1.4×10^9	8.0×10^7

The expected attack scenario concerns a multiple-objective attack on T6 and T7, maximizing the losses of the plants. Therefore, the expected losses can be regarded as a baseline loss for decision-making on protection strategies. Table 6.9 lists the predicted attack scenarios and the corresponding benefits of each protection strategy.

Table 6.9 The *NPVB* of each protection strategy

Protection strategies	Attack scenarios	PVB (€)	NPVB (€)
PS1	S9: T6 & T7	3.2×10^8	3.2×10^8
PS2	S9: T6 & T7	0	-2.9×10^6
PS3	S9: T6 & T7	2.9×10^8	2.9×10^8
PS4	S24: T16 & T17	5.5×10^8	5.4×10^8
PS5	S9: T6 & T7	5.3×10^8	5.3×10^8
PS6	S45: T31	4.4×10^8	4.4×10^8

As shown in Table 6.9, all the proposals are recommended except PS2 (*NPVB*<0). PS4 has the largest hypothetical benefit but its cost exceeds the protection budget. The results of the domino effect analysis using dynamic graphs demonstrate that domino effects are impossible due to the use of fireproof coatings on all the tanks. In other words, the expected loss with the baseline security system will be €14 M per year rather than €80 M per/year if we do not consider domino effects. Besides, the attack strategy will be S9 but not S24. Therefore, neglecting domino effects in security management may underestimate the loss of attacks and lead to unreasonable allocation of protection measures, resulting in large losses. Domino effect analysis is inevitable in chemical security management.

6.6.8 Optimization (Step 3 of the PROTOPT algorithm)

Both the results of cost analysis (Table 6.7) and benefit analysis (Table 6.9) show that PS2 is not advisable since *NPVB*<0 and *PVC*> C_{Budget}. Although PS2 is much more expensive than the other proposals, it has no effect on the chemical plant's security. Domino effect analysis demonstrates that PS4 can effectively prevent the escalation of all 48 primary scenarios while the cost of PS4 is much higher than the available budget of €2.5 M. As a result, PS2 and PS4 can not be recommended. Installing a fence sensor (PS1) can provide a faster response force, largely reducing the likelihood of successful attacks. Since it is a border security strategy, the attacker's strategy can be assumed to be unchanged. PS3 also reduces the likelihood of success of all 48 attacks by shortening the needed time for response. Therefore, the combination of PS1 and PS3 becomes the optimal cost-benefit strategy under the available budget of €2.5 M.

Besides PS5, PS6 is a cost-benefit strategy combining a detection measure and a safety barrier. To reduce the cost of fireproof coatings, only part of the tanks, those more vulnerable to domino effects, can be protected. The optimization algorithm proposed in Section 6.5 is used to obtain the number and position of the tanks where the fireproof coating should be installed. Figure 6.8 shows the optimization results of PS6 based on a maximin strategy.

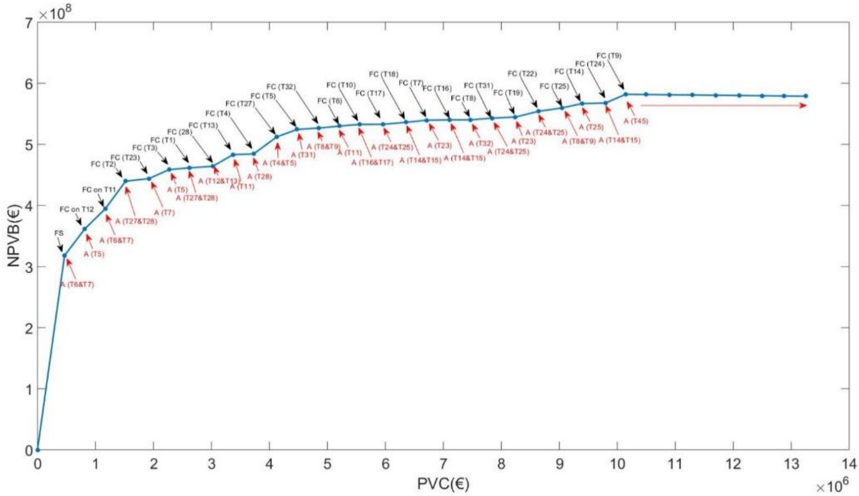

*The blue curve shows the *NPVB* (net present value of benefits) with increasing *PVC* (present value of costs). The black text arrows denote the new protection measures while the red text arrows represent attack scenarios corresponding to different protection investments (FS: fence sensor; FC: fireproof coating; A: attack).

Figure 6.8 The optimization results of PS6
(Chen et al., 2020b)

The adversary's attack strategies vary with increasing the present value of costs (*PVC*). First, *NPVB* increases from 0 to €318 M due to the installation of fence sensors on the plant perimeter. Next, fireproof coatings are sequentially installed on T12, T11, T2, T23, and T3. As a result, *NPVB* furtherly increases by €141M while PVC increases to €2.27 M. If more tanks are protected using fireproof coatings, *PVC* will excess the protection budget of 2.5M, and the increase ratio of *NPVB* decreases gradually. After applying fireproof coatings on T9, the likelihood of domino effects becomes impossible and further investment in the fireproof coating will be unprofitable. These results demonstrate that the investment in protection measures follows the law of diminishing returns[2]. (Anderson and Mittal, 2000)

This case study shows that we can obtain the most cost-effective protection strategy by applying the developed PROTOPT algorithm. However, various chemical plants are located in different places and face different threats. As a result, the likelihood of threats is different for each chemical plant, which may have an important impact on the profitability of protection investments. Taking PS5 as an example, Figure 6.9 shows the NPVB values with different threat probabilities.

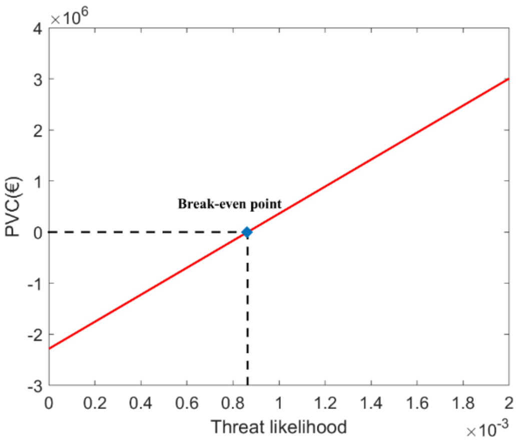

Figure 6.9 *NPVB* values with different threat probabilities (Chen et al., 2020b)

Figure 6.9 indicates that *NPVB* is proportional to the threat likelihood. The threat probability at the break-even point (P^*) is 0. 86×10^{-3}, which means that the protection is profitable only when the threat likelihood $P_T > 0.86\times10^{-3}$. However, the results do not mean that the protection is not recommended when $P_T < 0.86\times10^{-3}$. In that case, cost-benefit indicators or disproportion factor analysis may be used to facilitate the decision-making on the prevention of intentional domino effects.

[2] In economics, diminishing returns indicates the decrease in marginal output (impact) from increasing one unit of input factor, while the amounts of all other input factors stay constant.

6.7 Conclusions

In this Chapter, an integrated methodology based on cost-benefit analysis is developed to protect chemical industrial areas from domino effects. A protection strategy may consist of three types of protection measures: detection measures, delay barriers, and emergency response actions. According to the Stackelberg leadership model, the defender is considered as the "leader" while the attacker is viewed as the "follower" who knows the protection strategy before launching an attack. As a result, the net present value of benefits (*NPVB*) is obtained to identify the recommended protection strategies. Finally, an optimization algorithm (PROTOPT) based on the "maximin" strategy is developed to obtain the optimal protection strategy. The results obtained from the application of the methodology to a case study demonstrated that domino effects have a great impact on the payoffs and strategies of adversaries, and should therefore not be neglected in safety and security management; multiple kinds of protection measures are recommended in chemical industrial areas since they follow the law of diminishing returns. The likelihood of threats plays a critical role in a protection strategy's profitability, so the optimal protection strategy varies from a chemical industrial area to the other. In brief, the optimal protection strategy (including the types, quantities, and position of protection measures) can be obtained using the developed methodology and PROTOPT algorithm, addressing the technical and financial issues in safety and security resources.

Chapter 7 A resilience-based approach for managing domino effects

A disruption to chemical plants may trigger domino effects, resulting in more severe performance losses and making the performance restoration more difficult. The disruption, such as an intentional attack, may be difficult to predict and prevent, thus developing a resilient chemical plant may be a practical and effective way to deal with domino effects. This study develops a dynamic stochastic methodology to quantify the resilience of chemical plants. In this methodology, resilience evolution scenarios are modeled as a dynamic process that consists of four stages: disruption, escalation, adaption, and restoration stages. The resistant capability in the disruption stage, mitigation capability in the escalation stage, adaption capability in the adaption stage, and restoration capability in the restoration stage are quantified to obtain a chemical plant's resilience. The uncertainties in the disruption stage and the mitigation stage are considered, and the dynamic Monte Carlo method is used to simulate possible resilience scenarios and thus quantify chemical plant resilience. A case study is used to illustrate the developed methodology, and a discussion based on the case study is provided to find out the critical parameters and resilience measures.

The content of this chapter is based on the following submitted paper:
Chen, C., Yang, M., Reniers, G., 2021. A dynamic stochastic methodology for quantifying HAZMAT storage resilience. Reliability Engineering & System Safety.

7.1 Introduction

The petrochemical industry plays a critical role in industrial production by providing various chemical products such as petroleum, natural gas, and acrylonitrile. These hazardous materials (HAZMAT) are always stored, transferred, and processed via different equipment and installations located nearby within a chemical plant or chemical cluster. Most of these chemical products are flammable, explosive, or toxic, making chemical facilities vulnerable to disruptions, resulting in major accidents such as fire, explosion, and hazardous release (Khan et al., 2015; Fuentes-Bargues et al., 2017; Yang et al., 2018; Chen et al., 2020c; Pasman et al., 2020; Tong et al., 2020). Besides, these major accident scenarios in a hazardous installation may escalate to installations nearby, leading to a chain of accidents, resulting in the overall consequences more severe than the primary event, which is called “domino effects” or “knock-on effects” (Reniers and Cozzani, 2013).

Chemical plants may encounter various disruptions. According to the nature of the disruption events, the disruptions may be divided into three categories: unintentional accidents, natural disasters, and intentional attacks (Cozzani et al., 2014; Reniers and Audenaert, 2014; Chen et al., 2020c). Accidental disruptions may be caused by mechanical failure, corrosion, fatigue, and human errors, etc., such as the Intercontinental Terminal Company Tank Fire in March 2019 at Deer Park, the U.S (CNN, 2019). Compared with accidental disruptions, natural hazards may result in more severe consequences due to the damage of multiple chemical facilities, safety barriers, and other emergency response infrastructures. The damage to industrial facilities caused by natural disasters is called the Natech event (Cozzani et al., 2010; Khakzad and Van Gelder, 2018). For instance, the hurricane of Harvey in 2017 led to the release of at least 18 hazardous storage tanks in Texas (Misuri et al., 2019; Qin et al., 2020). Both the accidental disruptions and the disruptions caused by natural hazards are unintentional, while intentional attacks may aim to cause damage to the attack objective by using external weapons besides the hazardous materials inside chemical facilities. For example, on June 26, 2015, two tanks in a France chemical plant were damaged due to an explosion attack (Chen et al., 2020b).

Many studies dealing with unintentional and intentional threats have been conducted on various topics: inherent safety (Khan and Amyotte, 2003; Cozzani et al., 2007; Landucci et al., 2008; Tanabe and Miyake, 2012; Eini et al., 2015), hazard identification (Khan et al., 2001a; Cameron et al., 2017), safety risk assessment (Cozzani et al., 2005; Villa et al., 2016; Chen et al., 2020a; Guo et al., 2020), Natech risk assessment (Cozzani et al., 2014; Antonioni et al., 2015; Yang et al., 2019), security risk assessment (Reniers et al., 2015; Zhou et al., 2017; Khakzad et al., 2018e; Matteini et al., 2018), safety barrier management (Gnoni et al., 2009; Reniers et al., 2009; Reniers and Pavlova, 2013a), security measure management (Reniers et al., 2008; Zhang and Reniers, 2016; Khakzad and Reniers, 2019), emergency response (Zhou, 2013; Hosseinnia et al., 2018b; Du et al., 2020), etc.

Resilience engineering is becoming a more active and substantial research topic in the safety and security domain. Although no identical definition of resilience exists

currently in the academic domain (Hosseini et al., 2016), the capabilities (metrics) of a resilient system for responding to unexpected disruptions can be summarized as follows (Hosseini and Barker, 2016; Cincotta et al., 2019; Yarveisy et al., 2020):
(i) Absorptive capacity: the capability of a system to resist, absorb, or withstand the impact of disruptive events; (ii) Adaptive capacity: the capability of a system to adapt itself to maintain its operational performance without any recovery activity; (iii) Restoration capacity: the capability of a system to repair or restore damages from a disruption to recover the loss performance of the system, making the system to reach a new stable state.

Safety management aims to take measures to reduce the likelihood and consequences caused by disruptions for avoiding and mitigating human loss, economic loss, environmental loss, etc. Different from safety management, resilience engineering is to enhance a system's capabilities to absorb, adapt, and recover from a disruption, reduce the impacts of the disruptions on the system's performance. Safety management may be used to enhance absorption capability while has no direct impacts on adaption and recovery capabilities. As a result, safety management is not as wide as that of resilience management/engineering. In light of the unpredictable or indefensible threats (e.g., intentional attacks and natural disasters), enhancing the resilience capability is an ideal approach to reduce the losses caused by disruptions and to quickly recover its performance. (Zinetullina et al., 2021).

The advancement of resilience engineering research will contribute significantly to chemical process safety (Hollnagel et al., 2006; Dinh et al., 2012; Cincotta et al., 2019; Pasman et al., 2020; Provan et al., 2020). Past research attempts on resilience in the process industry identified the process resilience influence factors (Dinh et al., 2012; Jain et al., 2018a), resilience hazards (Azadeh et al., 2014; Jain et al., 2018b; Alrabghi, 2020). Besides, the Bayesian network was used to quantify process resilience (Abimbola and Khan, 2019; Tong et al., 2020; Zinetullina et al., 2021). However, Little attention has been paid to chemical plant resilience in which domino effects may play an essential role (Reniers et al., 2014; Cincotta et al., 2019). Therefore, this study aims to develop a methodology for quantifying the resilience of chemical plants, considering the dynamic stochastic evolution of disruptions due to domino effects, adaptation performance, and the dynamic restoration process. This chapter is organized as follows: Section 7.2 defines chemical plant resilience and introduces the possible measures to enhance the resilience of chemical plants. a stochastic dynamic methodology for quantifying the chemical plant resilience is elaborated in Section 7.3. Section 7.4 develops an algorithm to obtain chemical resilience. A case study is provided in Section 7.5 and a discussion based on the case study is illustrated in Section 7.6. Finally, the conclusions drawn from this study are present in Section 7.7.

7.2 Chemical plant resilience

7.2.1 The definition of chemical plant resilience

Although the resilience concept has been used in various industries and systems, there is no widely accepted definition of resilience available in the academic domain (Hosseini et al., 2016). In light of resilience capacities (Hosseini and Barker, 2016) and the possible catastrophic effects in chemical plants, we define chemical plant resilience as the capability of a chemical plant to resist, mitigate, adapt and recover from undesired events, to maintain its operation. Safety and security measures aim to prevent undesired events and mitigate the consequences caused by the events. Resilience engineering measures intend to enhance a system's capability to anticipate and prepare for disruption and its ability to adapt and recover from the disruption. To improve the resilience of chemical plants, operators should apply measures in different stages to resist the impacts of an undesired event, mitigate the consequences by preventing possible domino effects, and adjust operation strategies to improve the operation performance before recovery and to rapidly recover the plants. Figure 7.1 shows the chemical plant performance changing over time.

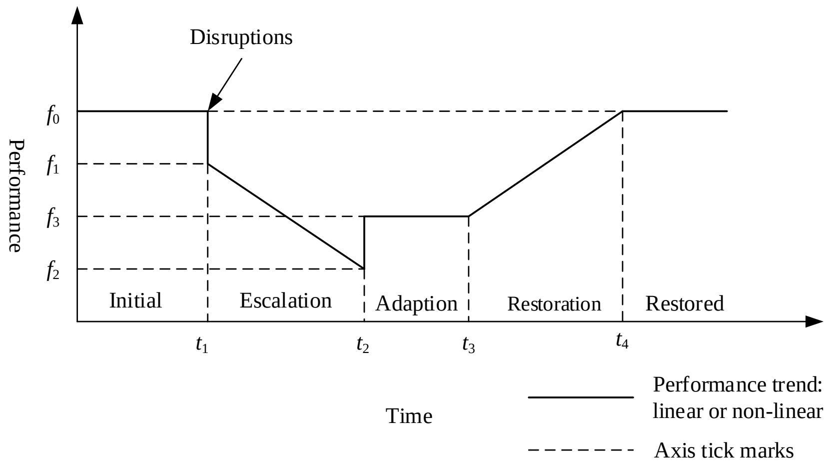

Figure 7.1 Chemical plant performance varies over time
(adapted from Henry and Emmanuel Ramirez-Marquez (2012))

According to the chemical plant resilience definition, a chemical plant may be in six stages when it comes to undesired events. Before the occurrence of undesired events, the chemical plant is in the initial stage, i.e., the performance is the maximum value f_0. When a disruption (undesired event) occurs, the performance may decrease immediately and cause major accident scenarios due to the damage to one or more than one installation. The primary major accident scenarios may escalate to installations nearby, resulting in domino effects. This will further reduce chemical plant performance. When the escalation is prevented (t_2), the residual performance reaches the minimum value f_2. At that time, the chemical plant may adapt its operation strategies to improve its performance. For instance, a chemical plant may utilize reserve installations or adjust chemical production strategies to improve performance. The last resilience strategy is to recover the performance by repairing or rebuilding the damaged installations (t_3~t_4). t_4 is the time that the performance of the chemical plant is fully recovered rather than the end of the restoration since the final restored performance may exceed the initial performance. In real cases, the performance of a recovered chemical plant may be different from the plant in the initial stage. In this study, the entire resilience process is time-dependent, which is called a resilience evolution scenario. It is also a stochastic process due to the uncertainties in the vulnerability of installations, hazardous scenario escalation, emergency response, etc.

7.2.2 Resilience metrics

As shown in Figure 7.1, chemical plant performance varies over time. According to the resilience framework proposed by Bruneau et al. (2003), resilience loss can be the expected degradation in performance over time. Based on the concept, we defined the chemical plant resilience metrics as a dimensionless ratio, as follows:

$$R = \frac{\int_{t_1}^{t_4} f(t)}{f(t_0)\left(t_4 - t_1\right)} \tag{7.1}$$

The numerator of formula (7.1) indicates the accumulation of chemical plant performance $f(t)$ between t_1 (disruption) and t_4 (fully recovered). The denominator represents the accumulation of initial performance $f(t_0)$ between t_1 and t_4. Although the resilience metrics is illustrated by the case of chemical plants, it may be applied to other fields by substituting other performance functions for the chemical plant performance function $f(t)$.

There may be many possible resilience evolution scenarios in terms of the uncertainties in resilience (which can be seen as different performance curves). Considering X resilience evolution scenarios and the maximum value of t_4 is $t_{\max}$, then the resilience metrics can be adapted, as follows:

$$R = \frac{1}{X}\sum_{i=1}^{X} \frac{\int_{t_1}^{t_{\max}} f(t)}{f(t_0)\left(t_{\max} - t_1\right)} \tag{7.2}$$

In Eq. 7.2, t_4 is substituted with $t_{\max}$ to unify the time dimension and thus avoid overestimating the resilience with longer resilience evolution time t_4. The most resilient system (R = 1) is an ideal condition in which the disruption does not induce any performance degradation. In such case, the impact of the disruption on the system is fully absorbed. If the system is destructed and the recovery is impossible, R is equal to zero. The value of R is between 0 and 1. It should be marked that t_4 is the time the system is fully recovered rather than the end of the restoration. The performance at the end of the restoration may exceed the original performance while the maximum of restored performance at t_4 cannot exceed its initial performance and R is no more than 1.

7.2.3 Capabilities of chemical plant resilience

According to the performance function curve in Figure 7.1 and the resilience metrics in Eq. (7.1), the capabilities of chemical plant resilience consist of resistance capability, mitigation capability, adaptation capability, and restoration capability, as shown in Figure 7.2. Resistance capability is the capability to resist descriptive events to avoid failure and maintain operation. Various measures can enhance resistance capability, and different measures may be taken to tackling different disruptions. For instance, installing lightning masts around installations and installing air terminals on the installations can prevent the damage of installations caused by lightning strikes (Necci et al., 2016; Yang et al., 2018); while security measures such as closed-circuit television (CCTV) cameras may be used to detect illegal invasions and thus prevent intentional attacks (Zhang and Reniers, 2016; Chen et al., 2020b). By applying these measures, resistance capability can be improved and thus increase the value of S_1 in Figure 7.2, enhancing resilience.

Mitigation capability is the capability to prevent the escalation of possible major accident scenarios caused by disruptions. This capability is essential for hazardous infrastructures due to possible domino effects. Safety barriers are always used to prevent the escalation of domino effects in the process industries, such as active protection measures (e.g., pressure relief valve), passive protection measures (e.g., fireproof coating), procedural and emergency response (e.g., firefighting) (Landucci et al., 2015a; Khakzad et al., 2017a; Chen et al., 2020c). Since safety barriers can prevent the escalation of domino effects and avoid catastrophic events, they can increase f_2 and shorten the time between t_1 and t_2, thus reducing the performance loss and improve resilience.

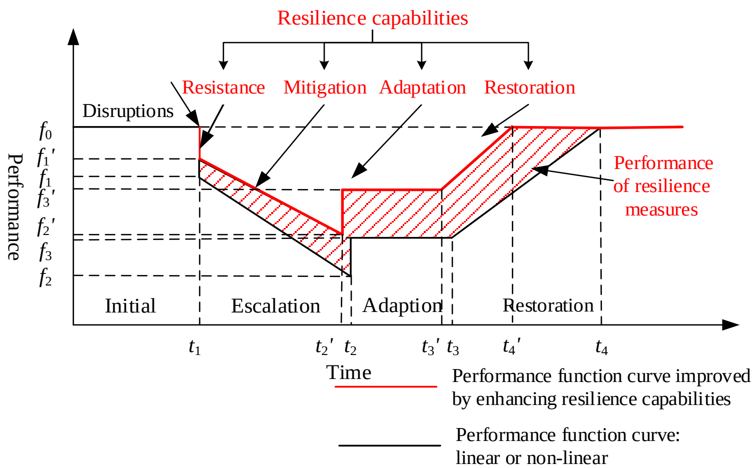

Figure 7.2 Chemical plant performance with resilience capabilities

Adaptation capability is the capability to adapt a new operation state to fully or partly recover the performance before restoration. This capability can be achieved in chemical plants by adjusting operation strategies, such as utilizing reserve equipment, speeding inventory turnover ratio, or adjusting chemical production strategies. Enhancing the adaptation capability can increase the value of f_3 in Figure 7.2 and improve the chemical plant performance before the restoration of the damaged chemical plant.

Restoration capability refers to the capability to quickly repair or rebuild the damaged installations to recover the performance of the chemical plant. In this stage, the restoration capability mainly depends on the time to fully recover (*TTR*). Therefore, shortening the *TTR* (t_3-t_4) can effectively reduce the lost performance and achieve a more resilient chemical plant.

Modeling the resilience capabilities based on the performance curve is the key step to quantify the resilience of a chemical plant. There, the next section is to develop a framework to quantify the resilience metrics by modeling these resilience capabilities.

7.3 A quantification framework of chemical plant resilience

Chemical plants are industrial infrastructures that manufacture, process, and storage chemical materials. The performance of a chemical plant mainly depends on its operation and products. For instance, hazardous material storage plants are industrial facilities for storing hazardous chemicals such as petroleum, benzene, and other chemical products. These products are delivered to end-users, process facilities, and other storage facilities. As a result, the total storage volume of the plant or the average daily chemical flow rate at the initial stage of a hazardous material storage plant can be used to represent the chemical plant performance. According to the chemical plant performance, the performance function f(t) can be established by quantified the capability of resistance, mitigation, adaptation, and restoration.

7.3.1 Resistance modeling

The resistance capability is the ability to withstand and retain operation and avoid being damaged (Yarveisy et al., 2020). Resistance may be viewed as the antonym of vulnerability, representing the inability of an installation to withstand strains and the consequent failures (Johansson et al., 2013). The vulnerability of installations is often represented by the failure probability of installations exposed to a disruption. Therefore, the resistance capability of an installation can be obtained as follows:

$$C_r = 1 - P_f \tag{7.3}$$

where P_f is the failure probability of an installation exposed to a disruption, and C_r is the resilience capability of the installation exposed to the disruption. In terms of a chemical plant, there are usually multiple installations. Due to disruption such as a terrorist attack (Chen et al., 2020b) or a natural disaster, multiple installations may be simultaneously damaged, resulting in a sudden decrease in chemical plant performance (f_0-f_1). f_1 is the performance of the undamaged installations. The vulnerability of an installation depends on different disruptions. Let us take an intentional attack using explosive devices as an example, the overpressure caused by the explosion is the main threat for installations, possible to be calculated by the TNT equivalency method (Van Den Bosh and Weterings, 1997; Landucci et al., 2015b).

In this method, the point-source TNT explosion model is adopted by transferring the net explosive mass to be an equivalent amount of TNT. Then the scaling distance can be determined as follows:

$$Z = \frac{r}{{m_{TNT}}^{1/3}} \tag{7.4}$$

where Z denotes the scaled distance; m_{TNT} represents the equivalent mass of TNT, kg; r represents the distance between installations and the explosion. The overpressure is a function of the scaling distance, which can be read from the TNT blast chart or obtained from empirical formulas. Since the blast chart needs to be read by humans and thus may not suitable for computer computation, many empirical formulas were developed in the past years. Eq. (7.5) provides an empirical formula of overpressure (P_o) based on the TNT blast chart (Assael and Kakosimos, 2010).

$$P_o = \frac{80800\left(1+\left(\frac{Z}{4.5}\right)^2\right)}{\sqrt{1+\left(\frac{Z}{0.048}\right)^2}\sqrt{1+\left(\frac{Z}{0.32}\right)^2}\sqrt{1+\left(\frac{Z}{1.35}\right)^2}} \tag{7.5}$$

To obtain the failure probability of installations, the probit model (Cozzani and Salzano, 2004b; Cozzani et al., 2005) is adopted in this study, as follows:

$$Y_p = \begin{cases} -18.96 + 2.44\ln\left(P_s\right) & \text{Atmospheric vessels} \\ -42.44 + 4.33\ln\left(P_s\right) & \text{Pressurised vessels} \end{cases} \tag{7.6}$$

where Y_{p} is the probit value. The failure probability (P_f) caused by overpressure is thus calculated using the cumulative distribution function of the standard normal distribution (ϕ).

In each resilience evolution scenario, the damaged installations in the disruption stage can be determined by sampling random numbers according to P_f (see the illustrations in Section 7.4). Therefore, the total performance at t_1 (f_1) can be obtained according to the damaged performance in the disruption stage (f_{di}), as follows:

$$f_1 = f_0 - f_{di} \tag{7.7}$$

7.3.3 Mitigation modeling

In chemical plants, hazardous installations are located nearby. Domino effects may occur due to possible major accident scenarios (e.g., fire and explosion) caused by disruptions. If domino effects occur, the consequences may be more severe than the primary disruptions. The mitigation capability in chemical plants thus refers to preventing or mitigating the escalation of domino effects. As shown in Figure 7.2, enhancing the mitigation capability can raise f_2 and may decrease t_2, to improve chemical plant resilience. When a hazardous installation is damaged and results in a loss of containment of hazardous materials, major hazards such as fire and explosion can occur, resulting in the nearby installations exposed to heat radiation or overpressure. Once the physical force damage the nearby installations, the major accident scenarios may propagate, resulting in a chain of accidents and a decrease in performance (t_1-t_2 in Figure 7.2). To avoid the failure of installations, safety barriers such as passive barriers, active barriers, and emergency response barriers may be implemented (Landucci et al., 2015a; Khakzad et al., 2017a). The passive fire protection measures refer to these safety measures that do not need external activation to trigger the protection functions for containing fire or delaying fire escalation, such as fireproof coating, pressure safety valves, and fire-resistant walls. These protection measures are based on different mechanisms and thus have different performances for fire protection. In terms of active protection measures, external activations are needed to trigger the protection function, such as the water spray system (WSS). The third safety barrier is emergency response. Emergency response actions such as firefighting are essential to prevent domino effects while a period is needed for the emergency response team to arrive. The emergency response system can be regarded as a socio-technical system with some uncertainties. The performance of these safety barriers has been illustrated in Chapter 6. Applying the Domino Evolution Graph (DEG) model in this study, we can obtain the time t_2 and the failure likelihood of installations due to domino effects. At the end of the escalation stage (t_2), the total performance (f_2) can be obtained according to the damaged performance in the escalation stage (f_{es}), as follows:

$$f_2 = f_1 - f_{es} \tag{7.8}$$

7.3.4 Adaptation modeling

The adaptation capability in this study refers to operation adjustments, which can lead to improved chemical plant performance. These operation strategies include utilizing reserve installations, speeding inventory turnover ratio and adjusting chemical production strategies, etc. Reserve installations can quickly replace the damaged installations and thus increase the chemical plant performance. Speeding the inventory turnover ratio can increase the daily chemical flow rate and also increase the chemical plant performance. adjusting chemical production strategies may reduce the dependence of operation on damaged installation. These adaptation strategies can be used alone or in combination according to the adaptation capabilities of chemical plants. Due to adaptation strategies, the loss of chemical plant performance caused by the disruption and the sequential cascading effect can be partially recovered, as follows:

$$f_3 = f_2 + f_{ad} \tag{7.9}$$

7.3.5 Restoration modeling

The loss of performance may be fully recovered by restoring the damaged installations. In this study, all the damaged installations are considered to be reconstructed. In this stage, the time to full recovery (TTR) is a quantitative indicator. The reconstruction of an installation is a time-consuming process. For example, the construction of a tank includes several steps: installing the tank bottom, installing the hydraulic jacking system, installing the tank roof, assembling and lifting the first ring (top) of the tank wall, assembling and lifting the second ring of the tank wall, installing the accessories. The construction time of installations depends on many factors, such as the construction method, the number of people, and resources invested in the construction. If multiple installations are damaged, the rebuilding sequence may also affect the TTR. The restoration capability is negatively correlated with the construction time. As a result, increasing the investments in construction can shorten the TTR and thus enhance the chemical plant resilience. Besides, a company may improve the level of preparedness to quickly recover from disruptions, such as the availability of drawings, construction and maintenance teams, and financing, etc.

7.4 Simulation Algorithm

This section provides a stochastic dynamic algorithm to obtain the resilience of chemical plants exposed to disruptions. Figure 7.3 shows the flow diagram of the algorithm for obtaining resilience. This algorithm is based on the dynamic Monte Carlo method. Firstly, we need to input the number of iterations N, the disruption time $t_1 = 0$, and the initial iteration $n = 1$. Given a disruption, vulnerability analysis will be conducted using the models in Section 7.3.2 to determine the failure probability of installations exposed to the disruption. Based on the failure probabilities, a set of random data (between 0 and 1) is sampled to determine the damaged installations. If a random number is less than the failure probability, the installation is considered damaged. Then, possible escalation is assessed using the escalation models in section 7.3.3 to obtain the failure installations in the escalation stage. Again, random data will be generated and used to determine the end time of escalation t_2. According to the results of vulnerability models and escalation models, the performance from t_1 to t_2 can be gained. Next, the improved performance due to adaptation measures needs to be determined. Furthermore, the restoration start time (t_3) and end time (t_4) should be determined based on the restoration strategy. Based on these calculations, the entire performance curve (t_1-t_4) can be obtained. The above steps need to be repeated until n exceeds N. To calculate the resilience in each iteration, the maximum value of t_4 (t_{max}) can be found out. Setting the integral interval [0 t_{max}], the resilience in each iteration is calculated based on Eq. (7.1). Finally, the resilience can be obtained according to Eq. (7.2), considering the dynamic resilience evolution process and uncertainties in the disruption and escalation stages.

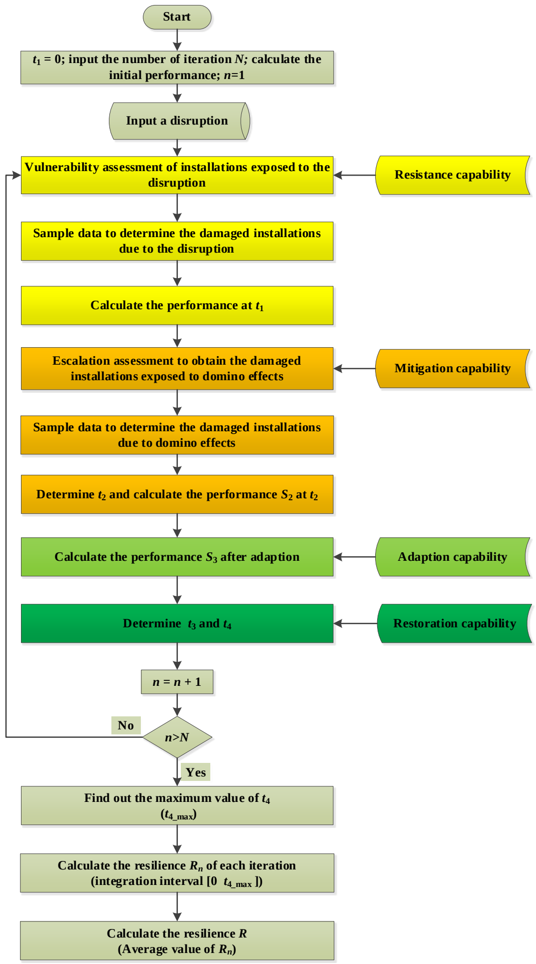

Figure 7.3 Flow diagram of the algorithm for obtaining resilience

7.5 Case study

7.5.1 Case study descriptions

In this section, the resilience of a refined oil storage farm is examined using the resilience quantification methodology proposed in this study. The storage farm consists of 14 tanks (numbering T1-T14) and stores two hazardous materials: gasoline (T2-T5, T12-T14) and diesel (T1, T6, T7-T11). The characteristics of the tanks are listed in Table 7.1, and the layout of the storage farm is shown in Figure 7.4. The total storage volume in the initial stage (initial) is 30500 m^3. The flow rate in the initial stage of gasoline and diesel is 1088.6 m^3/d (3×10^8 kg/y) and 658.6 m^3/d (2×10^8 kg/y), respectively. The inventory turnover ratio of the storage farm is 20.9. Assuming that the average value of *TER* (μ) is 15 min and the variance (σ) is 5 min.

Table 7.1 Features of hazardous material storage tanks

Tank	Type	Dimensions (m)	Volume (m^3)	Material	Density (kg/m^3)	Restoration time (day)
T1	Atmospheric, fixed-roof	8.9×8.0	500	Diesel	832	15
T2-T5	Atmospheric, floating-roof	11.5×12.0	1000	Gasoline	755	30
T6	Atmospheric, fixed-roof	11.5×9.6	1000	Diesel	832	30
T7-T11	Atmospheric, fixed-roof	15.7×10.4	2000	Diesel	832	60
T12-T14	Atmospheric, floating-roof	21.7×16.0	5000	Gasoline	755	150

Assume that a disruption due to an intentional explosion occurs at the storage farm (represented by a red asterisk in Figure 7.4) induced by a suitcase bomb with an improvised explosive device (IED), the explosion is assumed to be equivalent to 23 kg TNT (Hosseinnia et al., 2018a). The distances between different storage tanks and the explosion position are shown in Table 7.2. The explosion may lead to fire on tanks, and the heat radiation generated by each tank to other tanks can be obtained by using the ALOHA software (ALOHA, 2016). The parameters for heat radiation calculation and the results are shown in the Appendix (Table A.7). Once the attack results in tank damage, a suspended time (t_2-t_3) of 30 days is assumed for incident investigation, preparation for restoration. In the restoration stage, the damaged tanks are rebuilt according to the tank volume (descending order).

Figure 7.4 Layout of the oil tank farm

Table 7.2 The distance between storage tanks and the explosion position

Tank	T1	T2	T3	T4	T5	T6	T7	T8	T9	T10	T11	T12	T13	T14
T1	0	17	25	35	-	-	-	-	-	-	-	52	75	-
T2	17	0	18	18	25	35	54	45	-	-	-	60	76	-
T3	25	18	0	25	18	40	54	39	69	58	53	46	57	84
T4	35	18	25	0	18	18	36	32	58	53	59	71	80	-
T5	-	25	18	18	0	25	37	22	53	43	44	60	64	83
T6	-	35	40	18	25	0	20	20	42	44	56	85	87	-
T7	-	54	54	36	37	20	0	22	22	31	50	96	91	-
T8	-	45	39	32	22	20	22	0	31	23	31	76	69	80
T9	-	-	69	58	53	42	22	31	0	23	45	-	93	94
T10	-	-	58	53	43	44	31	23	23	0	22	88	72	71
T11	-	-	53	59	44	56	50	31	45	22	0	72	50	51
T12	52	60	46	71	60	85	96	76	-	88	72	0	36	71
T13	75	76	57	80	64	87	91	69	93	72	50	36	0	35
T14	-	-	84	-	83	-	-	80	94	71	51	71	35	0
EP	26	28	14	39	29	53	66	47	79	64	53	16	37	68

*EP represents the explosion position; “-” denotes the distance that extends 100m.

7.5.2 Results

According to the case study description, a stochastic dynamic resilience simulation can be conducted according to the methodology presented in Section 7.3 and the algorithm in Section 7.4. A desktop PC (CPU: Intel(R) Core(TM) i5, RAM: 8G) is used to carry out the simulation. If the number of iterations N is set to be 10^4, the computation time is around 2s and the difference of storage resilience values between two calculations is less than 5/1000. While the computation time is around 105 s the difference is lower than 1/1000 when the N is equal to 10^5. Since the accuracy difference between $N = 10^5$ and $N = 10^4$ is ignored, we select $N = 10^5$ for the computation in this chapter. The storage resilience R (average value) is equal to 0.822. The maximum value of R is 1 while the minimum value is 0.417. Figure 7.5 shows the resilience distribution of the storage tank farm.

In light of the large difference between the minimal value and the maximum value, the stochastic characteristics of resilience cannot be ignored. Figure 7.5 shows three resilience scenarios of the storage tank farm. The black curve represents the resilience scenario with the maximum resilience in which the disruption doesn’t lead to any damage and performance reduction. The red curve represents a resilience evolution scenario with the mean resilience while the blue curve denotes a resilience evolution scenario with the minimum resilience. Due to the overpressure caused by the explosion, two tanks (T3 and T12) close to the explosion position failed immediately in the two resilience scenarios. However, during the escalation stage, the residual 12 tanks are damaged in the minimal resilience scenario while only 5 tanks (T2, T5, T1, T4, T13) failed in the mean resilience scenario. As a result, the needed time to full recovery of the minimal resilience scenario (465 days) is much longer than that of the mean resilience scenario (945 days).

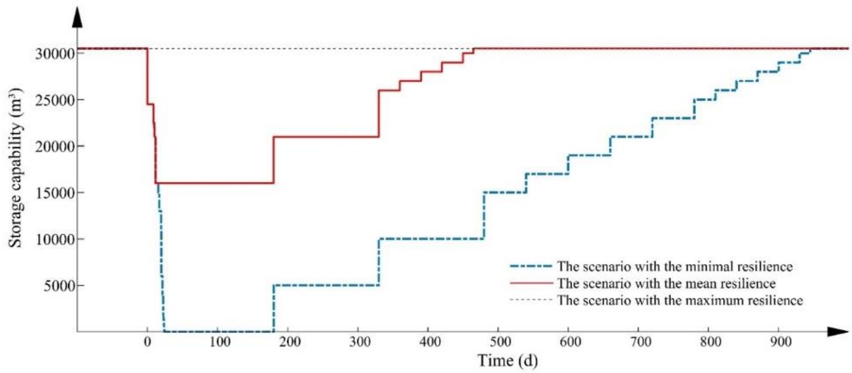

Figure 7.5 Resilience evolution scenarios of the storage plant

Suppose the domino effects are not considered in the case study, the resilience increase from 0.821 to 0.905. Figure 7.6 shows a typical resilience scenario without domino effects (red curve) and a typical resilience scenario considering domino effects. Most of the red curve is lower than the blue curve, indicating that domino effects have an ignored impact on the storage resilience of hazardous materials. Consequently, the resilience of hazardous material storage plants may be overestimated if domino effects are neglected.

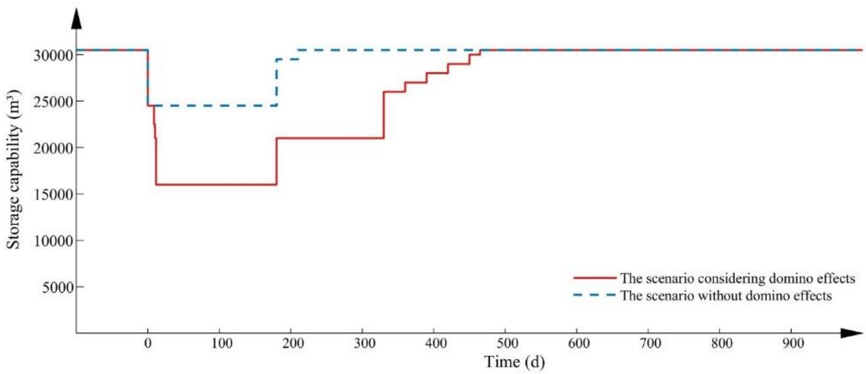

Figure 7.6 Resilience scenarios with and without domino effects

To further explain the role of domino effects in storage resilience, Figure 7.7 shows the failure probabilities of storage tanks exposed to only the attack and both attacks and possible domino effects.

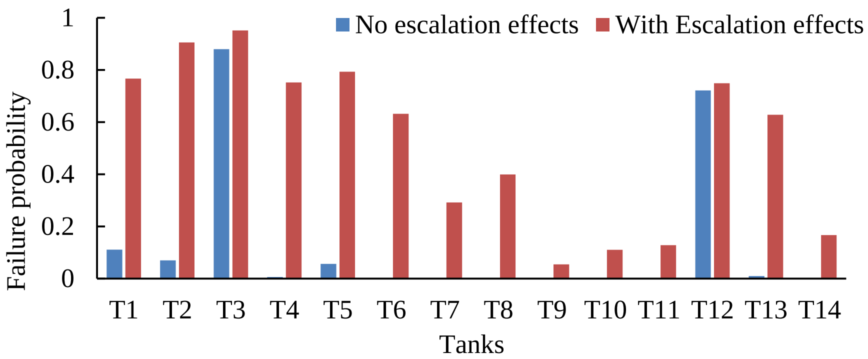

Figure 7.7 Failure probability of storage tanks exposed to the attack

The blue bars represent the failure probability directly caused by the explosion, while the orange bars denote the failure probability considering domino effects. It shows that T3 and T12 are prone to be directly damaged by the explosion attack since they are close to the explosion position. However, other tanks are more likely to be damaged by the domino effects caused by the explosion attack. For example, T2 has a low probability to be directly damaged by the attack while the failure probability is over 0.9 due to the possible domino effects. If domino effects are neglected, the failure probabilities of tanks would be underestimated, resulting in an overestimation of storage performance and resilience.

7.6 Discussion

Based on the case study in Section 7.5, this section will discuss the resilience model parameters and possible resilience measures to improve the resilience of hazardous material storage plants.

7.6.1 Resistance capability analysis

In light of explosion attacks, the resistance capability of storage tanks mainly depends on the TNT equivalent mass of the explosive, as shown in Figure 7.8a. With increasing the TNT equivalent mass of the explosive, the storage resilience (red curve) rapidly decreases and then approaches the minimal resilience value. The result indicates that storage resilience depends on the intensity of disruptions. The maximum resilience value (black curve) decreases with the increase of TNT equivalent mass, while the minimal resilience value almost remains unchanged. The result demonstrates that the uncertainty of resilience also decreases with increasing the TNT equivalent mass. These resilience trends can be explained by Figure 7.8b. Figure 7.8b shows the failure probability of storage tanks. The failure probability of each tank increases with increasing TNT equivalent mass, resulting in decreased storage performance. Besides, with the further increase of the TNT equivalent mass, the failure probabilities of tanks are close to 1, resulting in uncertainty reduction.

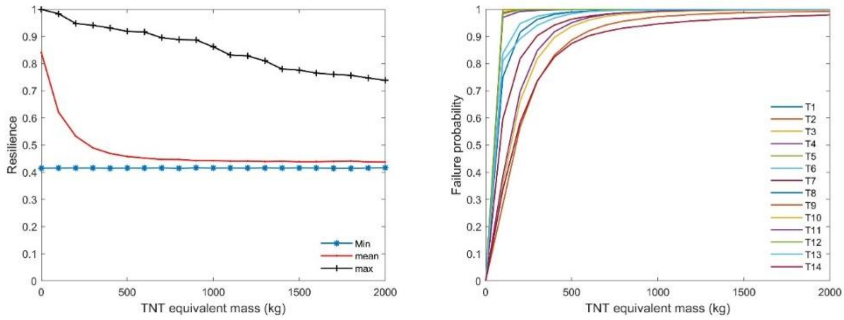

(a) (b)

Figure 7.8 Effects of TNT equivalent mass on (a) resilience and (b) failure

7.6.2 Mitigation capability analysis

In hazardous material storage plants, a disruption may lead to major accident scenarios and result in domino effects. The mitigation capability refers to the safety barriers that can mitigate the consequences of disruptions by preventing or mitigating domino effects. By applying a water spray system (WSS), the possible heat radiation can be partly reduced, thus increasing the resilience, as shown in Figure 7.9a.

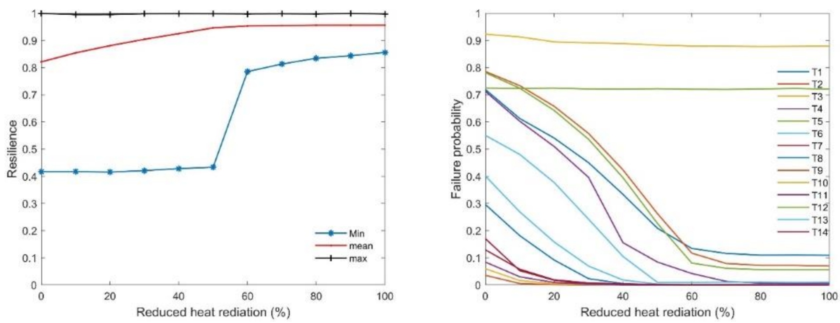

(a) (b)

Figure 7.9 Effects of WSS on (a) resilience and (b) tank failure

The storage resilience increases with the reduced heat radiation increasing until domino effects are almost prevented (60%). The minimal resilience value largely increases when the reduced heat radiation increases from 50% to 69% since domino effects are almost impossible when the reduced heat radiation exceeds 60%. This can be seen in the failure probability curves in Figure 7.9b. When the reduced heat radiation exceeds 60%, the failure probability of each tank remains unchanged (i.e., the tank failure can only be directly caused by the overpressure caused by the attack rather than domino effects). The results indicate that further decreasing the possible heat radiation may not be cost-effective when the reduced heat radiation is more than 60%.

Similar to the water spray system (WSS), an emergency response such as firefighting can also be used to prevent domino effects. The mean time for emergency response u is a critical parameter for mitigation capability, as shown in Figure 7.10. The storage resilience (i.e., the red curve in Figure 7.10a) decreases with increasing μ because the failure probability of most of the tanks increases with increasing μ, as shown in Figure 7.10b. In Figure 7.10b, the failure probabilities of T3 and T12 are much higher than other tanks when μ is less than 10 min since they are more likely to be directly damaged by the blast overpressure caused by the explosion, as shown in Figure 7.7. The failure probabilities of residual tanks increase with increasing μ since delayed emergency response can lead to more severe domino effects. The failure probabilities of T12-T14 cannot exceed the failure probability of T12 since there are two domino islands where no domino effects can occur in between (Reniers and Audenaert, 2008). One island consists of T1-T11 and another consists ofT12-T14. As a result, T13 and T14 can only be damaged by the domino effects caused by T12 when T12 is damaged by the attack.

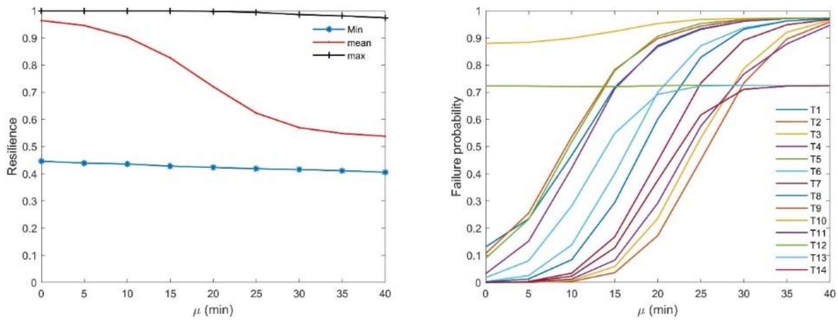

(a) (b)

Figure 7.10 Effects of emergency response on (a) resilience and (b) failure

7.6.3 Adaption capability analysis

Adaption measures such as utilizing reserve tanks and speeding inventory turnover ratio may partially compensate for the performance loss caused by a disruption before the storage plant is fully restored. The adaption capability is limited by the storage equipment (reserve tanks), loading, and unloading facilities. Figure 7.11a shows the effects of speeding inventory turnover (represented by the increased inventory turnover rate (%) based on the storage capability at the end of the escalation stage) on storage resilience. As shown in Figure 7.11a, the storage resilience (red curve) increases with an increasing inventory turnover rate in the adaption stage. The minimum resilience value is constant since all tanks are damaged in the minimal resilience scenario and speeding inventory turnover does not work. Besides the performance adaption, shortening the adaption time (t_2-t_3) can also improve the adaption capability, as shown in Figure 7.11b. Both the storage resilience (red curve) and the minimal storage resilience (blue curve) in Figure 7.11b show a decreasing trend with increasing adaption time. As a result, reducing the adaption time and starting restoration early is also an adaption measure to enhance resilience.

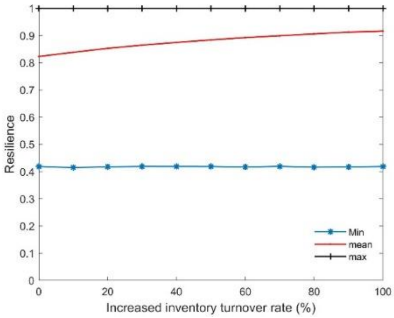

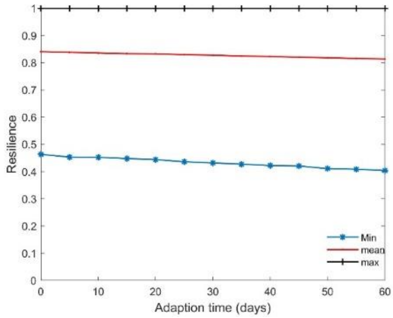

(a) (b)

Figure 7.11 effects of (a) inventory turnover rate and (b) adaption time

7.6.4 Restoration capability analysis

Restoration is the final stage of a resilience process. The restoration time is a crucial parameter for the restoration capability, as shown in Figure 7.12.

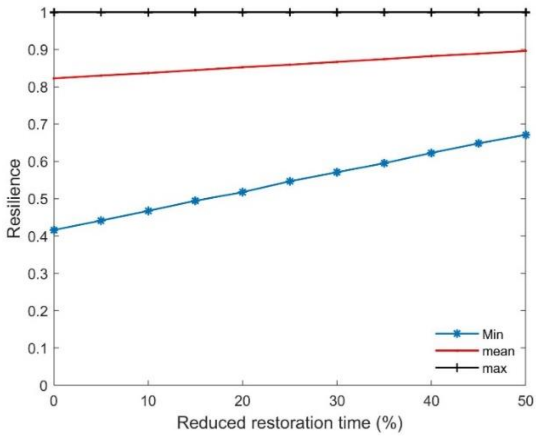

Figure 7.12 The effects of restoration time on storage resilience

As shown in Figure 7.12, the resilience is inversely proportional to the restoration time. Both the resilience value and the minimal resilience value increase with the decrease of restoration time. As a result, a quick restoration capability is essential for developing a resilient hazardous material storage plant. Different restoration strategies (e.g., restoration sequence) may lead to different resilience capabilities. In this study, the restoration sequence is based on the tank volume: ascending order (from small to large) and descending order (from large to small). There is no apparent difference (both are 0.822) between ascending order restoration and descending order restoration since the tank construction time is proportional to the tank volume. If the construction time is not proportional to the tank volume, the restoration sequence makes a difference. For instance, the resilience based on the descending sequence (0.861) is much higher than that based on the ascending sequence (0.777).

According to the above analysis, there are many measures in different resilience stages to enhance the resilience of hazardous material storage, such as safety barriers in the escalation stage, speeding inventory turnover in the adaptation stage, and shortening restoration time in the restoration stage. Besides, these measures, inherent safety design (Cozzani et al., 2009) may also be used to improve storage resilience by preventing and mitigating the primary major accident scenarios and possible escalations. In this study, the costs of different resilience measures are not considered. In the future, resilience management approaches may be developed by combining the resilience quantification method developed in this study with economic tools such as cost-benefit analysis and cost-effectiveness analysis.

7.7 Conclusions

The resilience of chemical plants is time-dependent and uncertain. This chapter proposes a dynamic stochastic methodology to measure it, considering possible domino effects and the recovery of damaged installations. In this methodology, the dynamic resilience process is divided into four stages: disruption, escalation, adaption, and restoration stages. This model considers the uncertainties related to the vulnerability of tanks exposed to disruptions, domino effects, and emergency response time. The dynamic Monte Carlo method is used to simulate possible resilience evolution scenarios and thus obtain storage resilience. Compared with traditional safety and security risk assessment, the developed resilience methodology addressing the roles of adaptation and restoration, which is more suitable for tackling unpredictable disruptions. Finally, a case study is provided to demonstrate and test the proposed methodology and algorithm. The primary conclusions are: (1) the resilience values can range in a large interval (in the case study, they are between 0.4 and 1) due to the uncertainties in the dynamic resilience process. As a result, the uncertainties in the resilience process cannot be ignored in resilience modeling; (2) domino effects play an essential role in hazardous material resilience; neglecting possible domino effects may underestimate the resilience; (3). the resilience depends on the intensity of disruptions, the plant's resistance capability, mitigation capability, adaption capability, and restoration capability; (4) resilience measures such as safety barriers in the escalation stage, speeding inventory turnover in the adaptation stage, and shortening restoration time in restoration stage are effective for developing a more resilient plant; (5) economic tools such as cost-benefit analysis and cost-effectiveness analysis may be used in this study to develop a resilience management approach chemical plants.

Chapter 8 Conclusions and future research

This study develops a Dynamic and Integrated Approach for MOdeling and maNaging Domino-effects in the chemical process industry, which is named "DIAMOND". This approach can contribute to modeling domino effects, decision-making on domino effect management, and developing a resilient chemical plant. The main conclusions and the answers to research questions are illustrated in Section 8.1. The research limitations and future research issues are discussed in Section 8.2.

8.1 Answer to research questions

The research provided in this dissertation is summarized in this section to answer the research questions proposed in Chapter 1.

Main research question

How can domino effects be modeled and managed, considering the time-dependencies and evolution uncertainties, for preventing and mitigating domino effects?

When a hazardous scenario (toxic release, fire, and explosion) occurs in a chemical industrial area, many hazardous installations are mutually linked via escalation vectors (e.g., heat radiation, overpressure), forming a system. The spatial-temporal evolution of hazardous scenarios within the system leads to domino effects. In light of the characteristics, a dynamic tool is better to model the temporal evolution and a graph/network-based approach is suitable to model the spatial escalation. As a result, a domino evolution graph (DEG) model based on dynamic graphs is proposed in Chapter 3 to model the spatial-temporal evolution of fire-induced domino effects. In Chapter 4, a dynamic event tree is used to model the dynamic evolution of vapor cloud explosion. Besides, Monte Carlo method is integrated into the dynamic graph model (called "Dynamic Graph Monte Carlo" (DGMC)) in Chapter 5 to tackle the evolution uncertainties in domino effects. In the DGMC model, hazardous installations, humans, and ignition sources are modeled as graph nodes and the physical effects between different nodes are modeled as graph edges. The Monte Carlo method is employed to automatically update graphs and deal with uncertainties, obtaining numerical evolution results.

In terms of domino effect management, not only safety barriers but also security measures should be considered due to possible catastrophic consequences caused by intentional attacks. In decision-making on prevention and mitigation of domino effects, economic issues need to be considered because chemical companies usually face budget limitations and pursue more profit. As a result, safety and security resources are integrated into domino effect management, and a cost-benefit analysis is conducted in Chapter 6 to obtain the optimal protection strategy. Besides safety and security measures, adaptation and restoration should also be considered to deal with unpredicted and unpreventable domino effects. Therefore, a resilience-based approach is developed in Chapter 7 in which the roles of resistance, mitigation, adaptation, and restoration in domino effect management are quantified.

Sub-research question on the state-of-the-art:

1. *What methods have been used in modeling and managing domino effects, and what research gaps need to be filled for better preventing and mitigating domino effects?*

To answer the question, a literature review focusing on modeling and managing domino effects in the process industry was conducted. Since the 1990s, increasing attention has been paid to domino effects in the process industry. In the past three decades, various methods have been developed to model and manage domino effects in the process industry. The modeling methods were divided into three categories: analytical approaches, graphical approaches, and simulation approaches. Some analytical methods-based software was developed in early research of domino effects to quantify the likelihood of domino effects. Graphical approaches, such as Bayesian network and Petri-net obtain increasing attention in recent years and can be used to map higher-order escalation of domino effects and thus estimate the probability of domino effects and the vulnerability of installations. Simulation approaches based on the Monte Carlo method can simplify probability calculation and may be used to deal with complex escalations while requiring longer calculation time. Although current methods have contributed enormously to modeling domino effects, many challenges still exist. The problems include modeling the spatial-temporal evolution of domino effects involving higher-order escalations, modeling the VCE-induced domino effects, and modeling the evolution of multi-hazardous scenarios in one domino effect.

In terms of the prevention and mitigation of domino effects, various management strategies were proposed: inherent safety, management of safety barriers, emergency response, cooperative prevention, and security strategies. Safety managers may select one protection strategy or a combination of multiple strategies. These strategies with different performances and costs may be used in different stages of the entire operating life. Thus, both the protection costs and financial implications related to potential avoided losses should be considered since protection resources are always limited and essential for the company’s profitability in the long term. Besides, both safety and security measures should be used to deal with intentional domino effects in which multiple failures of installations are possible. Once domino effects are inevitable, a quick repair or reconstruction may reduce the consequences of domino effects. As a result, the adaptation and restoration of chemical plants should also be considered in the whole to deal with unpredictable or unpreventable domino effects.

Sub-research question on modeling fire-induced domino effects:
2. *How can the spatial-temporal evolution of domino effects induced by fire be modeled, considering superimposed effects and synergistic effects?*

To answer the question, a domino evolution graph (DEG) model based on dynamic graphs is developed in Chapter 3. In the model, hazardous installations are modeled as graph nodes and the escalation vectors are modeled as graph edges. The graph structure can model possible complex phenomena in spatial evolution, such as synergistic effects and parallel effects. Besides, graph update can model the time dependencies in temporal evolution such as superimposed effects. Moreover, the model can also overcome the limitation of the probit model in higher-level escalation and rapidly obtain the evolution paths, evolution time, and the failure probabilities of installations.

An illustrated case study demonstrates that the synergistic effects and the superimposed effects considered in the DEG play a vital role in domino effect evolution. The domino effect risk may be underestimated if they are ignored in domino effect modeling. The primary scenario involving the failure of multiple installations that are more likely to occur in intentional domino effects can speed up the escalation of domino effects, leading to the prevention of domino effects more difficult and more severe consequences. Since the evolution process and the damage probability of installations can be rapidly obtained using the dynamic graph approach, the developed model can be applied to realistic chemical clusters with a large number of installations, significantly supporting the decision-making on the allocation of safety and security resources.

Sub-research question on modeling VCE-induced domino effects:
3. *How can the vapor dispersion and delayed ignition time be considered in VCE-induced domino effects?*

Chapter 4 establishes a dynamic VCE evolution assessment (DVEA) model based on a dynamic event tree. The DVEA model integrates the dispersion process of vapor cloud and ignition uncertainty into a stochastic simulation engine (a dynamic event tree) to assess the vapor cloud explosion risk in chemical industrial areas and obtain the damage probabilities of installations exposed to VCEs and the likelihood of domino effects. Both the time dependencies in vapor cloud dispersion and the uncertainty of delayed ignitions are addressed in the DVEA model.

Applying the DVEA model in a real case shows that both the time dependencies in vapor cloud dispersion and the uncertainty of delayed ignition are crucial for reflecting the characteristics of possible large VCEs and avoiding underestimating consequences. The vulnerability of installations to VCEs depends on the congestion of the plant layout and delayed ignition time (DIT). A long-delayed explosion may result in multiple-failure of installations, resulting in catastrophic disasters. The influence factors of DIT include the distance between the release position and the ignition sources, the type of ignition sources, and the ignition control measures in place. Ignition control measures in a chemical plant can decrease the ignition probability of single sources while may lead to a larger VCE and more severe consequences if the vapor cloud disperses outside the plant in which ignition sources are not fully eliminated. As a result, ignition control may be regarded as a delay measure but not as a preventive measure. Combining ignition control measures with emergency response actions may be an effective way to prevent VCEs since ignition control might provide enough time for emergency response actions to prevent VCEs.

Sub-research question on coupling domino effects:
4. *How can the evolution of multi-hazardous scenarios be modeled in domino effects?*

Based on the research of the DEG model of fire-induced domino effects in Chapter 3 and the DVEA model of VCE-induced domino effects in Chapter 4, a dynamic model called “Dynamic Graph Monte Carlo” (DGMC) is developed to model the evolution of multi-hazardous scenarios and assess the vulnerability of humans and installations exposed to such hazards. Since the DGMC model integrates dynamic graphs and Monte Carlo method, it has the advantages of both methods: graphs can provide a structure for model spatial evolution, graph update can model temporal evolution, and the random number generator in Monte Carlo simulation can deal with uncertainties in domino effect evolution. In the DGMC model, a chemical plant is modeled as a multi-agent system including three kinds of agents: hazardous installations, ignition sources, and humans. The uncertainties and interdependencies among these agents and their impacts on the evolution of hazards are considered in the DGMC model.

Therefore, the DGMC model can effectively model multiple hazardous scenarios that may simultaneously or sequentially occur in one domino effect. Neglecting any hazardous scenarios may underestimate the consequences of domino effects, resulting in an unreasonable allocation of safety barriers and personal protection equipment (PPE). The study results show that humans in different locations may be threatened by different hazards, thus different protection measures may be formulated for different people. A long-delayed ignition can damage multiple installations and acute toxicity of people around the release source. As a result, VCE-induced domino effects may result in more severe consequences than fire-induced domino effects. The safety distances based on fire hazards are not sufficient for the prevention of VCE-induced domino effects. People close to the release source are prone to the threat of multi-hazardous scenarios, while the distant deaths are mainly induced by acute toxicity and overpressure.

Sub-research question related to prevention and mitigation of domino effects
5. *How can safety and security resources be integrated and optimized for preventing and mitigating domino effects?*

Because both safety and security resources can contribute to prevent and mitigate domino effects, safety and security resources should be integrated better protect chemical plants and overcome resource overlaps. In Chapter 6, safety and security measures are divided into three categories (detection, delay, and emergency response) and the performance of a protection strategy (a combination of those measures) is considered in the DEG model. Based on the performance of protection strategies, the protection benefits and costs are quantified and a cost-benefit analysis is conducted to support decision-making on the allocation of safety and security measures. The expected avoided loss caused by a protection strategy is considered the Benefit while the investment related to the protection strategy is regarded as the cost. As a result. The net present value of benefits (NPVB) is obtained based on the cost-benefit analysis to determine whether a protection strategy is profitable or not. Besides, an optimization algorithm called “PROTOPT” is developed to achieve the most profitable protection strategy with the maximum NPVB.

The study demonstrates that multiple kinds of protection measures should be employed in chemical industrial areas since they follow the law of diminishing returns. The likelihood of threats plays a critical role in a protection strategy’s benefits. Therefore the optimal protection strategy varies with different plants and different threats. The protection is profitable only when the threat likelihood is no less than the threat probability at the break-even point. At the break-even point, the protection benefit is equal to the protection cost.

Sub-research question related to unpreventable domino effects
6. *How can unpreventable domino effects be tackled?*

Domino effects may be unpreventable such as the escalation caused by simultaneous attacks or natural disasters. In that case, protection measures may not prevent domino effects. A feasible way to deal with these unpreventable domino effects is to reduce the effects on the operation of companies by adjusting operation strategies and rapidly restoring the damaged installations. Resilience is the ability of a system to resist, mitigate, adapt and recover from disruptions. As a result, enhancing the resilience of a chemical plant can promote to prevent and mitigate domino effects, adapt, and recover from the damaged situation. A resilience-based approach is thus proposed in Chapter 7 to deal with domino effects. In this chapter, a dynamic stochastic model is developed to quantify the resilience of chemical plants. A resilience evolution scenario is modeled as a dynamic process that consists of four stages: disruption, escalation, adaption, and restoration stages. A simulation algorithm is developed to generate possible resilience evolution scenarios for obtaining chemical plant resilience.

Besides safety and security measures, the developed resilience approach highlights the roles of adaptation and restoration in dealing with domino effects, which is more suitable for tackling unpredictable and unpreventable disruptions. Chemical plant resilience depends on resistance capability, mitigation capability, adaption capability, and restoration capability. Improving any of these capabilities can contribute to the prevention and mitigation of domino effects. Various resilience measures such as safety barriers in the escalation stage, speeding inventory turnover in the adaptation stage, and shortening restoration time in the restoration stage are effective for developing a more resilient chemical plant and thus reducing the likelihood and consequences of domino effects.

8.2 Recommendations for future research

1. Recommendations on probit models

Probit models are used in this study for the risk assessment of domino effects and significantly impact the reasonable risk assessment results. The probit models for assessing fire-induced domino effects depend on the time to failure (TTF) of vessels exposed to fire. The common-used calculation method for TTF is developed for small vessels (atmospheric vessels: 25-17,500 m^3; pressurized vessels: 5-250m^3). However, using large storage vessels for hazardous materials is a development trend in the process industry (Yang et al., 2006). Besides vessel types, volumes considered in probit models, other vessel parameters such as wall thickness and wall material may also impact the vessel vulnerability. To extend the application of probit models and this study, vulnerability experiments may be used to improve the probit models. But experiments of large vessels may be expensive and dangerous, numerical simulations may be conducted using advanced consequence simulation software, such as ANSYS, FLUENT, FLACS, FDS, etc.

2. Recommendation on uncertainty modeling in domino effects

This study develops graphical-based models for modeling the spatial-temporal evolution of domino effects, addressing the time-dependencies, ignition uncertainty, and possible multiple hazardous scenarios in domino effects. However, accurately modeling domino effects is still challenging due to the uncertainty involved in the evolution of domino effects. The uncertainty can be divided into two parts, the intensity uncertainty of hazardous scenarios and the uncertainty of propagation. The former refers to heat radiation intensity, overpressure value, and the number, weight, and velocity of fragments. The latter involves the failure likelihood of installations subject to hazardous scenarios, failure types, and the subsequent scenarios. These uncertainties may be tackled in future research to support domino effect risk assessment and management.

3. Recommendation on modeling VCE-induced domino effects

In this study, vapor cloud dispersion is considered in VCE-induced domino effects. However, the vapor cloud dispersion model based on empirical formulas may not extend to model all possible release scenarios. Besides, the empirical model neglects VCE dilution with distance, the influences of wind velocity, and the effects of obstacles on dispersion. Thus, dynamic CFD methods may be integrated into domino effect risk assessment to obtain more accurate results in future studies. With the rapid improvement of computational resources, applying dynamic CFD methods in risk assessment may become easier and acceptable for researchers and practitioners in the future.

4. Recommendation on domino effect management

In chapter 6, a management approach is established to prevent and mitigate domino effects in chemical plants. However, there may be multiple chemical plants belonging to different companies in a chemical cluster. In terms of the cross-plant areas, safety and security resources allocated in one chemical plant has a benefit for nearby plants due to the mitigation of possible external domino effects while it may also relatively increase the security risk of nearby plants because of the change of attractiveness for possible common adversaries. To get the optimal strategy in a chemical plant, the protection strategies of other plants should be considered. Hence, the cost-benefit management may be extended to support decision-making on domino effects in chemical luster. Besides, the management approach proposed in this study neglects inherent safety design. Future research may consider inherent safety measures in a protection strategy to develop a life cycle management tool.

5. Recommendations on economic aspects of safety and security

In this study, cost-benefit analysis is used to support decision-making on protection strategies. The reliability of the optimal protection obtained by economic approaches depends on the monetization of costs. However, economic data is difficult to collect and a database for economic values of accident costs and the costs of safety measures may be developed in the future. Besides, some costs are difficult to be monetized or unethical to be monetized, such as the value of human life, reputational costs, and psychological costs. Therefore, other economic approaches such as cost-effectiveness analysis may be used to reduce the monetization work. Moreover, multiple-criteria decision (MCD) may be developed to deal with these costs and multi-objective optimization may be used to obtain the optimal protection strategy.

6. Recommendations on resilience-based approach

Chapter 7 develops a resilience-based approach for tackling domino effects, considering safety measures, security measures, adaptation measures, and restoration measures. Besides these measures, more design and operation options may be identified and quantified in the future to improve chemical plant resilience. Furthermore, the costs of different resilience measures are not considered and the benefits of resilience are not monetized. To support decision-making on resilience investment, resilience management approaches may be developed by combining the resilience quantification method developed in this study with economic tools such as cost-benefit analysis and cost-effectiveness analysis. Furthermore, the resilience quantification method developed for chemical plants may be applied to other interdependent infrastructure systems such as water supply systems and energy transportation systems.

Appendix

A.1 Appendix of Chapter 2

Table A.1 Characterization of current researches

Publication	Topic	Research issue	Research approach	Other keywords
Alileche et al. (2015)	Modeling	Vulnerability	Threshold methods	Heat radiation, overpressure
Cozzani et al. (2006b)	Modeling	Vulnerability	Threshold methods	Heat radiation, overpressure
Salzano and Cozzani (2006)	Modeling	Vulnerability	Threshold methods	overpressure
Cozzani and Salzano (2004c)	Modeling	Vulnerability	Probabilistic methods	Overpressure
Gubinelli et al. (2004)	Modeling	Vulnerability	Probabilistic methods	fragments
Gubinelli and Cozzani (2009b)	Modeling	Vulnerability	Probabilistic methods	fragments
Gubinelli and Cozzani (2009a)	Modeling	Vulnerability	Probabilistic methods	fragments
Hauptmanns (2001a)	Modeling	Vulnerability	Probabilistic methods	fragments
Hauptmanns (2001b)	Modeling	Vulnerability	Probabilistic methods	fragments
Jia et al. (2017)	Modeling	Vulnerability	Probabilistic methods	Heat radiation
Jujuly et al. (2015)	Modeling	Vulnerability	Probabilistic methods	Heat radiation
Landucci et al. (2009a)	Modeling	Vulnerability	Probabilistic methods	Heat radiation
Landucci et al. (2015b)	Modeling	Vulnerability	Probabilistic methods	Overpressure
Lisi et al. (2014)	Modeling	Vulnerability	Probabilistic methods	fragments
Lisi et al. (2015)	Modeling	Vulnerability	Probabilistic methods	fragments
Mukhim et al. (2017)	Modeling	Vulnerability	Probabilistic methods	Overpressure
Pula et al. (2007)	Modeling	Vulnerability	Probabilistic methods	fragments
Salzano and Cozzani (2005)	Modeling	Vulnerability	Probabilistic methods	overpressure
Salzano et al. (2014)	Modeling	Vulnerability	Probabilistic methods	Overpressure
Sun et al. (2012)	Modeling	Vulnerability	Probabilistic methods	fragments
Sun et al. (2013b)	Modeling	Vulnerability	Probabilistic methods	Overpressure
Sun et al. (2013a)	Modeling	Vulnerability	Probabilistic methods	Heat radiation
Sun et al. (2016b)	Modeling	Vulnerability	Probabilistic methods	fragments
Sun et al. (2017)	Modeling	Vulnerability	Probabilistic methods	fragments
Tugnoli et al. (2014b)	Modeling	Vulnerability	Probabilistic methods	fragments
Tugnoli et al. (2014a)	Modeling	Vulnerability	Probabilistic methods	fragments
Zhang and Jiang (2008)	Modeling	Vulnerability	Probabilistic methods	Overpressure
Zhang and Chen (2009)	Modeling	Vulnerability	Probabilistic methods	fragments
Ahmadi et al. (2019)	Modeling	Vulnerability	CFD/FEM methods	Heat radiation
Argentia et al. (2014)	Modeling	Vulnerability	CFD/FEM methods	Heat radiation
Landucci et al. (2009c)	Modeling	Vulnerability	CFD/FEM methods	Heat radiation
Landucci et al. (2016b)	Modeling	Vulnerability	CFD/FEM methods	Heat radiation
Rum et al. (2018)	Modeling	Vulnerability	CFD/FEM methods	Heat radiation
Antonioni et al. (2009b)	Modeling	Risk assessment	Analytical method	Heat radiation, overpressure
Antonioni et al. (2015)	Modeling	Risk assessment	Analytical method	Natech
Baesi et al. (2013)	Modeling	Risk assessment	Analytical method	Heat radiation, overpressure
Bagster and Pitblado (1991)	Modeling	Risk assessment	Analytical method	Heat radiation, overpressure
Cozzani et al. (2006a)	Modeling	Risk assessment	Analytical method	Heat radiation, overpressure
Cozzani et al. (2005)	Modeling	Risk assessment	Analytical method	Heat radiation, overpressure
Cozzani and Salzano (2004b)	Modeling	Risk assessment	Analytical method	Overpressure
Cozzani and Salzano (2004a)	Modeling	Risk assessment	Analytical method	Overpressure

Cozzani et al. (2014)	Modeling	Risk assessment	Analytical method	Natech
Kadri et al. (2013)	Modeling	Risk assessment	Analytical method	Heat radiation, overpressure
Khan and Abbasi (1998a)	Modeling	Risk assessment	Analytical method	Accidental domino effects
Khan and Abbasi (2001)	Modeling	Risk assessment	Analytical method	Accidental domino effects
Khan and Abbasi (1996)	Modeling	Risk assessment	Analytical method	Accidental domino effects
Khan and Abbasi (1998b)	Modeling	Risk assessment	Analytical method	Accidental domino effects
Khan and Abbasi (2000)	Modeling	Risk assessment	Analytical method	Accidental domino effects
Khan et al. (2001b)	Modeling	Risk assessment	Analytical method	Accidental domino effects
Khan et al. (2001c)	Modeling	Risk assessment	Analytical method	Accidental domino effects
Ramirez-Camacho et al. (2015)	Modeling	Risk assessment	Analytical method	Heat radiation
Silva et al. (2016)	Modeling	Risk assessment	Analytical method	overpressure
van der Voort et al. (2007)	Modeling	Risk assessment	Analytical method	overpressure
Zhang and Chen (2013)	Modeling	Risk assessment	Analytical method	Heat radiation, overpressure
Zhou and Reniers (2018a)	Modeling	Risk assessment	Analytical method	Heat radiation
Alileche et al. (2017)	Modeling	Risk assessment	Graphical method	Event tree
Chen et al. (2018)	Modeling	Risk assessment	Graphical method	Dynamic graphs
Jiang et al. (2019)	Modeling	Risk assessment	Graphical method	BN
Ji et al. (2018)	Modeling	Risk assessment	Graphical method	DBN
Kamil et al. (2019)	Modeling	Risk assessment	Graphical method	Petri-net
Khakzad (2015)	Modeling	Risk assessment	Graphical method	DBN
Khakzad (2018b)	Modeling	Risk assessment	Graphical method	DBN, Natech
Khakzad (2019)	Modeling	Risk assessment	Graphical method	DBN, Natech
Khakzad et al. (2018a)	Modeling	Risk assessment	Graphical method	DBN
Khakzad et al. (2018b)	Modeling	Risk assessment	Graphical method	DBN, Natech
Khakzad et al. (2013)	Modeling	Risk assessment	Graphical method	BN
Khakzad and Reniers (2015b)	Modeling	Risk assessment	Graphical method	Graph metrics
Khakzad et al. (2016)	Modeling	Risk assessment	Graphical method	Graph metrics
Reniers and Dullaert (2007)	Modeling	Risk assessment	Graphical method	Network
Yuan et al. (2016)	Modeling	Risk assessment	Graphical method	BN
Yang et al. (2018)	Modeling	Risk assessment	Graphical method	BN, Natech
Zhou and Reniers (2017b)	Modeling	Risk assessment	Graphical method	Petri-net
Abdolhamidzadeh et al. (2010b)	Modeling	Risk assessment	Simulation method	Monte Carlo

Ahmed et al. (2012)	Modeling	Risk assessment	Simulation method	Monte Carlo
Rad et al. (2014)	Modeling	Risk assessment	Simulation method	Monte Carlo
Zhang et al. (2018)	Modeling	Risk assessment	Simulation method	Agent-based modeling
Cozzani et al. (2007)	Management	Inherent safety	Inherent safety indexes	Heat radiation, overpressure
Cozzani et al. (2009)	Management	Inherent safety	Inherent safety indexes	Heat radiation, overpressure
Landucci et al. (2008)	Management	Inherent safety	Inherent safety indexes	Heat radiation
Tugnoli et al. (2008b)	Management	Inherent safety	Inherent safety indexes	Heat radiation, overpressure
Tugnoli et al. (2008a)	Management	Inherent safety	Inherent safety indexes	Heat radiation, overpressure
Bernechea and Arnaldos (2014)	Management	Inherent safety	Layout optimization	Heat radiation, overpressure
Dan et al. (2015)	Management	Inherent safety	Layout optimization	Heat radiation
de Lira-Flores et al. (2014)	Management	Inherent safety	Layout optimization	Heat radiation, overpressure
de Lira-Flores et al. (2018)	Management	Inherent safety	Layout optimization	Heat radiation, overpressure
Jung et al. (2011)	Management	Inherent safety	Layout optimization	Heat radiation, overpressure
Khakzad and Reniers (2015a)	Management	Inherent safety	Layout optimization	Heat radiation
Latifi et al. (2017)	Management	Inherent safety	Layout optimization	Accidental domino effects
Lee et al. (2005)	Management	Inherent safety	Layout optimization	Accidental domino effects
Lee et al. (2006)	Management	Inherent safety	Layout optimization	Accidental domino effects
López-Molina et al. (2013)	Management	Inherent safety	Layout optimization	Overpressure
Nomen et al. (2014)	Management	Inherent safety	Layout optimization	Heat radiation, overpressure
So et al. (2011)	Management	Inherent safety	Layout optimization	Heat radiation, overpressure
Khakzad et al. (2014)	Management	Inherent safety	Inventory optimization	Heat radiation
Bucelli et al. (2018)	Management	Safety barriers	Performance assessment	Heat radiation
Janssens et al. (2015)	Management	Safety barriers	Performance assessment	Heat radiation
Khakzad et al. (2017a)	Management	Safety barriers	Performance assessment	Heat radiation
Khakzad et al. (2017c)	Management	Safety barriers	Performance assessment	Heat radiation
Landucci et al. (2015a)	Management	Safety barriers	Performance assessment	Heat radiation
Landucci et al. (2016a)	Management	Safety barriers	Performance assessment	Heat radiation
Landucci et al. (2017a)	Management	Safety barriers	Performance assessment	Heat radiation
Landucci et al. (2017b)	Management	Safety barriers	Performance assessment	Heat radiation
Sun et al. (2016a)	Management	Safety barriers	Performance assessment	Projectiles, experiments
Tugnoli et al. (2012)	Management	Safety barriers	Performance assessment	Heat radiation
Tugnoli et al. (2013)	Management	Safety barriers	Performance assessment	Heat radiation

Ghasemi and Nourai (2017)	Management	Safety barriers	Optimization of barriers	Heat radiation
Khakzad and Reniers (2017)	Management	Safety barriers	Optimization of barriers	Heat radiation
Khakzad et al. (2017b)	Management	Safety barriers	Optimization of barriers	Heat radiation
Khakzad et al. (2018c)	Management	Safety barriers	Optimization of barriers	Heat radiation
Tsai et al. (2018)	Management	Emergency	Procedural action analysis	Heat radiation
Zhou et al. (2016)	Management	Emergency	Procedural action analysis	Heat radiation
Zhou and Reniers (2016b)	Management	Emergency	Procedural action analysis	Heat radiation
Zhou and Reniers (2017a)	Management	Emergency	Procedural action analysis	Heat radiation
Zhou and Reniers (2018c)	Management	Emergency	Procedural action analysis	Heat radiation
Cincotta et al. (2019)	Management	Emergency	Firefighting analysis	Heat radiation
Khakzad (2018a)	Management	Emergency	Firefighting analysis	Heat radiation
Khakzad (2018d)	Management	Emergency	Firefighting analysis	Heat radiation
Hosseinnia et al. (2018b)	Management	Emergency	Emergency alert	Chemical industrial clusters
Reniers et al. (2005a)	Management	Cooperative	Cooperative prevention	Traditional risk analysis tools
Reniers et al. (2005b)	Management	Cooperative	Cooperative prevention	Standardized method
Reniers et al. (2009)	Management	Cooperative	Cooperative prevention	Game theory
Reniers and Soudan (2010)	Management	Cooperative	Cooperative prevention	Game theory
Pavlova and Reniers (2011)	Management	Cooperative	Enhancing cooperation	Game theory
Reniers (2010)	Management	Cooperative	Enhancing cooperation	Game theory
Reniers et al. (2012)	Management	Cooperative	Enhancing cooperation	Systemic risk index
Reniers et al. (2008)	Management	Security	Security of critical installations	Intentional attacks
Reniers et al. (2014)	Management	Security	Security of critical installations	Intentional attacks
Khakzad and Reniers (2019)	Management	Security	Mitigation of consequences	Intentional attacks
Reniers and Audenaert (2014)	Management	Security	Mitigation of consequences	Intentional attacks
Srivastava and Gupta (2010)	Management	Security	Mitigation of consequences	Intentional attacks
(Chen et al., 2019b)	Management	Security	Reduction of attractiveness	Intentional attacks
Khakzad (2018c)	Management	Security	Reduction of attractiveness	Intentional attacks

A.2 Appendix of Chapter 4

A.2.1 Values of AIT and MIE

Table A.2 Values of AIT and MIE for some common chemicals (Moosemiller, 2011)

Chemicals	MIE (mJ)	AIT (F)
Hydrogen	0.011/00.17	752-1085
Methane	0.28/0.3	999-1103
Propane	0.25/0.26/0.48	842-919
Gasoline	0.23-0.29/0.8	824/853

A.2.2 Strength coefficient

There are several methods based on qualitative factors available in the literature, such as the method developed by Kinsella (1993). The method is based on three factors: (i) degree of obstruction by obstacles inside the vapor cloud, (ii) ignition energy, (iii) degree of confinement. The first factor is divided into three levels: high (obstacles in the gas cloud with a volume blockage fraction no less than 30% and with spacing between obstacles no more than 3 m), low (obstacles in a gas cloud with a blockage fraction less than 30% and/or spacing between obstacles in excess of 3 m) and none (no obstacles within the gas cloud). The factor of parallel plane confinement is divided into two levels: confined (gas clouds, or parts of it, are confined by walls/barriers on two or three sides), and unconfined (gas cloud is not confined, other than by the ground). The factor of ignition strength is divided into two levels: high (high energy source), and low (low energy source). The strength coefficient then can be estimated according to Table A.3.

Table A.3 Blast Strength Index (Kinsella, 1993)

Category	Ignition energy		Degree of obstruction			Parallel plane confinement		Strength coefficient
	Low (L)	High (H)	High (H)	Low (L)	No (N)	Confined (C)	Unconfined (U)	
1		H	H			C		7-10
2		H	H				U	7-10
3	L		H			C		5-7
4		H		L		C		5-7
5		H		L			U	4-6
6		H			N	C		4-6
7	L		H				U	4-5
8		H			N		U	4-5
9	L			L		C		3-5
10	L			L			U	2-3
11	L				N	C		1-2
12	L				N		U	1

A.2.3 Blast chart

The scaled overpressure (P_{sc}), as a function of the scaled distance (r_{sc}) and the strength coefficient (SC) of the explosion blast, can be read from a blast chart, as shown in Figure A.1. The blast chart was obtained on the basis that explosion strength is a function of the coefficient of strength and the scaled distance. Such blast was numerically simulated by means of a Flux-Corrected Transport code (van den Berg, 1980). As shown in Figure A.1, the horizontal axis represents the scaled distance (r_{sc}), the inner vertical axis represents the strength coefficient (SC) while the outside vertical axis represents the scaled overpressure (P_{sc}).

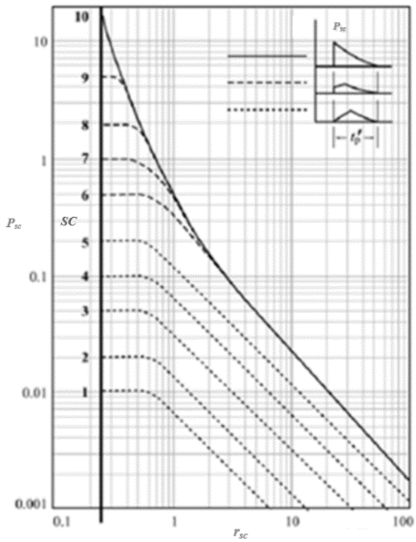

Figure A.1 The blast chart used in the Multi-Energy method (Van Den Bosh and Weterings, 1997)

A.3 Appendix of Chapter 6

Table A.4 The Heat flux q_{ij} between each pair of tanks in kW/m^2. Values lower than 10 kW/m2 are excluded (-)

Tank	1	2	3	4	5	6	7	8	9	10	11	12	13	14	15	16	17	18	19	20	21	22	23	24	25	26	27	28	29	30	31	32	33	34
1	-	14	-	-	11	-	-	-	-	-	-	-	-	-	-	-	-	-	-	-	-	-	-	-	-	-	-	-	-	-	-	-	-	-
2	14	-	28	-	-	11	-	-	-	-	-	-	-	-	-	-	-	-	-	-	-	-	-	-	-	-	-	-	-	-	-	-	-	-
3	-	28	-	-	-	-	11	-	-	-	-	-	-	-	-	-	-	-	-	-	-	-	-	-	-	-	-	-	-	-	-	-	-	-
4	-	-	-	-	28	-	-	-	-	11	-	-	-	-	-	-	-	-	-	-	-	-	-	-	-	-	-	-	-	-	-	-	-	-
5	11	-	-	28	-	14	-	-	-	-	11	-	-	-	-	-	-	-	-	-	-	-	-	-	-	-	-	-	-	-	-	-	-	-
6	-	11	-	-	14	-	28	-	-	-	-	11	-	-	-	-	-	-	-	-	-	-	-	-	-	-	-	-	-	-	-	-	-	-
7	-	-	11	-	-	28	-	14	-	-	-	-	11	-	-	-	-	-	-	-	-	-	-	-	-	-	-	-	-	-	-	-	-	-
8	-	-	-	-	-	-	14	-	28	-	-	-	-	11	-	-	-	-	-	-	-	-	-	-	-	-	-	-	-	-	-	-	-	-
9	-	-	-	-	-	-	-	28	-	-	-	-	-	-	11	-	-	-	-	-	-	-	-	-	-	-	-	-	-	-	-	-	-	-
10	-	-	-	11	-	-	-	-	-	-	28	-	-	-	-	-	-	-	-	-	-	-	-	-	-	-	-	-	-	-	-	-	-	-
11	-	-	-	-	11	-	-	-	-	28	-	14	-	-	-	-	-	-	-	-	-	-	-	-	-	-	-	-	-	-	-	-	-	-
12	-	-	-	-	-	11	-	-	-	-	14	-	28	-	-	-	-	-	-	-	-	-	-	-	-	-	-	-	-	-	-	-	-	-
13	-	-	-	-	-	-	11	-	-	-	-	28	-	14	-	-	-	-	-	10	-	-	-	-	-	-	-	-	-	-	-	-	-	-
14	-	-	-	-	-	-	-	11	-	-	-	-	14	-	28	-	-	-	-	-	-	-	-	-	-	-	-	-	-	-	-	-	-	-
15	-	-	-	-	-	-	-	-	11	-	-	-	-	28	-	-	-	-	-	-	-	-	-	-	-	-	-	-	-	-	-	-	-	-
16	-	-	-	-	-	-	-	-	-	-	-	-	-	-	-	-	26	-	-	-	-	-	-	-	-	-	-	-	-	-	-	-	-	-
17	-	-	-	-	-	-	-	-	-	-	-	-	-	-	-	26	-	-	-	-	-	-	-	-	-	-	-	-	-	-	-	-	-	-
18	-	-	-	-	-	-	-	-	-	11	12	-	-	-	-	-	-	-	26	-	-	-	-	-	-	-	-	-	-	-	-	-	-	-
19	-	-	-	-	-	-	-	-	-	-	11	10	-	-	-	-	-	26	-	-	-	-	-	-	-	-	-	-	-	-	-	-	-	-
20	-	-	-	-	-	-	-	-	-	-	-	-	10	10	-	-	-	-	-	-	26	-	-	-	-	-	-	-	-	-	-	-	-	-
21	-	-	-	-	-	-	-	-	-	-	-	-	-	11	11	-	-	-	-	26	-	-	-	-	-	-	-	-	-	-	-	-	-	-
22	-	-	-	-	-	-	-	-	-	-	-	-	-	-	-	-	-	-	-	-	-	-	26	-	-	-	-	-	-	-	-	-	-	-
23	-	-	-	-	-	-	-	-	-	-	-	-	-	-	-	-	-	-	-	-	-	26	-	-	-	-	-	-	-	-	-	-	-	-
24	-	-	-	-	-	-	-	-	-	-	-	-	-	-	-	-	-	-	-	-	-	-	-	-	26	-	-	-	-	-	-	-	-	-
25	-	-	-	-	-	-	-	-	-	-	-	-	-	-	-	-	-	-	-	-	-	-	-	26	-	-	-	-	-	-	-	-	-	-
26	-	-	-	-	-	-	-	-	-	-	-	-	-	-	-	-	-	-	-	-	-	-	-	-	-	-	-	-	-	-	-	-	-	-
27	-	-	-	-	-	-	-	-	-	-	-	-	-	-	-	-	-	-	-	-	-	-	-	-	-	-	-	26	-	-	-	-	-	-
28	-	-	-	-	-	-	-	-	-	-	-	-	-	-	-	-	-	-	-	-	-	-	-	-	-	-	26	-	-	-	-	-	-	-
29	-	-	-	-	-	-	-	-	-	-	-	-	-	-	-	-	-	-	-	-	-	-	-	-	-	-	-	-	-	26	-	-	-	-
30	-	-	-	-	-	-	-	-	-	-	-	-	-	-	-	-	-	-	-	-	-	-	-	-	-	-	-	-	26	-	-	-	-	-
31	-	-	-	-	-	-	-	-	-	-	-	-	-	-	-	-	-	-	-	-	-	-	-	-	-	-	11	-	-	-	-	11	-	-
32	-	-	-	-	-	-	-	-	-	-	-	-	-	-	-	-	-	-	-	-	-	-	-	-	-	-	-	-	-	-	11	-	-	-
33	-	-	-	-	-	-	-	-	-	-	-	-	-	-	-	-	-	-	-	-	-	-	-	-	-	-	-	-	-	-	-	-	-	-
34	-	-	-	-	-	-	-	-	-	-	-	-	-	-	-	-	-	-	-	-	-	-	-	-	-	-	-	-	-	-	-	-	-	-

Table A.5 The evolution path of domino effects caused by different primary hazardous scenarios

Primary scenarios	Domino evolution path																						
	1	**2**	**3**	**4**	**5**	**6**	**7**	**8**	**9**	**10**	**11**	**12**	**13**	**14**	**15**	**16**	**17**	**18**	**19**	**20**	**21**	**22**	**23**	**24**
T1 on fire	T1	T2	T5	T3	T6	T4	T7	T11	T12	T8	T10	T13	T14	T9	T15	T19	T18	T20	T21	T24	T21	T26	T29	T30
T2 on fire	T2	T3	T1	T6	T7	T5	T4	T8	T12	T13	T11	T9	T14	T10	T15	T19	T20	T18	T21	T24	T25	T26	T29	T30
T3 on fire	T3	T2	T7	T6	T1	T5	T8	T4	T12	T13	T11	T9	T14	T10	T15	T19	T20	T18	T21	T24	T25	T26	T29	T30
T4 on fire	T4	T5	T1	T11	T6	T10	T12	T7	T2	T13	T3	T19	T18	T8	T14	T9	T15	T20	T21	T24	T25	T26	T29	T30
T5 on fire	T5	T4	T6	T1	T11	T10	T7	T12	T2	T3	T13	T8	T19	T18	T14	T9	T15	T20	T21	T24	T25	T26	T29	T30
T6 on fire	T6	T7	T5	T2	T12	T3	T13	T8	T1	T11	T4	T14	T9	T10	T15	T19	T20	T18	T21	T24	T25	T26	T29	T30
T7 on fire	T7	T6	T8	T3	T13	T2	T12	T5	T9	T14	T1	T11	T15	T4	T10	T20	T21	T19	T18	T26	T25	T24	T29	T30
T8 on fire	T8	T9	T7	T14	T15	T13	T6	T12	T3	T2	T5	T21	T11	T20	T1	T4	T10	T19	T18	T26	T25	T24	T29	T30
T9 on fire	T9	T8	T15	T14	T7	T13	T6	T12	T3	T21	T20	T2	T5	T11	T1	T4	T10	T19	T18	T26	T25	T24	T29	T30
T10 on fire	T10	T11	T4	T5	T12	T18	T19	T6	T13	T7	T1	T2	T3	T14	T8	T24	T25	T20	T15	T9	T21	T26	T29	T30
T11 on fire	T11	T10	T12	T5	T4	T19	T18	T13	T6	T7	T1	T2	T14	T8	T3	T20	T15	T24	T25	T9	T21	T26	T29	T30
T12 on fire	T12	T13	T11	T6	T7	T14	T10	T5	T8	T4	T15	T20	T19	T2	T3	T9	T1	T18	T21	T24	T25	T26	T29	T30
T13 on fire	T13	T12	T14	T7	T6	T11	T20	T15	T8	T5	T9	T21	T10	T3	T2	T4	T19	T1	T18	T26	T25	T24	T29	T30
T14 on fire	T14	T15	T13	T8	T9	T7	T12	T21	T20	T6	T3	T11	T5	T2	T19	T4	T10	T1	T26	T18	T25	T24	T29	T30
T15 on fire	T15	T14	T9	T8	T13	T21	T7	T20	T12	T6	T3	T11	T5	T2	T19	T4	T1	T10	T26	T18	T25	T24	T29	T30
T16 on fire	T16	T17	T23	T22	T27	T28	T31	T32	-	-	-	-	-	-	-	-	-	-	-	-	-	-	-	-
T17 on fire	T17	T16	T23	T22	T27	T28	T31	T32	-	-	-	-	-	-	-	-	-	-	-	-	-	-	-	-
T18 on fire	T18	T11	T19	T10	T12	T13	T5	T4	T6	T7	T25	T24	T14	T1	T20	T8	T2	T3	T15	T9	T21	T29	T30	T26
T19 on fire	T19	T18	T11	T10	T12	T13	T25	T24	T5	T6	T4	T7	T14	T20	T8	T1	T2	T15	T3	T9	T21	T29	T30	T26
T20 on fire	T20	T21	T14	T13	T15	T12	T26	T8	T7	T9	T6	T11	T5	T3	T19	T2	T10	T4	T18	T1	T25	T24	T29	T30
T21 on fire	T21	T20	T14	T15	T13	T12	T26	T8	T9	T7	T6	T11	T5	T3	T19	T2	T10	T4	T18	T1	T25	T24	T29	T30
T22 on fire	T22	T23	T27	T28	T16	T17	T31	T32	-	-	-	-	-	-	-	-	-	-	-	-	-	-	-	-
T23 on fire	T23	T22	T27	T28	T16	T17	T31	T32	-	-	-	-	-	-	-	-	-	-	-	-	-	-	-	-

T24 on fire	T24	T25	T29	T30	T18	T19	T11	T10	T12	T13	T5	T4	T6	T7	T14	T20	T8	T1	T2	T3	T15	T9	T21	T26
T25 on fire	T25	T24	T29	T30	T18	T19	T11	T10	T12	T13	T5	T4	T6	T7	T14	T20	T8	T1	T2	T3	T15	T9	T21	T26
T26 on fire	T26	-	-	-	-	-	-	-	-	-	-	-	-	-	-	-	-	-	-	-	-	-	-	-
T27 on fire	T27	T28	T31	T22	T23	T32	T16	T17	-	-	-	-	-	-	-	-	-	-	-	-	-	-	-	-
T28 on fire	T28	T27	T31	T22	T23	T32	T16	T17	-	-	-	-	-	-	-	-	-	-	-	-	-	-	-	-
T29 on fire	T29	T30	T24	T25	T18	T19	T11	T10	T12	T13	T5	T4	T6	T7	T14	T20	T8	T1	T2	T3	T15	T9	T21	T26
T30 on fire	T30	T29	T24	T25	T18	T19	T11	T10	T12	T13	T5	T4	T6	T7	T14	T20	T8	T1	T2	T3	T15	T9	T21	T26
T31 on fire	T31	T32	T27	T28	T22	T23	T16	T17	-	-	-	-	-	-	-	-	-	-	-	-	-	-	-	-
T32 on fire	T32	T31	T27	T28	T22	T23	T16	T17	-	-	-	-	-	-	-	-	-	-	-	-	-	-	-	-
T33 on fire	T33	-	-	-	-	-	-	-	-	-	-	-	-	-	-	-	-	-	-	-	-	-	-	-
T34 on fire	T34	-	-	-	-	-	-	-	-	-	-	-	-	-	-	-	-	-	-	-	-	-	-	-
T2&T3 on fire	T2	T3	T6	T7	T1	T5	T8	T4	T12	T13	T11	T9	T14	T10	T15	T19	T20	T18	T21	T24	T25	T26	T29	T30
T4&T5 on fire	T4	T5	T1	T11	T6	T10	T12	T7	T2	T3	T13	T19	T18	T8	T14	T9	T15	T20	T21	T24	T25	T26	T29	T30
T6&T7 on fire	T6	T7	T2	T3	T12	T5	T8	T13	T1	T11	T14	T4	T9	T15	T10	T20	T19	T21	T18	T26	T25	T24	T29	T30
T8&T9 on fire	T8	T9	T14	T15	T7	T13	T6	T12	T3	T21	T2	T20	T5	T11	T1	T4	T10	T19	T18	T26	T25	T24	T29	T30
T10&T11 on fire	T10	T11	T4	T12	T18	T19	T5	T13	T6	T7	T1	T2	T14	T3	T8	T24	T25	T20	T15	T9	T21	T26	T29	T30
T12&T13 on fire	T12	T13	T7	T14	T11	T6	T8	T5	T20	T15	T10	T9	T4	T3	T2	T19	T21	T1	T18	T26	T25	T24	T29	T30
T14&T15 on fire	T14	T15	T8	T9	T13	T21	T20	T7	T12	T6	T3	T11	T5	T2	T19	T4	T10	T26	T1	T18	T25	T24	T29	T30
T16&T17 on fire	T16	T17	T23	T22	T27	T28	T31	T32	T0	T0	T0	T0	T0	T0	T0	T0	T0	T0	T0	T0	T0	T0	T0	T0
T18&T19 on fire	T18	T19	T11	T10	T12	T13	T24	T25	T5	T4	T6	T7	T14	T20	T8	T1	T2	T3	T15	T29	T30	T9	T21	T26
T20&T21 on fire	T20	T21	T14	T15	T13	T26	T12	T8	T9	T7	T6	T11	T5	T3	T19	T2	T10	T4	T18	T1	T25	T24	T29	T30
T22&T23 on fire	T22	T23	T27	T28	T16	T17	T31	T32	-	-	-	-	-	-	-	-	-	-	-	-	-	-	-	-
T24&T25 on fire	T24	T25	T29	T30	T18	T19	T11	T10	T12	T13	T5	T4	T6	T7	T14	T20	T8	T1	T2	T3	T15	T9	T21	T26
T27&T28 on fire	T27	T28	T31	T22	T23	T32	T16	T17	-	-	-	-	-	-	-	-	-	-	-	-	-	-	-	-
T29&T30 on fire	T29	T30	T24	T25	T18	T19	T11	T10	T12	T13	T5	T4	T6	T7	T14	T20	T8	T1	T2	T3	T15	T9	T21	T26

Table A.6 The costs of different protection strategies

<table>
<tr><th>Cost categories</th><th>PS1</th><th>PS2</th><th>PS3</th><th>PS4</th><th>PS5</th><th>PS6</th></tr>
<tr><td>Initial costs (€)</td><td>118000</td><td>786220</td><td>52900</td><td rowspan="2">7371872</td><td>170900</td><td rowspan="2">1552009</td></tr>
<tr><td>Installation costs (€)</td><td>162000</td><td>1114463</td><td>39000</td><td>201000</td></tr>
<tr><td>Annual operating costs (€/Year)</td><td>4170</td><td>0</td><td>201480</td><td>0</td><td>205650</td><td>4170</td></tr>
<tr><td>Annual maintenance costs (€/Year)</td><td>8400</td><td>57020</td><td>2757</td><td>221156</td><td>11157</td><td>46560</td></tr>
<tr><td>Annual inspection costs (€/Year)</td><td>5600</td><td>38014</td><td>1838</td><td>147437</td><td>7438</td><td>31040</td></tr>
<tr><td>Annual logistics and transport costs (€/Year)</td><td>2800</td><td>19007</td><td>919</td><td>73719</td><td>3719</td><td>15520</td></tr>
<tr><td>Annual other costs (€/Year)</td><td>1400</td><td>9503</td><td>460</td><td>36859</td><td>1860</td><td>7760</td></tr>
<tr><td>Present value of costs (€)</td><td>466042</td><td>2928151</td><td>1817208</td><td>11356951</td><td>2283250</td><td>2425673</td></tr>
</table>

A.4 Appendix of Chapter 7

The parameters for heat radiation calculation by the software ALOHA are as follows: a wind speed of 1 m/s measured at 10 m above the ground and blowing from East, partly cloudy, air temperature of 25 °C, 50% relative humidity, and stability class of E. According to these parameters, the heat Radiation between each pair of tanks can be obtained by the ALOHA software, as shown in Table A.7.

Table A.7 The Heat Radiation (kW/m^2) from installation *i* to installation *j*

Tank *i*, *j*	T1	T2	T3	T4	T5	T6	T7	T8	T9	T10	T11	T12	T13	T14
T1	0	11	6	0	0	0	0	0	0	0	0	0	0	0
T2	19	0	18	18	11	6	0	0	0	0	0	0	0	0
T3	11	18	0	11	18	0	0	0	0	0	0	0	0	0
T4	6	18	11	0	18	18	6	7	0	0	0	0	0	0
T5	0	11	19	19	0	11	5	13	0	0	0	0	0	0
T6	0	0	0	15	9	0	13	13	0	0	0	0	0	0
T7	0	0	0	8	8	21	0	18	18	11	0	0	0	0
T8	0	5	7	10	18	21	18	0	11	17	11	0	0	0
T9	0	0	0	0	0	6	18	11	0	17	5	0	0	0
T10	0	0	0	0	6	5.5	11	17	17	0	18	0	0	0
T11	0	0	0	0	6	0	0	11	5	18	0	0	0	0
T12	9	7	12	5	7	0	0	0	0	0	5	0	17	5
T13	0	0	8	0	6.3	0	0	5	0	5	10	17	0	18
T14	0	0	0	0	0	0	0	0	0	5	10	5	18	0

References

Abdolhamidzadeh, B., Abbasi, T., Rashtchian, D., Abbasi, S.A., 2010a. A new method for assessing domino effect in chemical process industry. J Hazard Mater 182, 416-426. 10.1016/j.jhazmat.2010.06.049

Abdolhamidzadeh, B., Abbasi, T., Rashtchian, D., Abbasi, S.A., 2010b. A new method for assessing domino effect in chemical process industry. Journal of hazardous materials 182, 416-426. 10.1016/j.jhazmat.2010.06.049

Abdolhamidzadeh, B., Abbasi, T., Rashtchian, D., Abbasi, S.A., 2011. Domino effect in process-industry accidents – An inventory of past events and identification of some patterns. Journal of Loss Prevention in the Process Industries 24, 575-593. 10.1016/j.jlp.2010.06.013

Abimbola, M., Khan, F., 2019. Resilience modeling of engineering systems using dynamic object-oriented Bayesian network approach. Computers & Industrial Engineering 130, 108-118. 10.1016/j.cie.2019.02.022

Acosta, C., Siu, N., 1993. Dynamic event trees in accident sequence analysis: application to steam generator tube rupture. Reliability Engineering & System Safety 41, 135-154.

AFP, 2012. Total Subsidiary Ex-boss Jailed for Deadly French Blast. Retrieved from: https://www.expatica.com/fr/total-subsidiary-ex-boss-jailed-for-deadly-french-blast/. (Accessed April 15, 2019).

Ahmadi, O., Mortazavi, S.B., Pasdarshahri, H., Mohabadi, H.A., 2019. Consequence analysis of large-scale pool fire in oil storage terminal based on computational fluid dynamic (CFD). Process Safety and Environmental Protection 123, 379-389. 10.1016/j.psep.2019.01.006

Ahmed, M., Jerez, S., Matasic, I., Prodhomme, G., Reimeringer, M., 2012. Explosions and Structural Fragments as Industrial Hazard: Domino Effect and Risks. Procedia Engineering 45, 159-166. 10.1016/j.proeng.2012.08.137

Aldemir, T., 2018. Advanced Concepts in Nuclear Energy Risk Assessment and Management. World Scientific Publishing Company Pte. Limited.

Alessandri, S., Caputo, A.C., Corritore, D., Giannini, R., Paolacci, F., Phan, H.N., 2018. Probabilistic risk analysis of process plants under seismic loading based on Monte Carlo simulations. Journal of Loss Prevention in the Process Industries 53, 136-148. 10.1016/j.jlp.2017.12.013

Alileche, N., Cozzani, V., Reniers, G., Estel, L., 2015. Thresholds for domino effects and safety distances in the process industry: A review of approaches and regulations. Reliability Engineering & System Safety 143, 74-84. 10.1016/j.ress.2015.04.007

Alileche, N., Olivier, D., Estel, L., Cozzani, V., 2017. Analysis of domino effect in the process industry using the event tree method. Safety Science 97, 10-19. 10.1016/j.ssci.2015.12.028

ALOHA, 2016. ALOHA user manual. Retrieved from: https://www.epa.gov/cameo/aloha-software. (Accessed May 5, 2019).

Alrabghi, A., 2020. Modelling condition-based maintenance for nonidentical two-component systems considering four types of dependencies. Journal of quality in maintenance engineering ahead-of-print. 10.1108/jqme-09-2019-0091

American Petroleum Institute (API), 2004. Recommended practice for security vulnerability assessment for petroleum and petrochemical facilities. American Petroleum Institute.
Anderson, C., Townsend, W., Zook, J., Cowgill, G., 1974. The effects of a fire environment on a rail tank car filled with LPG.
Anderson, E.W., Mittal, V., 2000. Strengthening the satisfaction-profit chain. Journal of Service research 3, 107-120.
Antonioni, G., Bonvicini, S., Spadoni, G., Cozzani, V., 2009a. Development of a framework for the risk assessment of Na-Tech accidental events. Reliability Engineering & System Safety 94, 1442-1450. 10.1016/j.ress.2009.02.026
Antonioni, G., Landucci, G., Necci, A., Gheorghiu, D., Cozzani, V., 2015. Quantitative assessment of risk due to NaTech scenarios caused by floods. Reliability Engineering & System Safety 142, 334-345. 10.1016/j.ress.2015.05.020
Antonioni, G., Spadoni, G., Cozzani, V., 2007. A methodology for the quantitative risk assessment of major accidents triggered by seismic events. J Hazard Mater 147, 48-59. 10.1016/j.jhazmat.2006.12.043
Antonioni, G., Spadoni, G., Cozzani, V., 2009b. Application of domino effect quantitative risk assessment to an extended industrial area. Journal of Loss Prevention in the Process Industries 22, 614-624. 10.1016/j.jlp.2009.02.012
API, 2013. ANSI/API Standard 780 – Security risk assessment methodology for the petroleum and petrochemical industry. American Petroleum Institute.
Apostolakis, G.E., Lemon, D.M., 2005. A screening methodology for the identification and ranking of infrastructure vulnerabilities due to terrorism. Risk Analysis: An International Journal 25, 361-376.
Argentia, F., Landucci, G., Antonionib, G., Cozzanib, V., 2014. Frequency evaluation for domino scenarios triggered by heat radiation exposure. Chemical Engineering Transactions 36, 373-378.
Assael, M.J., Kakosimos, K.E., 2010. Fires, explosions, and toxic gas dispersions: effects calculation and risk analysis. CRC Press.
Atkins, W., 1998. Development of methods to assess the significance of domino effects from major hazard sites. Health and Safety Executive, London, UK.
Atkinson, G., 2017. Development of heavy vapour clouds in very low wind speeds. Journal of Loss Prevention in the Process Industries 48, 162-172. 10.1016/j.jlp.2017.04.011
Atkinson, G., Coldrick, S., 2012. Vapour cloud formation: Experiments and modelling. Debyshire, UK: Health and Safety Laboratory.
Atkinson, G., Cowpe, E., Halliday, J., Painter, D., 2017a. A review of very large vapour cloud explosions: Cloud formation and explosion severity. Journal of Loss Prevention in the Process Industries 48, 367-375. 10.1016/j.jlp.2017.03.021
Atkinson, G., Hall, J., McGillivray, A., 2017b. Review of Vapour Cloud Explosion Incidents. Health and Safety Executive, Buxton, UK.
Azadeh, A., Salehi, V., Arvan, M., Dolatkhah, M., 2014. Assessment of resilience engineering factors in high-risk environments by fuzzy cognitive maps: A petrochemical plant. Safety Science 68, 99-107. 10.1016/j.ssci.2014.03.004
Badri, N., Nourai, F., Rashtchian, D., 2013. A multivariable approach for estimation of vapor cloud explosion frequencies for independent congested spaces to be used in

occupied building risk assessment. Process Safety and Environmental Protection 91, 19-30. 10.1016/j.psep.2011.12.002
Baesi, S., Abdolhamidzadeh, B., Hassan, C.R.C., Hamid, M.D., Reniers, G., 2013. Application of a multi-plant QRA: A case study investigating the risk impact of the construction of a new plant on an existing chemical plant's risk levels. Journal of Loss Prevention in the Process Industries 26, 895-903. 10.1016/j.jlp.2012.11.005
Bagster, D.F., Pitblado, R.M., 1991. The Estimation of Domino Incident Frequencies—An Approach. Process Safety & Environmental Protection 69, 195-199.
Baker, Q.A., Doolittle, C.M., Fitzgerald, G.A., Tang, M.J., 1998. Recent developments in the Baker-Strehlow VCE analysis methodology. Process Safety Progress 17, 297-301.
Baker, Q.A., Tang, M.J., Scheier, E.A., Silva, G.J., 1996. Vapor cloud explosion analysis. Process Safety Progress 15, 106-109.
Bakke, J.R., van Wingerden, K., Hoorelbeke, P., Brewerton, B., 2010. A study on the effect of trees on gas explosions. Journal of Loss Prevention in the Process Industries 23, 878-884. 10.1016/j.jlp.2010.08.007
Baybutt, P., 2002. Assessing risks from threats to process plants: Threat and vulnerability analysis. Process Safety Progress 21, 269-275.
Baybutt, P., 2017. Issues for security risk assessment in the process industries. Journal of Loss Prevention in the Process Industries 49, 509-518. 10.1016/j.jlp.2017.05.023
BBC News, 2015. France explosions: Devices found near Berre-L'Etang plant.
Bellamy, L., Geyer, T., Astley, J., 1989. Evaluation of the human contribution to pipework and in-line equipment failure frequencies. Health and Safety Executive.
Bernechea, E.J., Arnaldos, J., 2014. Optimizing the design of storage facilities through the application of ISD and QRA. Process Safety and Environmental Protection 92, 598-615. 10.1016/j.psep.2013.06.002
Bier, V.M., Nagaraj, A., Abhichandani, V., 2005. Protection of simple series and parallel systems with components of different values. Reliability Engineering & System Safety 87, 315-323. 10.1016/j.ress.2004.06.003
Birk, A.M., 2014. Cost-effective application of thermal protection on LPG road transport tanks for risk reduction due to hot BLEVE incidents. Risk Anal 34, 1139-1148. 10.1111/risa.12148
Blomberg, S.B., Hess, G.D., Weerapana, A., 2004. An economic model of terrorism. Conflict Management and Peace Science 21, 17-28.
Bollinger, R.E., Crowl, D.A., 1997. Inherently safer chemical processes: a life cycle approach. Wiley-AIChE.
Bondy, J.A., Murty, U.S.R., 1976. Graph theory with applications. Citeseer.
Brazdil, J.F., 2000. Acrylonitrile. Ullmann's Encyclopedia of Industrial Chemistry.
Brück, T., 2007. The economic analysis of terrorism. Routledge.
Bruneau, M., Chang, S.E., Eguchi, R.T., Lee, G.C., O'Rourke, T.D., Reinhorn, A.M., Shinozuka, M., Tierney, K., Wallace, W.A., Von Winterfeldt, D., 2003. A framework to quantitatively assess and enhance the seismic resilience of communities. Earthquake Spectra 19, 733-752.

Bubbico, R., Mazzarotta, B., 2014. Security risk assessment of process plants: the role of layout, In: Garzia, F., Thomas, G., Pritchard, D.A. (Eds.), 2014 International Carnahan Conference on Security Technology. Ieee, New York.
Bucelli, M., Landucci, G., Haugen, S., Paltrinieri, N., Cozzani, V., 2018. Assessment of safety barriers for the prevention of cascading events in oil and gas offshore installations operating in harsh environment. Ocean Engineering 158, 171-185. 10.1016/j.oceaneng.2018.02.046
Buncefield Major Incident Investigation Board, 2008. The Buncefield incident, 11 December 2005: the final report of the Major Incident Investigation Board. Health and Safety Executive.
Cameron, I., Mannan, S., Németh, E., Park, S., Pasman, H., Rogers, W., Seligmann, B., 2017. Process hazard analysis, hazard identification and scenario definition: Are the conventional tools sufficient, or should and can we do much better? Process Safety and Environmental Protection 110, 53-70. 10.1016/j.psep.2017.01.025
Campedel, M., Cozzani, V., Garcia-Agreda, A., Salzano, E., 2008. Extending the quantitative assessment of industrial risks to earthquake effects. Risk Anal 28, 1231-1246. 10.1111/j.1539-6924.2008.01092.x
Casteigts, A., Flocchini, P., Quattrociocchi, W., Santoro, N., 2012. Time-varying graphs and dynamic networks. International Journal of Parallel, Emergent and Distributed Systems 27, 387-408.
CBS, 2015. Final investigation report CARIBBEAN petroleum tank terminal explosion and multiple tank fires. Retrieved from: https://www.csb.gov/assets/1/17/06.09.2015_final_capeco_draft_report__for_board_vote.pdf?15462. (Accessed September 20, 2020).
CCPS, 1996. Guidelines for use of vapor cloud dispersion models. Wiley-AIChE.
CCPS, 2001. Layer of Protection Analysis: Simplified Process Risk Assessment. AIChE–CCPS, NewYork.
CCPS, 2011. Layer of protection analysis: simplified process risk assessment. American Institute of Chemical Engineers - Center of Chemical Process Safety, New York.
Chakraborty, S., Goyal, N.K., Mahapatra, S., Soh, S., 2020. A Monte-Carlo Markov chain approach for coverage-area reliability of mobile wireless sensor networks with multistate nodes. Reliability Engineering & System Safety 193, 14. 10.1016/j.ress.2019.106662
Chang, J.I., Lin, C.-C., 2006. A study of storage tank accidents. Journal of Loss Prevention in the Process Industries 19, 51-59. 10.1016/j.jlp.2005.05.015
Chen, C., Khakzad, N., Reniers, G., 2020a. Dynamic vulnerability assessment of process plants with respect to vapor cloud explosions. Reliability Engineering & System Safety 200. 10.1016/j.ress.2020.106934
Chen, C., Li, C., Reniers, G., Yang, F., 2021a. Safety and security of oil and gas pipeline transportation: A systematic analysis of research trends and future needs using WoS. Journal of Cleaner Production 279. 10.1016/j.jclepro.2020.123583
Chen, C., Reniers, G., 2018. Risk Assessment of Processes and Products in Industrial Biotechnology, Adv Biochem Eng Biotechnol.

Chen, C., Reniers, G., 2020. Chemical industry in China: The current status, safety problems, and pathways for future sustainable development. Safety Science 128. 10.1016/j.ssci.2020.104741

Chen, C., Reniers, G., Khakzad, N., 2019a. Exploring loading and unloading operations in relation to domino effects in chemical industrial parks. Chemical Engineering Transactions 75. 10.3303/CET1977010

Chen, C., Reniers, G., Khakzad, N., 2019b. Integrating safety and security resources to protect chemical industrial parks from man-made domino effects: a dynamic graph approach. Reliability Engineering & System Safety 191. 10.1016/j.ress.2019.04.023

Chen, C., Reniers, G., Khakzad, N., 2020b. Cost-Benefit Management of Intentional Domino Effects in Chemical Industrial Areas. Process Safety and Environmental Protection 134, 392-405. 10.1016/j.psep.2019.10.007

Chen, C., Reniers, G., Khakzad, N., 2020c. A thorough classification and discussion of approaches for modeling and managing domino effects in the process industries. Safety Science 125. 10.1016/j.ssci.2020.104618

Chen, C., Reniers, G., Khakzad, N., 2021b. A dynamic multi-agent approach for modeling the evolution of multi-hazard accident scenarios in chemical plants. Reliability Engineering & System Safety 207. 10.1016/j.ress.2020.107349

Chen, C., Reniers, G., Zhang, L., 2018. An innovative methodology for quickly modeling the spatial-temporal evolution of domino accidents triggered by fire. Journal of Loss Prevention in the Process Industries 54, 312-324. 10.1016/j.jlp.2018.04.012

Chen, P., Huang, Y., Mou, J., van Gelder, P.H.A.J.M., 2019c. Probabilistic risk analysis for ship-ship collision: State-of-the-art. Safety Science 117, 108-122. 10.1016/j.ssci.2019.04.014

Cincotta, S., Khakzad, N., Cozzani, V., Reniers, G., 2019. Resilience-based optimal firefighting to prevent domino effects in process plants. Journal of Loss Prevention in the Process Industries 58, 82-89. 10.1016/j.jlp.2019.02.004

Clini, F., Darbra, R.M., Casal, J., 2010. Historical Analysis Of Accidents Involving Domino Effect, In: Buratti, S.S. (Ed.), Cisap4: 4th International Conference on Safety & Environment in Process Industry. Aidic Servizi Srl, Milano, pp. 335-340.

CNN, 2019. Texas district attorney files charges against chemical plant for its 4-day fire. Retrieved from: https://edition.cnn.com/2019/04/29/us/deer-park-itc-plant-fire-charges/index.html. (Accessed April 30, 2019).

Coster, M.N., Hankin, R.K., 2003. Risk assessment of antagonistic hazards. Journal of Loss Prevention in the Process Industries 16, 545-550.

Council Directive96/82/EC, 1997. Council Directive 96/82/EC of 9 December 1996 on the Control of Major-Accident Hazards Involving Dangerous Substances. Official Journal of the European Communities, 1–38.

Council Directive 2012/18/EU, 2012. On the control of major-accident hazards involving dangerous substances. Official Journal of the European Communities, 1–38.

Cozzani, V., Antonioni, G., Landucci, G., Tugnoli, A., Bonvicini, S., Spadoni, G., 2014. Quantitative assessment of domino and NaTech scenarios in complex industrial areas. Journal of Loss Prevention in the Process Industries 28, 10-22. 10.1016/j.jlp.2013.07.009

Cozzani, V., Antonioni, G., Spadoni, G., 2006a. Quantitative assessment of domino scenarios by a GIS-based software tool. Journal of Loss Prevention in the Process Industries 19, 463-477. 10.1016/j.jlp.2005.11.007
Cozzani, V., Campedel, M., Renni, E., Krausmann, E., 2010. Industrial accidents triggered by flood events: analysis of past accidents. J Hazard Mater 175, 501-509. 10.1016/j.jhazmat.2009.10.033
Cozzani, V., Gubinelli, G., Antonioni, G., Spadoni, G., Zanelli, S., 2005. The assessment of risk caused by domino effect in quantitative area risk analysis. J Hazard Mater 127, 14-30. 10.1016/j.jhazmat.2005.07.003
Cozzani, V., Gubinelli, G., Salzano, E., 2006b. Escalation thresholds in the assessment of domino accidental events. J Hazard Mater 129, 1-21. 10.1016/j.jhazmat.2005.08.012
Cozzani, V., Salzano, E., 2004a. The quantitative assessment of domino effect caused by overpressure: Part II. Case studies. Journal of hazardous materials 107, 81-94.
Cozzani, V., Salzano, E., 2004b. The quantitative assessment of domino effects caused by overpressure: Part I. Probit models. Journal of hazardous materials 107, 67-80.
Cozzani, V., Salzano, E., 2004c. Threshold values for domino effects caused by blast wave interaction with process equipment. Journal of Loss Prevention in the Process Industries 17, 437-447. 10.1016/j.jlp.2004.08.003
Cozzani, V., Tugnoli, A., Salzano, E., 2007. Prevention of domino effect: from active and passive strategies to inherently safer design. J Hazard Mater 139, 209-219. 10.1016/j.jhazmat.2006.06.041
Cozzani, V., Tugnoli, A., Salzano, E., 2009. The development of an inherent safety approach to the prevention of domino accidents. Accid Anal Prev 41, 1216-1227. 10.1016/j.aap.2008.06.002
Cozzani, V., Zanelli, S., 2001. An approach to the assessment of domino accidents hazard in quantitative area risk analysis, Loss Prevention and Safety Promotion in the Process Industries. Elsevier, pp. 1263-1274.
Craftsman, 2018. 2018 National Concrete and Masonry Estimator. Retrieved from: https://www.craftsman-book.com/downloads/national-estimator. (Accessed April 10, 2017).
CSB, 2015. Final investigation report Caribbean petroleum tank terminal explosion and multiple tank fires. U.S. Chemical Safety and Hazard Investigation Board.
Dan, S., Shin, D., Yoon, E.S., 2015. Layout optimization of LNG-liquefaction process on LNG-FPSO preventing domino effects. Journal of chemical engineering of Japan 48, 646-655.
Darbra, R.M., Palacios, A., Casal, J., 2010. Domino effect in chemical accidents: main features and accident sequences. J Hazard Mater 183, 565-573. 10.1016/j.jhazmat.2010.07.061
Dasgotra, A., Varun Teja, G.V.V., Sharma, A., Mishra, K.B., 2018. CFD modeling of large-scale flammable cloud dispersion using FLACS. Journal of Loss Prevention in the Process Industries 56, 531-536. 10.1016/j.jlp.2018.01.001
David, R., Alla, H., 2005. Discrete, continuous, and hybrid Petri nets. Springer.

De Dianous, V., Fievez, C., 2006. ARAMIS project: A more explicit demonstration of risk control through the use of bow–tie diagrams and the evaluation of safety barrier performance. Journal of hazardous materials 130, 220-233.
de Lira-Flores, J., Vázquez-Román, R., López-Molina, A., Mannan, M.S., 2014. A MINLP approach for layout designs based on the domino hazard index. Journal of Loss Prevention in the Process Industries 30, 219-227. 10.1016/j.jlp.2013.07.007
de Lira-Flores, J.A., Gutiérrez-Antonio, C., Vázquez-Román, R., 2018. A MILP approach for optimal storage vessels layout based on the quantitative risk analysis methodology. Process Safety and Environmental Protection 120, 1-13. 10.1016/j.psep.2018.08.028
Delvosalle, C., 1998. A methodology for the identification and evaluation of domino effects. Rep. CRC/MT/003, Belgian Ministry of Employment and Labour, Bruxelles (B).
Ding, L., Ji, J., Khan, F., 2020. Combining uncertainty reasoning and deterministic modeling for risk analysis of fire-induced domino effects. Safety Science 129. 10.1016/j.ssci.2020.104802
Dinh, L.T.T., Pasman, H., Gao, X., Mannan, M.S., 2012. Resilience engineering of industrial processes: Principles and contributing factors. Journal of Loss Prevention in the Process Industries 25, 233-241. 10.1016/j.jlp.2011.09.003
Directive, E., 2012. Directive 2012/19/EU of the European Parliament and of the Council of 4 July 2012 on waste electrical and electronic equipment, WEEE. Official Journal of the European Union L 197, 38-71.
Dorman, P., 2000. The economics of safety, health, and well-being at work: an overview. ILO Geneva.
Du, Y., Sun, J., Duan, Q., Qi, K., Xiao, H., Liew, K.M., 2020. Optimal Assignments of Allocating and Scheduling Emergency Resources to Accidents in Chemical Industrial Parks. Journal of Loss Prevention in the Process Industries 65. 10.1016/j.jlp.2020.104148
Dugan, J.B., Bavuso, S.J., Boyd, M.A., 1992. Dynamic fault-tree models for fault-tolerant computer systems. IEEE Transactions on reliability 41, 363-377.
Durga Rao, K., Gopika, V., Sanyasi Rao, V.V.S., Kushwaha, H.S., Verma, A.K., Srividya, A., 2009. Dynamic fault tree analysis using Monte Carlo simulation in probabilistic safety assessment. Reliability Engineering & System Safety 94, 872-883. 10.1016/j.ress.2008.09.007
Dweck, J., Boutillon, S., Asbill, S., 2004. Deadly LNG incident holds key lessons for developers, regulators. Pipeline and Gas Journal, 39-42.
Eini, S., Abdolhamidzadeh, B., Reniers, G., Rashtchian, D., 2015. Optimization procedure to select an inherently safer design scheme. Process Safety and Environmental Protection 93, 89-98. 10.1016/j.psep.2014.05.002
Eisenberg, N.A., Lynch, C.J., Breeding, R.J., 1975. Vulnerability model. A simulation system for assessing damage resulting from marine spills. Enviro control inc rockville md.
Evans, D., 2002. Database searches for qualitative research. Journal of the Medical Library Association 90, 290.

Explorer, S., 2019. Average Salary in France 2019. Retrieved from: http://www.salaryexplorer.com/salary-survey.php?loc=74&loctype=1. (Accessed April 10, 2019).
Fabbrocino, G., Iervolino, I., Orlando, F., Salzano, E., 2005. Quantitative risk analysis of oil storage facilities in seismic areas. J Hazard Mater 123, 61-69. 10.1016/j.jhazmat.2005.04.015
Fuentes-Bargues, J.L., González-Cruz, M., González-Gaya, C., Baixauli-Pérez, M., 2017. Risk Analysis of a Fuel Storage Terminal Using HAZOP and FTA. International journal of environmental research and public health 14, 705.
Galbusera, L., Trucco, P., Giannopoulos, G., 2020. Modeling interdependencies in multi-sectoral critical infrastructure systems: Evolving the DMCI approach. Reliability Engineering & System Safety 203. 10.1016/j.ress.2020.107072
Gant, S.E., Atkinson, G.T., 2011. Dispersion of the vapour cloud in the Buncefield Incident. Process Safety and Environmental Protection 89, 391-403. 10.1016/j.psep.2011.06.018
Garcia, M.L., 2007. Design and evaluation of physical protection systems. Elsevier.
Gavious, A., Mizrahi, S., Shani, Y., Minchuk, Y., 2009. The costs of industrial accidents for the organization: developing methods and tools for evaluation and cost–benefit analysis of investment in safety. Journal of Loss Prevention in the Process Industries 22, 434-438.
Ge, W., Sun, H., Zhang, H., Li, Z., Guo, X., Wang, X., Qin, Y., Gao, W., van Gelder, P., 2020. Economic risk criteria for dams considering the relative level of economy and industrial economic contribution. Science of the Total Environment 725. 10.1016/j.scitotenv.2020.138139
Georgiadou, P.S., Papazoglou, I.A., Kiranoudis, C.T., Markatos, N.C., 2007. Modeling emergency evacuation for major hazard industrial sites. Reliability Engineering & System Safety 92, 1388-1402. 10.1016/j.ress.2006.09.009
Gexcon, 2018a. EFFECTS. Retrieved from: https://www.gexcon.com/products-services/EFFECTS/31/en. (Accessed July 17, 2019).
Gexcon, 2018b. Software. Retrieved from: https://www.gexcon.com/products-services-index/Software/5/en. (Accessed June 6, 2019).
Ghasemi, A.M., Nourai, F., 2017. A framework for minimizing domino effect through optimum spacing of storage tanks to serve in land use planning risk assessments. Safety Science 97, 20-26. 10.1016/j.ssci.2016.04.017
GlobalPetrolPrices, 2019. France Gasoline prices, liter. Retrieved from: https://www.globalpetrolprices.com/France/gasoline_prices/. (Accessed April 09, 2019).
Gnoni, M.G., Lettera, G., Bragatto, P.A., 2009. A decision model for preventing knock-on risk inside industrial plant. Crc Press-Taylor & Francis Group, Boca Raton.
Goldbeck, N., Angeloudis, P., Ochieng, W.Y., 2019. Resilience assessment for interdependent urban infrastructure systems using dynamic network flow models. Reliability Engineering & System Safety 188, 62-79. 10.1016/j.ress.2019.03.007
Gomez-Mares, M., Zarate, L., Casal, J., 2008. Jet fires and the domino effect. Fire Safety Journal 43, 583-588.
Greenawald, L.A., Karwacki, C.J., Palya, F., Browe, M.A., Bradley, D., Szalajda, J.V., 2020. Conducting an evaluation of CBRN canister protection capabilities

against emerging chemical and radiological hazards. Journal of Occupational and Environmental Hygiene, 1-15. 10.1080/15459624.2020.1798452
Gubinelli, G., Cozzani, V., 2009a. Assessment of missile hazards: evaluation of the fragment number and drag factors. J Hazard Mater 161, 439-449. 10.1016/j.jhazmat.2008.03.116
Gubinelli, G., Cozzani, V., 2009b. Assessment of missile hazards: identification of reference fragmentation patterns. J Hazard Mater 163, 1008-1018. 10.1016/j.jhazmat.2008.07.056
Gubinelli, G., Zanelli, S., Cozzani, V., 2004. A simplified model for the assessment of the impact probability of fragments. J Hazard Mater 116, 175-187. 10.1016/j.jhazmat.2004.09.002
Guo, X., Ji, J., Khan, F., Ding, L., 2020. Fuzzy bayesian network based on an improved similarity aggregation method for risk assessment of storage tank accident. Process Safety and Environmental Protection 144, 242-252. 10.1016/j.psep.2020.07.030
Guowen, S., Paskaluk, S., Sati, R., Crown, E.M., Doug Dale, J., Ackerman, M., 2010. Thermal protective performance of protective clothing used for low radiant heat protection. Textile Research Journal 81, 311-323. 10.1177/0040517510380108
Haase, H., 1977. Electrostatic hazards: their evaluation and control. Wiley-VCH.
Harary, F., 1969. Graph theory. Addison-Wesley, Reading, MA.
Harary, F., Gupta, G., 1997. Dynamic graph models. Mathematical and Computer Modelling 25, 79-87.
Hauptmanns, U., 2001a. A Monte-Carlo based procedure for treating the flight of missiles from tank explosions. Probabilistic Engineering Mechanics 16, 307-312.
Hauptmanns, U., 2001b. A procedure for analyzing the flight of missiles from explosions of cylindrical vessels. Journal of Loss Prevention in the Process Industries 14, 395-402.
Hauptmanns, U., 2004. Semi-quantitative fault tree analysis for process plant safety using frequency and probability ranges. Journal of Loss Prevention in the Process Industries 17, 339-345.
He, Z., Weng, W., 2019. Synergic effects in the assessment of multi-hazard coupling disasters: Fires, explosions, and toxicant leaks. Journal of hazardous materials. 10.1016/j.jhazmat.2019.121813
Health and Safety Executive, 2009. Buncefield Explosion Mechanism Phase 1. Health and Safety Executive.
Hemmatian, B., Abdolhamidzadeh, B., Darbra, R.M., Casal, J., 2014. The significance of domino effect in chemical accidents. Journal of Loss Prevention in the Process Industries 29, 30-38. 10.1016/j.jlp.2014.01.003
Henry, D., Emmanuel Ramirez-Marquez, J., 2012. Generic metrics and quantitative approaches for system resilience as a function of time. Reliability Engineering & System Safety 99, 114-122. 10.1016/j.ress.2011.09.002
Hessami, A.G., 2004. A systems framework for safety and security: the holistic paradigm. Systems Engineering 7, 99-112.
Hollnagel, E., Woods, D.D., Leveson, N., 2006. Resilience engineering: Concepts and precepts. Ashgate Publishing, Ltd.

Hosseini, S., Barker, K., 2016. Modeling infrastructure resilience using Bayesian networks: A case study of inland waterway ports. Computers & Industrial Engineering 93, 252-266. 10.1016/j.cie.2016.01.007

Hosseini, S., Barker, K., Ramirez-Marquez, J.E., 2016. A review of definitions and measures of system resilience. Reliability Engineering & System Safety 145, 47-61. 10.1016/j.ress.2015.08.006

Hosseinnia, B., Khakzad, N., Reniers, G., 2018a. An emergency response decision matrix against terrorist attacks with improvised device in chemical clusters. International Journal of Safety and Security Engineering 8, 187-199.

Hosseinnia, B., Khakzad, N., Reniers, G., 2018b. Multi-plant emergency response for tackling major accidents in chemical industrial areas. Safety Science 102, 275-289. 10.1016/j.ssci.2017.11.003

HSE, 1978. Canvey: An investigation of potential hazards from operations in the Canvey Island/Thurrock area. HM Stationery Office.

HSE, 2011. Buncefield: Why did it happen. HSE Books.

HSE, 2016. Internal guidance on cost benefit analysis (CBA) in support of safety-related investment decisions. Retrieved from: http://orr.gov.uk/__data/assets/pdf_file/0018/18009/revised-safety-cba-guidance-05022016.pdf. (Accessed April 10, 2019).

ICCA, 2019. The Global Chemical Industry: Catalyzing Growth and Addressing Our World's Sustainability Challenges. Retrieved from: https://icca-chem.org/wp-content/uploads/2020/10/Catalyzing-Growth-and-Addressing-Our-Worlds-Sustainability-Challenges-Report.pdf. (Accessed November 2, 2020).

Jafari, S., Ajorlou, A., Aghdam, A.G., 2011. Leader localization in multi-agent systems subject to failure: A graph-theoretic approach. Automatica 47, 1744-1750.

Jain, P., Mentzer, R., Mannan, M.S., 2018a. Resilience metrics for improved process-risk decision making: Survey, analysis and application. Safety Science 108, 13-28. 10.1016/j.ssci.2018.04.012

Jain, P., Rogers, W.J., Pasman, H.J., Keim, K.K., Mannan, M.S., 2018b. A Resilience-based Integrated Process Systems Hazard Analysis (RIPSHA) approach: Part I plant system layer. Process Safety and Environmental Protection 116, 92-105. 10.1016/j.psep.2018.01.016

Jallon, R., Imbeau, D., de Marcellis-Warin, N., 2011. Development of an indirect-cost calculation model suitable for workplace use. J Safety Res 42, 149-164. 10.1016/j.jsr.2011.05.006

Janssens, J., Talarico, L., Reniers, G., Sörensen, K., 2015. A decision model to allocate protective safety barriers and mitigate domino effects. Reliability Engineering & System Safety 143, 44-52. 10.1016/j.ress.2015.05.022

Jensen, H.A., Jerez, D.J., Valdebenito, M., 2020. An adaptive scheme for reliability-based global design optimization: A Markov chain Monte Carlo approach. Mechanical Systems and Signal Processing 143. 10.1016/j.ymssp.2020.106836

Ji, J., Tong, Q., Khan, F., Dadashzadeh, M., Abbassi, R., 2018. Risk-Based Domino Effect Analysis for Fire and Explosion Accidents Considering Uncertainty in Processing Facilities. Industrial & Engineering Chemistry Research 57, 3990-4006. 10.1021/acs.iecr.8b00103

Jia, M., Chen, G., Reniers, G., 2017. An innovative framework for determining the damage probability of equipment exposed to fire. Fire Safety Journal 92, 177-187. 10.1016/j.firesaf.2017.05.015
Jiang, D., Pan, X.-H., Hua, M., Mébarki, A., Jiang, J.-C., 2019. Assessment of tanks vulnerability and domino effect analysis in chemical storage plants. Journal of Loss Prevention in the Process Industries 60, 174-182.
Jiang, D., Wu, B., Cheng, Z., Xue, J., van Gelder, P.H.A.J.M., 2020. Towards a probabilistic model for estimation of grounding accidents in fluctuating backwater zone of the Three Gorges Reservoir. Reliability Engineering & System Safety. 10.1016/j.ress.2020.107239
Johansson, J., Hassel, H., Zio, E., 2013. Reliability and vulnerability analyses of critical infrastructures: Comparing two approaches in the context of power systems. Reliability Engineering & System Safety 120, 27-38. 10.1016/j.ress.2013.02.027
Johnson, D., 2013. Vapour cloud explosion at the IOC terminal in Jaipur. Loss Prevention Bulletin.
Johnson, D., Tam, V., 2017. Why DDT is the only way to explain some vapor cloud explosions. Process Safety Progress 36, 292-300.
Jones, M.L., 2004. Application of systematic review methods to qualitative research: practical issues. Journal of advanced nursing 48, 271-278.
Joy, D.C., 1995. Monte Carlo modeling for electron microscopy and microanalysis. Oxford University Press.
Jujuly, M., Rahman, A., Ahmed, S., Khan, F., 2015. LNG pool fire simulation for domino effect analysis. Reliability Engineering & System Safety 143, 19-29. 10.1016/j.ress.2015.02.010
Jung, S., Ng, D., Diaz-Ovalle, C., Vazquez-Roman, R., Mannan, M.S., 2011. New Approach To Optimizing the Facility Siting and Layout for Fire and Explosion Scenarios. Industrial & Engineering Chemistry Research 50, 3928-3937. 10.1021/ie101367g
Kadri, F., Châtelet, E., Chen, G., 2013. Method for quantitative assessment of the domino effect in industrial sites. Process Safety and Environmental Protection 91, 452-462. 10.1016/j.psep.2012.10.010
Kamil, M.Z., Taleb-Berrouane, M., Khan, F., Ahmed, S., 2019. Dynamic domino effect risk assessment using Petri-nets. Process Safety and Environmental Protection 124, 308-316. 10.1016/j.psep.2019.02.019
Khakzad, N., 2015. Application of dynamic Bayesian network to risk analysis of domino effects in chemical infrastructures. Reliability Engineering & System Safety 138, 263-272. 10.1016/j.ress.2015.02.007
Khakzad, N., 2018a. A Graph Theoretic Approach to Optimal Firefighting in Oil Terminals. Energies 11. 10.3390/en11113101
Khakzad, N., 2018b. Impact of wildfires on Canada's oil sands facilities. Natural Hazards and Earth System Sciences 18, 3153-3166. 10.5194/nhess-18-3153-2018
Khakzad, N., 2018c. Reducing the attractiveness of chemical plants to terrorist attacks: Dehorning rhinos. Process Safety Progress 37, 150-152. 10.1002/prs.11907
Khakzad, N., 2018d. Which Fire to Extinguish First? A Risk-Informed Approach to Emergency Response in Oil Terminals. Risk Anal 38, 1444-1454. 10.1111/risa.12946

Khakzad, N., 2019. Modeling wildfire spread in wildland-industrial interfaces using dynamic Bayesian network. Reliability Engineering & System Safety 189, 165-176. 10.1016/j.ress.2019.04.006

Khakzad, N., Amyotte, P., Cozzani, V., Reniers, G., Pasman, H., 2018a. How to address model uncertainty in the escalation of domino effects? Journal of Loss Prevention in the Process Industries 54, 49-56. 10.1016/j.jlp.2018.03.001

Khakzad, N., Dadashzadeh, M., Reniers, G., 2018b. Quantitative assessment of wildfire risk in oil facilities. Journal of environmental management 223, 433-443.

Khakzad, N., Khan, F., Amyotte, P., 2011. Safety analysis in process facilities: Comparison of fault tree and Bayesian network approaches. Reliability Engineering & System Safety 96, 925-932. 10.1016/j.ress.2011.03.012

Khakzad, N., Khan, F., Amyotte, P., 2012. Dynamic risk analysis using bow-tie approach. Reliability Engineering & System Safety 104, 36-44.

Khakzad, N., Khan, F., Amyotte, P., Cozzani, V., 2013. Domino effect analysis using Bayesian networks. Risk Anal 33, 292-306. 10.1111/j.1539-6924.2012.01854.x

Khakzad, N., Khan, F., Amyotte, P., Cozzani, V., 2014. Risk management of domino effects considering dynamic consequence analysis. Risk Anal 34, 1128-1138. 10.1111/risa.12158

Khakzad, N., Landucci, G., Cozzani, V., Reniers, G., Pasman, H., 2018c. Cost-effective fire protection of chemical plants against domino effects. Reliability Engineering & System Safety 169, 412-421. 10.1016/j.ress.2017.09.007

Khakzad, N., Landucci, G., Reniers, G., 2017a. Application of dynamic Bayesian network to performance assessment of fire protection systems during domino effects. Reliability Engineering & System Safety 167, 232-247. 10.1016/j.ress.2017.06.004

Khakzad, N., Landucci, G., Reniers, G., 2017b. Application of Graph Theory to Cost-Effective Fire Protection of Chemical Plants During Domino Effects. Risk analysis 37, 1652-1667. 10.1111/risa.12712

Khakzad, N., Martinez, I.S., Kwon, H.-M., Stewart, C., Perera, R., Reniers, G., 2018d. Security risk assessment and management in chemical plants: Challenges and new trends. Process Safety Progress 37, 211-220. 10.1002/prs.11914

Khakzad, N., Martinez, I.S., Kwon, H.M., Stewart, C., Perera, R., Reniers, G., 2018e. Security risk assessment and management in chemical plants: Challenges and new trends. Process Safety Progress 37, 211-220. 10.1002/prs.11914

Khakzad, N., Reniers, G., 2015a. Risk-based design of process plants with regard to domino effects and land use planning. J Hazard Mater 299, 289-297. 10.1016/j.jhazmat.2015.06.020

Khakzad, N., Reniers, G., 2015b. Using graph theory to analyze the vulnerability of process plants in the context of cascading effects. Reliability Engineering & System Safety 143, 63-73. 10.1016/j.ress.2015.04.015

Khakzad, N., Reniers, G., 2017. Cost-effective allocation of safety measures in chemical plants w.r.t land-use planning. Safety Science 97, 2-9. 10.1016/j.ssci.2015.10.010

Khakzad, N., Reniers, G., 2019. Low-capacity utilization of process plants: A cost-robust approach to tackle man-made domino effects. Reliability Engineering & System Safety 191. 10.1016/j.ress.2018.03.030

Khakzad, N., Reniers, G., Abbassi, R., Khan, F., 2016. Vulnerability analysis of process plants subject to domino effects. Reliability Engineering & System Safety 154, 127-136. 10.1016/j.ress.2016.06.004
Khakzad, N., Reniers, G., Landucci, G., 2017c. Application of Bayesian network to safety assessment of chemical plants during fire-induced domino effects, 26th Conference on European Safety and Reliability. ESREL 2016, Glasgow, UK, pp. 786-792.
Khakzad, N., Reniers, G., van Gelder, P., 2017d. A multi-criteria decision making approach to security assessment of hazardous facilities. Journal of Loss Prevention in the Process Industries 48, 234-243. 10.1016/j.jlp.2017.05.006
Khakzad, N., Van Gelder, P., 2018. Vulnerability of industrial plants to flood-induced natechs: A Bayesian network approach. Reliability Engineering & System Safety 169, 403-411. 10.1016/j.ress.2017.09.016
Khan, F., Abbasi, S., 1996. Simulation of accidents in a chemical industry using the software package MAXCRED. Indian Journal of Chemical Technology 3, 338-344.
Khan, F., Rathnayaka, S., Ahmed, S., 2015. Methods and models in process safety and risk management: Past, present and future. Process Safety and Environmental Protection 98, 116-147. 10.1016/j.psep.2015.07.005
Khan, F.I., Abbasi, S., 1998a. Models for domino effect analysis in chemical process industries. Process Safety Progress 17, 107-123.
Khan, F.I., Abbasi, S., 1999. Major accidents in process industries and an analysis of causes and consequences. Journal of Loss Prevention in the Process Industries 12, 361-378.
Khan, F.I., Abbasi, S., 2001. An assessment of the likelihood of occurrence, and the damage potential of domino effect (chain of accidents) in a typical cluster of industries. Journal of Loss Prevention in the Process Industries 14, 283-306.
Khan, F.I., Abbasi, S.A., 1998b. DOMIFFECT (DOMIno eFFECT): user-friendly software for domino effect analysis. Environmental Modelling & Software 13, 163-177.
Khan, F.I., Abbasi, S.A., 2000. Studies on the probabilities and likely impacts of chains of accident (domino effect) in a fertilizer industry. Process Safety Progress 19, 40-56. 10.1002/prs.680190110
Khan, F.I., Amyotte, P.R., 2003. How to make inherent safety practice a reality. The Canadian Journal of Chemical Engineering 81, 2-16.
Khan, F.I., Husain, T., Abbasi, S.A., 2001a. Safety weighted hazard index (SWeHI): a new, user-friendly tool for swift yet comprehensive hazard identification and safety evaluation in chemical process industrie. Process Safety and Environmental Protection 79, 65-80.
Khan, F.I., Iqbal, A., Abbasi, S.A., 2001b. Rapid risk assessment of a fertilizer industry using recently developed computer-automated tool TORAP. Journal of Loss Prevention in the Process Industries 14, 413-427. 10.1016/s0950-4230(00)00055-3
Khan, F.I., Iqbal, A., Abbasi, S.A., 2001c. Risk analysis of a petrochemical industry using ORA (Optimal Risk Analysis) procedure. Process Safety Progress 20, 95-110. 10.1002/prs.680200207

Khan, F.I., Rani, J.D., Abbasi, S.A., 1998. Accident simulation as a tool for assessing and controlling environmental risks in chemical process industries: A case study. Korean Journal of Chemical Engineering 15, 124-135. 10.1007/bf02707064
Kinney, R., Crucitti, P., Albert, R., Latora, V.J.T.E.P.J.B.-C.M., Systems, C., 2005. Modeling cascading failures in the North American power grid. 46, 101-107.
Kinsella, K., 1993. A rapid assessment methodology for the prediction of vapour cloud explosion overpressure, International Conference and Exhibition on Safety, Health and Loss Prevention in the Oil, Chemical and Process Industries, Singapore.
Kletz, T.A., 2003. Inherently safer design—its scope and future. Process Safety and Environmental Protection 81, 401-405.
Krausmann, E., Cozzani, V., Salzano, E., Renni, E., 2011a. Industrial accidents triggered by natural hazards: an emerging risk issue. Natural Hazards and Earth System Sciences 11, 921-929. 10.5194/nhess-11-921-2011
Krausmann, E., Renni, E., Campedel, M., Cozzani, V., 2011b. Industrial accidents triggered by earthquakes, floods and lightning: lessons learned from a database analysis. Natural Hazards 59, 285-300. 10.1007/s11069-011-9754-3
Kroshl, W.M., Sarkani, S., Mazzuchi, T.A., 2015. Efficient Allocation of Resources for Defense of Spatially Distributed Networks Using Agent-Based Simulation. Risk Anal 35, 1690-1705. 10.1111/risa.12325
Kuczera, G., Parent, E., 1998. Monte Carlo assessment of parameter uncertainty in conceptual catchment models: the Metropolis algorithm. Journal of Hydrology 211, 69-85.
Kuhn, A., Ruf, O., 2013. The Value of a Statistical Injury: New Evidence from the Swiss Labor Market. Swiss Journal of Economics and Statistics (SJES) 149, 57-86. 10.1016/j.psep.2017.03.023
Landucci, G., Antonioni, G., Tugnoli, A., Cozzani, V., 2012a. Probabilistic Assessment of Domino Effect Triggered by Fire: Implementation in Quantitative Risk Assessment. Chemical Engineering Transactions 26, 195-200.
Landucci, G., Antonioni, G., Tugnoli, A., Cozzani, V., 2012b. Release of hazardous substances in flood events: Damage model for atmospheric storage tanks. Reliability Engineering & System Safety 106, 200-216. 10.1016/j.ress.2012.05.010
Landucci, G., Argenti, F., Spadoni, G., Cozzani, V., 2016a. Domino effect frequency assessment: The role of safety barriers. Journal of Loss Prevention in the Process Industries 44, 706-717. 10.1016/j.jlp.2016.03.006
Landucci, G., Argenti, F., Tugnoli, A., Cozzani, V., 2015a. Quantitative assessment of safety barrier performance in the prevention of domino scenarios triggered by fire. Reliability Engineering & System Safety 143, 30-43. 10.1016/j.ress.2015.03.023
Landucci, G., Bonvicini, S., Cozzani, V., 2017a. A methodology for the analysis of domino and cascading events in Oil & Gas facilities operating in harsh environments. Safety Science 95, 182-197. 10.1016/j.ssci.2016.12.019
Landucci, G., D'Aulisa, A., Tugnoli, A., Cozzani, V., Birk, A.M., 2016b. Modeling heat transfer and pressure build-up in LPG vessels exposed to fires. International Journal of Thermal Sciences 104, 228-244. 10.1016/j.ijthermalsci.2016.01.002
Landucci, G., Gubinelli, G., Antonioni, G., Cozzani, V., 2009a. The assessment of the damage probability of storage tanks in domino events triggered by fire. Accident Analysis & Prevention 41, 1206-1215. 10.1016/j.aap.2008.05.006

Landucci, G., Gubinelli, G., Antonioni, G., Cozzani, V., 2009b. The assessment of the damage probability of storage tanks in domino events triggered by fire. Accid Anal Prev 41, 1206-1215. 10.1016/j.aap.2008.05.006
Landucci, G., Molag, M., Cozzani, V., 2009c. Modeling the performance of coated LPG tanks engulfed in fires. J Hazard Mater 172, 447-456. 10.1016/j.jhazmat.2009.07.029
Landucci, G., Necci, A., Antonioni, G., Argenti, F., Cozzani, V., 2017b. Risk assessment of mitigated domino scenarios in process facilities. Reliability Engineering & System Safety 160, 37-53. 10.1016/j.ress.2016.11.023
Landucci, G., Necci, A., Antonioni, G., Tugnoli, A., Cozzani, V., 2014. Release of hazardous substances in flood events: Damage model for horizontal cylindrical vessels. Reliability Engineering & System Safety 132, 125-145. 10.1016/j.ress.2014.07.016
Landucci, G., Reniers, G., Cozzani, V., Salzano, E., 2015b. Reliability Engineering & System Safety 143, 53-62. 10.1016/j.ress.2015.03.004
Landucci, G., Tugnoli, A., Cozzani, V., 2008. Inherent safety key performance indicators for hydrogen storage systems. J Hazard Mater 159, 554-566. 10.1016/j.jhazmat.2008.02.080
Latifi, S.E., Mohammadi, E., Khakzad, N., 2017. Process plant layout optimization with uncertainty and considering risk. Computers & chemical engineering 106, 224-242. 10.1016/j.compchemeng.2017.05.022
Lea, C., Ledin, H., 2002. A review of the state-of-the-art in gas explosion modelling. Health and Safety Laboratory Buxton, UK.
Lee, J.Y., Kim, H.S., Yoon, E.S., 2006. A new approach for allocating explosive facilities in order to minimize the domino effect using NLP. Journal of chemical engineering of Japan 39, 731-745. 10.1252/jcej.39.731
Lee, J.Y., Lee, J.W., Ko, J.W., Yoon, E.S., 2005. Optimization for allocating the explosive facilities in order to minimize ptimiz the domino effect using nonlinear programming. Korean Journal of Chemical Engineering 22, 649-656. 10.1007/bf02705777
Lees, F., 2012. Lees' Loss prevention in the process industries: Hazard identification, assessment and control. Butterworth-Heinemann.
Li, Wang, Ge, Wei, Li, 2019. Risk Analysis of Earth-Rock Dam Breach Based on Dynamic Bayesian Network. Water 11. 10.3390/w11112305
Li, J., Reniers, G., Cozzani, V., Khan, F., 2017. A bibliometric analysis of peer-reviewed publications on domino effects in the process industry. Journal of Loss Prevention in the Process Industries 49, 103-110. 10.1016/j.jlp.2016.06.003
Li, Z., Li, W., Ge, W., 2018. Weight analysis of influencing factors of dam break risk consequences. Natural Hazards & Earth System Sciences 18.
Lisi, R., Consolo, G., Maschio, G., Milazzo, M., 2014. Domino effects due to the projection of fragments: estimation of the impact probability using a Monte Carlo simulation. Chem. Eng. Trans. 36, 361-366.
Lisi, R., Consolo, G., Maschio, G., Milazzo, M.F., 2015. Estimation of the impact probability in domino effects due to the projection of fragments. Process Safety and Environmental Protection 93, 99-110. 10.1016/j.psep.2014.05.003

Liu, K., Wu, J., Liu, H., Sun, M., Wang, Y., 2021. Reliability analysis of thermal error model based on DBN and Monte Carlo method. Mechanical Systems and Signal Processing 146. 10.1016/j.ymssp.2020.107020

López-Molina, A., Vázquez-Román, R., Mannan, M.S., Félix-Flores, M.G., 2013. An approach for domino effect reduction based on optimal layouts. Journal of Loss Prevention in the Process Industries 26, 887-894. 10.1016/j.jlp.2012.11.001

Maremonti, M., Russo, G., Salzano, E., Tufano, V., 1999. Post-accident analysis of vapour cloud explosions in fuel storage areas. Process Safety and Environmental Protection 77, 360-365.

Matches, 2014. Tank Cost Estimate. Retrieved from: http://www.matche.com/equipcost/Tank.html. (Accessed April 11, 2019).

Matteini, A., Argenti, F., Salzano, E., Cozzani, V., 2018. A comparative analysis of security risk assessment methodologies for the chemical industry. Reliability Engineering & System Safety.

Mishra, K.B., 2018. The influence of volume blockage ratio on IOCL Jaipur explosion. Journal of Loss Prevention in the Process Industries 54, 196-205. 10.1016/j.jlp.2018.03.007

Mishra, K.B., Wehrstedt, K.-D., Krebs, H., 2013. Lessons learned from recent fuel storage fires. Fuel Processing Technology 107, 166-172. 10.1016/j.fuproc.2012.08.003

Mishra, K.B., Wehrstedt, K.-D., Krebs, H., 2014. Amuay refinery disaster: The aftermaths and challenges ahead. Fuel Processing Technology 119, 198-203. 10.1016/j.fuproc.2013.10.025

Misuri, A., Casson Moreno, V., Quddus, N., Cozzani, V., 2019. Lessons learnt from the impact of hurricane Harvey on the chemical and process industry. Reliability Engineering & System Safety 190. 10.1016/j.ress.2019.106521

Misuri, A., Landucci, G., Cozzani, V., 2020. Assessment of safety barrier performance in Natech scenarios. Reliability Engineering & System Safety 193. 10.1016/j.ress.2019.106597

Moodie, K., 1988. Experiments and modelling:-An overview with particular reference to fire engulfment. Journal of hazardous materials 20, 149-175.

Moore, D.A., Fuller, B., Hazzan, M., Jones, J.W., 2007. Development of a security vulnerability assessment process for the RAMCAP chemical sector. Journal of hazardous materials 142, 689-694.

Moosemiller, M., 2011. Development of algorithms for predicting ignition probabilities and explosion frequencies. Journal of Loss Prevention in the Process Industries 24, 259-265.

Mueller, J., Stewart, M.G., 2011. Terror, security, and money: Balancing the risks, benefits, and costs of homeland security. Oxford University Press.

Mukhim, E.D., Abbasi, T., Tauseef, S.M., Abbasi, S.A., 2017. Domino effect in chemical process industries triggered by overpressure—Formulation of equipment-specific probits. Process Safety and Environmental Protection 106, 263-273. 10.1016/j.psep.2017.01.004

Murata, T., 1989. Petri nets: Properties, analysis and applications. Proceedings of the IEEE 77, 541-580.

Necci, A., Antonioni, G., Bonvicini, S., Cozzani, V., 2016. Quantitative assessment of risk due to major accidents triggered by lightning. Reliability Engineering & System Safety 154, 60-72. 10.1016/j.ress.2016.05.009

Necci, A., Antonioni, G., Cozzani, V., Krausmann, E., Borghetti, A., Alberto Nucci, C., 2013. A model for process equipment damage probability assessment due to lightning. Reliability Engineering & System Safety 115, 91-99. 10.1016/j.ress.2013.02.018

Necci, A., Argenti, F., Landucci, G., Cozzani, V., 2014. Accident scenarios triggered by lightning strike on atmospheric storage tanks. Reliability Engineering & System Safety 127, 30-46. 10.1016/j.ress.2014.02.005

Necci, A., Cozzani, V., Spadoni, G., Khan, F., 2015. Assessment of domino effect: State of the art and research Needs. Reliability Engineering & System Safety 143, 3-18. 10.1016/j.ress.2015.05.017

Nomen, R., Sempere, J., Mariotti, V., 2014. QRA Including Domino Effect as a Tool for Engineering Design. Procedia Engineering 84, 23-32. 10.1016/j.proeng.2014.10.406

Olivar, O.J.R., Mayorga, S.Z., Giraldo, F.M., Sánchez-Silva, M., Pinelli, J.-P., Salzano, E., 2020. The effects of extreme winds on atmospheric storage tanks. Reliability Engineering & System Safety 195. 10.1016/j.ress.2019.106686

OSHA, 2019. Personal Protective Equipment. Retrieved from: https://www.osha.gov/Publications/osha3151.pdf. (Accessed August 30, 2020).

Paltrinieri, N., Bonvicini, S., Spadoni, G., Cozzani, V., 2012. Cost-benefit analysis of passive fire protections in road LPG transportation. Risk Anal 32, 200-219; discussion 220-203. 10.1111/j.1539-6924.2011.01654.x

Papadakis, G., Amendola, A., 1997. Guidance on the preparation of a safety report to meet the requirements of Council Directive 96/82/EC (Seveso II). Joint Research Centre, European Commission.

Pasman, H., Kottawar, K., Jain, P., 2020. Resilience of Process Plant: What, Why, and How Resilience Can Improve Safety and Sustainability. Sustainability 12. 10.3390/su12156152

Paté-Cornell, E., Guikema, S., 2002. Probabilistic modeling of terrorist threats: A systems analysis approach to setting priorities among countermeasures. Military Operations Research 7, 5-23.

Pavlova, Y., Reniers, G., 2011. A sequential-move game for enhancing safety and security cooperation within chemical clusters. J Hazard Mater 186, 401-406. 10.1016/j.jhazmat.2010.11.013

Pietersen, C., 1988. Analysis of the LPG-disaster in Mexico City. Journal of hazardous materials 20, 85-107.

Pietersen, C., 1990. Consequences of accidental releases of hazardous material. Journal of Loss Prevention in the Process Industries 3, 136-141.

Pita, J., Jain, M., Ordóñez, F., Tambe, M., Kraus, S., Magori-Cohen, R., 2009. Effective solutions for real-world stackelberg games: When agents must deal with human uncertainties, Proceedings of The 8th International Conference on Autonomous Agents and Multiagent Systems-Volume 1. International Foundation for Autonomous Agents and Multiagent Systems, pp. 369-376.

Poole, R.W., 2008. Toward risk-based aviation security policy. OECD/ITF Joint Transport Research Centre Discussion Paper.
Provan, D.J., Woods, D.D., Dekker, S.W.A., Rae, A.J., 2020. Safety II professionals: How resilience engineering can transform safety practice. Reliability Engineering & System Safety 195. 10.1016/j.ress.2019.106740
Pula, R., Khan, F.I., Veitch, B., Amyotte, P.R., 2007. A model for estimating the probability of missile impact: Missiles originating from bursting horizontal cylindrical vessels. Process Safety Progress 26, 129-139. 10.1002/prs.10178
Qi, R., Ng, D., Cormier, B.R., Mannan, M.S., 2010. Numerical simulations of LNG vapor dispersion in Brayton Fire Training Field tests with ANSYS CFX. Journal of hazardous materials 183, 51-61.
Qiao, A., Zhang, S., 2010. Advanced CFD modeling on vapor dispersion and vapor cloud explosion. Journal of Loss Prevention in the Process Industries 23, 843-848. 10.1016/j.jlp.2010.06.006
Qin, R., Khakzad, N., Zhu, J., 2020. An overview of the impact of Hurricane Harvey on chemical and process facilities in Texas. International Journal of Disaster Risk Reduction 45. 10.1016/j.ijdrr.2019.101453
Rad, A., Abdolhamidzadeh, B., Abbasi, T., Rashtchian, D., 2014. FREEDOM II: An improved methodology to assess domino effect frequency using simulation techniques. Process Safety and Environmental Protection 92, 714-722. 10.1016/j.psep.2013.12.002
Rai, S., Hu, X., 2018. Hybrid agent-based and graph-based modeling for building occupancy simulation, Proceedings of the 4th ACM International Conference of Computing for Engineering and Sciences, pp. 1-12.
Ramírez-Camacho, J.G., Pastor, E., Amaya-Gómez, R., Mata, C., Muñoz, F., Casal, J., 2019. Analysis of crater formation in buried NG pipelines: A survey based on past accidents and evaluation of domino effect. Journal of Loss Prevention in the Process Industries 58, 124-140. 10.1016/j.jlp.2019.01.011
Ramirez-Camacho, J.G., Pastor, E., Casal, J., Amaya-Gomez, R., Munoz-Giraldo, F., 2015. Analysis of domino effect in pipelines. J Hazard Mater 298, 210-220. 10.1016/j.jhazmat.2015.05.033
Ramírez-Marengo, C., Diaz-Ovalle, C., Vázquez-Román, R., Mannan, M.S., 2015. A stochastic approach for risk analysis in vapor cloud explosion. Journal of Loss Prevention in the Process Industries 35, 249-256.
Reniers, G., 2009. Terrorism security in the chemical industry: Results of a qualitative investigation. Security Journal 24, 69-84. 10.1057/sj.2009.10
Reniers, G., 2010. An external domino effects investment approach to improve cross-plant safety within chemical clusters. J Hazard Mater 177, 167-174. 10.1016/j.jhazmat.2009.12.013
Reniers, G., Brijs, T., 2014. Major accident management in the process industry: An expert tool called CESMA for intelligent allocation of prevention investments. Process Safety and Environmental Protection 92, 779-788. 10.1016/j.psep.2014.02.003
Reniers, G., Cozzani, V., 2013. Domino Effects in the Process Industries, Modeling, Prevention and Managing. Elsevier, Amsterdam, The Netherlands.

Reniers, G., Cuypers, S., Pavlova, Y., 2012. A game-theory based Multi-plant Collaboration Model (MCM) for cross-plant prevention in a chemical cluster. J Hazard Mater 209-210, 164-176. 10.1016/j.jhazmat.2012.01.004
Reniers, G., Dullaert, W., Audenaert, A., Ale, B.J., Soudan, K., 2008. Managing domino effect-related security of industrial areas. Journal of Loss Prevention in the Process Industries 21, 336-343.
Reniers, G., Dullaert, W., Karel, S., 2009. Domino effects within a chemical cluster: a game-theoretical modeling approach by using Nash-equilibrium. J Hazard Mater 167, 289-293. 10.1016/j.jhazmat.2008.12.113
Reniers, G., Dullaert, W., Soudan, K., 2004. A domino effect evaluation model.
Reniers, G., Khakzad, N., Cozzani, V., Khan, F., 2018a. The impact of nature on chemical industrial facilities: Dealing with challenges for creating resilient chemical industrial parks. Journal of Loss Prevention in the Process Industries. 10.1016/j.jlp.2018.09.010
Reniers, G., Khakzad, N., Gelder, P.V., 2018b. Security Risk Assessment In the Chemical and Process Industry. Walter de Gruyter GmbH & Co KG.
Reniers, G., Pavlova, Y., 2013a. Safety Management in Chemical Industrial Clusters: The State of the Art.
Reniers, G., Pavlova, Y., 2013b. Using game theory to improve safety within chemical industrial parks. Springer.
Reniers, G., Soudan, K., 2010. A game-theoretical approach for reciprocal security-related prevention investment decisions. Reliability Engineering & System Safety 95, 1-9.
Reniers, G., Van Lerberghe, P., Van Gulijk, C., 2015. Security risk assessment and protection in the chemical and process industry. Process Safety Progress 34, 72-83. 10.1002/prs.11683
Reniers, G.L., Sorensen, K., 2013. An approach for optimal allocation of safety resources: using the knapsack problem to take aggregated cost-efficient preventive measures. Risk Anal 33, 2056-2067. 10.1111/risa.12036
Reniers, G.L., Van Erp, H.N., 2016. Operational safety economics: a practical approach focused on the chemical and process industries. John Wiley & Sons.
Reniers, G.L.L., Audenaert, A., 2008. Preventing intentional disasters by investigating the security of chemical industrial areas. Disaster Advances 1, 14-19.
Reniers, G.L.L., Audenaert, A., 2014. Preparing for major terrorist attacks against chemical clusters: Intelligently planning protection measures w.r.t. domino effects. Process Safety and Environmental Protection 92, 583-589. 10.1016/j.psep.2013.04.002
Reniers, G.L.L., Dullaert, W., 2007. DomPrevPlanning©: User-friendly software for planning domino effects prevention. Safety Science 45, 1060-1081. 10.1016/j.ssci.2006.10.004
Reniers, G.L.L., Dullaert, W., 2008. Knock-on accident prevention in a chemical cluster. Expert Systems with Applications 34, 42-49. 10.1016/j.eswa.2006.08.033
Reniers, G.L.L., Dullaert, W., Ale, B.J.M., Soudan, K., 2005a. Developing an external domino accident prevention framework: Hazwim. Journal of Loss Prevention in the Process Industries 18, 127-138. 10.1016/j.jlp.2005.03.002

Reniers, G.L.L., Dullaert, W., Ale, B.J.M., Soudan, K., 2005b. The use of current risk analysis tools evaluated towards preventing external domino accidents. Journal of Loss Prevention in the Process Industries 18, 119-126. 10.1016/j.jlp.2005.03.001

Reniers, G.L.L., Jongh, K.D., Gorrens, B., Lauwers, D., Leest, M.V., Witlox, F., 2010. Transportation Risk ANalysis tool for hazardous Substances (TRANS) – A user-friendly, semi-quantitative multi-mode hazmat transport route safety risk estimation methodology for Flanders. Transportation Research Part D: Transport and Environment 15, 489-496. 10.1016/j.trd.2010.07.001

Reniers, G.L.L., Sörensen, K., Khan, F., Amyotte, P., 2014. Resilience of chemical industrial areas through attenuation-based security. Reliability Engineering & System Safety 131, 94-101. 10.1016/j.ress.2014.05.005

Reuters, 2015. CORRECTED-COLUMN-Oil storage business is booming: Kemp. Retrieved from: https://www.reuters.com/article/oil-storage-kemp-idUSL8N13S4ZQ20151204. (Accessed April 11, 2019).

Rew, P., Daycock, L., 2004. Development of a method for the determination of on-site ignition probabilities, HSE Contractor Report WSA/226. HSE Books, London (UK).

Rubinstein, R.Y., Kroese, D.P., 2016. Simulation and the Monte Carlo method. John Wiley & Sons.

Rum, A., Landucci, G., Galletti, C., 2018. Coupling of integral methods and CFD for modeling complex industrial accidents. Journal of Loss Prevention in the Process Industries 53, 115-128. 10.1016/j.jlp.2017.09.006

Safety, C.f.C.P., 2000. Guidelines for chemical process quantitative risk analysis. Center for Chemical Process Safety/AIChE.

Salzano, E., Cozzani, V., 2003. The use of probit functions in the quantitative risk assessment of domino accidents caused by overpressure. A a Balkema Publishers, Leiden.

Salzano, E., Cozzani, V., 2005. The analysis of domino accidents triggered by vapor cloud explosions. Reliability Engineering & System Safety 90, 271-284. 10.1016/j.ress.2004.11.012

Salzano, E., Cozzani, V., 2006. A fuzzy set analysis to estimate loss intensity following blast wave interaction with process equipment. Journal of Loss Prevention in the Process Industries 19, 343-352. 10.1016/j.jlp.2005.08.002

Salzano, E., Landucci, G., Reniers, G., Cozzani, V., 2014. Domino effects related to home-made explosives. Chemical Engineering Transactions 36, 349-354.

Scarponi, G.E., Landucci, G., Heymes, F., Cozzani, V., 2018. Experimental and numerical study of the behavior of LPG tanks exposed to wildland fires. Process Safety and Environmental Protection 114, 251-270. 10.1016/j.psep.2017.12.013

Schmidt, S., Mishra, K.B., Wehrstedt, K.-D., 2016. CFD based reproduction of Amuay refinery accident 2012. CHEMICAL ENGINEERING 48.

Shaluf, I.M., Ahmadun, F., Shariff, R., Mustafa, S., Said, A.M., 2003. Fire and explosion at mutual major hazard installations: review of a case history. Journal of Loss Prevention in the Process Industries 16, 149-155. 10.1016/s0950-4230(02)00094-3

Sharma, R.K., Gurjar, B.R., Wate, S.R., Ghuge, S.P., Agrawal, R., 2013. Assessment of an accidental vapour cloud explosion: Lessons from the Indian Oil Corporation

Ltd. accident at Jaipur, India. Journal of Loss Prevention in the Process Industries 26, 82-90. 10.1016/j.jlp.2012.09.009
Sierra, D., Briceno, J., Buitrago, H., Rozo, B., Montecchi, L., Mura, I., 2018. Probabilistic Modeling of Failure Domino Effects in Chemical Plants.
Silva, E.P., Nele, M., e Melo, P.F.F., Könözsy, L., 2016. Underground parallel pipelines domino effect: An analysis based on pipeline crater models and historical accidents. Journal of Loss Prevention in the Process Industries 43, 315-331. 10.1016/j.jlp.2016.05.031
Siu, N., 1994. Risk assessment for dynamic systems: an overview. Reliability Engineering & System Safety 43, 43-73.
So, W., Kim, Y.-H., Lee, C.J., Shin, D., Yoon, E.S., 2011. Optimal layout of additional facilities for minimization of domino effects based on worst-case scenarios. Korean Journal of Chemical Engineering 28, 656-666. 10.1007/s11814-010-0445-7
Šrekl, J., Golob, J., 2011. New approach to calculate the probability of ignition. Journal of Loss Prevention in the Process Industries 24, 288-291.
Srivastava, A., Gupta, J.P., 2010. New methodologies for security risk assessment of oil and gas industry. Process Safety and Environmental Protection 88, 407-412. 10.1016/j.psep.2010.06.004
Stewart, M.G., Mueller, J., 2011. Cost-benefit analysis of advanced imaging technology full body scanners for airline passenger security screening. Journal of Homeland Security and Emergency Management 8.
Stewart, M.G., Mueller, J., 2012. Terror, security, and money: balancing the risks, benefits, and costs of critical infrastructure protection, pp. 513-533.
Stewart, M.G., Mueller, J., 2013. Terrorism risks and cost-benefit analysis of aviation security. Risk Anal 33, 893-908. 10.1111/j.1539-6924.2012.01905.x
Stewart, M.G., Mueller, J., 2014. A risk and cost–benefit analysis of police counter-terrorism operations at Australian airports. Journal of Policing, Intelligence and Counter Terrorism 9, 98-116.
Stroeve, S.H., Blom, H.A., Bakker, G.B., 2013. Contrasting safety assessments of a runway incursion scenario: Event sequence analysis versus multi-agent dynamic risk modelling. Reliability Engineering & System Safety 109, 133-149.
Su, H., Zio, E., Zhang, J.J., Li, X.Y., 2018. A systematic framework of vulnerability analysis of a natural gas pipeline network. Reliability Engineering & System Safety 175, 79-91. 10.1016/j.ress.2018.03.006
Sun, D., Huang, G., Jiang, J., Zhang, M., Wang, Z., 2013a. Influence of the Protective Layer of Polyvinylchloride Resin on Failure of LPG Vessel Caused by Heat Radiation. Procedia Engineering 62, 564-572. 10.1016/j.proeng.2013.08.101
Sun, D., Huang, G., Jiang, J., Zhang, M., Wang, Z., 2013b. Study on the Rationality and Validity of Probit Models of Domino Effect to Chemical Process Equipment caused by Overpressure. Journal of Physics: Conference Series 423, 012002. 10.1088/1742-6596/423/1/012002
Sun, D., Jiang, J., Zhang, M., Wang, Z., 2016a. Ballistic experiments on the mechanism of protective layer against domino effect caused by projectiles. Journal of Loss Prevention in the Process Industries 40, 17-28. 10.1016/j.jlp.2015.11.020

Sun, D., Jiang, J., Zhang, M., Wang, Z., Huang, G., Qiao, J., 2012. Parametric approach of the domino effect for structural fragments. Journal of Loss Prevention in the Process Industries 25, 114-126. 10.1016/j.jlp.2011.06.029
Sun, D., Jiang, J., Zhang, M., Wang, Z., Zhang, Y., Cai, L., 2016b. Investigation of multiple domino scenarios caused by fragments. Journal of Loss Prevention in the Process Industries 40, 591-602. 10.1016/j.jlp.2016.01.023
Sun, D., Jiang, J., Zhang, M., Wang, Z., Zhang, Y., Yan, L., Zhang, H., Du, X., Zou, Y., 2017. Investigation on the approach of intercepting fragments generated by vessel explosion using barrier net. Journal of Loss Prevention in the Process Industries 49, 989-996. 10.1016/j.jlp.2016.10.012
Swuste, P., van Nunen, K., Reniers, G., Khakzad, N., 2019. Domino effects in chemical factories and clusters: An historical perspective and discussion. Process Safety and Environmental Protection.
Talarico, L., Reniers, G., 2016. Risk-informed decision making of safety investments by using the disproportion factor. Process Safety and Environmental Protection 100, 117-130. 10.1016/j.psep.2016.01.003
Tanabe, M., Miyake, A., 2012. Approach enhancing inherent safety application in onshore LNG plant design. Journal of Loss Prevention in the Process Industries 25, 809-819. 10.1016/j.jlp.2012.04.005
Tauseef, S.M., Rashtchian, D., Abbasi, T., Abbasi, S.A., 2011. A method for simulation of vapour cloud explosions based on computational fluid dynamics (CFD). Journal of Loss Prevention in the Process Industries 24, 638-647. 10.1016/j.jlp.2011.05.007
Taveau, J., 2012. The Buncefield explosion: Were the resulting overpressures really unforeseeable? Process Safety Progress 31, 55-71. 10.1002/prs.10468
Taylor, J.R., 2003. Risk analysis for process plant, pipelines and transport. Routledge.
The accident investigation team for “11.28” accident, 2019. The investigation report of “11.28” large explosion-fire accident of Shenghua Chemical Company, Zhangjiakou China Chemical Industry Group. Retrieved from: http://www.xinhuanet.com/energy/2019-05/24/c_1124535295.htm. (Accessed June 13, 2020).
Tong, Q., Yang, M., Zinetullina, A., 2020. A Dynamic Bayesian Network-based approach to Resilience Assessment of Engineered Systems. Journal of Loss Prevention in the Process Industries 65. 10.1016/j.jlp.2020.104152
Tsai, S.-F., Huang, A.-C., Shu, C.-M., 2018. Integrated self-assessment module for fire rescue safety in a chemical plant – A case study. Journal of Loss Prevention in the Process Industries 51, 137-149. 10.1016/j.jlp.2017.12.011
Tseng, J., Su, T., Kuo, C., 2012. Consequence evaluation of toxic chemical releases by ALOHA. Procedia Engineering 45, 384-389.
Tugnoli, A., Cozzani, V., Di Padova, A., Barbaresi, T., Tallone, F., 2012. Mitigation of fire damage and escalation by fireproofing: A risk-based strategy. Reliability Engineering & System Safety 105, 25-35. 10.1016/j.ress.2011.11.002
Tugnoli, A., Cozzani, V., Padova, A., Barbaresi, T., Tallone, F., 2013. Reducing the Consequences of Accidental Fires in Oil & Gas Facilities: a Risk-Based Procedure for Identification of the Fireproofing Zones. Chemical Engineering Transactions 32, 103-108.

Tugnoli, A., Gubinelli, G., Landucci, G., Cozzani, V., 2014a. Assessment of fragment projection hazard: probability distributions for the initial direction of fragments. J Hazard Mater 279, 418-427. 10.1016/j.jhazmat.2014.07.034
Tugnoli, A., Khan, F., Amyotte, P., Cozzani, V., 2008a. Safety assessment in plant layout design using indexing approach: implementing inherent safety perspective. Part 1 - guideword applicability and method description. J Hazard Mater 160, 100-109. 10.1016/j.jhazmat.2008.02.089
Tugnoli, A., Khan, F., Amyotte, P., Cozzani, V., 2008b. Safety assessment in plant layout design using indexing approach: implementing inherent safety perspective. Part 2-Domino Hazard Index and case study. J Hazard Mater 160, 110-121. 10.1016/j.jhazmat.2008.02.091
Tugnoli, A., Milazzo, M.F., Landucci, G., Cozzani, V., Maschio, G., 2014b. Assessment of the hazard due to fragment projection: A case study. Journal of Loss Prevention in the Process Industries 28, 36-46. 10.1016/j.jlp.2013.08.015
U.S. Department of Homeland Security, 2013. Critical Infrastructure Sectors, Washington.
U.S. National Transport Safety Board, 1993. National Transport Safety Board Pipeline Accident Report: Brenham, Texas. U.S. Chemical Safety and Hazard Investigation Board.
Uijt de Haag, Ale, 1999. Guidelines for quantitative risk assessment. Committee for the Prevention of Disasters, The Hague (NL).
UPI, 2019. Death toll rises to 78 in Chinese chemical plant explosion. Retrieved from: https://www.upi.com/Top_News/World-News/2019/03/26/Death-toll-rises-to-78-in-Chinese-chemical-plant-explosion/1601553571988/. (Accessed April 30, 2019).
van den Berg, A., 1980. A ID variable flame speed blast simulation code using a Flux-Corrected Transport algorithm. Report No. PML 162.
Van den Berg, A., 1985. The multi-energy method: a framework for vapour cloud explosion blast prediction. Journal of hazardous materials 12, 1-10.
Van den Berg, A., Lannoy, A., 1993. Methods for vapour cloud explosion blast modelling. Journal of hazardous materials 34, 151-171.
Van Den Bosh, C., Merx, W., Jansen, C., De Weger, D., Reuzel, P., Leeuwen, D., Blom-Bruggerman, J., 1989. Methods for the calculation of possible damage (Green Book). Committee for the Prevention of Disasters, The Hague (NL).
Van Den Bosh, C., Weterings, R., 1997. Methods for the calculation of physical effects (Yellow Book). Committee for the Prevention of Disasters, The Hague (NL).
van der Voort, M.M., Klein, A.J.J., de Maaijer, M., van den Berg, A.C., van Deursen, J.R., Versloot, N.H.A., 2007. A quantitative risk assessment tool for the external safety of industrial plants with a dust explosion hazard. Journal of Loss Prevention in the Process Industries 20, 375-386. 10.1016/j.jlp.2007.04.024
Vilchez, J.A., Sevilla, S., Montiel, H., Casal, J., 1995. Historical analysis of accidents in chemical plants and in the transportation of hazardous materials. Journal of Loss Prevention in the Process Industries 8, 87-96.
Villa, V., Paltrinieri, N., Khan, F., Cozzani, V., 2016. Towards dynamic risk analysis: A review of the risk assessment approach and its limitations in the chemical process industry. Safety Science 89, 77-93. 10.1016/j.ssci.2016.06.002

Villa, V., Reniers, G.L.L., Paltrinieri, N., Cozzani, V., 2017a. Development of an economic model for counter terrorism measures in the process-industry. Journal of Loss Prevention in the Process Industries 49, 437-460. 10.1016/j.jlp.2017.06.001

Villa, V., Reniers, G.L.L., Paltrinieri, N., Cozzani, V., 2017b. Development of an economic model for the allocation of preventive security measures against environmental and ecological terrorism in chemical facilities. Process Safety and Environmental Protection 109, 311-339. 10.1016/j.psep.2017.03.023

Wang, B., Li, D., Wu, C., 2020. Characteristics of hazardous chemical accidents during hot season in China from 1989 to 2019: A statistical investigation. Safety Science 129. 10.1016/j.ssci.2020.104788

Wang, B., Wu, C., 2020. Safety informatics as a new, promising and sustainable area of safety science in the information age. Journal of Cleaner Production 252. 10.1016/j.jclepro.2019.119852

Wang, B., Wu, C., Reniers, G., Huang, L., Kang, L., Zhang, L., 2018. The future of hazardous chemical safety in China: Opportunities, problems, challenges and tasks. Science of the Total Environment 643, 1-11. 10.1016/j.scitotenv.2018.06.174

Whiteley, J.R., Mannan, M.S., 2004. Initial perspectives on process threat management. J Hazard Mater 115, 163-167. 10.1016/j.jhazmat.2004.05.011

wisselkoers, 2019. Exchange rate. Retrieved from: https://www.wisselkoers.nl/. (Accessed April 09, 2019).

Yang, Y., Chen, G., Chen, P., 2018. The probability prediction method of domino effect triggered by lightning in chemical tank farm. Process Safety and Environmental Protection 116, 106-114. 10.1016/j.psep.2018.01.019

Yang, Y., Chen, G., Reniers, G., 2019. Vulnerability assessment of atmospheric storage tanks to floods based on logistic regression. Reliability Engineering & System Safety, 106721.

Yang, Y., Chen, G., Reniers, G., Goerlandt, F., 2020. A bibliometric analysis of process safety research in China: Understanding safety research progress as a basis for making China's chemical industry more sustainable. Journal of Cleaner Production 263. 10.1016/j.jclepro.2020.121433

Yang, Y., Kim, J., Seo, H., Lee, K., Yoon, I., 2006. Development of the world's largest above-ground full containment LNG storage tank, 23rd World Gas Conference, Amsterdam, pp. 1-14.

Yarveisy, R., Gao, C., Khan, F., 2020. A simple yet robust resilience assessment metrics. Reliability Engineering & System Safety 197. 10.1016/j.ress.2020.106810

Yuan, Z., Khakzad, N., Khan, F., Amyotte, P., 2016. Domino effect analysis of dust explosions using Bayesian networks. Process Safety and Environmental Protection 100, 108-116. 10.1016/j.psep.2016.01.005

Zarei, E., Jafari, M.J., Badri, N., 2013. Risk assessment of vapor cloud explosions in a hydrogen production facility with consequence modeling. Journal of research in health sciences 13, 181-187.

Zeng, T., Chen, G., Yang, Y., Chen, P., Reniers, G., 2019. Developing an advanced dynamic risk analysis method for fire-related domino effects. Process Safety and Environmental Protection.

Zhang, L., Landucci, G., Reniers, G., Khakzad, N., Zhou, J., 2017. DAMS: A Model to Assess Domino Effects by Using Agent-Based Modeling and Simulation. Risk Anal. 10.1111/risa.12955

Zhang, L., Landucci, G., Reniers, G., Khakzad, N., Zhou, J., 2018. DAMS: A Model to Assess Domino Effects by Using Agent-Based Modeling and Simulation. Risk analysis 38, 1585-1600. 10.1111/risa.12955

Zhang, L., Reniers, G., 2016. A Game-Theoretical Model to Improve Process Plant Protection from Terrorist Attacks. Risk Anal 36, 2285-2297. 10.1111/risa.12569

Zhang, M., Jiang, J., 2008. An improved probit method for assessment of domino effect to chemical process equipment caused by overpressure. Journal of hazardous materials 158, 280-286. 10.1016/j.jhazmat.2008.01.076

Zhang, N., Si, W., 2020. Deep reinforcement learning for condition-based maintenance planning of multi-component systems under dependent competing risks. Reliability Engineering & System Safety 203. 10.1016/j.ress.2020.107094

Zhang, X.-m., Chen, C., 2013. Mechanism analysis and risk assessment of escalation scenario in chemical industry zones. Process Safety and Environmental Protection 91, 79-85. 10.1016/j.psep.2012.02.003

Zhang, X.-m., Chen, G.-h., 2009. The analysis of domino effect impact probability triggered by fragments. Safety Science 47, 1026-1032. 10.1016/j.ssci.2008.11.005

Zhang, X., Chen, G., 2011. Modeling and algorithm of domino effect in chemical industrial parks using discrete isolated island method. Safety Science 49, 463-467. 10.1016/j.ssci.2010.11.002

Zheng, J.-F., Gao, Z.-Y., Zhao, X.-M., 2007. Modeling cascading failures in congested complex networks. Physica A: Statistical Mechanics and its Applications 385, 700-706. 10.1016/j.physa.2007.07.031

Zhou, J., 2013. Petri net modeling for the emergency response to chemical accidents. Journal of Loss Prevention in the Process Industries 26, 766-770. 10.1016/j.jlp.2013.02.002

Zhou, J., Reniers, G., 2016a. Petri-net based modeling and queuing analysis for resource-oriented cooperation of emergency response actions. Process Safety and Environmental Protection 102, 567-576. 10.1016/j.psep.2016.05.013

Zhou, J., Reniers, G., 2016b. Petri-net based simulation analysis for emergency response to multiple simultaneous large-scale fires. Journal of Loss Prevention in the Process Industries 40, 554-562. 10.1016/j.jlp.2016.01.026

Zhou, J., Reniers, G., 2017a. Analysis of emergency response actions for preventing fire-induced domino effects based on an approach of reversed fuzzy Petri-net. Journal of Loss Prevention in the Process Industries 47, 169-173. 10.1016/j.jlp.2017.03.011

Zhou, J., Reniers, G., 2017b. Petri-net based cascading effect analysis of vapor cloud explosions. Journal of Loss Prevention in the Process Industries 48, 118-125. 10.1016/j.jlp.2017.04.017

Zhou, J., Reniers, G., 2018a. A matrix-based modeling and analysis approach for fire-induced domino effects. Process Safety and Environmental Protection 116, 347-353. 10.1016/j.psep.2018.02.014

Zhou, J., Reniers, G., 2018b. Modeling and analysis of vapour cloud explosions knock-on events by using a Petri-net approach. Safety Science 108, 188-195. 10.1016/j.ssci.2018.04.019

Zhou, J., Reniers, G., 2018c. Petri-net based evaluation of emergency response actions for preventing domino effects triggered by fire. Journal of Loss Prevention in the Process Industries 51, 94-101. 10.1016/j.jlp.2017.12.001

Zhou, J., Reniers, G., 2020. Probabilistic Petri-net addition enabling decision making depending on situational change: The case of emergency response to fuel tank farm fire. Reliability Engineering & System Safety 200. 10.1016/j.ress.2020.106880

Zhou, J., Reniers, G., Khakzad, N., 2016. Application of event sequence diagram to evaluate emergency response actions during fire-induced domino effects. Reliability Engineering & System Safety 150, 202-209. 10.1016/j.ress.2016.02.005

Zhou, J., Reniers, G., Zhang, L., 2017. A weighted fuzzy Petri-net based approach for security risk assessment in the chemical industry. Chemical Engineering Science 174, 136-145. 10.1016/j.ces.2017.09.002

Zinetullina, A., Yang, M., Khakzad, N., Golman, B., Li, X., 2021. Quantitative resilience assessment of chemical process systems using functional resonance analysis method and Dynamic Bayesian network. Reliability Engineering & System Safety 205. 10.1016/j.ress.2020.107232

Summary

In light of the catastrophic consequences of past escalation accidents in the process industry, domino effects have raised an increasing concern in the scientific and technical domain. To prevent and mitigate domino effects, growing research on modeling and managing domino effects was conducted in recent decades. However, modeling and managing domino effects are still challenging concerning the time-dependencies and evolution uncertainties. As a result, this dissertation aims to deal with these limitations, supporting decision-making on preventing and mitigating domino effects. The contributions of this study are summarized as follows:

Insights into modeling and managing domino effects in the process industry

A systematic literature review is conducted to summarize and classify the methods used for modeling and managing domino effects, analyze current research trends, and discuss future research needs. The models are divided into three categories (analytical methods, graphical methods, and simulation methods) and the management strategies are grouped into five types (inherent safety, management of safety barriers, emergency response, cooperative prevention, and security strategies). Graphical methods such as Bayesian network and graph theory are increasingly used to model domino effects. Increasing attention is paid to managing intentional domino effects and Natech domino effects. Although past work has contributed a lot to modeling and managing domino effects, many challenges are still left, such as modeling the evolution of coupled domino effects, management of domino effects in extreme conditions, integrating safety and security resources to prevent domino effects, decision-making on managing domino effects in chemical clusters.

A spatial-temporal evolution model of fire-induced domino effects

A domino evolution graph (DEG) model based on dynamic graphs is established to model the spatial-temporal evolution of domino accidents triggered by fire. The proposed model extends the TTF (time to failure) to RTF (residual time to failure) to dynamically model the higher-level escalation of domino effects, considering synergistic effects, parallel effects, and superimposed effects. Ignoring these physical effects may underestimate domino effect risk because they can speed up fire escalations and thus make the control of domino effects more difficult. Compared with previous probabilistic models, the DEG model concerns more on physical mechanisms and it is more flexible and visible to model the dynamic escalation process. The Minimum Evolution Time (MET) algorithm proposed for the DEG model can rapidly obtain the evolution paths, evolution time, and the failure probability of installations. Therefore, the model can be used to assess domino effects in chemical industrial areas with a large number of hazardous installations.

A dynamic evolution model of VCE induced domino effects

Past risk assessment methods on VCEs ignore the effects of vapor cloud dispersion and delayed ignitions on the vulnerability of installations. In light of this limitation, a dynamic VCE evolution assessment (DVEA) model is developed based on a dynamic event tree, considering the spatial-temporal evolution of VCEs and the uncertainty of delayed ignition time (DIT). Multiple ignition sources can be

considered in this model, addressing the uncertainties of ignition time and ignition position. The study shows that a long-delayed explosion may lead to multi-failure of installations, resulting in catastrophic disasters. The result is consistent with past VCE-induced domino accidents. It indicates that the DVEA model can reflect the characteristics of possible large VCEs and avoid underestimating the consequences. Besides, this study demonstrates that only using ignition control measures in chemical plants is not enough for preventing VCEs and may aggravate the consequences. Combining ignition control measures with emergency response actions (e.g., diluting oil vapor by water vapor) may be an effective way to prevent VCEs.

A multi-agent evolution model of coupling domino effects

Accident analysis indicates that major accident scenarios such as acute toxicity, fire, and explosion may simultaneously or sequentially occur in a domino effect event. However, most of the previous domino effect models only concern one hazardous scenario in domino effects, neglecting the evolution between different hazardous scenarios. Therefore, a multi-agent approach called “Dynamic Graph Monte Carlo” (DGMC) is developed based on dynamic graphs and the Monte Carlo method to model the evolution of multi-hazardous scenarios in domino effects. In the model, chemical plants are regarded as a multi-agent system with three kinds of agents: hazardous installations, ignition sources, and humans. Hazardous effects caused by domino effects are modeled as the dependencies of agents and the evolution of domino effects is determined by the behavior of agents. This study demonstrates that the model can avoid underestimating domino effect risk since the spatial-temporal evolution of multi-hazard scenarios is addressed. The hazardous effect of VCE may be more severe than that of fire, and the safety distance designed based on fire hazard may not be sufficient to prevent domino effects triggered by VCEs.

An approach for decision-making on preventing and mitigating domino effects

Previous research on managing domino effects mainly focused on the performance of safety barriers, neglecting the role of security measures in intentional domino effects. Besides, the financial issues related to the investment of safety and security measures are always ignored while the protection budget is always limited. As a result, a cost-benefit management approach is proposed to support the decision-making on the investment and allocation of domino effects. This method considers the costs of protection measures and the expected benefits obtained from the protection investment. This study finds that investment in safety and security measures follows the law of diminishing returns. The protection strategies including multiple kinds of protection measures are recommended in terms of preventing and mitigating domino effects. The likelihood of threats plays a critical role in a protection strategy’s profitability, so different companies should formulate their optimal strategies based on their threats.

A resilience strategy for the prevention and mitigation of domino effects

Safety barriers can be used to prevent and mitigate accidental domino effects and intentional domino effects. Security measures can be used to prevent intentional attacks and thus prevent intentional domino effects. As a result, protection strategies based on safety and security measures are always recommended for preventing and mitigating domino effects. Limited attention has been paid to mitigating the consequences of domino effects after the events. Therefore, a resilience-based approach is developed to prevent and mitigate domino effects. Besides safety and security measures, adaptation and restoration are considered for mitigating the consequences of domino effects on the operation of the companies. To support the decision-making on resilience measures, a chemical resilience indicator is developed, considering the capabilities of resistance, mitigation, adaptation, and restoration. A sensitive analysis for the indicator demonstrates that adaptation and restoration measures can effectively enhance the resilience of chemical plants, mitigating the consequences of domino effects.

In summary, this study establishes evolution models for assessing domino effects and proposes two protection strategies based on the developed models for preventing and mitigating domino effects. The developed domino effect models can contribute to a better understanding of the evolution of domino effects and the protection strategies can support the decision-making on the investment and allocation of protection measures.

Curriculum Vitae

Personal Information

Name: Chao Chen
M/F: Male
DOB: Jan 29, 1991
POD: Guang'an, Sichuan, China
Nationality: Chinese
Tel.: +31 621742978, +86 18782950228
E-mail: c.chen-1@tudelft.nl; chenchaoswpu@gmail.com
Page: https://www.researchgate.net/profile/Chao_Chen113

Educations

- **Ph.D. candidate: Safety and Security Science** 10/2017 – present
  - 3S Group, Delft University of Technology, Delft, The Netherlands;
  - Promoter/daily supervisor: Prof. Genserik Reniers/ Dr. Ming Yang
  - **Research topics**: Process safety and security, Domino effects, Safety economics, Resilience
- **Master of Science: Petroleum Engineering** 09/2014 – 06/2017
  - College of Petroleum Engineering, Southwest Petroleum University, Chengdu, China
  - Supervisor: Prof. Changjun Li
- **Bachelor of Management: Business Management** 09/2012 – 06/2014
  - School of Economics and Management, Southwest Petroleum University, Chengdu, China
  - Subject: DuPont Process Safety Management Systems
  - Supervisor: Prof. Xiaozhong Yu
- **Bachelor of Science: Petroleum Engineering** 09/2010 – 06/2014
  - School of Petroleum Engineering, Southwest Petroleum University, Chengdu, China
  - Supervisor: Prof. Changjun Li

Publications

- **Journal papers**

[1] **Chen, C.**, Yang, M., Reniers, G., 2021. A dynamic stochastic methodology for quantifying HAZMAT storage resilience. Reliability Engineering & System Safety. (under review)

[2] **Chen, C.**, Reniers, G., Khakzad, N., Yang, M., 2021. Operational safety economics: Foundations, current approaches and paths for future research. Safety Science. 105326

[3] **Chen, C**., Reniers, G., Khakzad, N., 2021. A dynamic multi-agent approach for modeling the evolution of multi-hazard accident scenarios in chemical plants. Reliability Engineering & System Safety 207. 10.1016/j.ress.2020.107349

[4] **Chen, C.**, Li, C., Reniers, G., Yang, F., 2021. Safety and security of oil and gas pipeline transportation: A systematic analysis of research trends and future needs using WoS. Journal of Cleaner Production 279. 10.1016/j.jclepro.2020.123583

[5] **Chen, C.**, Reniers, G., Khakzad, N., 2020. A thorough classification and discussion of approaches for modeling and managing domino effects in the process industries. Safety Science 125. 10.1016/j.ssci.2020.104618

[6] **Chen, C.**, Reniers, G., Khakzad, N., 2020. Cost-Benefit Management of Intentional Domino Effects in Chemical Industrial Areas. Process Safety and Environmental Protection 134, 392-405. 10.1016/j.psep.2019.10.007

[7] **Chen, C.**, Khakzad, N., Reniers, G., 2020a. Dynamic vulnerability assessment of process plants with respect to vapor cloud explosions. Reliability Engineering & System Safety 200. 10.1016/j.ress.2020.106934

[8] Yang, F., Tao, J., **Chen, C.**, Ge, F., Reniers, G., 2020. Determining the perceived safety and security attitude and knowledge of urban residents towards bus fires. Burns. 10.1016/j.burns.2019.09.009

[9] **Chen, C.**, Reniers, G., 2020. Chemical industry in China: The current status, safety problems, and pathways for future sustainable development. Safety Science 128. 10.1016/j.ssci.2020.104741

[10] **Chen, C.**, Reniers, G., Khakzad, N., 2019b. Integrating safety and security resources to protect chemical industrial parks from man-made domino effects: a dynamic graph approach. Reliability Engineering & System Safety 191. 10.1016/j.ress.2019.04.023

[11] **Chen, C.**, Reniers, G., Khakzad, N., 2019a. Exploring loading and unloading operations in relation to domino effects in chemical industrial parks. Chemical Engineering Transactions 75. 10.3303/CET1977010

[12] **Chen, C.**, Reniers, G., Zhang, L., 2018. An innovative methodology for quickly modeling the spatial-temporal evolution of domino accidents triggered by fire. Journal of Loss Prevention in the Process Industries 54, 312-324. 10.1016/j.jlp.2018.04.012

[13] **Chen C**, Reniers G. Goede praktijken ter verbetering van de veiligheid bij het laden en lossen van vloeibare chemische stoffen [J]. PreventFocus, 2018, 2: 12-14.

[14] Li, C., **Chen, C.**, Liao, K., Jia, W., Huang, Q., 2016. Theoretical research on the characteristics of the self-magnetic leakage field induced by ferromagnetic pipelines. Insight - Non-Destructive Testing and Condition Monitoring 58, 601-608. 10.1784/insi.2016.58.11.601

[15] Li, C., **Chen, C.**, Liao, K., 2015. A quantitative study of signal characteristics of non-contact pipeline magnetic testing. Insight-Non-Destructive Testing and Condition Monitoring 57, 324-330. 10.1784/insi.2015.57.6.324

- **Monograph**

[1] Chen C, Reniers G, Ming Yang. Integrating Safety and Security Management to Protect Chemical Industrial Area. Springer, 2021.

- **Chapters**

[1] **Chen, C.**, Reniers, G., 2021. Economic Model for Tackling Intentional Domino Effects in a Chemical Facility, Dynamic Risk Assessment and Management of Domino Effects and Cascading Events in the Process Industry. (In Press)

[2] **Chen, C.**, Reniers, G., 2020. Economic approaches for making prevention and safety investment decisions in the process industry

[3] **Chen, C.**, Reniers, G., 2018. Risk Assessment of Processes and Products in Industrial Biotechnology, Adv Biochem Eng Biotechnol

- **Conference presentations**

[1] **Chen, C.**, Reniers, G., 2021. Economic approach for tackling domino effects. International Symposium on Urban and Industrial Safety, 15-17 November 2019. Nanjing, China.

[2] **Chen, C.**, Reniers, G., 2021. Exploring loading and unloading operations in relation to domino effects in chemical industrial parks. 16th International Symposium on Loss Prevention and Safety Promotion in the Process Industries and accompanying exhibition. 16-19 June 2019. Delft, The Netherlands.